

https://dspace.org/

Electron paramagnetic resonance and optical investigations of defect centres in diamond

Du Preez, L

1965-09-01
University of the Witwatersrand, Johannesburg
http://hdl.handle.net/10539/20866

Downloaded from a DSpace repository. https://dspace.org/

ELECTRON PARAMAGNETIC RESONANCE AND OPTICAL INVESTIGATIONS OF DEFECT CENTRES IN DIAMOND

A THESIS

PRESENTED TO

THE DEPARTMENT OF PHYSICS

IN THE FACULTY OF SCIENCE

UNIVERSITY OF THE WITWATERSRAND, JOHANNESBURG

IN FULFILMENT

OF THE REQUIREMENTS FOR THE DEGREE

DOCTOR OF PHILOSOPHY

BY

L. DU PREEZ.

SEPTEMBER, 1965.

lustrial Distributors (1946) Limited
CORPORATED IN THE REPUBLIC OF SOUTH AFRICA)

ephone 35-7441 Telex 43-7707 Telegrams "Tesremos"

Diamond
Research
Laboratory

P.O. Box 916
Johannesburg

1st September, 1965

I declare that this thesis is my own work and that it was not submitted previously for any degree at any university.

L. DU PREEZ

ACKNOWLEDGEMENTS.

I am especially indebted to my supervisors Prof. J.H.N. Loubser of the University of the Witwatersrand, and Dr. H.B. Dyer, Director of Research of the Diamond Research Laboratory, for their help, enthusiasm and encouragement throughout the course of this project.

My thanks are due to Dr. F.A. Raal of the Diamond Research Laboratory for his constant interest, advice, and for valuable assistance in obtaining the diamond samples through the courtesy of the Diamond Corporation.

It is a pleasure to acknowledge helpful discussions with Prof. F.R.N. Nabarro, Dr. F.R.L. Schöning and Mr. L.A. Vermeulen of the University of the Witwatersrand; Prof. E.W.J. Mitchell and Dr. C.D. Clark of the University of Reading, and Dr. W.A. Runciman of the A.E.R.E., Harwell.

For much assistance in computation and preparation of this thesis I am grateful to Mrs. C. Swemmer of the Diamond Research Laboratory.

Financial assistance was provided by Industrial Distributors (1946) Ltd. to whom I wish to express my gratitude.

NOTE

Some of the results which are reported in this thesis have been published in the following papers:-

1) IRRADIATION DAMAGE IN TYPE I DIAMOND.
Dyer, H.B., and Du Preez, L., 1965, J. Chem. Phys., 42, 1898.

2) NEW LINES IN THE ELECTRON SPIN RESONANCE SPECTRUM OF SUBSTITUTIONAL NITROGEN DONORS IN DIAMOND.
Loubser, J.H.N., and Du Preez, L., 1965, Brit. J. Appl. Phys., 16, 457.

3) OPTICAL ABSORPTION FEATURES ASSOCIATED WITH PARAMAGNETIC NITROGEN IN DIAMOND.
Dyer, H.B., Raal, F.A., Du Preez, L., and Loubser, J.H.N., 1965, Phil. Mag., 11, 763.

4) EXCHANGE INTERACTION EFFECTS IN THE E.S.R. SPECTRUM OF SUBSTITUTIONAL NITROGEN IN DIAMOND,
Loubser, J.H.N., Van Ryneveld, W.P., and Du Preez, L., Solid State Communications, 1965, In Press.

ELECTRON PARAMAGNETIC RESONANCE AND OPTICAL INVESTIGATIONS OF DEFECT CENTRES IN DIAMOND

ABSTRACT

A survey of the optical and electron paramagnetic resonance (E.P.R.) absorption in a large number of diamonds from all major sources of production has revealed that perfect diamond is virtually non-existent. One or more of eleven different types of defect centres is found in each specimen. The presence or absence of nitrogen has long been known to give rise to the distinctive properties of Type I and Type II diamond. The present survey has shown that the form in which the nitrogen is present is significant. In most specimens the nitrogen is present in substitutional, non-paramagnetic platelet form, and these specimens were classified as Type Ia diamonds.

A small group of transparent natural diamonds was found to contain dispersed paramagnetic nitrogen. The optical properties of these diamonds are unlike those of other diamond types and have hitherto not been reported. It is proposed that these diamonds be classified as Type Ib.

Three new systems of E.P.R. lines were found in Type Ib diamond. They are shown to be due to: (i) ^{13}C

atoms situated in different positions relative to the substitutional nitrogen, (ii) interaction of the small quadrupole moment of the nitrogen with the electric field gradient, and (iii) the presence of the ^{15}N isotope.

Synthetic diamonds are found to be exclusively of the Type Ib variety, whereas natural Type Ib diamond are rare exceptions. This is attributed to the growth history of the specimens.

In order to investigate the defect centres associated with nitrogen in diamond, Type Ia and Ib diamond were irradiated with 0.78 MeV electrons. The effects observed were complicated and therefore led to a general investigation of irradiation damage, and the annealing of irradiation damage in diamond.

In addition to the G.R.1 and U.V. bands induced in all diamond by irradiation damage, another optical absorption feature, the N.D.1 band, is found in all Type Ia diamond after irradiation and limited heating. It is suggested that the N.D.1 centre arises from the combination of a carbon interstitial, and nitrogen in platelet form, and that the other primary product of irradiation damage, a vacancy, is responsible for both the G.R.1 and U.V. bands.

The N.D.1 centre acts as an acceptor, the G.R.1 centre as a donor. In the ionized state G.R.1 is inactive in optical absorption; N.D.1 is active. Electron transfer by thermal excitation results in the bleaching of G.R.1 and the enhancement of N.D.1. Illumination with light in the N.D.1 band causes electron transfer in the reverse direction, restoring band strengths to their former condition. A model is proposed which defines the energies within the forbidden gap of the ground and excited states of G.R.1 and N.D.1.

On heat treatment at temperatures of 500°C and above, the G.R.1 band in all diamonds anneals out. The rate of annealing, however, is found to be dependent on the nitrogen concentration. Thus in Type IIa diamond (which contains no nitrogen) G.R.1 anneals very slowly, resulting in the formation of an absorption tail. In Type Ia diamond G.R.1 anneals much faster (the actual rate depending on the nitrogen concentration), and two optical absorption bands, 5032A and H2, are formed.

It is proposed that the vacancy in diamond becomes mobile at about 500°C, and that the G.R.1 band in Type IIa diamond anneals because of the agglomeration of vacancies, which results in the formation of defects

responsible for the absorption tail. In Type Ia diamond the nitrogen platelets are ideal sinks for vacancies, because the lattice on either side of a platelet is in compression. G.R.1 therefore anneals more rapidly and 5032A centres are formed due to the combination of a vacancy and a nitrogen platelet. The nature of the H2 centre is much more obscure, but a possible explanation is that H2 centres are formed in addition, because the N.D.1 centres (nitrogen platelets with embedded interstitials) also succeed in trapping vacancies. Vacancy/interstitial recombinations are prevented since these defects are pinned to different locations in the platelet region.

In Type Ib diamonds N.D.1 centres were found to form at a lower temperature than in Type Ia diamond. It is suggested that the carbon interstitial in diamond is mobile, and combines with substitutional nitrogen in isolated positions at temperatures below 250°C. In Type Ia specimens, where the nitrogen is segregated in platelets, this process only occurs at about 250°C, when the interstitial has enough kinetic energy to overcome the energy barrier preventing it from combining with nitrogen inside the platelet region where it will relieve strain. Because of the different substitutional nitrogen configuration, the energy levels of N.D.1 centres in Type Ib diamond are

such that electron transfer by thermal excitation from G.R.1 to N.D.1 occurs at room temperature. Most of the G.R.1 centres are therefore permanently ionized and optically inactive.

After heat treatment, a new band called the 6400A band is formed in irradiated Type Ib diamond. It is suggested that 6400A centres are formed by the combination of mobile vacancies with substitutional nitrogen in isolated positions. The 6400A band is therefore analogous to the 5032A band produced in Type Ia diamond. As expected no analogue of the H2 is formed in Type Ib diamond, as both an interstitial and a vacancy cannot co-exist in combination with a single isolated substitutional nitrogen atom.

CONTENTS.

Page

Acknowledgements

Note

Abstract i

List of Tables xi

List of Figures xiii

CHAPTER I : Introduction.

1.1 General Properties of Diamond 1

1.2 Imperfections in Diamond 2

1.3 Outline of this Study 3

CHAPTER II : Experimental Methods.

2.1 Introduction 7

2.2 Methods for Studying Defect Centres in Diamond 8

2.3 Methods for Producing or Changing Defect Centres in Diamond 22

2.4 Discussion 35

CHAPTER III : Apparatus.

3.1 Introduction 37

3.2 Apparatus for Studying Diamonds Containing Defects 37

Page

3.3 Apparatus for Producing Or Modifying Defect Centres 42

CHAPTER IV : Survey of Natural Diamond.

4.1 Introduction 46

4.2 Non-Paramagnetic Nitrogen 48

4.3 4150A-Centres 55

4.4 Paramagnetic Nitrogen 63

4.5 Graphitic Regions 68

4.6 Acceptor Centres 72

4.7 G.R.1-Centres 75

4.8 5032A-Centres 76

4.9 Pink and Mauve Centres 77

4.10 4800A-Centres 79

4.11 Amber Centres 82

4.12 General Discussion 84

CHAPTER V : Paramagnetic Nitrogen in Natural Diamond.

5.1 Introduction 87

5.2 Electron Paramagnetic Resonance Absorption 87

5.3 Optical Absorption in the Ultra-violet and Visible Region 98

		Page
5.4	Optical Absorption in the Infra-red Region	99
5.5	Correlation Between the Absorption Features	101
5.6	Discussion	103
CHAPTER VI : Classification of Diamonds.		
6.1	Introduction	105
6.2	Proposed New Classification	106
6.3	Discussion	107
CHAPTER VII : Synthetic Diamonds.		
7.1	Introduction	109
7.2	Ferro-Magnetic Impurities	110
7.3	Electron Paramagnetic Resonance Measurements	111
7.4	Optical Measurements in the Ultra-violet and Visible Region	114
7.5	Infra-red Measurements	114
7.6	Doping Experiments	116
7.7	Discussion	121
CHAPTER VIII : Irradiation Damage in Type Ia Diamond.		
8.1	Introduction	123
8.2	Existing Knowledge	124

		Page
8.3	Specimen Selection	127
8.4	Results	127
8.5	Discussion of the Cycling Effects in Irradiated Type Ia Diamond	133
8.6	Investigation of the N.D.1-Centre	138
8.7	Investigation of the Thermal Activation Process	142
8.8	Discussion	148

CHAPTER IX : Annealing of Irradiation Damage in Type Ia Diamond.

9.1	Introduction	153
9.2	Existing Knowledge	154
9.3	Isothermal Annealing	156
9.4	Effects of Isothermal Heat Treatment	158
9.5	5032A-Centres	168
9.6	Annealing of G.R.1-Centres	170
9.7	H2-Centres	176

CHAPTER X : Irradiation Damage in Type Ib Diamond.

10.1	Introduction	180
10.2	Defects Induced Below Room Temperature	181

Page

10.3 Comparison of the N.D.1-Centres in Type Ia and Ib Diamond 182

10.4 N.D.1-Centres in Type Ib Diamond 185

10.5 Investigation of the Electron Exchange Effects 187

10.6 The Effects of Heat Treatment 189

10.7 6400A-Centres 193

10.8 Defects Induced at Room Temperature 194

CHAPTER XI : Conclusion.

11.1 Results of this Study 200

11.2 Suggestions for Further Research 204

REFERENCES 207

LIST OF TABLES

Number		Previous Page
5.1	^{13}C Hyperfine Lines - Spectrum (C)	92
5.2	^{14}N Quadrupole Hyperfine Lines - Spectrum (D)	93
5.3	Linear Correlations Between the Absorption Features in Paramagnetic Nitrogen Containing Diamonds	102
6.1	Characteristic Absorption Properties of the Diamond Types	107
7.1	Synthetic Diamond - Growth Doping with Nitrogen	119
8.1	Description of the Specimens	127
8.2	Energies of the Main Optical Absorption Features of the N.D.1 and 4150A Bands	128
8.3	Effects of Illumination on the N.D.1 Band in D_{14}	137
8.4	Effects of Treatment on the N.D.1 Band in D_{14} and D_{15}	139

Number		Previous Page
9.1	Effect of Isothermal Heat Treatment on the Optical Absorption Bands in D_{11}	158
9.2	Effect of Isothermal Heat Treatment on the Optical Absorption Bands in D_{13}	158
9.3	Effect of Isothermal Heat Treatment on the Optical Absorption Bands in D_{12}	158
9.4	Effect of Illumination with Monochromatic Light on the 5032A and H2 Bands in D_{14}	167
9.5	Energies of the Main Optical Absorption Features of the H2 Band	176
10.1	Optical Absorption Bands Produced by Irradiation at Low Temperatures	181
10.2	Effects of Illumination with Monochromatic Light on the Optical Absorption Bands in D_{18}	188
10.3	Effect of Heat Treatment on the Optical Absorption Bands in D_{18}	189
10.4	Energies of the Main Optical Absorption Features of the 6400A Band	193

LIST OF FIGURES

Number		Previous Page
3.1	Schematic Illustration of the Optical Cryostat	39
3.2	Block Diagram of the E.P.R. Spectrometer	40
4.1	Model for Nitrogen Platelets in Diamond	52
4.2	E.P.R. Line Associated with Graphitic Regions	70
4.3	E.P.R. Spectra of D_2-a Pink Diamond	78
4.4	Optical Absorption Spectrum of D_3- Illustrating the 4800A Band	80
4.5	Infra-red Absorption Spectrum of D_3	80
4.6	E.P.R. Spectra of D_3	80
4.7	E.P.R. Spectrum of D_4	82
4.8	E.P.R. Line Associated with Amber Centres in D_5	82
4.9	Optical Absorption Spectrum of D_5	82

Number		Previous Page
4.10	The 14,500A Optical Absorption Band in Specimen D_5	83
4.11	Infra-red Absorption Spectrum of D_5	83
4.12	Proposed Programme for Changing the Nitrogen Configurations in Diamond	86
5.1	E.P.R. Systems Associated with Paramagnetic Nitrogen in Diamond	90
5.2	The ^{13}C Centres Responsible for the Group (C) Spectra	92
5.3	Optical Absorption Spectra of D_6 and D_7 Which Contain Paramagnetic Nitrogen	99
5.4	Infra-red Absorption Spectrum of D_6 Which Contains Paramagnetic Nitrogen	100
5.5	Infra-red Absorption Spectrum of D_8	100
5.6	Infra-red Absorption Spectrum of D_9	101
7.1	E.P.R. Spectrum of Synthetic Diamond Which Contains Ferromagnetic Inclusions	112

Number		Previous Page
7.2	E.P.R. Spectrum of Synthetic Diamond Grown from a Non-Ferromagnetic Solvent	112
7.3	Optical Transmission Curves Obtained from Natural and Synthetic Diamond	114
7.4	Infra-red Spectrum of a Synthetic Diamond Crystal	115
7.5	E.P.R. Spectra of Nitrogen-Doped Synthetic Diamond	119
8.1	Optical Absorption Spectra of the Irradiated Type IIa Diamond D_{11}	124
8.2	Optical Absorption Spectra of the Irradiated Type Ia Diamond D_{12}	128
8.3	The N.D.1 Optical Absorption Band	128
8.4	E.P.R. Spectra of the Irradiated Type Ia Diamond D_{12}	130
8.5	Optical Absorption Spectra of D_{12} after Post Irradiation Treatment	132
8.6	Cycling in the Strength of the Absorption Features in the Irradiated Specimens	133

Number		Previous Page
8.7	Illustration of the Electron Transfer Involved in the Cycling of the N.D.1 G.R.1 and U.V. Bands	134
8.8	Optical Absorption Spectra of D_{14} Before and After Irradiation at 200°K	139
8.9	Rate Curves Obtained by Heating D_{15} - Illustrating the Similar Behaviour of N.D.1 and G.R.1	142
8.10	Effect of Isothermal Heating on N.D.1 in D_{15} Where Considerable Clustering of N.D.1-Centres is Expected	143
8.11	Effect of Isothermal Heating on N.D.1 in D_{14} Where Clustering of N.D.1-Centres is Expected to be a Minimum	146
9.1	Effect of Isothermal Heat Treatment on the Irradiation Induced Optical Bands	158
9.2	Optical Absorption Features in D_{12} After 550 hours at 500°C	166
9.3	Cycling of H2 and 5032A in D_{12} After Annealing up to 1200°C	166

Number		Previous Page
9.4	Effect of Heat Treatment in the Dark on the H2 and 5032A Bands	167
9.5	Schematic Illustration of the Results of Clark (1962)	169
9.6	The H2 Optical Absorption Band	176
10.1	Optical Absorption Spectra of D_{18} Before and After Irradiation at 200°K	182
10.2	E.P.R. Spectra of D_{18} Before and After Irradiation at 200°K	182
10.3	Comparison of the N.D.1 Bands in Type Ia and Ib Diamond	183
10.4	The 6400A Optical Absorption Band	193
10.5	Optical Absorption Spectra of D_{21}	194
10.6	E.P.R. Spectra of D_{21}	195
10.7	Optical Absorption Spectra of D_{21} After Heat Treatment	197

CHAPTER I

INTRODUCTION

1.1. General Properties of Diamond

Diamond has been known for centuries as a natural mineral of exceptional hardness and a gem of astonishing outward beauty. From the scientific point of view it is the prototype of crystals which show covalent bonding, and is of great interest since the whole crystal can be regarded as one giant molecule.

Diamond, like graphite, consists of carbon only. Each carbon atom is tetrahedrally bonded to four neighbouring atoms and provides one of the two electrons in each bond. The crystal structure exhibits cubic symmetry and may be regarded as consisting of two interpenetrating face-centered cubic lattices, displaced from each other quarter way along a body diagonal. The carbon atoms are held together by strong covalent bonding, the nearest neighbour separation being 1.54A. The unit cell contains eight atoms and has sides of length 3.57A. The structure is very open with no close-packed directions but with tunnels along $\langle 110 \rangle$ directions in the lattice.

As a result of the strong covalent bonding diamond is very hard and also has a high refractive index (2.42 at 5890A). Both these properties contribute to its value as a gem stone. For a non-metal, diamond has an exceptionally high thermal conductivity, this being about four times higher than that of copper at room temperature.

When heated above 500°C diamond is attached by oxygen and carbon dioxide is formed. In vacuo diamond reverts to graphite at temperatures above 1700°C. The melting point of diamond is estimated to be about 3600°C.

1.2. Imperfections in Diamond.

The diamond specimens encountered in practice exhibit many diverse physical properties which one would not expect from such a simple covalent solid. Most striking of these is the large variety of colours, which encompasses practically the whole of the visible spectrum. During the last two decades it became increasingly apparent that a number of physical properties of solids are determined more by the number and the nature of the imperfections present, than by the host lattice itself. It is therefore not unexpected that a natural mineral such as diamond exhibits such varying physical properties, since

these specimens probably contain many imperfections.

The imperfections in diamond can be of more than one type. Crystal imperfections such as cracks, flaws and inclusions of foreign compounds, will in general affect only the mechanical properties, and not the electronic properties. Imperfections in the lattice bonding such as vacant atomic sites, interstitial atoms and foreign atoms in solid solution, will change the electronic configuration in diamond, and for the purpose of this study such imperfections will be referred to as defect centres.

1.3. Outline of this Study.

This project involves a study of the defect centres in diamond, and is of course not the first attempt at such a study. Since 1932 defect centres in diamond were studied by workers at many research institutions all over the world, and altogether about two hundred papers have been published. Before embarking on this study therefore, a comprehensive literature survey was undertaken. It is beyond the scope of this thesis to review all the work previously conducted; only those contributions of direct interest to this particular study will

therefore be discussed.

Although a lot of information about the nature of defect centres in diamond was obtained by previous authors, a great deal of uncertainty still exists. Diamond is an especially costly commodity and difficult to shape to experimental requirements. Previous studies were therefore mainly concerned with specific defect centres in a few isolated samples. Very little is known about the occurence of defects in run-of-mine diamonds and the relationship between different defect centres. In an attempt to obtain more information on these aspects, this project was undertaken.

A large variety of defect centres is involved; to facilitate presentation of the results, the work of previous authors is therefore not presented in a single chapter, but is discussed in appropriate sections throughout this thesis.

This project was approached in two ways. Firstly experimental methods were used to study the electronic properties of diamonds containing defect centres, and secondly experimental methods were employed to produce defect centres in diamond and to change existing defects in these specimens. The experimental methods used are

discussed in Chapter II and the apparatus employed to conduct these experiments in Chapter III.

The first step was to conduct a survey of natural diamonds from all major sources of production. This survey, described in Chapter IV, revealed that perfect diamond is virtually non-existent and that most natural diamonds contain defect centres which are probably associated with either nitrogen atoms in solid solution, or combinations of nitrogen atoms and lattice defects.

The nitrogen could be positively identified as being present in either of two substitutional forms, these are a well known non-paramagnetic configuration, and a relatively unknown paramagnetic configuration. The electronic properties arising from the defects centres which are associated with paramagnetic nitrogen, are described in Chapter V. In Chapter VI the historic classification of diamonds is reviewed. A new classification system, based on the presence or absence of defect centres due to nitrogen in solid solution is proposed.

The defect centres encountered in synthetic diamonds are discussed in Chapter VII, where a comparison is made between natural and synthetic diamond.

In order to study in more detail the interaction

between various defect types, diamonds containing the two known nitrogen configurations were subjected to irradiation damage and subsequent heat treatment. The effects of irradiation damage in diamond are reviewed, and new mechanisms are proposed to explain these effects in Chapter VIII, where the effects of irradiation damage on specimens containing non-paramagnetic nitrogen are discussed. The results of annealing the irradiation damage in these specimens are described in Chapter IX. In view of these results new mechanisms for the annealing of irradiation damage in diamond are proposed.

In Chapter X the effects of irradiation damage and subsequent heat treatment in diamonds containing paramagnetic nitrogen are discussed. A comparison is made between the effects observed in specimens containing: no-nitrogen, non-paramagnetic nitrogen and paramagnetic nitrogen. A model is proposed to explain these effects.

Finally some concluding remarks and suggestions for further research are given in Chapter XI.

CHAPTER II.

EXPERIMENTAL METHODS.

2.1. Introduction.

It is convenient to divide the experimental methods used in this study into two groups:

a) Those used to study the physical properties of diamonds containing defect centres.

b) Those employed to create, or change, defect centres in diamond.

A number of well developed experimental methods are available for studying the physical properties of insulating crystals such as diamond. Because of the availability of equipment, the sensitivity of the techniques and the amount of information that can be obtained, the following two methods were used to study the properties of specimens containing defect centres:

1) Optical Absorption (O.A.) methods in the photon energy regions:

   a) Ultra-violet (U.V.) between 3.0 and 5.5 eV.

   b) Visible (VIS) between 1.5 and 3.0 eV.

   c) Infra-red (I.R.) between 0.6 and 1.5 eV.

2) Electron Paramagnetic Resonance (E.P.R.) absorption at an x-band frequency in the vicinity of 9.3 Gc/s.

To introduce and to modify defect centres in diamond the methods employed were:

1) Irradiation damage; using 0.78 MeV electrons.
2) Subsequent heat treatment in the range 100 to 1000°C.
3) Illumination with high intensity monochromatic light.

In addition, some of these methods were used at temperatures below room temperature, and standard x-ray diffraction procedures were used in some cases to determine crystal orientation.

These methods are all described in detail in the literature, e.g. in the volumes edited by Lark-Horovitz and Johnson (1959). The underlying principles will therefore only be discussed in connection with their application to a study of defects in diamond.

2.2. Methods for Studying Defect Centres in Diamond.

2.2.1. Optical Absorption in the U.V. - VIS Region.

The band theory of solids predicts a completely

filled valence band, a forbidden energy gap and an unfilled conduction band at $0^{o}K$ for perfect diamond. The O.A. spectrum in the U.V. - VIS region of perfect diamond at room temperature will therefore only exhibit an intrinsic or fundamental absorption edge at about 5.4 eV, broadened through the influence of lattice vibrations and the presence of excitons, corresponding to electronic transitions from the valence band to the conduction band by optical excitation.

The presence of defect centres in perfect diamond will introduce new electronic levels in the forbidden gap. These additional energy states, corresponding to electrons localized in the vicinity of defect centres differ from the valence or conduction bands of the crystal, since the latter are due to interaction between identical atoms. When an electron is freed from a defect, it can enter the conduction band and the centre becomes ionized. Hence the ground state of a defect centre can be represented by an energy level lower than the bottom of the conduction band. If the density of defects is low, the wavefunctions of similar centres do not overlap and the resulting energy levels in the forbidden gap are discrete.

Electronic transitions between the valence band,

the ground and excited states of defect centres, and the conduction band will be possible by optical excitation. Neglecting thermal vibrations of the crystal, transitions between the ground and excited states of defect centres will result in sharp optical absorption lines. Transitions to the conduction band will give a region of continuous absorption. At higher temperatures, the modes of vibration of the atomic nuclei of solids will affect the transitions. Since the amount of vibrational energy that may be involved has a finite range, the allowed optical frequencies extend over a finite range. Thus O.A. bands of diamond exhibit a line broadening that increases with increasing temperature.

Since each kind of defect gives a particular set of energy levels the O.A. spectrum of diamond can be used to observe different defect centres independently. Because of the difficulty in calculating exactly the energy levels of a defect, it is not possible to identify a defect centre unambiguously from its observed O.A. spectrum.

The relationship between the strength of an O.A. band and the number of centres from which it arises in a solid was derived originally by Smakula (1930). More

recently Dexter (1958) has obtained an expression in the form.

$$N.f_{if} = 8.21 \times 10^{16} \frac{n}{(n^2+2)^2} \int \mu_{if}(E)\, dE. \quad (2.1.)$$

Where

N = Number of centres /cc absorbing through a transition from state i to state f.

f_{if} = Oscillator strength for the transition.

n = Refractive index, being 2.417 for diamond.

$\int \mu_{if}(E)dE$ = Absorption coeficient μ in cm^{-1} measured as a function of the photon energy E in eV and integrated over the absorption band.

If in diamond out of a concentration N of a particular type of defect, only a fraction p is in a state to be observed optically, eqn. (2.1) reduces to

$$N_{f_{if}} P = 3.23 \times 10^{15} \int \mu_{if}(E)\, dE. \quad (2.2)$$

If the concentration of defects varies through the thickness of the diamond as is the case with electron-irradiation induced defects, the general expression is of the form

$$N_{f_{if}} P = 3.23 \times 10^{15} \int_{x=o}^{x=d} \int \mu_{if} (x,E)\, dEdx \quad (2.3)$$

Where d is the extent of the distribution of absorbing centres and, in this case, N is the total number of absorbing defects per cm^2 on the diamond face.

The f-value depends on the overlap of the wave functions of an electron in the initial and final states and is difficult to calculate as the effective electron mass and the internal electric field at the absorbing centre are involved in the theory. The f-value is therefore usually treated as an experimental parameter limiting the sensitivity of O.A. as a means of detecting defect centres. The f-value of many centres in solids are found to lie between 0.1 and 1.0, but may be as low as 0.01.

O.A. spectra can be constructed by representing the absorption coefficient μ in cm^{-1} as a function of photon energy in eV. The μ-values are calculated from the observed transmission of incident light normal to the specimen by using the relationship

$$I = \frac{Im}{Io} = \frac{(1 - r)^2\, e^{-\mu t}}{1 - r^2\, e^{-2\mu t}} \quad (2.4)$$

Where

$\frac{Im}{Io}$ = Measured fractional transmission.

t = Thickness of the specimen in cm.

$r = \left\{\frac{n-1}{n+1}\right\}^2$ The fraction of light reflected at at each surface.

n = Refractive index of diamond.

Values of n for various wavelengths of light were obtained from the data given by Peter (1923).

In order to avoid calculating μt for every value of I, the actual conversion of I to μt was carried out by interpolation between lines of constant wavenumber values on graphs of μt as the abscissa and I as the ordinate. This method provided evaluations of μt to a higher accuracy than that required, the errors being less than the errors in measuring I.

2.2.2. Optical Absorption in the I.R. Region.

In addition to electronic transitions, dealt with in the previous section, the atoms in a solid may change their energy in another way. This is accomplished by the vibrations of the nuclei within the solid. The vibrational energies are quantized so that certain definite vibrational states are allowed in a crystal. The transitions between different vibrational energy levels give rise to near infra-red absorption spectra and are

stimulated, provided there is a change of dipole moment connected with such a transition.

The vibrational transitions may also be induced in another way; by the scattering of light. Under certain conditions, the electric field of incident radiation may induce a dipole moment and energy can be interchanged with a photon. This exchange produces the Raman spectrum, which in its structure resembles the I.R. spectrum, although the two originate from two different processes, namely light scattering and absorption of radiation.

The selection rules governing the transitions associated with I.R. absorption spectra and Raman Spectra may be different. The I.R. selection rules are derived by calculating the matrix element of the dipole moment vector between the two states concerned, whereas the Raman selection rules are derived from the matrix elements of the polarizability.

Because of the crystal symmetry of the perfect diamond lattice (Oh; two carbon atoms per Bravais cell) a factor group analysis predicts only one triply degenerate fundamental frequency, active in Raman scattering, but inactive in I.R. absorption. The calorimetric value of the Debye characteristic temperature of diamond is about 1860°K,

which corresponds to a frequency limit of 1293 cm^{-1}. A strong Raman line is observed at 1332 cm^{-1} (0.165 eV). It is therefore generally accepted that the fundamental optical vibration of diamond is at 0.165 eV and that single phonon absorption of radiation in this region is forbidden for the perfect diamond lattice.

Sutherland et al (1954) found that all diamonds exhibit I.R. absorption. The absorption in the region 0.13 to 0.18 eV is highly specimen dependent, whereas the bands in the region 0.224 to 0.495 eV appear in all specimens and can be regarded as an intrinsic property of perfect diamond.

Lax and Burstein (1955) have shown that the intrinsic I.R. absorption bands in diamond may be due to multiphonon processes. Lattice absorption may be associated with two-phonon processes arising from second-order terms in the electric moment produced by charge deformation. Absorption by three-phonon processes can occur through third order terms in the electric moment.

Subsequently, Smith, Hardy and Mitchell (1962) have analysed the intrinsic I.R. absorption bands of diamond and found that they can be attributed to two-phonon processes in the 0.224 to 0.330 eV region and to

three phonon processes in the region 0.330 to 0.495 eV.

The I.R. absorption bands in the region 0.13 to 0.18 eV occur in the region of the fundamental optical vibrational frequencies of the diamond lattice, in spite of the fact that absorption associated with single-phonon processes is explicitly forbidden by the selection rules associated with the symmetry of the lattice.

Lax and Burnstein (1955) showed that such absorption may be possible when certain types of defect centres are present in the diamond lattice, because they can destroy locally the symmetry of the diamond structure and thereby permit an electromagnetic coupling to the fundamental optical vibrational frequencies.

2.2.3. E.P.R. Absorption.

E.P.R. spectroscopy involves the resonant absorption of electro-magnetic radiation by unpaired electrons in a magnetic field. Before a magnetic field is applied to a system containing unpaired electrons, the energy levels are degenerate in electron spin. Upon application of an external field the degeneracy will be removed and each level will split.

If a free paramagnetic ion with a resultant

angular momentum J is placed in a magnetic field H, the energy levels are given by

$$W = g \beta H M \qquad (2.5)$$

Where

$g = 1 + \frac{J(J+1) + S(S+1) - L(L+1)}{2J(J+1)}$ the Landé factor.

$\beta = \frac{eh}{4\pi mc}$ the Bohr Magneton.

M = Component of the electric angular momentum J along the field acting on the ion.

L = Orbital angular momentum.

S = Spin angular momentum.

If an alternating field of frequency ν is applied at right angles to H, magnetic dipole transitions are produced, according to the selection rule

$$\Delta M = \pm 1 \qquad (2.6)$$

Thus the photons which are resonantly absorbed are those whose energy is equal to the separation between adjacent levels i.e.

$$h\nu = g \beta H \qquad (2.7)$$

The simplest case is that of a single electron whose orbital moment L is zero. Then $g = 2.00229$.

From a classical point of view one can think of the unpaired spins in a magnetic field being oriented parallel or anti-parallel to the applied field H. The anti-parallel orientation corresponding to the higher of the energy levels. The magnetic moment vector processes about the direction of H with a frequency;

$$\nu = \frac{g\beta}{h} H \qquad (2.7)$$

which corresponds to the frequency of radiation required to cause a spin flip between the parallel and anti-parallel orientations, whereby microwave energy is absorbed. If the converse occurs it is termed induced emission. Both transitions have the same "a priori" probability. In a system at thermal equilibrium the lower state has a greater population and a net absorption of energy will occur until the levels are equally populated. If this is to continue the system of spins must be in thermal equilibrium.

Spin-lattice relaxation is one mechanism by which thermal equilibrium can be re-established. Coupling between the lattice and the spin system results in the

spins losing energy to the lattice and the restoration of the thermal equilibrium. If this coupling is weak, the system has a long spin-lattice relaxation time, and sufficient microwave power can be introduced to saturate the E.P.R. signal.

In addition to the external magnetic field, an unpaired electron may be associated with a nucleus possessing a magnetic moment, which produces an internal field. This will cause a splitting of the simple energy levels, known as hyperfine splitting, depending on the nuclear spin. A nucleus of spin I will cause hyperfine splitting into (2I+1) component levels.

The simple picture of free unpaired electrons in a solid, even including hyperfine interaction, can be further complicated by many interactions such as those of the orbital motion and spin with each other, with the applied magnetic field, and with magnetic moments of nearby nuclei. There are also electrostatic and covalent interactions with the crystalline environment. Generally the theoretical description of a paramagnetic entity is so complex that a complete solution for the energy levels and wave functions is impractical. Commonly, the interpretation of E.P.R. phonomena are limited to a set of

low-lying energy levels whose magnetic behaviour is described by an expression known as the "spin-Hamiltonian."

The concept of the spin-Hamiltonian was introduced by Pryce (1950) and the theory was further developed by Abragam and Pryce (1951). The spin-Hamiltonian is a polynomial in $\underline{S}$, the effective electron spin, where $2S + 1$ is the number of levels whose properties are being described. It also contains terms describing the interactions of nuclear spins $\underline{I}$, and yields the energy levels, transitions between which give rise to the E.P.R. spectrum, as the eigen values of:

$$\mathcal{H} = \underline{H}\cdot\underline{g}\cdot\underline{S} + \underline{S}\cdot\underline{D}\cdot\underline{S} + \underline{S}\cdot\underline{A}\cdot\underline{I} + \underline{I}\cdot\underline{Q}'\cdot\underline{I} - \gamma\beta_n \underline{H}\cdot\underline{I} - \beta_n \underline{H}\cdot\underline{R}\cdot\underline{I} \qquad (2.9)$$

Where

β = Bohr magneton.

β_n = Nuclear magneton.

γ = Nuclear gyromagnetic ratio.

In general the other quantities are tensors whose values may be determined experimentally. The first term in eqn (2.9) describes the Zeeman splitting of the lowest energy levels, whilst the second describes the zero

field splitting produced by crystalline field or spin-spin interactions. The remaining four terms describe nuclear interactions, the first of these being the magnetic hyperfine interaction; the second the quadrupolar interaction, and the last two the direct interaction between the nucleus and the magnetic field.

Perfect diamond is intrinsically diamagnetic and will exhibit no E.P.R. absorption. The presence of defect centres may, however, provide a paramagnetic system and hence E.P.R. absorption can be used as a very sensitive method for detecting the presence of certain defects. The type of defects expected to give rise to E.P.R. are twofold:

a) Damaged lattice sites involving electrons localized in broken bonds. In this case nuclear interactions can be neglected because $I_{12_C} = 0$. ($I_{13_C} = \frac{1}{2}$, but this isotope is only 1.11% abundant). For a spectrum exhibiting axial symmetry the spin-Hamiltonian will then reduce to

$$\mathcal{H} = g_{\parallel} \beta H_z S_z + \beta g_{\perp} (H_x S_x + Hy\ Sy) + DS_z^2 \qquad (2.10)$$

The term D represents the presence of initial splitting of the electronic levels due to second order effects of the crystalline field. $g_{||}$ and $g_{\perp}$ are the principal values of the g tensor.

b) Substitutional impurity atoms such as those of the Group III and V elements, will give rise to unpaired electrons in bonding with carbon (Gr.IV) atoms. As most of these impurity atoms have nuclear spin, nuclear interactions with the unpaired electrons are very important and may yield important information from which the impurity atoms may be identified.

2.3. Methods for Producing or Changing Defect Centres in Diamond.

2.3.1. Irradiation Damage.

Irradiation damage is one way in which defects may be introduced in a controlled way into solids and has been studied extensively in the last twenty years. Comprehensive review articles e.g. by Kinchin and Pease (1955) and Seitz and Koehler (1956) are available. Only

a brief discussion of the underlying principles of the production of defects in diamond by irradiation damage will therefore be given here.

When high energy charged particles pass through a solid, they can lose energy in two ways. They can excite the orbital electrons of an atom and thus cause partial or complete ionization, or they can interact with the atomic nuclei in the solid. The latter process, known as Coulomb interaction or Rutherford scattering, involves scattering of the incident particle by the Coulomb field. In this process energy and momentum, dependent on the angle of scatter, are given to the nucleus. Seitz (1949) estimated that only about 0.1% of the energy is lost in nuclear interactions.

In non-ionic solids, it is only by Coulomb interaction that sufficient energy can be transferred to an atom to displace it from its normal lattice site, thus producing a vacant atomic site (vacancy) and an interstitial atom (interstitial). The minimum energy which must be given to an atom to displace it from a lattice site when all the neighbouring atoms remain in their original positions, is known as the displacement energy Ed. Calculation of the values of Ed in solids is difficult and

Ed is therefore usually determined experimentally. From energies of sublimation Seitz (1949) estimated Ed to be about 25 eV for most solids. This agrees with experimentally determined values for many solids.

If the energy of a displaced atom in a solid, or primary recoil as it is termed, is greater than Ed, the primary itself may cause further displacements. These so-called secondaries may cause further atomic displacements and a displacement cascade may continue until the displaced atoms have insufficient energy to displace any more atoms.

A consequence of irradiation damage in solids is energy transfer to lattice vibrations. This may occur either from the excitation of electrons, which subsequently give up their energy to lattice vibrations, or by direct excitation of lattice vibrations in non-displacement collisions. In some cases this can lead to high temperature regions of the order of $1000^{o}K$, involving thousands of atoms over a duration of 10^{-10} to 10^{-11} seconds. Such regions, known as "thermal-spikes" (Seitz 1949), may remain as disordered regions in a crystal on cooling.

The ordered arrangement of atoms in a crystal lattice may affect energy transfer in irradiation damage processes. Silsbee (1957) suggested that energy could be

transferred over up to 150 atomic distances by successive collisions along lines of closely packed atoms, in what is termed "focussing collisions." Thompson et al (1956) considered a similar mode of energy transfer, the so-called "dynamic crowdion." In an open structure like the diamond lattice, however, focussing of this type is not regarded as very likely.

Effects of irradiation damage on diamond were reported 50 years ago. Crookes (1909) was one of the earliest investigators to notice that colour changes were produced in diamonds by radium radiation. Cork (1942) obtained a blue surface colouration in a diamond, as a result of 10 MeV deutron bombardment. Similar effects were obtained by Dugdale (1953) who used electrons of energy up to 3 MeV. Pough and Rogers (1947) showed that diamonds were not affected by x-ray irradiation.

More recently, detailed studies of irradiation damage effects in diamond were undertaken, mainly by the Reading group (e.g. Clark et al 1956 a & b, Clark et al 1961 and Duncan 1963). Since the optical absorption induced in diamond by various forms of irradiation is similar in many respects and because there exists a minimum energy below which no absorption can be produced, it is

now generally accepted that the induced absorption arises from electronic excitation in carbon interstitials, or in the atoms surrounding a vacancy, or in complexes of these defects.

Atomic displacements may be produced in diamond by the following methods:

a) Neutron Irradiation, whereby neutrons from an atomic pile lose energy only by hard sphere collisions with carbon nuclei. The probability of such collisions is low but when collisions do occur the recoil carbon atom receives high energy and creates a number of secondary displacements. The rate of energy loss of the recoil atom is such that initially secondary displacements are separated by several atomic diameters, but when the atom has lost a large fraction of its energy, secondary displacements are separated by less than the interatomic spacing of carbon atoms in diamond. In such a region all existing order is destroyed, and this method is therefore not attractive for producing isolated point defects.

b) Gamma Irradiation, whereby gamma rays dissipate their energy by electron-positron pair production, Compton scattering and photo-ionization. For gamma rays from ^{60}Co (1.17 and 1.33 MeV) Compton electrons are the

main agents in defect production. The disadvantage of using gamma-rays for producing lattice displacements in diamond is that the time involved in producing a reasonable amount of defects ($\pm$ 10^{17}/cc) is of the order of months.

c) Electron Irradiation, where relativistic electrons with energy higher than 0.3 MeV possess sufficient energy to displace carbon atoms from their lattice positions by elastic collisions. This provides a very useful method for producing single defects and was used in this study. The maximum recoil energy transferred by a relativistic electron to an atom in an elastic collision is given by

$$Em = \frac{4Ei}{Mc^2} \left(\frac{Ei}{2} + m_o c^2 \right) \qquad (2.11)$$

Where

Ei = Incident electron energy.

M = Mass of the struck atom.

When an electron is scattered through an angle θ, the recoil energy of the struck atom is given by

$$Ep = Em \sin^2 (\theta /2) \qquad (2.12)$$

There is a minimum electron scattering angle θd, below which the energy transferred to the target atom is insufficient to cause a displacement. This is given by

$$Ed = Em \sin^2(\theta_d/2) \qquad (2.13)$$

The number of primary displacements, N_P, when diamond is irradiated by relativistic electrons, is given by

$$N_P = \sigma_P \, Ni \, Na \qquad (2.14)$$

Ni = Incident dose ($\bar{e}/cm^2$)

Na = Concentration of carbon atoms.

σ_P = Total cross section for primary displacements.

The total cross section for primary displacements was evaluated by Seitz and Koehler (1956) in the form

$$\sigma_P = \int_{\theta_d}^{\pi} d\phi \; (\theta) \, 2\pi \sin\theta d\theta \qquad (2.15)$$

Where $d\phi(\theta)$ is the expression for the differential Coulomb scattering cross section of relativistic electrons by atomic nuclei derived by McKinley and Feshback (1948)

in the form

$$d\phi(\theta) = \frac{Z^2 e^4}{4m_o^2 c^4} \left(\frac{1-\beta^2}{\beta^4}\right) \text{cosec}^4 \theta/2 \left[1-\beta^2 \sin^2 \theta/2 + \pi\alpha\beta \sin \theta/2 \,(1-\sin \theta/2)\right] \qquad (2.16)$$

This is accurate to terms in α^2, where:

$$\alpha = \frac{Z}{137} = 0.044 \text{ for carbon.}$$

$$\beta = V/c.$$

By inserting this value for $d\phi(\theta)$ in eqn. (2.15), substituting Ep/Em from eqn. (2.12) and integrating between the limits Ed and Em, the expression for the total cross section for primary displacements is obtained as

$$\sigma_p = \frac{\pi Z^2 e^4 (1-\beta^2)}{m_o^2 c^4 \beta^4} \left\{ \left(\frac{Em}{Ed} - 1\right) + 2\pi\alpha\beta \left[\left(\frac{Em}{Ed}\right)^{\frac{1}{2}} - 1\right] - (\beta^2 + \pi\alpha\beta) \ln \frac{Em}{Ed} \right\} \qquad (2.17)$$

This treatment does not take into account secondary displacements. In this study on defects in diamond care was taken to choose electron irradiation conditions in such a way that secondary displacements will not be

involved. The theory also applies for mono-energetic electrons only, and hence a correction must be applied for the energy loss occurring by electron interaction within a diamond.

Clark et al (1961) derived such a correction for the energy loss by assuming that the range of an electron of given energy in diamond is the same as that reported for aluminium by Glendenin (1948) if the higher density of diamond is corrected for. By using the treatment outlined above they obtained theoretical curves for the energy dependence of the rate of production of vacancy/interstitial pairs in diamond by assuming values for Ed. These were compared with the experimental results for the rates of production of optical absorption (a physical property of diamond that is sensitive to the number of defects present). Their results which were taken as a guide for point defect production in diamond in this study, can be summarized as follows:

1) X-rays or electrons of energy less than 0.3 MeV produce no O.A. bands.
2) O.A. bands at 2.0 eV and 4.0 eV are produced linearly with the dose in all diamonds by electrons of energy 0.3 to 0.8 MeV, and are primary products of the damage process.

3) Electrons of energy greater than 0.8 MeV produce, in addition, O.A., most easily observed at 2.696 eV, which is also very marked after neutron irradiation. 0.8 MeV therefore appears to be the threshold for multiple defect production.

4) Ed $\approx$ 80 eV for single defect production.

2.3.2. Annealing of Irradiation Damage by Heat Treatment.

This implies the movement of irradiation induced defects in a solid, whereby the defect centres undergo such changes that they no longer exist in the same atomic configuration. Motion of defects in a solid can take place as a result of the thermal vibrations of all the atoms and will depend on the thermal energy E of the defect.

The probability of a lattice atom or defect having a thermal energy E is proportional to the Boltzman factor

$$e^{-E/kT}$$

Where T is the absolute temperature.

If E_i is the depth of the potential well in which a defect

is held, then the frequency Γ with which it jumps into a next lattice site is given by

$$\Gamma = \nu_o \, e^{-E_i/kT} \qquad (2.18)$$

Where ν_o is the vibrational frequency of the defect in its potential well and is usually of the order of 10^{13} per second (Seitz 1940).

The simplest type of annealing of irradiation damage is the mutual annihilation of interstitials and vacancies. This process usually proceeds by jumps of one defect (mostly the interstitial; Lomer and Cottrell 1955) towards the other. At high temperatures, however, the mobile interstitials or vacancies may be trapped by other defects.

Very little is known about the annealing of irradiation damage in diamond. The effects appear to be highly specimen dependent and probably involve combination with other defects. This will be fully discussed at a later stage.

2.3.3. Thermal Ionization of Defect Centres.

This process involves the transfer of electrons

by thermal activation between defect centres, or between defect centres and the host lattice. Such thermally-activated changes in the state of charge of defect centres influence optical and E.P.R. absorption measurements, although the atomic configuration of the defect remains unaltered.

In the band picture of solids, the defects generally produced by irradiation damage in diamond give rise to ground states in the forbidden gap. Transitions between occupied ground states and excited states give rise to optical absorption. Electrons may be thermally excited from ground states into the conduction band where they are free to move through the crystal and can then be trapped by empty acceptor states. This is one mechanism by which so-called "thermal-bleaching" can result. In this case the effective activation energy is the thermal energy gap between the ground state level of the defect centre and the conduction band. Because of relaxation of the atoms around the defect during the ionization process, this energy is expected to be less than the energy for optical bleaching of the centre.

On the other hand, thermal-activation of an electron from the valence band to the ground state of a

defect centre may occur under favourable circumstances. The positive hole so generated is free to move through the crystal and may be trapped by donor centres. In such a process the rate of thermal excitation to a defect ground state, R, will be given by

$$R = Nv\ Se\ v\ (G-g)\ e^{-E/kT} \qquad (2.19)$$

Where

v = Thermal velocity, assumed to be the same for electrons in the conduction band and holes in the valence band, and given by $\frac{1}{2}\ mv^2 = 3/2\ kT$.

Se = Capture cross-section of empty states for electrons.

G = Density of states.

g = Density of occupied states.

E = Activation energy of the process.

Heat treatment of irradiated diamonds in order to anneal irradiation damage may simultaneously affect thermal ionization of the defects. Care was therefore taken to assess the contribution of each of these possible effects of heat treatment.

2.3.4. Illumination with High Intensity Monochromatic Light.

The state of charge of defect centres may be altered permanently by illumination with light of certain energies. Most commonly this results in optical bleaching by which an electron is excited from the ground state of one defect centre to the conduction band and then trapped by another defect centre. This effect will depend on the occupancy and capture cross sections of the defect states involved. A quantitative treatment of the processes involved has been given by Bube (1960).

This method has, in the present study, proved useful in obtaining the positions of defect levels in the forbidden gap.

2.4. Discussion.

The methods described above for studying defect centres in diamond have proved useful but in most instances the defect centres could not be identified from these observations alone. The methods used to produce defects, or to alter existing defects, provided valuable additional information, with the result that in some cases a reasonable model could be proposed for a defect centre.

It must be emphasized that the methods employed are not the only ones available. Many other techniques can also be applied to a study of defect centres in diamond, and by taking all the evidence into account, one usually obtains the best understanding of the nature of a specific defect centre. Two such additional experimental methods are:

1) Excitation and luminescence spectra. This method was studied in some detail by Matthews (1956) and Maycraft (1960).

2) Photoconduction in normally insulating diamonds, which was studied by Vermeulen (1965).

The results of these authors, as well as some additional crude observations made in the course of this study, will be discussed in appropriate sections later on.

CHAPTER III.

APPARATUS.

3.1. Introduction.

The apparatus used to carry out the experimental methods described in Chapter II can also best be described in two sections; that for studying diamonds containing defects, and that used for producing or modifying defect centres in diamond. As the aim of this study was to make a large number of measurements on as many diamond samples as possible, rather than to apply a specific technique to the study of diamond, apparatus known to work satisfactorily was used as far as possible and no special equipment was developed.

3.2. Apparatus for Studying Diamonds Containing Defects.

3.2.1. Optical Absorption in the U.V.-VIS Region.

Absorption spectra were constructed from transmission values at various wavelengths of the incident light as described in Chapter II. The transmission values in the U.V.-VIS region were measured with a Unicam S.P.

700 recording double beam spectrophotometer, covering the spectral range 0.6 eV to 6.0 eV.

A tungsten filament lamp is used in the visible and near infra-red region and a hydrogen arc for the ultra-violet region, the change-over point being at 30 kc/cm. The beam of monochromatic light in the instrument is divided into two parts, which are chopped at 300 c/s, passed alternatively through the reference and sample compartments at 25 c/s, and then recombined on a single radiation detector producing a signal. This is then amplified and switched, synchronously with the alternation of the beams through the compartments, between two output channels; thus producing a sample and a reference spectrum. Two detectors are used; a photomultipher for the U.V. and VIS regions and a lead sulphide detector for the near I.R. region, the change-over point being at 13 kc/cm. The sample and reference compartments were adopted with 1 mm slits to accommodate small diamond specimens.

In order not to deflect the beam of the spectrophotometer from the detector, the diamond specimens used had to be provided with two opposed flat faces, parallel to each other to within better than 1° of arc. This was accomplished by a special technique developed by the

Diamond Research Laboratory.

The wavelength settings on the instrument were regularly checked against the 6563A, 4861A and 4341A hydrogen emission lines. The particular instrument available did not give reproducible transmission values over long periods of time. A reference transmission curve was therefore superimposed on every sample curve. Obtaining transmission values relative to these reference curves, provided reproducibility to within 1% at all wavelength settings over long periods of time.

In order to carry out transmission measurements at temperatures below room temperature, a cryostat was constructed to fit the sample compartment of the instrument. The design was essentially that of Wedepohl (1963) and is illustrated in Figure 3.1.

3.2.2. Optical Absorption in the I.R. Region.

Transmission values in the I.R. region were obtained with a Unicam S.P. 200 recording double beam spectrophotometer, covering the spectral range of 0.1 eV to 0.6 eV. Radiation is provided by a Nerst filament, this is switched between sample and reference at 10 c/s and detected with a Golay Cell. Specimen preparation was the

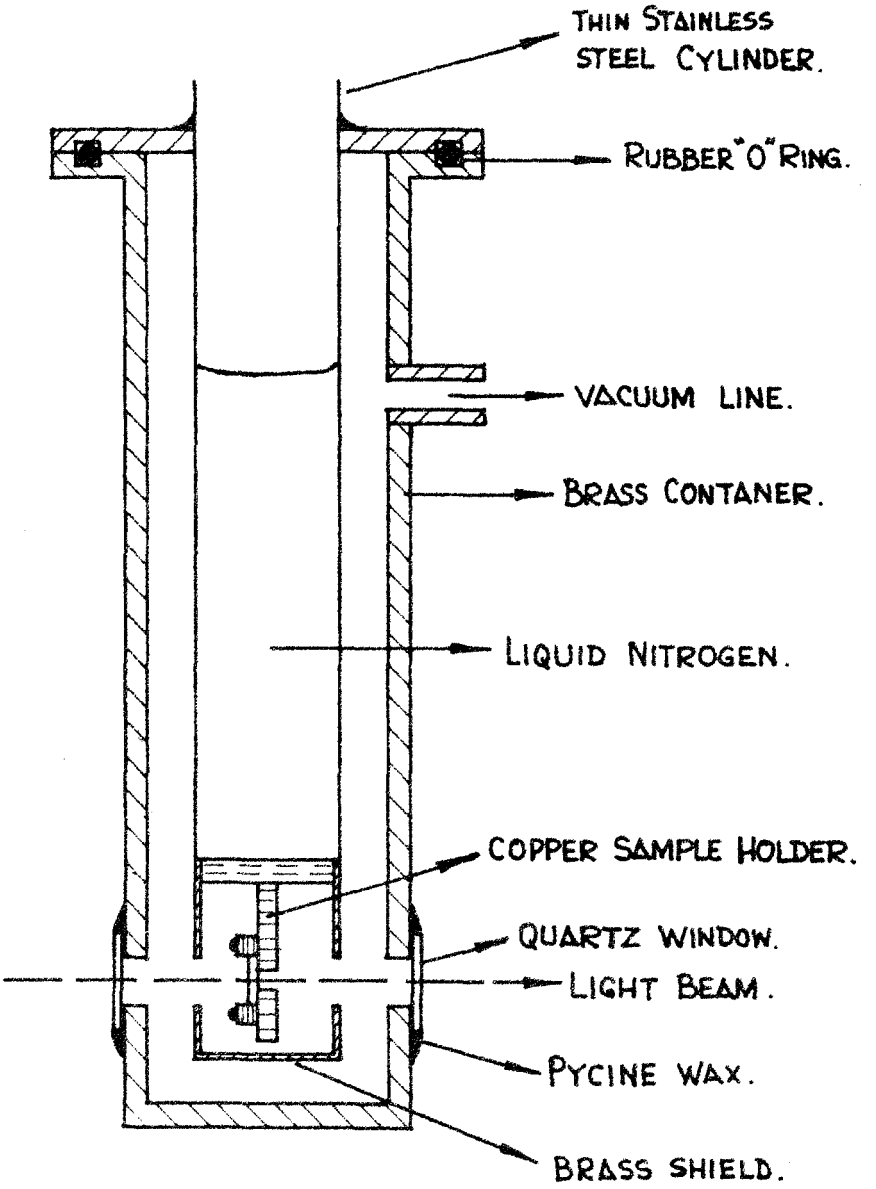

FIGURE 2.1 SCHEMATIC ILLUSTRATION OF THE OPTICAL CRYOSTAT.

same as for the U.V.-VIS region, and rock salt beam condensers were used to improve the intensity of light through the small windows on the specimens.

The wavelength settings of the instrument were checked against the known absorption lines in the polystyrene spectrum. The same procedure as for the U.V.-VIS region was adopted to ensure reproducible transmission values.

3.3.3. E.P.R. Measurements.

The E.P.R. spectrometer used was of conventional design, operating at an X-band microwave frequency in the vicinity of 9.3 Gc/s, with 100 Kc/s field modulation. The arrangement of the components in the form of a block-diagram is illustrated by Figure 3.2, which is self-explanatory.

Microwave frequency stabilisation was effected by locking the klystron frequency to the reference cavity with an automatic frequency control unit, which monitored the reflector voltage of the klystron. The sample cavity used was a reflection TE_{102} rectangular cavity, equipped with a small copper wire coil inside, to provide 100 Kc/s modulation of the d.c. magnetic field at the sample

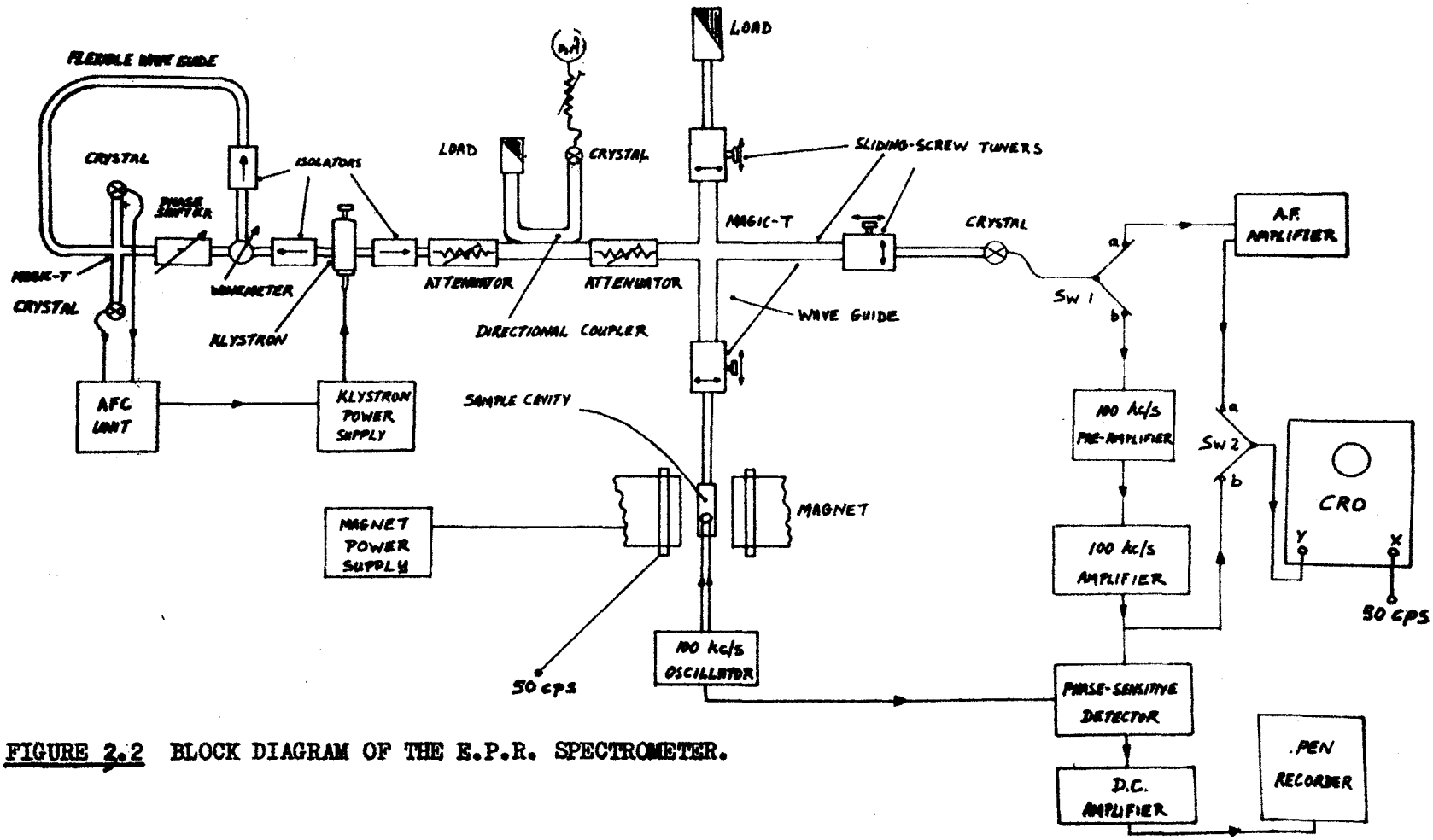

FIGURE 2.2 BLOCK DIAGRAM OF THE E.P.R. SPECTROMETER.

position. The electromagnet providing the d.c. magnetic field was operated by a 50 volt, 10 amp, voltage stabilized solid state power supply manufactured by Grundy and Partners. A good quality Helipot potentiometer was built into this, and the magnetic field was swept by driving this potentiometer with a synchronous electric motor through a variable gearbox.

A relative magnetic field calibration was obtained by scanning the known spectrum of substitutional nitrogen in diamond (Smith et al 1959a), with a fixed recorder chart speed, and various gear ratios for driving the power supply. The magnetic field sweeps so obtained were linear and reproducible. From the known separation between the lines of the nitrogen spectrum, each sweep rate could be calibrated as scanning a known number of oersteds per cm of recorder chart. Magnetic field spacings within about 100 Oe of $g = 2$ could hereby be measured to an accuracy of about 2%. No absolute calibration of the magnetic field strength was attempted.

The g-values of the systems studied were compared with the known values for Diphenylpicrylhydrazine (DPPH) and substitutional nitrogen in diamond, by simultaneously placing small amounts of these and the

specimens studied in the sample cavity. The sensitivity of the spectrometer was evaluated by detecting various amounts of a diluted sample of DPPH having a known amount of free spins. It is estimated that about (10^{13}. ΔH) free spins could be detected with the instrument; ΔH being the line width measured between the maximum and the minimum of the first derivative spectrum in oersted.

Normally no sample preparation was required, the specimens were inserted in the cavity in such a position that they were in the maximum r.f. magnetic field and minimum r.f. electric field. When specific crystal directions were required, the required orientations were obtained using standard back reflection x-ray diffraction techniques. Small facets were then polished on the specimens normal to these directions, and they were then fixed with one of these facets flush to a flat piece of quartz which could be aligned normal to the direction of the d.c. magnetic field.

3.3. Apparatus for Producing or Modifying Defect Centres.

3.3.1. Electron Irradiation.

A 2 MeV electron accelerator, developed for the

Diamond Research Laboratory by N.V. Philips, was used. This instrument was described in detail by Henneberke (1960). Briefly, the accelerator is of the cascade type incorporated in a tank with 10 atmospheres of nitrogen pressure. Electrons are emitted by a tungsten filament and accelerated down a 14 stage evacuated accelerating tube which is supplied by a 7 stage Cockcroft-Walton generator with selenium rectifying units.

The accelerating voltage is measured with a rotating voltmeter. The meter was calibrated by Horszowski (1963) with a stacked foil current measurement technique. The beam current density was measured by collecting all the electron beam which passed through a collimator of known area in a Faraday cage.

The specimens were held by Wood's metal in a recess in the top of a copper cold finger which was mounted in an evacuated container under the thin metal window of the accelerating tube, and was cooled by water or a solid-CO_2 and acetone mixture.

3.3.2. Heat Treatment.

Heat treatment of the specimens was carried out in two stages. Between 100°C and 500°C the specimens were

heated in air in a small copper cup containing a chromel-alumel thermocouple, which was inserted in a Wild and Barfield tube furnace. Because of the small size of the specimens and the copper cup, furnace temperature was attained very rapidly by the specimen. Since the furnace had a large thermal capacity, it was possible to control the temperature very accurately. After completion of a heat treatment the diamonds were dropped onto a water-cooled copper block where, because of their high thermal conductivity, they cooled very rapidly to room temperature.

Since diamonds are attacked by air above 500°C, heat treatment in the range 500°C to 1000°C was carried out in vacuo. The apparatus used was similar to that described by Clark (1955). It consists of a small furnace mounted in an evacuated bell-jar. Provision was made for dropping the specimens, with a magnetically operated release mechanism, onto a thermocouple junction, after the selected furnace temperature was obtained. Because of the low thermal capacity of the furnace the temperature fell between 10°C and 20°C on entry of the specimens and took 3 to 5 minutes to recover its original value. At the end of the heating time the furnace current was switched off, and after about 5 minutes when the

temperature was below 500°C, air was allowed into the system, and the specimens removed. In this temperature range the shortest heating time was 4 hours, so that the errors introduced by warming up to the desired temperature, and cooling to room temperature, was small.

3.3.3. Illumination.

The diamond specimens were illuminated with light from a quartz envelope high pressure mercury lamp. The light was focused onto the specimens using a quartz lens. When light of specific wavelengths were required, a Hilger quartz monochromator was used to select the particular emission line. By mounting the specimens in the cryostat described in § 3.2.1. illumination could be effected at temperatures below room temperature.

CHAPTER IV.

SURVEY OF NATURAL DIAMOND.

4.1. Introduction.

In all about 250 diamonds were selected for detailed study from about 10,000 individual stones, which were themselves surveyed for the more obvious visual characteristics such as colour, morphology etc. This large number of stones comprised a cross-section of production from all major sources of natural diamond, and the final selection of 250 for detailed work was done as far as possible to yield a sample which was representative of all the batches surveyed.

The specimens were studied using the O.A., I.R. and E.P.R. absorption techniques described in Chapter II. Perfect diamond without defect centres in detectable amounts should only exhibit the following absorption features:

1) The fundamental absorption edge at about 5.4 eV in O.A. in the U.V. region. No absorption bands in the VIS. region.
2) I.R. bands between 0.224 eV and 0.495

eV associated with two and three phonon processes.

3) No E.P.R. absorption.

No such perfect diamonds were found in this survey. All the specimens investigated exhibited additional absorption which can only be attributed to the presence of defects. The defect centres encountered do not always reveal themselves in I.R. or E.P.R. absorption; however, all exhibit characteristic C.A. systems in the U.V.-VIS region. Where the nature of the defect centres was not known, they were therefore labelled according to their characteristic absorption in the U.V.-VIS region.

Altogether eleven different defect centres were found, and they are therefore labelled:

1) Non-Paramagnetic Nitrogen.
2) 4150A-Centres.
3) Paramagnetic Nitrogen.
4) Graphitic Regions.
5) Acceptor Centres.
6) G.R.1-Centres.
7) 5032A-Centres.
8) Pink Centres.
9) Mauve Centres.

10) 4800A-Centres.

11) Amber Centres.

In this chapter the absorption systems produced by these defect centres are described individually. A discussion of the nature of these centres is added, however, it must be stressed that at this stage the emphasis is to catalogue the defects occurring in natural diamond, and that a detailed discussion of the nature of some of these centres is presented in the following chapters.

4.2. Non-Paramagnetic Nitrogen.

4.2.1. Existing Knowledge.

Sutherland et al (1954) reported an I.R. band system, the so-called A-bands, characterised by a strong band at 0.159 eV. The O.A. in the U.V.-VIS. of these A-centres was described in detail by Clark et al (1956 a). The characteristic feature is an absorption edge, the so-called secondary absorption edge, starting at 3.7 eV and extending to the fundamental absorption edge at 5.4 eV. No E.P.R. absorption associated with A-centres was reported in the literature.

Kaiser and Bond (1959) found nitrogen, generally

in a concentration of about 10^{20} atoms/cc, as an impurity in most diamonds. A linear correlation was demonstrated between the nitrogen concentration and the A-centre optical absorption features. From lattice dilation and density measurements, Kaiser and Bond concluded that the nitrogen atoms are present in substitutional solid solution.

Smith et al (1959 a) detected an E.P.R. spectrum in certain diamonds, which could be interpreted as arising from the presence of isolated substitutional nitrogen atoms in the diamond lattice. The amount of paramagnetic nitrogen present in the specimens, as estimated from the E.P.R. absorption, was between 10^{15} and 10^{17} atoms/cc. Smith et al therefore concluded that most of the nitrogen found by Kaiser and Bond must be present in a non-paramagnetic form.

It was not clear whether the secondary absorption edge is due entirely to non-paramagnetic nitrogen; nor was it known what effect the presence of paramagnetic nitrogen has on the optical properties of diamond.

The apparent absence of E.P.R. absorption, and the strong I.R. band at 0.159 eV, associated with these nitrogen centres, was discussed by Elliot (1960). He

proposed that the substitutional nitrogen atoms are located in a double nitrogen layer of the N-C-N type; thus effecting a non-paramagnetic configuration where intervening carbon atoms are surrounded by a tetrahedron of nitrogen atoms, with two extra electrons shared between the four bonds. As an alternative Elliot suggested a N-C-C-N layer arrangement, where extra electrons are confined to particular bonds. The possibility of pairs of nitrogen atoms, in the form of N_2-molecules, was ruled out by the requirement of considerable charge transfer, (defect either charged or a dipole) to account for the strong I.R. absorption with maximum at 0.159 eV.

This proposal of Elliot was supported by Evans and Phaal (1962), who observed platelets segregated in (100) planes in diamonds exhibiting the A-centre O.A. features, by transmission electron microscopy. Nitrogen is the only impurity found in a high enough concentration (10^{20} atoms/cc) to account for the observed platelet size and density. Small dislocation loops were found on (111) planes near the nitrogen platelets and were attributed to the condensation of vacancies following the formation of the platelets.

The nature of these nitrogen platelets was

further investigated by James and Evans (1965), who computed profiles for the electron microscope images of the platelets. By using the method described by Ashby and Brown (1963 a & b), estimates were obtained of the lattice displacements on either side of the platelets. Thus James and Evans suggested that the platelets contain a varying number of nitrogen-rich planes and that each impurity plane produces a lattice displacement of approximately 1/6 a, where a is the (400) interplaning spacing. The diamond lattice on either side of the platelets is therefore in compression and some strain could actually be detected in the plane of the platelets.

Tagaki and Lang (1964) demonstrated a general proportionality between the strength of the secondary absorption edge and the anamolous "spike" x-ray reflections, (commonly found in diamond Frank 1956) point-by-point in several stones. Further evidence on the nature of nitrogen platelets was obtained when Frank (1964) reported that an error, by a factor of 4 in the lattice displacement was contained in his 1956 interpretation of the x-ray diffraction spikes. These incorrect values of Frank (1956) were used by Elliot (1960) in his model for the nitrogen platelets.

Following Frank's correction Lang (1964) proposed a platelet structure with six carbon and four nitrogen atoms per unit cell, which produce, with standard bond lengths, an expansion normal to the platelet of 1.18A, in accord with the evidence from the x-ray diffraction spikes. This is illustrated in Figure 4.1. Such a structure produces no density change in agreement with observations of Mykolajewycz et al (1964).

Lang's model, however, does not seem to be able to account for the strong infra-red A-bands which characterizes non-paramagnetic nitrogen; it thus appears that while the general concept of nitrogen segregated into a platelet configuration is well established, the precise arrangement of the atoms in the platelet remains speculative.

4.2.2. Results of this Survey.

About 98% of all the diamonds investigated exhibited the optical absorption features shown to be characteristic of non-paramagnetic nitrogen in platelet form. The nitrogen concentration, estimated from the optical absorption features as described by Kaiser and Bond (1959) was found to be between 3×10^{19} and 10^{20} atoms/cc.

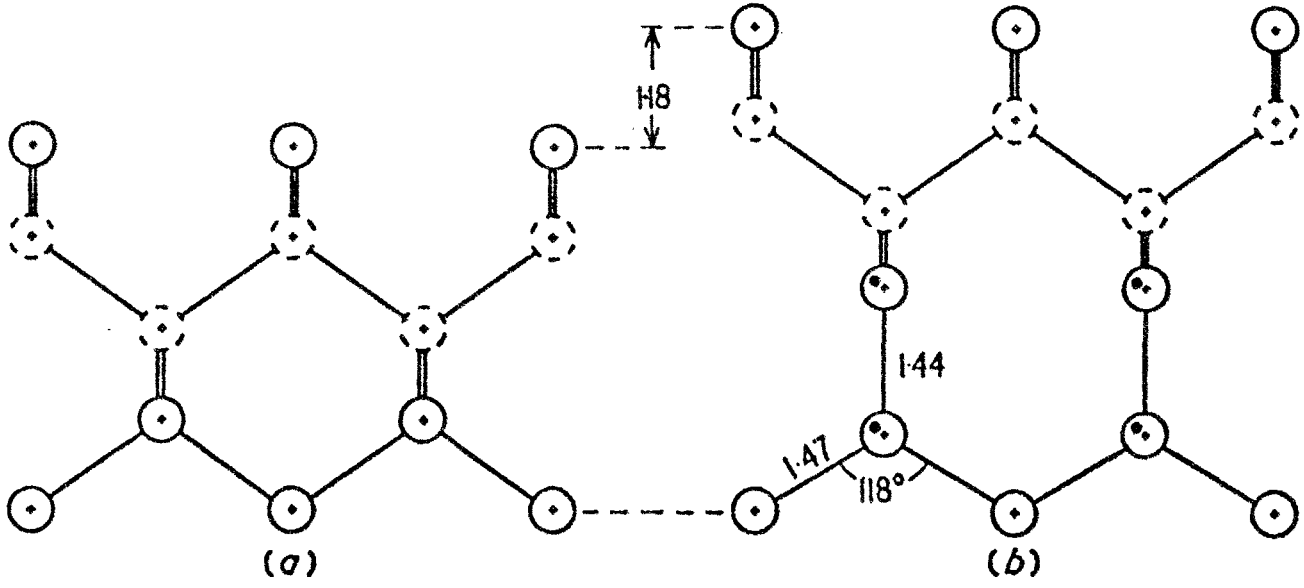

Figure 1. Sections on (110) of unit cells of (*a*) normal diamond and (*b*) platelet structure in a platelet layer parallel to (001). Full circles, C in plane of section; broken circles, C at $a_0/2\sqrt{2}$ above or below plane of section; circles with dot, N in plane of section.

FIGURE 4.1 MODEL FOR NON-PARAMAGNETIC SUBSTITUTIONAL NITROGEN PLATELETS IN DIAMOND. REPRODUCED FROM LANG (1964).

As rare exceptions, some specimens were found which contained only about 10^{18} non-paramagnetic atoms/cc. All these specimens exhibited in addition to the non-paramagnetic nitrogen absorption system an absorption system associated with the so-called 4150A-centres, which are discussed in the next section.

A small group - possibly 0.5% of all the diamonds exhibit only the absorption features arising from non-paramagnetic nitrogen. The 4150A-centres, if present, are below the threshold of detection by optical absorption methods. No E.P.R. absorption could be detected in these specimens, although some of the larger specimens ($\pm$ 0.5 cc) contained as much as 3×10^{20} non-paramagnetic nitrogen atoms/cc and about 10^{13} free spins could be detected by the instrument.

4.2.3. Discussion.

It appears evident that the A-centre optical absorption features are due entirely to non-paramagnetic nitrogen in platelets. Subsequently it will be shown that paramagnetic nitrogen, presumably nitrogen in a dispersed, substitutional form in the diamond lattice, give rise to completely different and hitherto unknown

optical absorption features which will be discussed in a later section.

The evidence suggests that 98% of all diamonds grew in a nitrogen rich environment. Nitrogen was incorporated in the diamond lattice in substitutional positions and probably by a vacancy mechanism migrated to form platelets. The vacancies then condensed into small dislocation loops.

It appears that the nitrogen platelets give rise to a level in the forbidden gap at about 3.7 eV below the conduction band. Transitions from this level to the conduction band may then explain the secondary absorption edge, stretching from 3.7 eV to 5.4 eV, in U.V. absorption.

This picture has support from Vermeulen (1965) who found a photoconduction peak at 4 eV which could be qualitatively correlated with the secondary absorption edge. The low energy limit of a photoconduction peak defines the energy of the level (Bube 1960) so that this peak may very well be associated with the transition of electrons from a level 3.7 eV below the conduction band.

The I.R. absorption system associated with the nitrogen platelets may conceivably arise from the creation

of a dipole moment which provides coupling between the normal lattice modes and the incident electro-magnetic radiation as suggested by Elliot (1960) and Smith and Hardy (1961).

4.3. 4150A-Centres.

4.3.1. Existing Knowledge.

In addition to the A-bands, Sutherland et al (1954) observed another common I.R. absorption system in diamond; the so-called "B-bands". The main features of this system are a strong band at 0.145 eV and a weaker sharp band at 0.165 eV. They reported that the B-bands correlated with the so-called 4150A O.A. system in the VIS. region. The 4150A system has been described in detail by Clark et al (1956 a). It is characterized by a set of absorption lines which consists of a sharp principal line of lowest energy at 2.99 eV (4150A) and a number of successively more diffuse ancillary lines at higher energies.

Dyer and Matthews (1957) examined the fluoresence spectrum associated with the 4150A system. The spectrum consists of a principal sharp line of highest

energy at 2.99 eV and a number of more diffuse lines at lower energies; i.e. the mirror image of the absorption system. The excitation spectrum of this fluoresence system followed the shape of the 4150A - absorption curve very closely.

Raal (1959) found another O.A. system, the so-called 2360A system, which appeared to be associated with 4150A - centres. This system consists of three O.A. bands between 5.2 eV and 5.4 eV; the strongest band being at 5.25 eV (2360A).

Recently Holland and Raal (1964) have investigated the correlation between the 2360A system in the U.V. region, the 4150A system in the VIS region and the B-bands in the I.R. region. The 4150A system was found to correlate well with the I.R. B-bands only in diamonds containing large amounts (about 10^{20} atoms/cc) of non-paramagnetic nitrogen. The correlation was weak or non-existent in diamonds containing less non-paramagnetic nitrogen. In these specimens the 4150A system was absent or much smaller than expected from the strength of the I.R. B-bands. The 2360A system correlated well with the B-bands.

No E.P.R. absorption associated with the 4150A

system was reported in the literature.

4.3.2. Results of this Survey.

About 98% of all the diamonds investigated exhibited the 4150A system. All these specimens also contained non-paramagnetic nitrogen. Strong 4150A systems were only observed when the non-paramagnetic nitrogen concentration was about 10^{20} atoms/cc; when lower, the 4150A system was much weaker. Although no correlation between the 4150A system and the non-paramagnetic nitrogen content exists, there appears to be some relation between these centres.

An E.P.R. absorption system, which will be referred to as the "14 line spectrum" was found to be associated with the 4150A O.A. system. This E.P.R. system was found to be precisely the same as that reported by Smith et al (1959 b) who did however, not associate it with the 4150A O.A. system. The 14 line spectrum was described in detail by Smith et al and as this investigation reveals nothing more than to confirm the earlier observations, it will only be described briefly here.

The 14 line E.P.R. system is characterised by a complicated anisotropic system of weak, narrow ($\Delta H \approx \frac{1}{3}$ Oe) lines near g = 2. There are between 14 and 30 or more lines in the spectrum, depending on the orientation

of the d.c. magnetic field, with respect to the crystallographic axes. The resonances are easily saturated, full resolution of the spectrum being very difficult. When the crystal is orientated so that the d.c. magnetic field Ho [100] direction; the minimum number of lines, namely 14, is found. In random orientation the whole spectrum is found in a magnetic field spread of approximately 30 Oe.

To investigate in more detail the correlation between this E.P.R. spectrum and the 4150A O.A. system in the VIS region, 10 diamonds were selected for careful study. From these specimens absorption coefficients were derived from transmission values at various photon energies across the 4150A system. Graphs of absorption coefficient versus photon energy were plotted. The background absorption continuum was sketched in for each graph and the resulting enclosed areas measured with a planimeter. These areas were used as a measure of the strength of the 4150A system, expressed in units of eV x cm^{-1}.

The 14 line E.P.R. spectra of these diamonds were obtained under as near identical conditions as pos[illegible] A high modulation current was used in these [illegible]nts so that the individual lines of this system [illegible]not resolved, and the spectra had the appearance of

of a broad single line, The first derivative spectra so obtained were integrated graphically at intervals of 1 Oe, and the actual E.P.R. spectra constructed. The areas under these curves were taken as a measure of the strength of the 14 line spectrum in a particular stone.

The degree of correspondence between the 4150A system and the 14 line spectrum was expressed in terms of a correlation coefficient. The correlation coefficient between two variables u and v is defined as

$$r = \frac{\overline{uv} - \bar{u}\bar{v}}{\sigma_u \sigma_v}$$

Where $$\sigma_u^2 = \overline{u^2} - \bar{u}^2$$

$$\sigma_v^2 = \overline{v^2} - \bar{v}^2$$

Thus r = 0 implies an absence of correlation between the variables, and r = 1 implies a perfect straight line relationship.

A correlation coefficient, r = 0.94 was obtained between the 4150A system and the 14 line spectrum. This significantly high value indicates that there is a common cause for these absorption systems which will be referred to as 4150A-centres.

4.3.3. Discussion.

Smith et al (1959 b) proposed that the 14 line E.P.R. spectrum could arise from substitutional aluminium atoms in the diamond lattice. They reasoned that when aluminium with 3 outer electrons is bound substitutionally, a large fraction of the resulting "holes" would be bound to their acceptor atoms at room temperature, because of the large ionization energy of diamond. The observed spectrum was then accounted for qualitatively as arising from an unpaired electron localized along one of the four tetrahedral bonds joining an aluminium atom with its nearest neighbour carbon atom.

As there are four equally probable bond directions along which the "hole" can be orientated, there will be four dissimilar and overlapping sets of lines for an arbitrary orientation of Ho. If Ho is parallel to the [100] direction, thus making an equal angle ($\Theta = 55^{\circ}$) with each of the tetrahedral bonds, the four sets should coincide and the minimum number of lines, 14, should be observed. The nuclear spin of aluminium, $I_{Al} = 5/2$; there will therefore be six lines due to hyperfine splitting. The interaction of the quadrupole moment of the aluminium nucleus ($+ 0.150 \times 10^{24} cm^2$) with the field

gradient of the unpaired electron will add so-called "forbidden" resonances. For $\Delta M_I = \pm 1$ eight transitions will be added. The 14 lines observed could therefore be the transitions $\Delta M_I = 0$ (six) and $\Delta M_I = \pm 1$ (eight).

It is difficult to reconstruct this spectrum theoretically because the hyperfine, quadrupole and nuclear magnetic energies are all of the same order of magnitude. Recently, however, Every (1965), using computer calculations, has shown that it is unlikely that such a spectrum could result from substitutional aluminium atoms in the diamond lattice. Furthermore, the results of spectrographic analysis (Raal 1957) indicate that although aluminium frequently occurs as an impurity in diamond, there is no correlation or relation between 4150A-centres and the aluminium content of diamond. This coupled with the fact that there is a very distinct relation between 4150A-centres and the presence of nitrogen platelets, indicates that the 4150A-centres are not due to the presence of substitutional aluminium atoms only.

The E.S.R. results indicate that the 14 line spectrum arises from centres having <111> symmetry. This is in agreement with the results of Maycraft (1960) on the polarisation of the luminesence associated with

the 4150A O.A. system, which indicated a complex having <111> symmetry.

Any more specific model for 4150A-centres, apart from that they are associated with nitrogen in some way and have <111> symmetry, will be very speculative. One possibility is that the centres consist of nearest neighbour substitutional aluminium and nitrogen donor-acceptor pairs. This proposal is favoured by Dean (1965) who from a study of luminesence in diamond suggested that the 4150A optical transition may be due to the creation of an exciton bound to this centre in which the donor and acceptor are in an ionized state.

Another possibility is that the centre involves nitrogen atoms in solid solution in a different state of aggregation than the non-paramagnetic nitrogen platelets. This would explain the relationship between these centres and the concentration of nitrogen platelets, as it is reasonable to expect that when the nitrogen content is high a large number of other nitrogen aggregates may be present as well. On this basis the simplest nitrogen defects responsible for 4150A-centres would be nitrogen pairs in interstitial or substitutional positions.

The 4150A O.A. band probably arises from

transitions between the ground state and excited states of the defect centre, in the forbidden gap. It has a principal line of lowest energy and additional less sharp lines arising from the interaction between the main electronic transition and vibrational states of the crystal. That such a model involving transitions within the forbidden gap and not involving the valence or conduction bands is feasible, was subsequently shown by Vermeulen (1965) who found a photoconduction minimum at the 4150A region in the photoconduction spectra of diamonds containing these centres; indicating that absorption of light in this region takes place, which does not involve the generation of charge carriers.

The mirror image similarity in shape of the 4150A luminesence and absorption systems indicates that the absorption process is the exact reversal of the luminesence process, both taking place at the same centre.

4.4. Paramagnetic Nitrogen.

4.4.1. Existing Knowledge.

As mentioned in § 4.2.1. Smith et al (1959 a) reported the presence of an E.P.R. spectrum which they

attributed to the presence of single, isolated, substitutional nitrogen atoms in the diamond lattice.

This spectrum consists of a triplet of equally spaced, equally intense, lines with the d.c. magnetic field Ho parallel to a [100] direction. The g factor of the resonance is isotropic being 2.0024 ± 0.0005. The nuclear spin of nitrogen $I_{14_N} = 1$. From nuclear splitting one would expect $2I + 1 = 3$ lines. In other orientations of the d.c. magnetic field the outer two lines of the triplet are resolved in as many as 4 lines each. This was explained by Smith et al by considering more than one centre. The model proposed by them comprises a substitutional nitrogen atom with one of the C-N bond directions a hyperfine axis. The spectrum from a given nitrogen centre will then consist of 3 lines whose spacing $|K|$ depends on the angle between the hyperfine axis and Ho. With Ho $\parallel$ [100] direction, an equal angle, $\theta = 55^{\circ}$, will result from all four possible C-N bond directions. The spacings will therefore be equal, all four spectra will be superimposed, and only three lines will be observed.

No information as regards the optical absorption properties of diamonds containing paramagnetic nitrogen

was reported in the literature.

4.4.2. Results of this Survey.

In a relatively common form of diamond, dispersed or paramagnetic nitrogen was found to occur. These diamonds, known to the trade as coated stones, consist of a clear diamond core with an opaque overgrowth, often very thick, of very imperfectly grown diamond or coat. Paramagnetic nitrogen is found only in the opaque coat in a concentration as high as 10^{18} atoms/cc (assessed from the intensity of the E.P.R. spectrum). As the coat consists of such imperfect, opaque diamond, containing large numbers of impurities, it has not been possible to obtain any more information about the properties associated with paramagnetic nitrogen in diamond. According to Kemmey and Mitchell (1960), the E.P.R. spectra of Smith et al were observed in opaque, greenish stones from the Belgian Congo and Sierra Leone, which probably were coated stones.

A rare group of clear diamonds—probably about 0.1% natural occurrence—was found to show the E.P.R. spectrum of dispersed substitutional nitrogen. These diamonds were used for a careful study of the effects of these defects. The results of this examination will be

described fully in the next chapter. Briefly, however, E.P.R. studies revealed the presence of many lines besides those found by Smith et al (1959 a). These lines, specifically those attributed to ^{15}N hyperfine splitting, provide additional evidence in support of the conclusion that the spectrum is due to single substitutional nitrogen atoms. The optical properties found to be associated with the presence of paramagnetic nitrogen were hitherto unknown, and unlike those of diamonds containing other defect centres.

4.4.3. Discussion.

It is now certain that the vast majority of all clear natural diamonds do not contain any paramagnetic nitrogen.* The coated diamonds of West Africa give every

---

*Note added in proof. Since this survey was undertaken a more sensitive E.P.R. spectrometer was used, and it was found that virtually all natural diamonds contain a very small amount (10^{12} to 10^{13} atoms/cc) of paramagnetic nitrogen. Paramagnetic nitrogen in concentrations higher than this is only found in coated diamonds and in the small group of transparent natural diamonds mentioned above

evidence of two growth phases. The first appears to have been relatively slow and controlled, with clear diamond cores being formed. These cores contain non-paramagnetic nitrogen and 4150A-centres, in varying concentrations. A subsequent, very different, and probably very rapid growth phase must then have occurred, leading to the deposition of the opaque coat which contains paramagnetic nitrogen, and is most imperfectly crystallised. This rapid growth may have been initiated by the changes in pressure and temperature immediately prior to, and during the volcanic erruption which led to kimberlite pipe formation. This would result in relatively rapid quenching of the newly grown diamond, and any included nitrogen would be expected to remain largely dispersed.

In the rare clear diamonds containing up to 10^{17} atoms/cc paramagnetic nitrogen, crystal perfection is such that very rapid growth processes appear improbable. It may be that this small group of specimens was grown under unusually low temperature conditions, where the equilibrium concentration of thermal vacancies presumably necessary for nitrogen migration to form platelets, was sufficiently low to prevent platelet formation.

4.5. Graphitic Regions.

4.5.1. Existing Knowledge.

Clark et al (1956 a & b) reported the existence of an absorption tail in all the so-called Type IIa specimens (non-nitrogen containing insulating diamonds) studied. The absorption tail comprises a monotonic increase of absorption, with increasing photon energy, starting at 1.5 eV and extending up to the fundamental absorption edge at 5.4 eV. Clark et al found that this absorption tail could be enhanced by heating specimens in which single vacancies and interstitials were produced by electron irradiation at temperatures between 700°C and 900°C. They suggested that the absorption tail is due to extensive regions of amorphous or graphitic carbon produced by the agglomeration of point defects. The point defects may either increase the number of these regions or migrate to and increase the size of existing regions.

Clark et al adduced further support for their model from neutron irradiation damage studies. In neutron irradiated Type IIa diamonds the absorption tail is produced without heating, by bombardment with pile neutrons, and is probably associated with regions of extensive

damage near the ends of the tracks of recoil carbon atoms. X-ray examination of heavily neutron-irradiated diamonds by Levy and Krammerer (1955) have revealed the presence of amorphous material.

Wedepohl (1957 a) showed that the wavelength dependence of the apparent absorption tail is $\lambda^{-3.6}$. As a result of this he pointed out that most of the tail might arise from a Rayleigh scattering effect (λ^{-4}). Bastin and Mitchell (1959) investigated this system in plane parallel specimens, using an integrating sphere, and concluded that the apparent absorption tail is real and that the wavelength dependence with that required for Rayleigh scattering is fortuitous.

Duncan (1963) found that the absorption tail could also be produced in Type IIa diamonds by 1.4 MeV electron irradiation without heating. He determined the displacement energy for these centres as Ed = 140 eV.

4.5.2. Results of this Survey.

From the specimens investigated it is estimated that between 1% and 2% of all natural diamonds do not contain nitrogen in detectable amounts. These specimens are commonly referred to as Type II diamonds (Robertson

et al 1934). Of the Type II diamonds most are good insulators and are referred to as Type IIa. A small percentage are semi-conductors and of the so-called Type IIb variety (Custers 1952).

All the Type IIa specimens were found to exhibit the absorption tail in varying strength. No I.R. absorption apart from the intrinsic diamond bands could be detected in these specimens. However a single isotropic E.P.R. line that appeared to be associated with the absorption tail was found.

This E.P.R. line in specimen D1 is illustrated by Figure 4.2. The g-value could not be distinguished experimentally from that of the resonance due to paramagnetic nitrogen in diamond (i.e. very close to the free electron value). The line width ΔH, measured between the maximum and minimum value of the first derivative spectrum, was found to vary between 3 Oe and 4 Oe in the ten specimens investigated. A linear correlation coefficient $r = 0.96$ was obtained between the intensity of the absorption tail and the relative strength of the E.P.R. line. This is in agreement with independent results of Duncan (1963), who studied the formation of the absorption tail and presumably the same E.P.R. line after

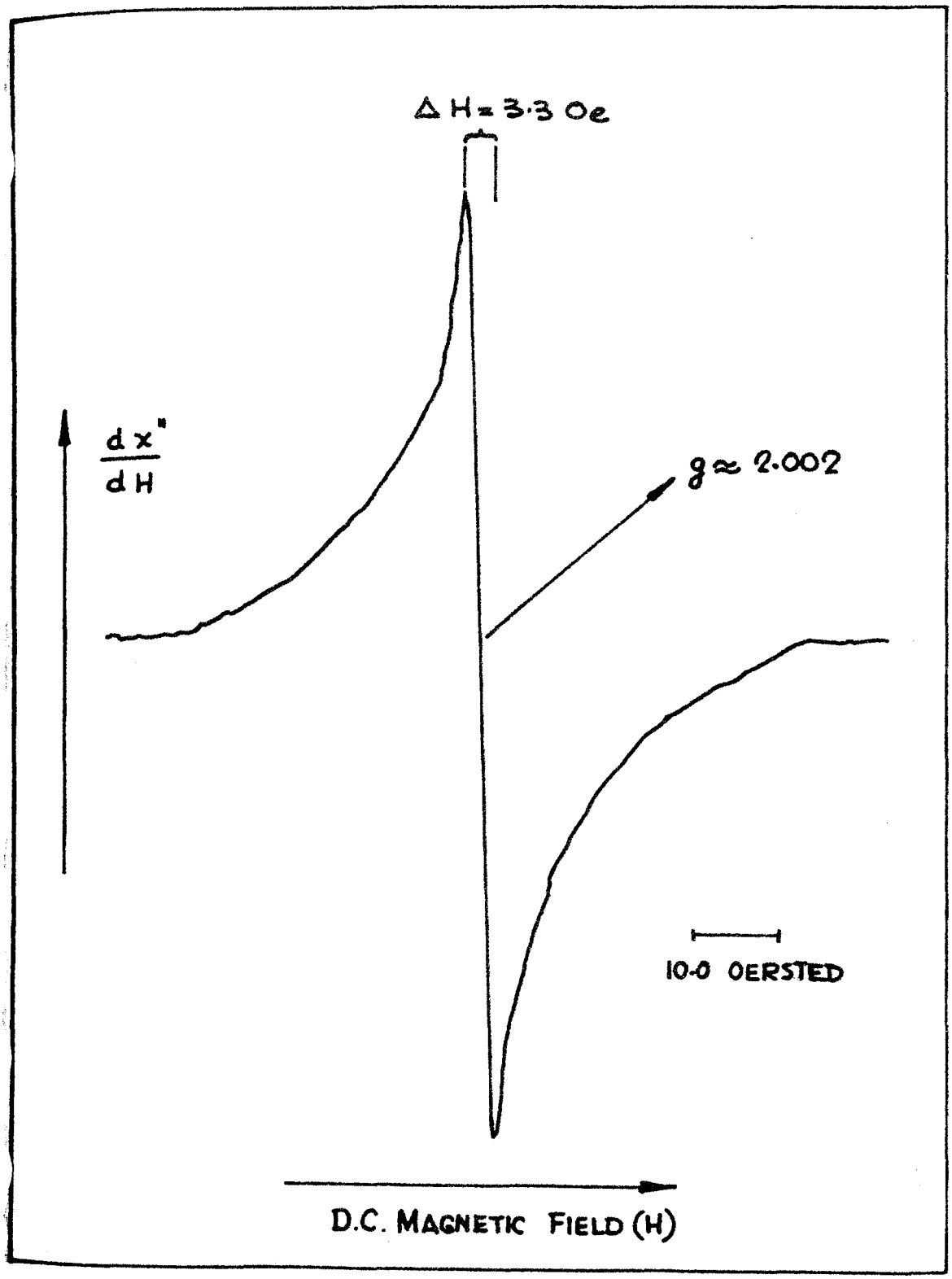

FIGURE 4.2 FIRST DERIVATIVE E.P.R. SPECTRUM OF SPECIMEN D1, ILLUSTRATING THE LINE ASSOCIATED WITH GRAPHITIC REGIONS.

electron irradiation at 1.75 MeV.

The absorption tail was also found in about 5% of the diamonds containing non-paramagnetic nitrogen. In most cases the associated E.P.R. line was superimposed on the 14 line spectrum present in these specimens due to the co-existence of 4150A-centres. The two spectra could be partially resolved at high levels of the microwave power in the resonant cavity. Under such conditions the intensity of the 14 line spectrum was reduced considerably due to saturation, whereas no saturation of the line due to graphitic regions could be detected.

4.5.3. Discussion.

From the evidence it appears reasonable to assume that the absorption tail and associated E.P.R. line originate from defect centres comprising regions of grossly disordered carbon atoms in the diamond lattice, which for the sake of briefness are referred to as graphitic regions. Whether the centres in fact consist of graphite, where carbon atoms are hexagonally close packed in basal planes which are bound loosely to one another, is not clear at all. Wagoner (1960) studied the free carrier resonance in graphite and found a line with an anisotropic g-value.

The values are:

$$g_{\parallel} = 2.0495 \quad (H \parallel \text{hexagonal axis})$$
$$g_{\perp} = 2.0026 \quad (H \perp \text{hexagonal axis})$$

No readily detectable changes in ΔH, of the E.P.R. line due to the graphitic regions, with orientation were observed, however, the orientation of the centres in the diamond structure is not known.

4.6. Acceptor Centres.

4.6.1. Existing Knowledge.

Custers (1952) discovered that a small group of Type II diamonds are semi-conducting. These specimens were classified as Type IIb and were investigated extensively by Wedepohl (1957 b). He concluded that these specimens are p-type semiconductors with an acceptor level at 0.34 eV above the valence band. In VIS absorption they are characterised by an absorption continuum starting at about 2.5 eV and extending to the I.R. region where characteristic bands at 0.508 eV, 0.344 eV and 0.306 eV are found.

Bell and Leivo (1961) reported E.P.R. spectra in two semi-conducting diamonds. In the first, which contained a high concentration of acceptor centres, a line, similar to that revealed by this survey to be due to graphitic regions, was found. The second diamond, which contained few acceptor centres but exhibited an unusual red luminesence, which is not characteristic of the acceptor centres, exhibited a broad unresolved resonance.

4.6.2. Results of this Survey.

As semi-conducting diamonds are very scarce, some were specially selected for study from the production of the Premier Mine (the only major source). Apart from the acceptor centres some of these specimens also revealed the presence of graphitic regions. No E.P.R. features were detected in any of the specimens containing only acceptor centres.

4.6.3. Discussion.

No E.P.R. absorption characteristic of the acceptor centres could be found. The line reported by Bell and Leivo (1961) in a diamond containing a large number of acceptor centres almost certainly derives from

the presence of some graphitic regions in the crystal. Similarly the other spectrum could be the result of defect centres other than the acceptor centres which could presumbaly also account for the unusual red luminescence.

The simplest and most probable atomic model for the acceptor centres would be a substitutionally bound Group III element in the diamond lattice such as boron or aluminium. The presence of such substitutional atoms is expected to be revealed by E.P.R. absorption, however, no resonances due to such shallow acceptor impurities could be detected in p-type silicon crystals. The failure to detect such resonances in silicon is thought to be related to the structure of the valence band (Ludwig and Woodbury 1962). The degeneracy of valence bands at $\underline{k} = 0$, the minimum hole energy in silicon, is related to the symmetry of the lattice, and can be lifted (except for spin) by subjecting the crystal to uniaxial stress. Feher et al (1960) observed a single resonance line in boron, aluminium, gallium and indium doped silicon crystals subjected to a uniaxial stress. Similar reasons may very well account for the absence of E.P.R. in unstrained diamonds containing acceptor centres.

4.7. GR1-Centres.

4.7.1. Existing Knowledge.

Clark et al (1956 a) found that an O.A. band, called GR1, consisting of a sharp principal line at 1.68 eV and successively more diffuse lines at higher energies, could be induced in all diamonds by irradiation damage. It was suggested that this band arose from the creation of vacancies or interstitials in the diamond lattice. No I.R. or E.P.R. absorption features, which could be associated with the GR1 band were reported.

4.7.2. Results of this Survey.

A GR1 band could be detected in only a few rare natural diamonds only in a surface layer, approximately 0.5 mm thick. No I.R. or E.P.R. absorption features, which could be associated with GR1-centres, were found.

4.7.3. Discussion.

The specimens in which a GR1 band could be detected are thought to have been subjected to irradiation damage during some stage of their geological environment. The defects associated with irradiation damage in diamond

are described in detail in Chapter VIII. GR1-centres may therefore more appropriately be discussed there.

4.8. 5032A-Centres.

4.8.1. Existing Knowledge.

An O.A. band with a principal line at 2.47 eV (5032A) and associated more diffuse lines on the high energy side, was found in natural diamond by Clark et al (1956 a). Clark et al (1956 b) demonstrated that this O.A. band can be produced in certain specimens if irradiation damage is followed by heat treatment in excess of 500°C. No associated I.R. or E.P.R. absorption features were reported.

4.8.2. Results of this Survey.

The 5032A O.A. band was observed only in about 0.1% of the specimens containing non-paramagnetic nitrogen. No associated I.R. or E.P.R. absorption features were observed.

4.8.3. Discussion.

The 5032A-centres appear to be associated with

vacancies or interstitials and nitrogen platelets and will be discussed in more detail in Chapter IX, where the effects of heat treatment on irradiated diamonds containing non-paramagnetic nitrogen are described.

4.9. Pink and Mauve Centres.

4.9.1. Existing Knowledge.

Raal (1958) found a broad O.A. band in the VIS region centered at approximately 2.23 eV in all pink and mauve coloured diamonds. This band could to some extent be correlated with the manganese impurity content of the specimens. Subsequently Wright (1961) reported that the band in pink diamonds only could be bleached by x-rays and again restored by exposure to U.V. light. Holland (1964) demonstrated that both pink and mauve diamonds have the O.A. band at 2.23 eV, but that the pink diamonds exhibit two additional overlapping bands with peaks at 3.13 eV and 3.18 eV respectively, while the mauve diamonds only exhibit an absorption tail extending from 2.7 eV to as far as the secondary absorption edge at about 3.7 eV.

4.9.2. Results of this Survey.

A very small percentage of the diamonds encountered normally exhibits pink or mauve centres. Some specimens were therefore specially selected. The diamonds containing mauve centres all contained large amounts of non-paramagnetic nitrogen ($\pm 10^{20}$ atoms/cc) and 4150A-centres. Only I.R. and E.P.R. absorption features characteristic of 4150A-centres and nitrogen platelets were observed in these specimens containing mauve centres.

The specimens containing pink centres all contained little or no non-paramagnetic nitrogen. No additional I.R. bands were found. A weak single isotropic E.P.R. line could be detected in these specimens. On exposure to x-rays this E.P.R. line nearly doubled in intensity and could be restored to its original condition by subsequent illumination with U.V. light. This is shown in Figure 4.3, for specimen D2, which in addition to pink centres also contained some graphitic regions as was evident from the O.A. spectrum.

4.9.3. Discussion.

It appears as though pink centres are normally not paramagnetic. The E.P.R. line detected in these

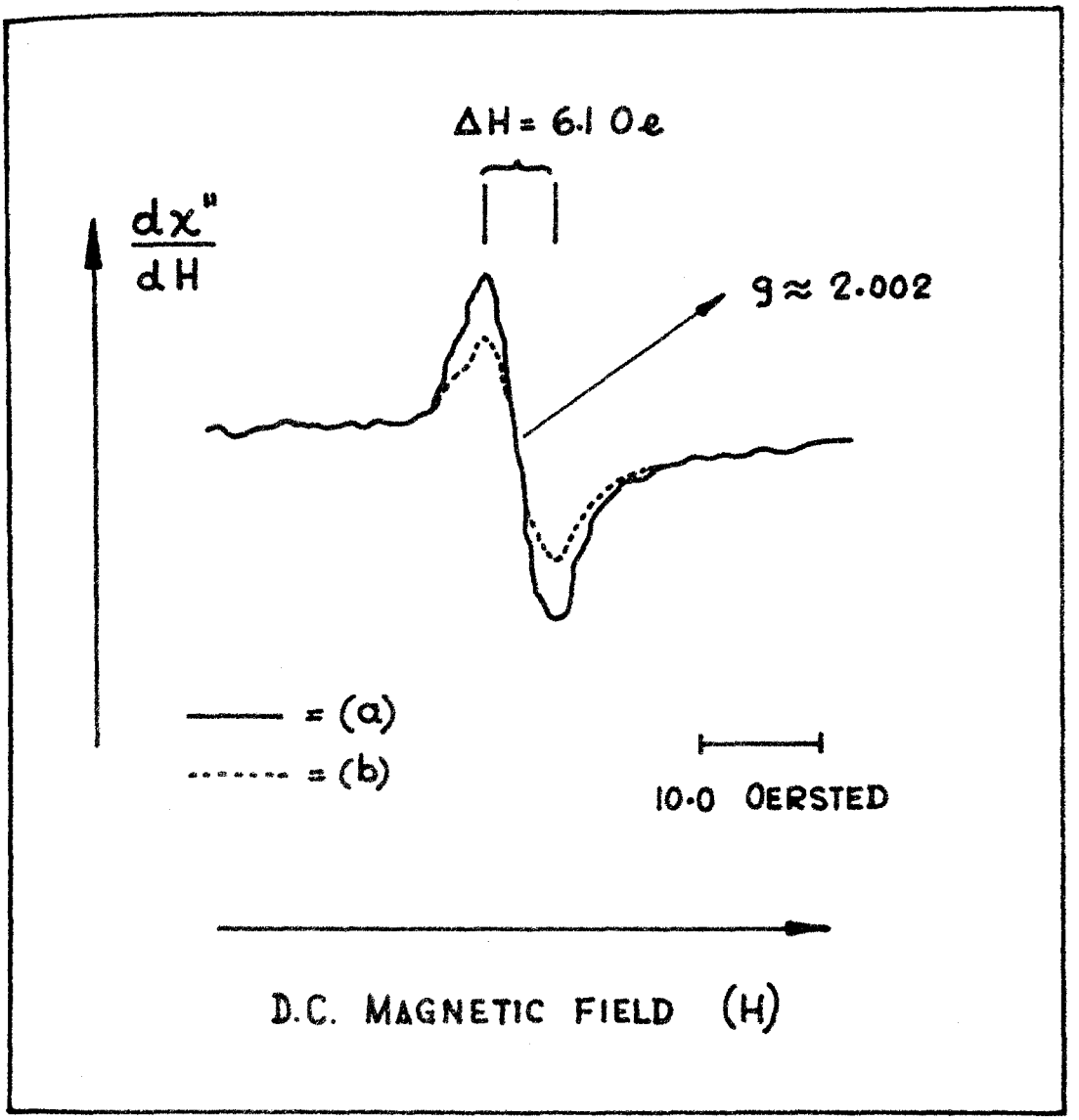

FIGURE 4.3 FIRST DERIVATIVE E.P.R. SPECTRA OF SPECIMEN D2, A TYPICAL PINK DIAMOND.

(a) AFTER EXPOSURE TO X-RAYS.

(b) AFTER SUBSEQUENT EXPOSURE TO SUNLIGHT.

specimens presumably arise from the graphitic regions present. When the pink diamonds are exposed to x-rays the O.A. bands are bleached and the pink centres presumably become paramagnetic, giving rise to a single line superimposed on the existing E.P.R. line. This additional E.P.R. absorption can be bleached by U.V. light, a process whereby the O.A. bands are restored.

From this scanty evidence no model for pink or mauve centres can be proposed. Presumably these centres do not arise from the presence of manganese in the diamond lattice, as no E.P.R. absorption which can be associated with manganese impurities is found.

4.10. 4800A-Centres.

4.10.1. Existing Knowledge.

None.

4.10.2. Results of this Survey.

These defect centres were encountered in most of the specimens containing paramagnetic nitrogen and also in some rare specimens containing about 10^{19} atoms/cc non-paramagnetic nitrogen. They are characterised

by a broad O.A. band in the VIS region, between 2.4 eV and 3.0 eV, with a maximum at 2.6 eV (4800A). This is illustrated in Figure 4.4 for specimen D3 which exhibits in addition a weak secondary absorption edge. As can be seen, only some imperfectly resolved structure at 2.5 eV was revealed at 80°K. All the specimens exhibiting 4800A-centres fluoresced strongly with a flesh colour under ultra-violet light.

In I.R. absorption 4800A-centres appear to be characterised by a weak band at 0.136 eV. This is illustrated in Figure 4.5 for specimen D3, which exhibits in addition a weak band at 0.159 eV due to the presence of non-paramagnetic nitrogen.

A complicated E.P.R. spectrum consisting of an anisotropic system of between 4 and 6 lines centered near g = 2 appears to be associated with the 4800A-centres. This is illustrated by Figure 4.6 with Ho applied in different crystallographic directions to specimen D3. It is evident that no symmetric pattern could be obtained in any of these orientations. Most commonly the 4800A-centres were detected in specimens containing paramagnetic nitrogen. The E.P.R. spectrum of Figure 4.6 was then found superimposed on the spectrum resulting from paramagnetic

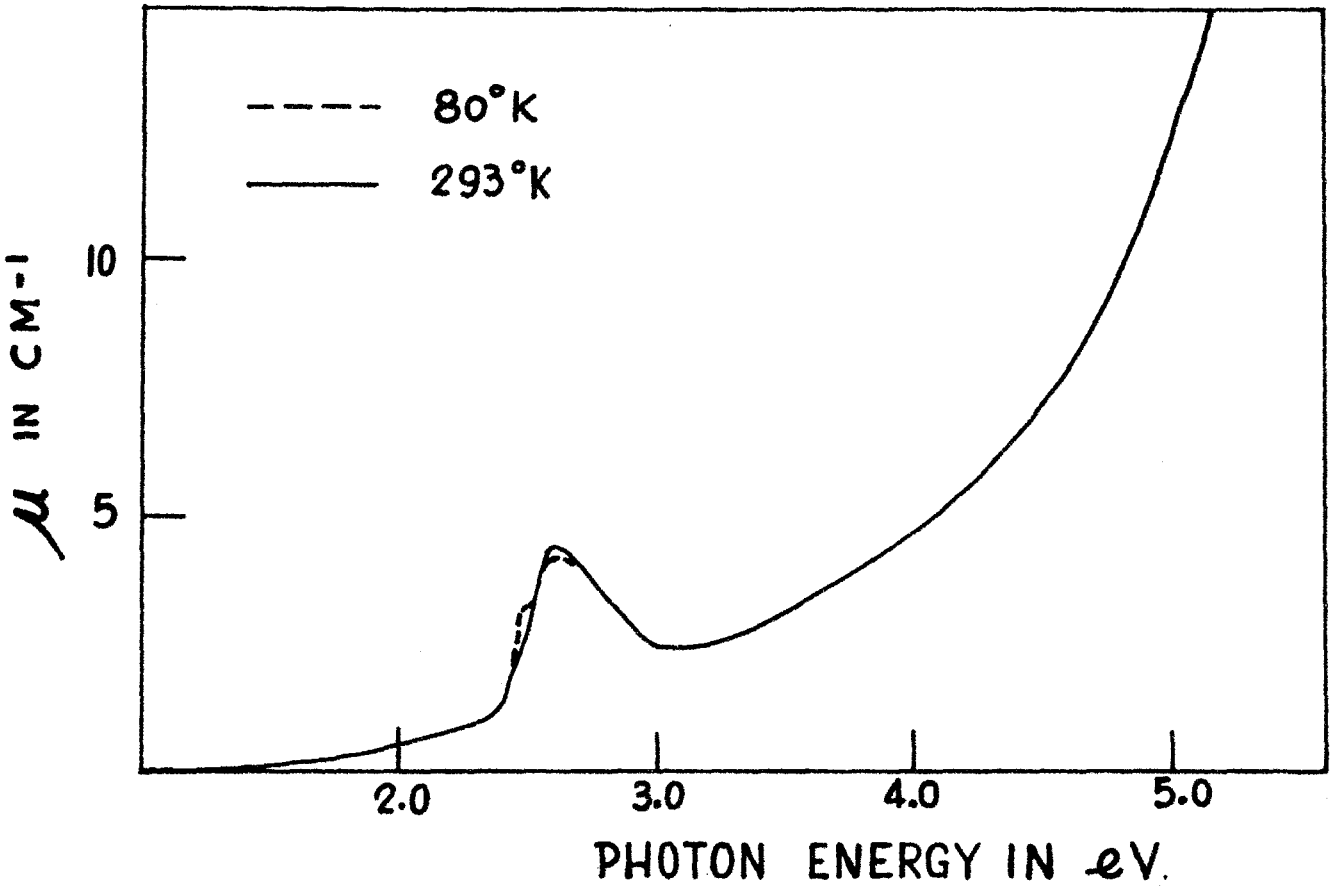

FIGURE 4.4 OPTICAL ABSORPTION SPECTRUM OF SPECIMEN D3, MEASURED AT ROOM TEMPERATURE AND AT 80°K, ILLUSTRATING THE 4800A BAND.

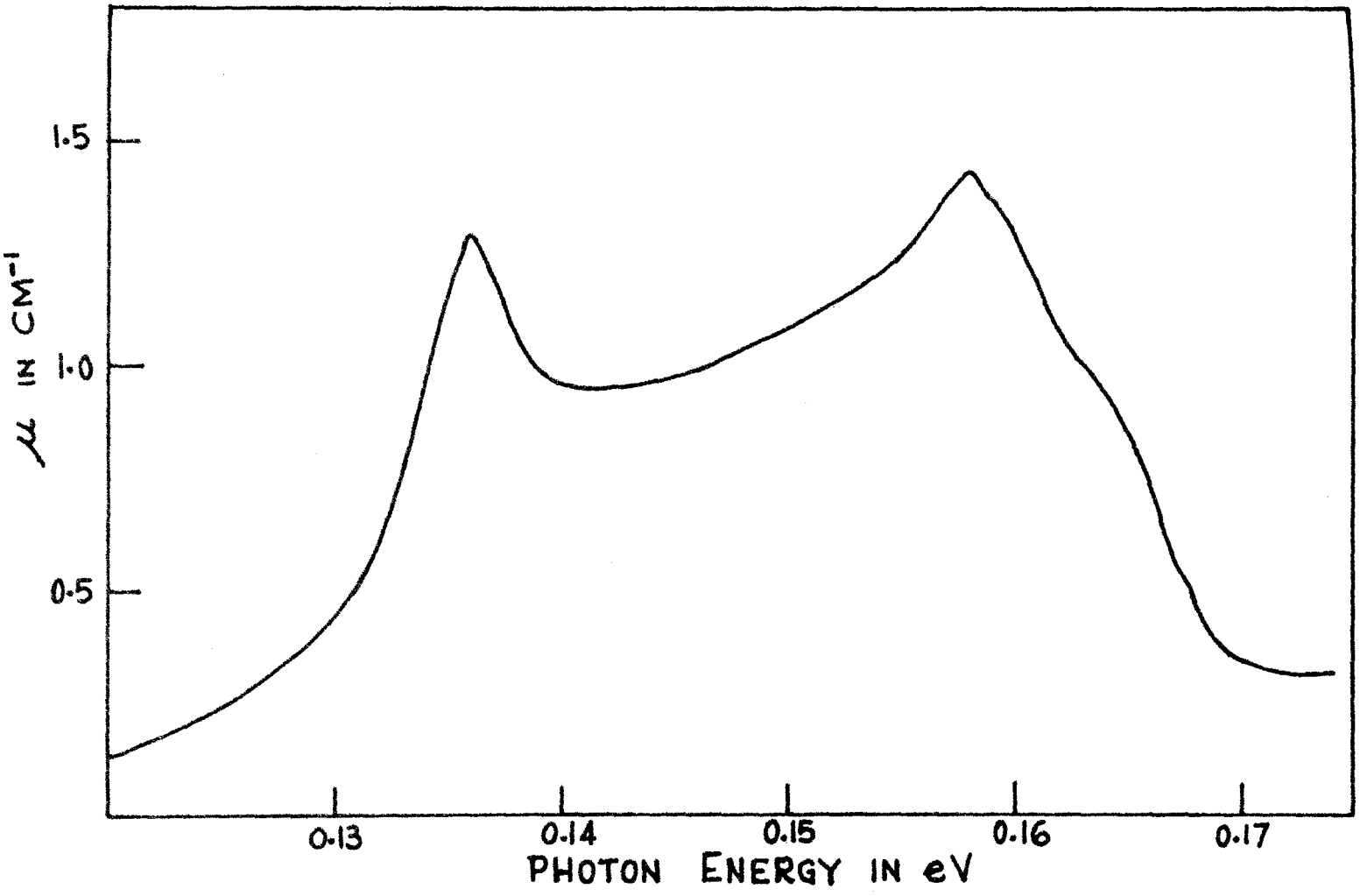

FIGURE 4.5 INFRA-RED ABSORPTION SPECTRUM OF SPECIMEN D3 IN THE SINGLE PHONON REGION.

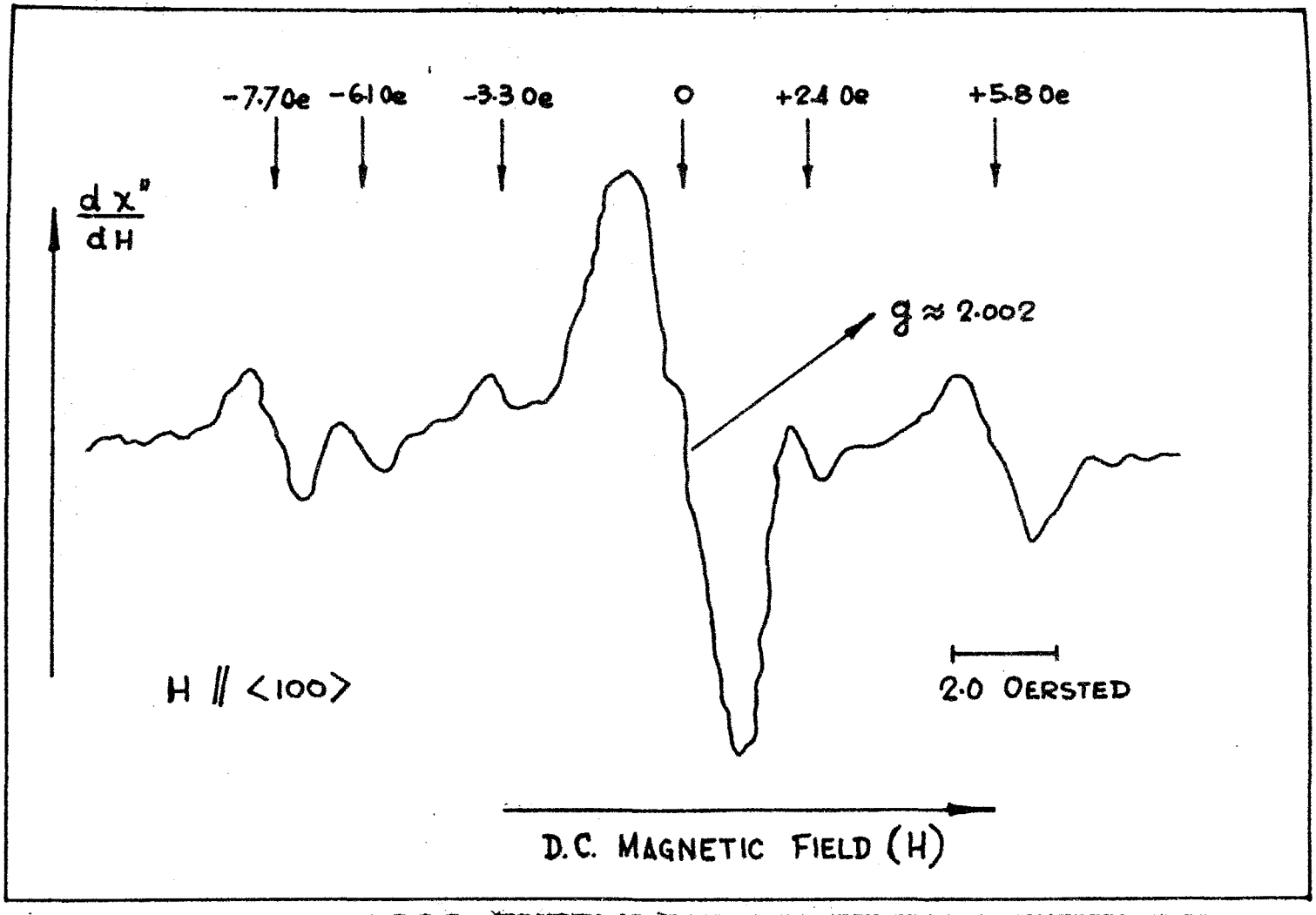

FIGURE 4.6a FIRST DERIVATIVE E.P.R. SPECTRUM OF SPECIMEN D3 WITH THE D.C. MAGNETIC FIELD APPLIED IN A (100) DIRECTION.

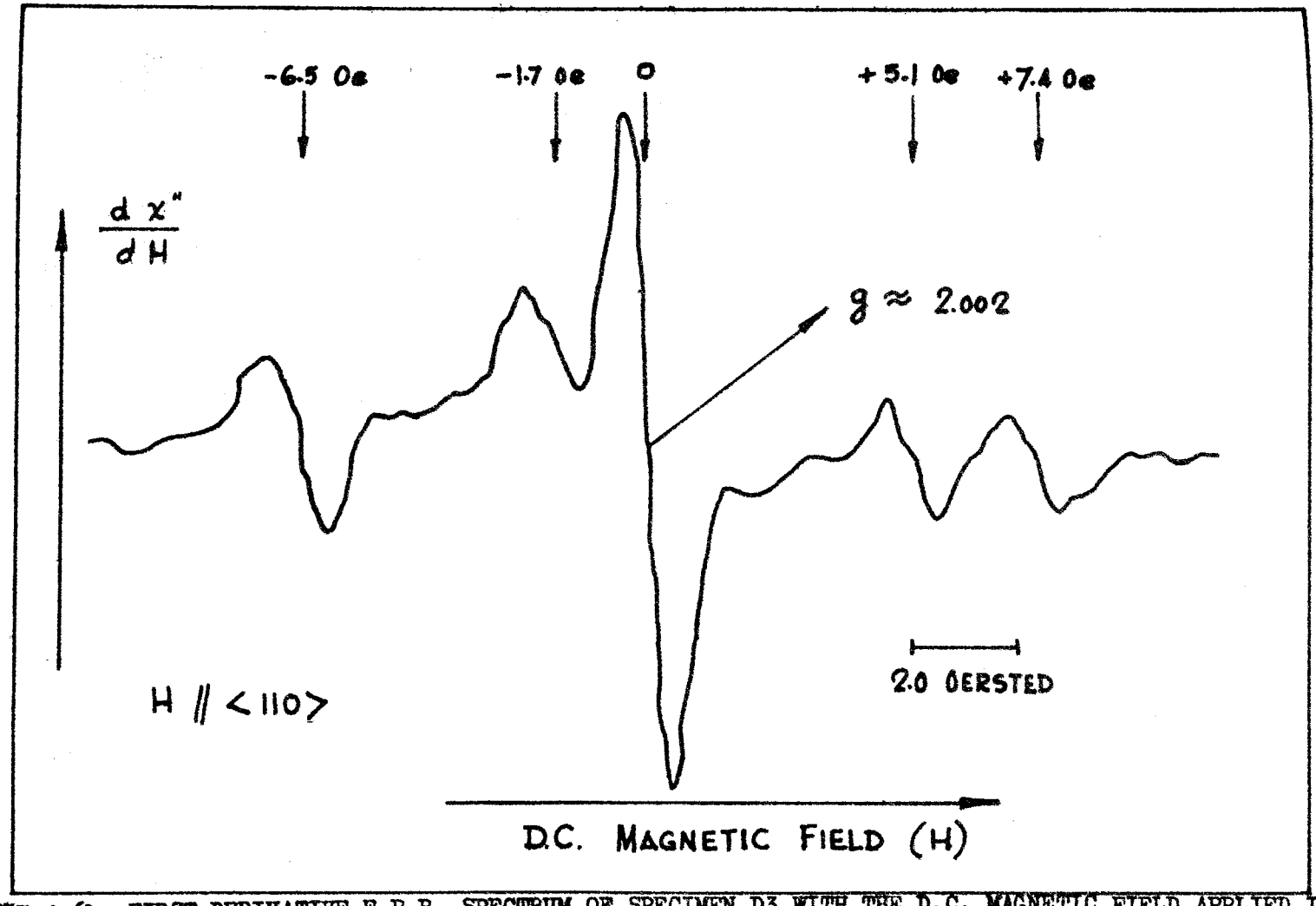

FIGURE 4.6b FIRST DERIVATIVE E.P.R. SPECTRUM OF SPECIMEN D3 WITH THE D.C. MAGNETIC FIELD APPLIED IN A (110) DIRECTION.

FIGURE 4.6c FIRST DERIVATIVE E.P.R. SPECTRUM OF SPECIMEN D3 WITH THE D.C. MAGNETIC FIELD APPLIED IN A (111) DIRECTION.

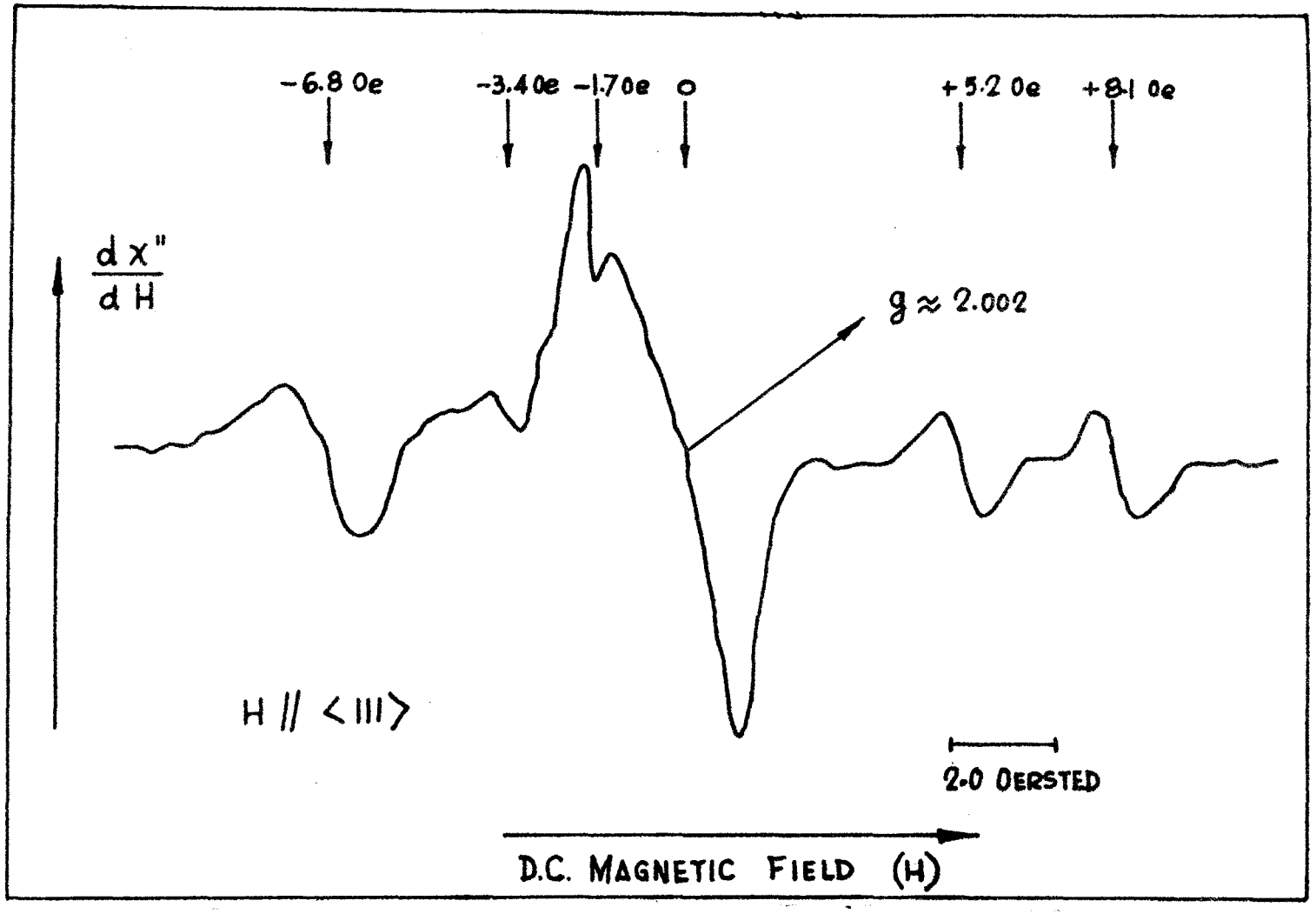

nitrogen in diamond.

No correlation coefficients could be calculated for the U.V.-VIS, I.R. and E.P.R. absorption spectra, as only a few specimens were availbale. The spectra described above were, however, always obtained when the 4800A optical absorption band was present.

4.10.3. Discussion.

The E.P.R. spectrum of 4800A-centres does not lend itself to any straightforward analysis. An attempt to obtain the symmetry of these centres was made by studying the E.P.R. spectrum in many different orientations, however without success. A more comprehensive study may yield useful information, but was not attempted at this stage in view of the many other centres that were studied.

Apart from the fact that the 4800A-centres appear to be associated with nitrogen in diamond and particularly nitrogen in the paramagnetic configuration, nothing can be said about the nature of the centres at this stage.

4.11. Amber Centres.

4.11.1. Existing Knowledge.

None.

4.11.2. Results of this Survey.

These centres were usually detected in specimens containing paramagnetic nitrogen, in which they appear to be very common. In these specimens the presence of additional amber centres was revealed by an apparent single, isotropic, narrow E.P.R. line superimposed on the central line of the paramagnetic nitrogen spectrum. This is illustrated in Figure 4.7 for specimen D4. In a few rare specimens no other paramagnetic absorption, except that from the amber centres, was found. This is illustrated in Figure 4.8 for specimen D5 which exhibits only a single isotropic line with $\Delta H = 1.8$ Oe $\pm$ 0.3 Oe. This E.P.R. line, thought to be due to amber centres, is quite different from the line associated with graphitic regions (§ 4.5.2.) in that it is about two times narrower and do not have such broad flanks.

The O.A. spectrum in the U.V.-VIS region of D5 is shown in Figure 4.9. The amber centres apparently

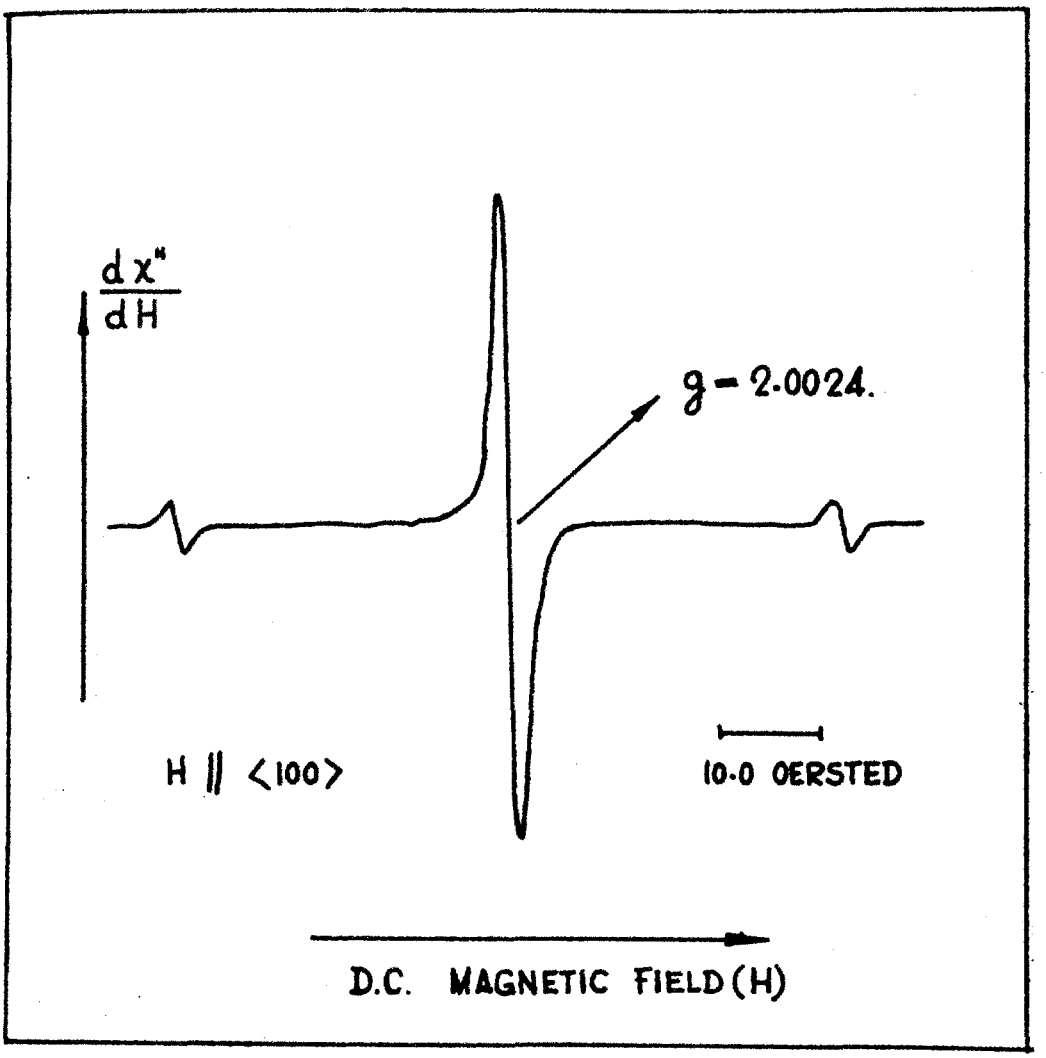

FIGURE 4.7 FIRST DERIVATIVE E.P.R. SPECTRUM OF SPECIMEN D4 WITH THE D.C. MAGNETIC FIELD APPLIED IN A (100) DIRECTION.

FIGURE 4.8 FIRST DERIVATIVE E.P.R. SPECTRUM OF SPECIMEN D5, ILLUSTRATING THE ISOTROPIC LINE ASSOCIATED WITH AMBER CENTRES.

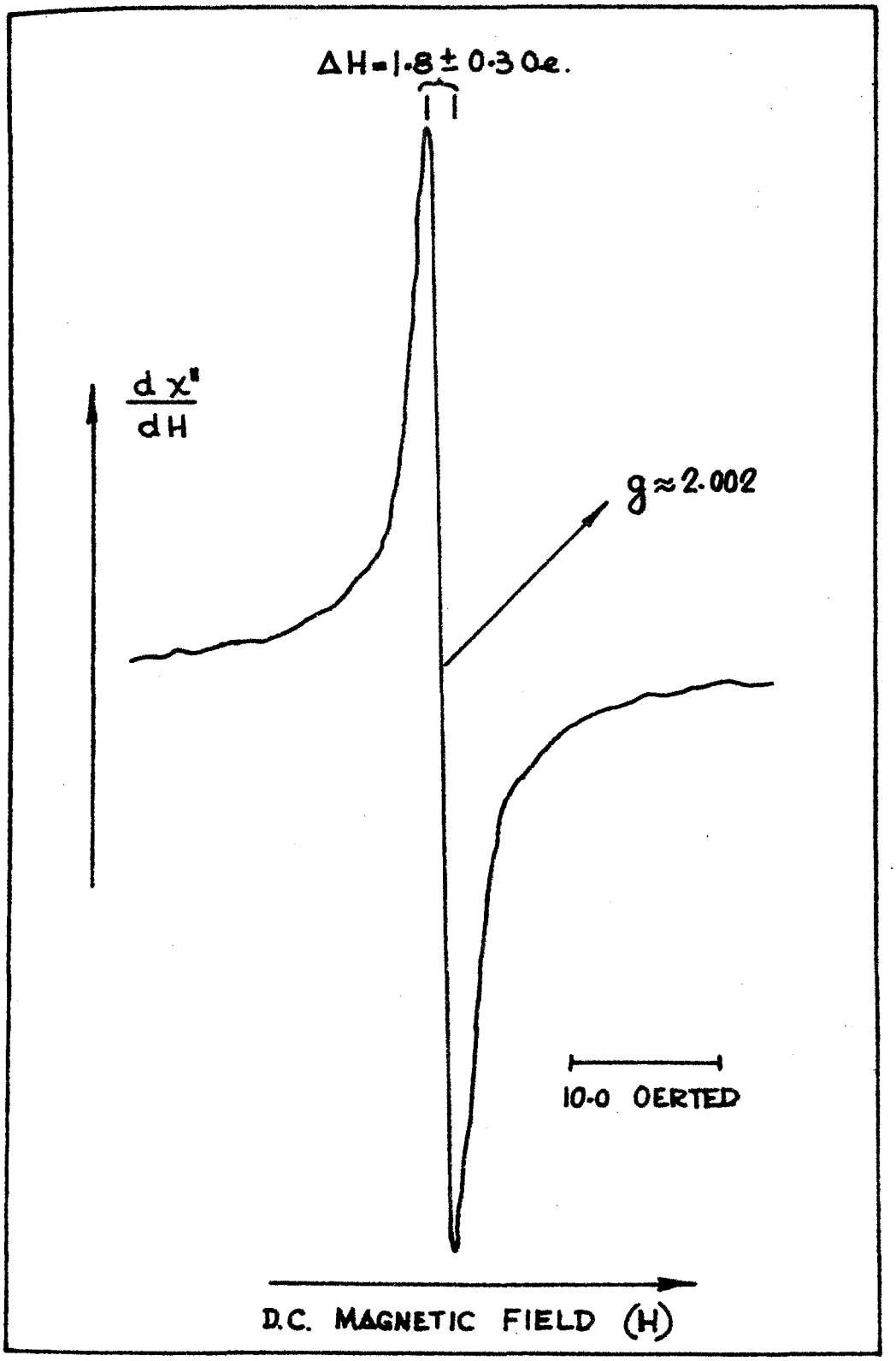

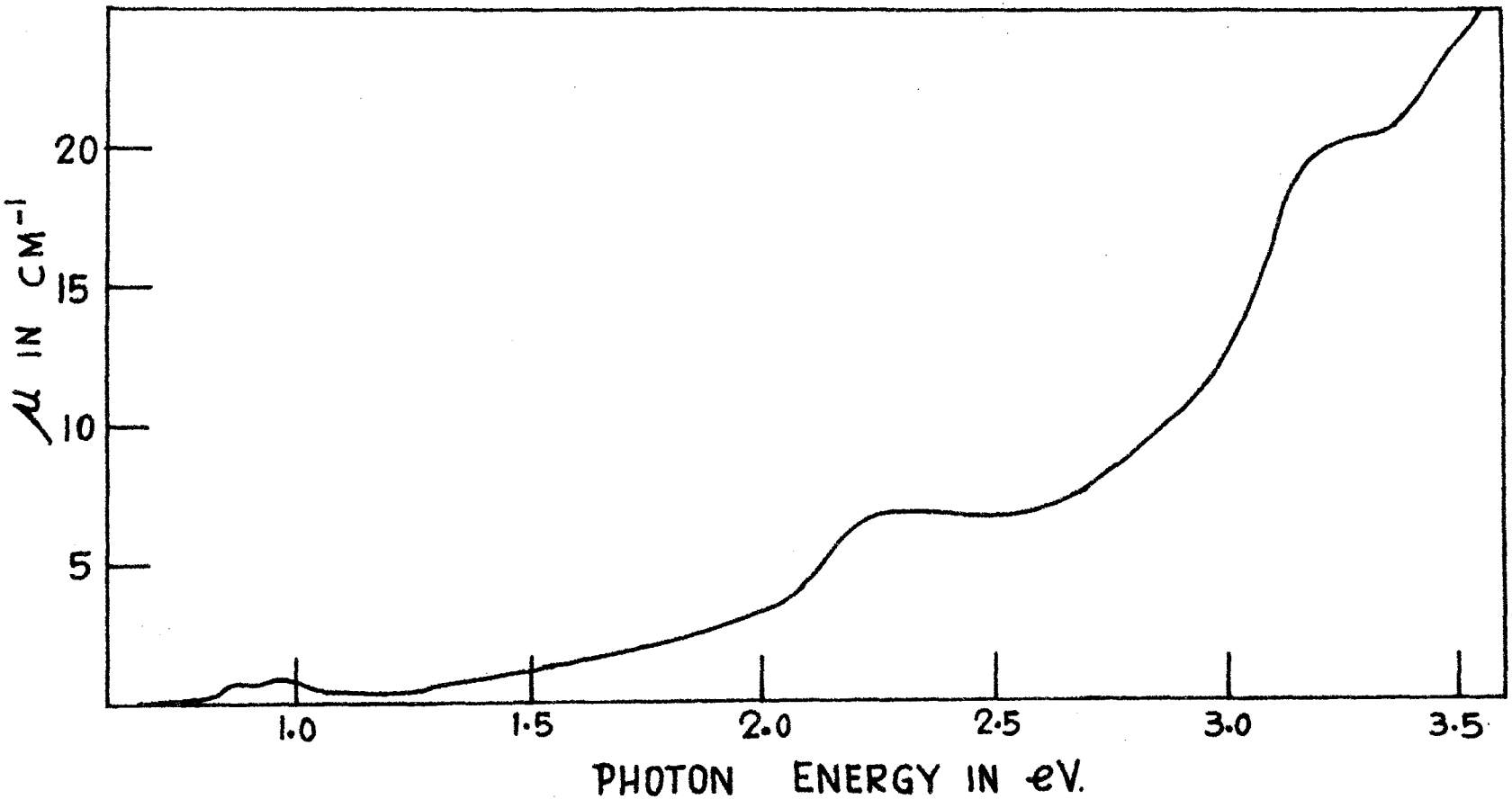

FIGURE 4.9 OPTICAL ABSORPTION SPECTRUM OF SPECIMEN D5.

give rise to: two broad structureless bands between 2.15 and 2.36 eV and between 3.1 and 3.55 eV; a weak system between 0.75 and 1.15 eV; and an absorption tail starting at 1.15 eV and continuing presumably to the fundamental absorption edge at 5.4 eV.

The first two broad bands did not change on cooling the specimen to liquid nitrogen temperature and unlike the bands in pink diamonds, they were not affected by exposure to x-rays. The weak system between 0.75 and 1.15 eV in the near I.R., measured at room temperature and at 80°K, is shown in more detail in Figure 4.10. It appears as if this band, which will be referred to as the 14,500A band, like the 4150A, GR1 and 5032A bands, also consists of a principal line at 0.77 eV and less sharp lines on the high energy side, two of which could be resolved at 0.83 eV and 0.85 eV with the lead-sulphide detector of the spectrophotometer, which does not offer good resolution but has to be used at these long wavelengths.

Furthermore, in the I.R. region all the specimens containing amber centres showed a weak band system between about 0.4 eV and 0.6 eV with a characteristic band at 0.52 eV. This is illustrated in Figure 4.11 for

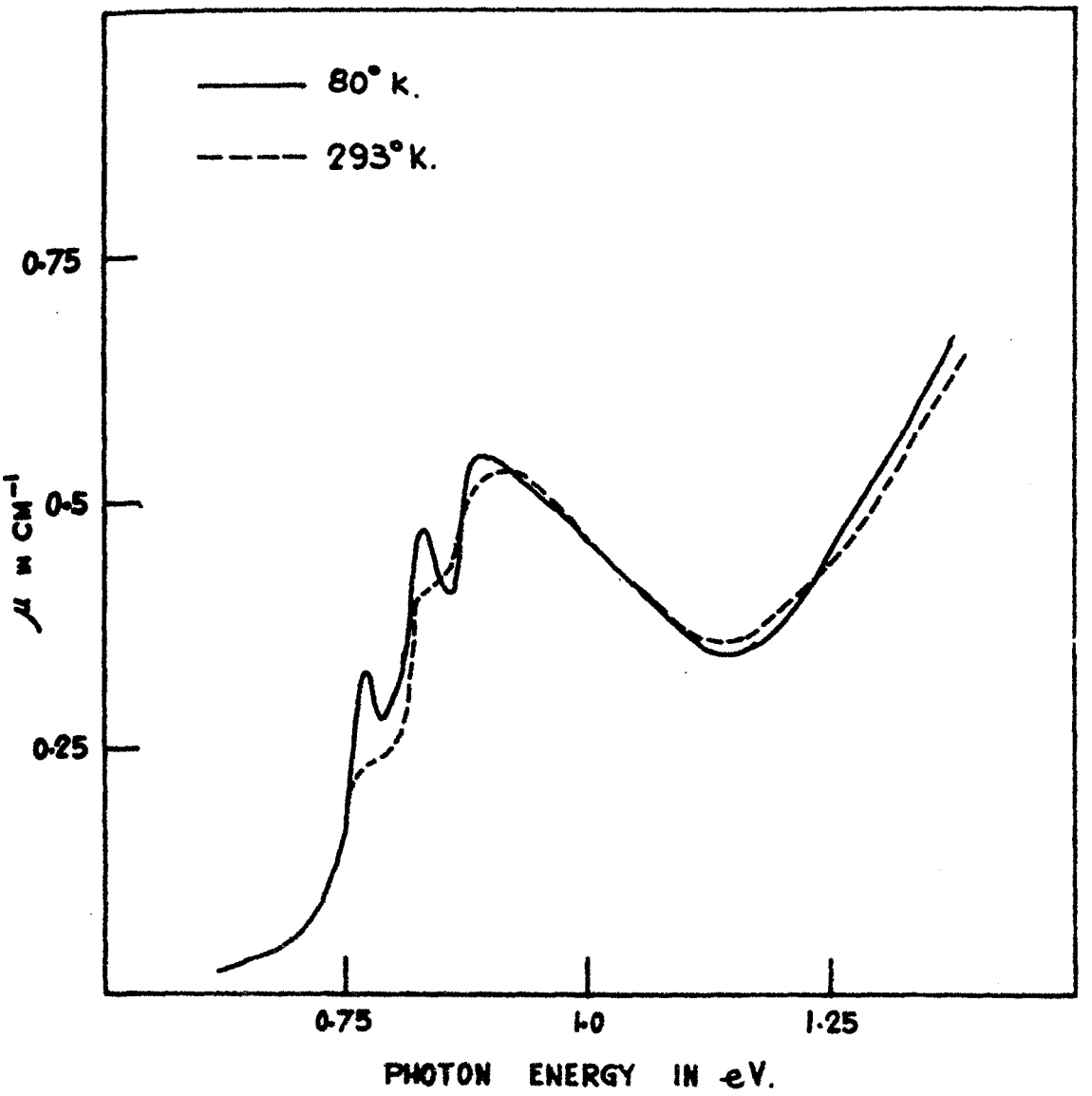

FIGURE 4.10 THE 14,500A OPTICAL ABSORPTION BAND IN SPECIMEN D5, AS MEASURED AT ROOM TEMPERATURE AND AT 80°K.

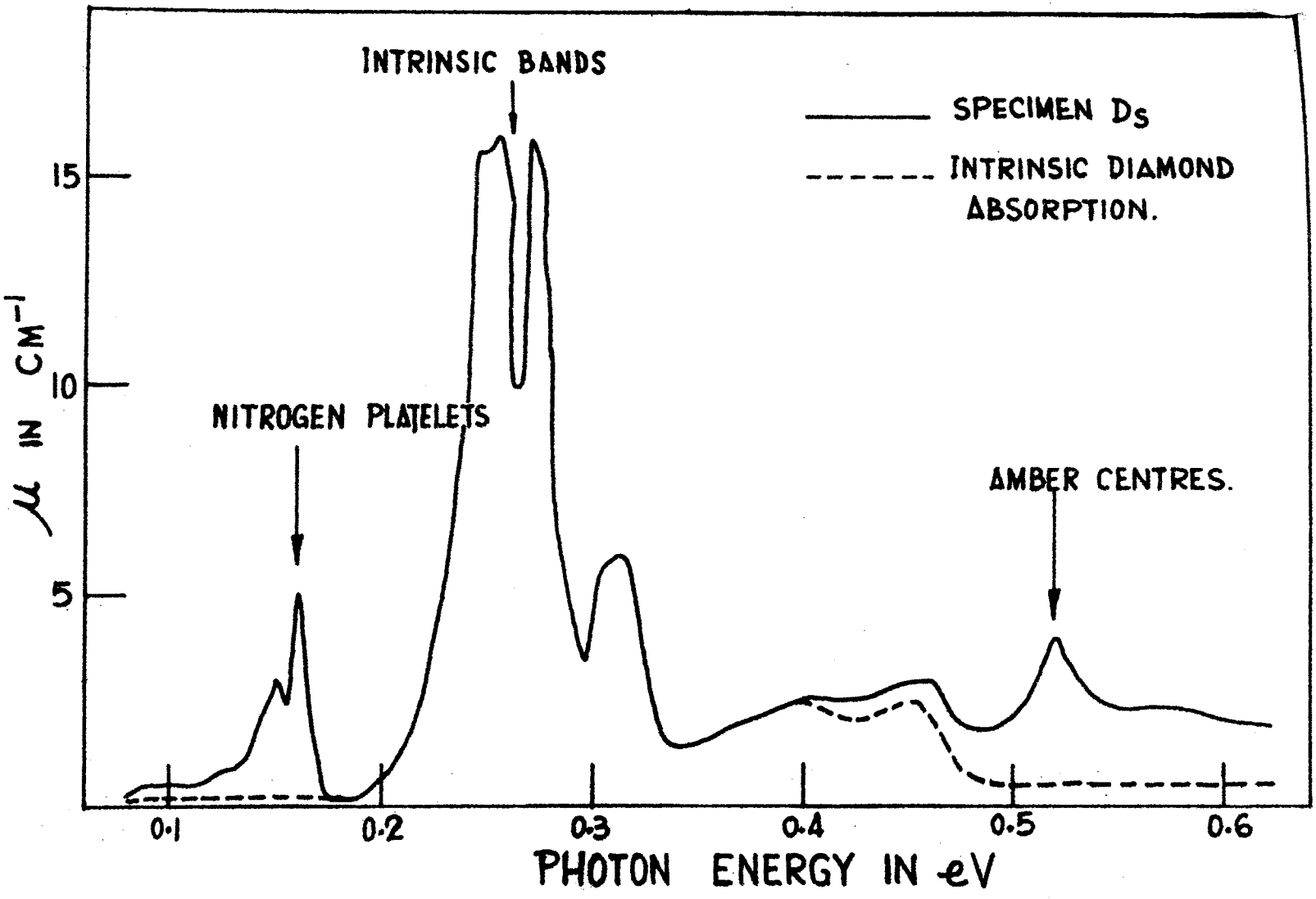

FIGURE 4.11 INFRA-RED ABSORPTION SPECTRUM OF SPECIMEN D5.

specimen D5. From this figure it is clear that D5 contains, in addition, some non-paramagnetic nitrogen.

4.11.3. Discussion.

The nature of the amber centres is not clear at all. The fact that the amber centres usually occur in diamonds containing paramagnetic nitrogen and give rise to a single narrow E.P.R. line may indicate substitutional nitrogen atoms in such a position in the diamond lattice that exchange interaction can take place along the bonds coupling the nitrogen atoms. Such a model was proposed by Slichter (1955) to explain the single E.P.R. line when silicon is heavily doped with phosphorous donors, but with the information available at present such an assignment to amber centres is mere speculation.

4.12. General Discussion.

From this survey it is evident that virtually all natural diamonds contain defect centres which could be detected by the absorption techniques used. A total of 11 different types of defect centres was observed. Of these, two could be definitely associated with the presence of substitutional nitrogen in diamond. Another

three, graphitic regions, GR1-centres and acceptor centres, are not associated with the presence of nitrogen in diamond. The remaining six defect centres could not be identified, but are associated in some way with the presence of nitrogen impurities.

The substitutional nitrogen found in diamond appears to have been included in a dispersed paramagnetic configuration, and subsequently, during growth and for millenia prior to kimberlite pipe formation, migrated by a vacancy mechanism to the more stable platelet configuration. It is reasonable to expect that some nitrogen remained in positions intermediate between the two known configurations. Such nitrogen, in intermediate stages of platelet formation, may be responsible for the unidentified defect centres observed in the nitrogen containing specimens.

In order to investigate the feasibility of this proposal and to determine whether any of the unidentified defect centres could be synthesised, it was decided to attempt the conversion of nitrogen in the paramagnetic configuration to the non-paramagnetic configuration and vice versa, in a step wise way.

In attempting such a programme the first step

would be to irradiate diamonds containing only the two nitrogen configurations in order to create vacancies in the diamond lattice. This would be followed by mild heat treatment to render the vacancies mobile so that they can migrate to, and become attached to substitutional nitrogen atoms. Following this with heat treatment up to very high temperatures may then promote nitrogen migration and the possible formation of intermediate nitrogen aggregates. This envisaged programme is illustrated schematically in Figure 4.12.

FIGURE 4.12 FLOW SHEET ILLUSTRATING THE PROPOSED PROGRAMME FOR CHANGING THE SUBSTITUTIONAL NITROGEN CONFIGURATIONS IN DIAMOND.

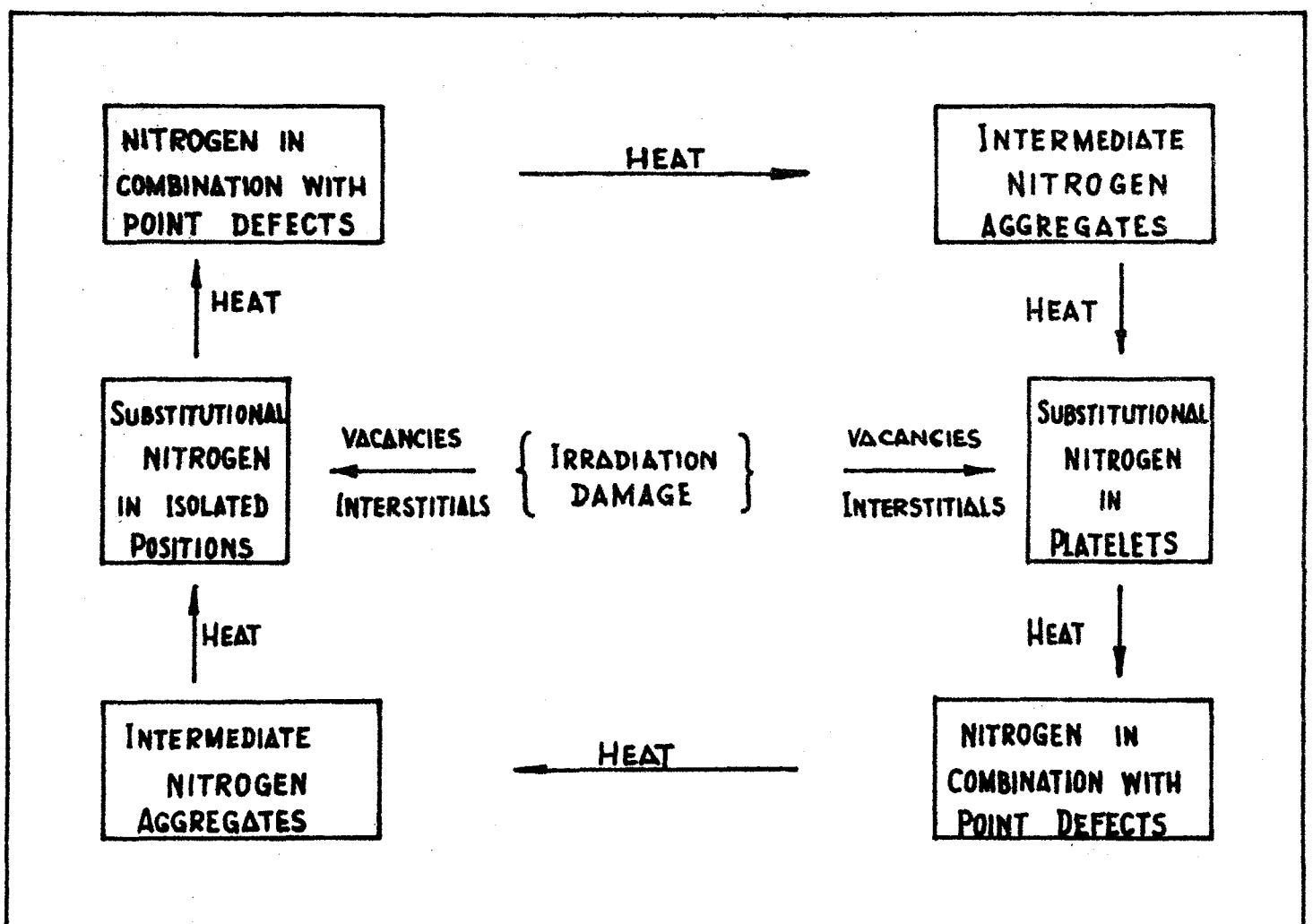

CHAPTER V.

PARAMAGNETIC NITROGEN IN NATURAL DIAMOND.

5.1. Introduction.

Before attempting a study of the conversion of substitutional nitrogen in the paramagnetic configuration to the non-paramagnetic configuration and vice versa, it was decided to investigate the absorption spectra due to paramagnetic nitrogen in detail. Such an investigation was necessary in order to avoid possible confusion of the spectra due to paramagnetic nitrogen, with those spectra that may arise from the formation of new defect centres.

From the specimens used for the survey, five transparent natural diamonds were specially selected as representing specimens containing only paramagnetic nitrogen defects in detectable amounts. The E.P.R., U.V.-VIS and I.R. absorption spectra observed in these specimens are described in this chapter, and the correlation between these spectra is discussed.

5.2. E.P.R. Absorption.

5.2.1. Existing Knowledge.

As mentioned in §4.4.1. Smith et al (1959 a) observed an anisotropic spectrum consisting of 3 equally intense, equally spaced lines with Ho || [100] direction. This was called spectrum (A), and was attributed to substitutional nitrogen donors in any one of four sites, which differ only in the symmetry axis for the hyperfine interaction with ^{14}N. The symmetry axis is in any of the four nearest neighbour directions. The spacing $|K|$ of the lines of the spectrum (A) was found to vary as;

$$K^2 = A^2 \cos^2\theta + B^2 \sin^2\theta \qquad (5.1)$$

and the hyperfine constants were determined as:

$$A = 38.1 \times 10^{-4} \text{ cm}^{-1}$$
$$B = 27.3 \times 10^{-4} \text{ cm}^{-1}$$

If the nitrogen donor electron occupied a hydrogen-like orbit of predominantly s character, the hyperfine interaction would be isotropic with A = B. As this is not the case, Smith et al concluded that there is a large admixture of p or a higher type orbit to the donor wave function, and proposed a model where the

electron with unpaired spin principally occupies an anti-bonding orbital between the nitrogen atom and one of its carbon nearest neighbours.

If the electron is in an orbital of this kind, the sites in which this particular neighbour is a ^{13}C atom ($I = \frac{1}{2}$; 1.1% natural abundance), should give rise to additional hyperfine lines 180 times weaker than the lines of spectrum (A). These lines, called spectrum (B), were found by Smith et al. The hyperfine constants, with a ^{14}N - ^{13}C bond being the hyperfine axis, are:

$$A = 113.5 \times 10^{-4} \text{ cm}^{-1}$$
$$B = 47.4 \times 10^{-4} \text{ cm}^{-1}$$

(The values actually quoted by Smith et al were $A = 56.75 \times 10^{-4}$ cm^{-1} and $B = 23.7 \times 10^{-4}$ cm^{-1}, i.e. half as much! An error must have slipped into their calculation.)

With Ho || [100] , Smith et al found an additional set of lines, called spectrum (C), spaced symmetrically 6.4 Oe on either side of the three lines of spectrum (A). This was attributed to hyperfine interactions with ^{13}C atoms in any one of the three positions, basal to the nitrogen of the N-C bond. Their calculated antibonding

wave function did not have the required density at such a large distance, and they suggested therefore a linear combination of antibonding orbitals.

No evidence of any quadrupole effects was found by Smith et al.

5.2.2. General.

By operating the spectrometer at very low energy densities in the cavity in order not to broaden the E.P.R. lines, many more lines due to the nitrogen donor could be detected. These new lines can be divided into three main groups, as they are due to three different causes. Following the notation used by Smith et al, the first group will be referred to as spectrum (C) as they are attributed to the interaction with the ^{13}C isotope. The other two groups will then be classified as spectrum (D) and spectrum (E) respectively.

These lines, in specimen D6, are illustrated in Figure 5.1 with Ho || [100]. The three lines of spectrum (A) are so much more intense that they overran the limits of the recorder.

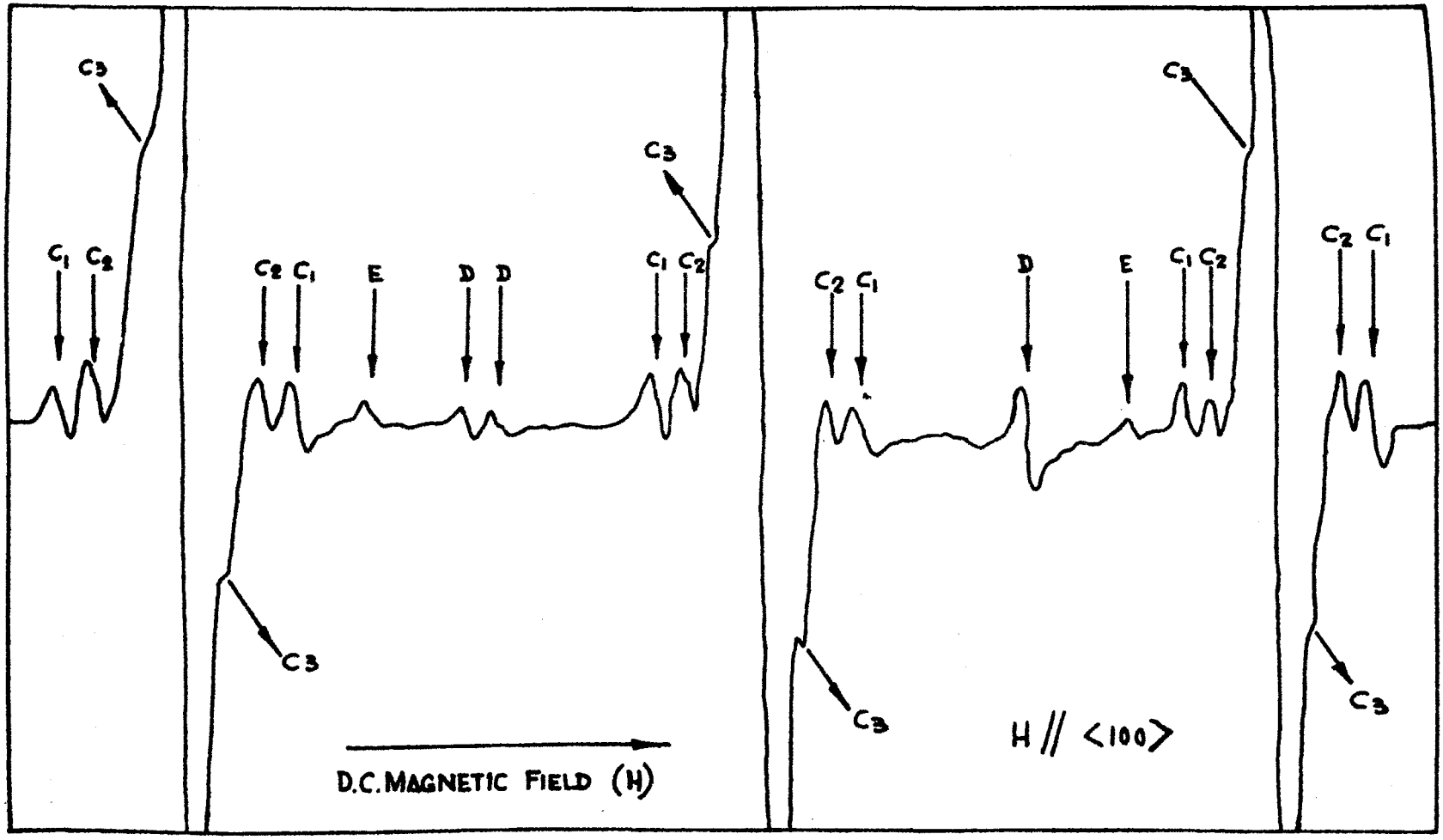

FIGURE 5.1 FIRST DERIVATIVE E.P.R. SPECTRUM OF SPECIMEN D6, ILLUSTRATING THE VARIOUS SYSTEMS ASSOCIATED WITH PARAMAGNETIC NITROGEN IN DIAMOND.

5.2.3. Spectrum (C).

This spectrum was found to consist of three pairs of lines symmetrically spaced on either side of the intense lines of spectrum (A). The outer pair is at 6.4 Oe ± 0.2 Oe. on each side of the central line of spectrum (A). This pair is therefore identified as the spectrum (C) lines of Smith et al, and will now be referred to as spectrum (C1). Smith et al could detect these lines only for Ho || ⟨100⟩; it is now evident that they can also be observed in the other orientations and that the hyperfine constants can therefore be evaluated.

The second pair of lines was observed at 4.6 Oe ± 0.3 Oe on either side of the intense spectrum (A) lines in all orientations. This will be referred to as spectrum (C2).

The third pair of lines closest to the intense lines of spectrum (A) could only be resolved for Ho||⟨100⟩, but did not seem to move with change of the applied field. They will be referred to as spectrum (C3).

The lines of all these spectra of the (C) series have equal intensity, and are about 60 times less intense than those of spectrum (A). They are therefore attributed to interaction with ^{13}C. The results of the

measurements on these lines are tabulated in Table 5.1. Also included in this table are the values of the hyperfine constants A and B calculated on the assumption that the hyperfine spacing $|K|$ depends on the angle Θ according to equation 5.1.

Smith et al suggested that the spectrum (C1) lines are caused by ^{13}C in one of the three basal carbon positions attached to the nitrogen atom, as illustrated by the C1 positions in Figure 5.2. This is a reasonable assumption since these carbon positions are closest to the nitrogen. It is suggested that the lines of spectrum (C2) are caused by ^{13}C in one of the carbon positions basal to the carbon in the N-C bond as illustrated by the C2 positions in Figure 5.2. The underlying assumption is that the unpaired electron in its antibonding orbital spends most of its time close to the nitrogen.

The probable positions of the ^{13}C giving rise to spectrum (C3) are as indicated by positions C3 in Figure 5.2. Again this is based on the assumption that the electron spends more of its time on the nitrogen in the N-C bond. That it is not one of the six next nearest neighbour positions in the plane perpendicular to the N-C bond containing the electron, is borne out by the

^{13}C HYPERFINE LINES - SPECTRUM (C)

θ = ANGLE BETWEEN Ho AND THE NITROGEN HYPERFINE AXIS	HYPERFINE SPLITTING DUE TO ^{13}C		
	SPECTRUM (C1)	SPECTRUM (C2)	SPECTRUM (C3)
$\theta = 0^{\circ}$	15.1 ± 0.5 Oe	9.2 ± 0.5 Oe	Could not be resolved
$\theta = 90^{\circ}$	11.4 ± 0.5 Oe	"	"
$\theta = 35^{\circ}$	13.7 ± 0.5 Oe	"	"
$\theta = 70^{\circ}$	11.7 ± 0.5 Oe	"	"
$\theta = 55^{\circ}$	12.8 ± 0.5 Oe	"	4.8 ± 0.5 Oe
CALCULATED HYPERFINE CONSTANTS (ASSUMING THE ^{13}C HYPERFINE AXES COINCIDENT WITH THE ^{14}N HYPERFINE AXIS)	$A_{(C1)} = 14.1 \pm 0.5 \times 10^{-4}$ cm^{-1} $B_{(C1)} = 10.7 \pm 0.5 \times 10^{-4}$ cm^{-1}	$A_{(C2)} = 8.6 \pm 0.5 \times 10^{-4}$ cm^{-1} $A_{(C2)} \approx B_{(C2)}$	$A_{(C3)} = 4.5 \pm 0.5 \times 10^{-4}$ cm^{-1} $A_{(C3)} \approx B_{(C3)}$ (probably)

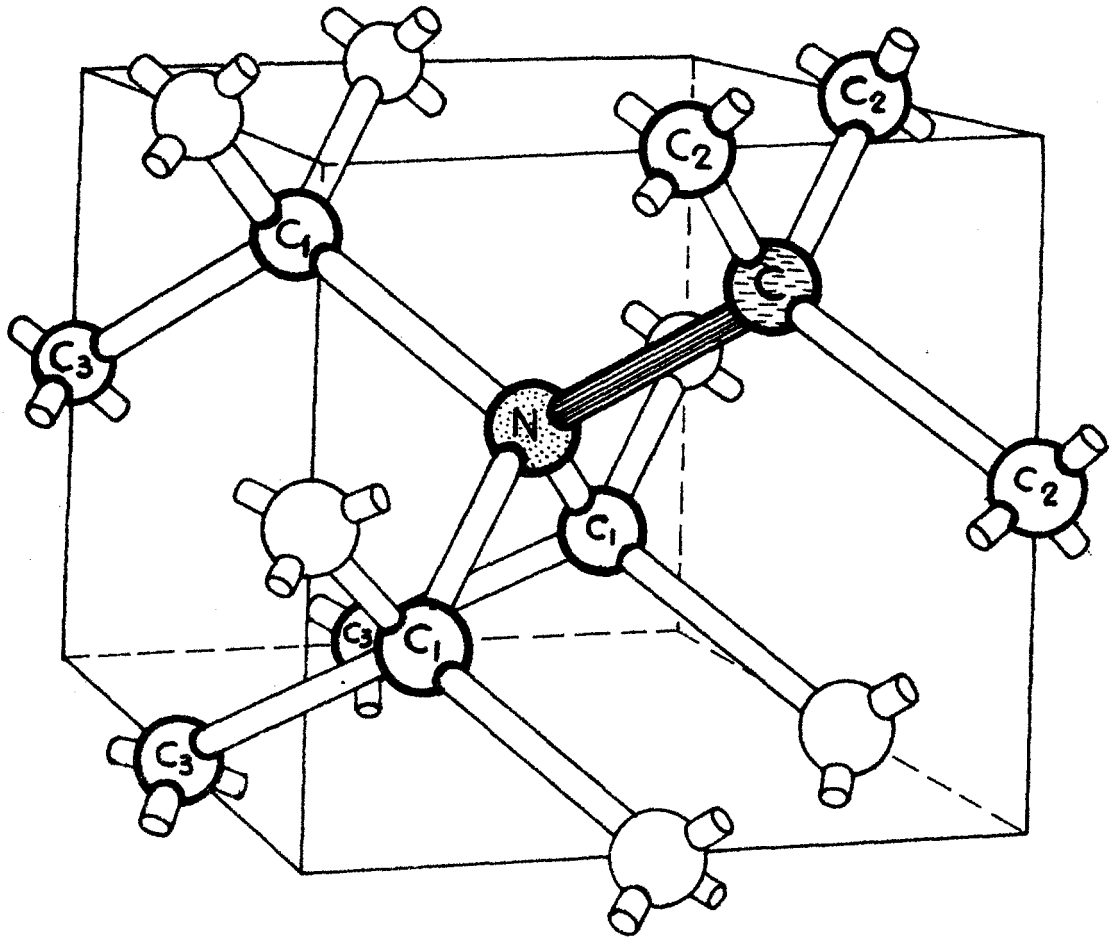

FIGURE 5.2 SCHEMATIC REPRESENTATION OF THE ^{13}C CENTRES RESPONSIBLE FOR THE GROUP (C) SPECTRA.

fact that the three (C) spectra all have the same intensity.

5.2.4. Spectrum (D).

This spectrum was first observed as two lines unequal in intensity approximately halfway between the intense lines of spectrum (A). The relative intensity of these lines varied with different orientations of Ho. The line at the higher magnetic field side is more intense than the line at the lower field side with Ho || <100>, of almost equal intensity with Ho || <110> and less intense with Ho || <111>.

These lines show no sign of saturation at the highest levels of microwave power available, whereas the lines of spectra (A), (B) and (C) give evidence of saturation at low energy levels.

Using the lowest 100 kc/s modulation possible, it was found that some of these lines are actually composed of two overlapping components. This is illustrated in Figure 5.1. The separation of the components that could be resolved, for different orientations of Ho, is given in Table 5.2. This difference in separation of the component lines would account for the different intensities

TABLE 5.2

^{14}N QUADRUPOLE HYPERFINE LINES - SPECTRUM (D)

θ = ANGLE BETWEEN Ho AND THE NITROGEN HYPERFINE AXIS		OBSERVED SEPARATION OF LINES		CALCULATED SEPARATION WITH P = -2.0 Oe	
		LOW FIELD SIDE	HIGH FIELD SIDE	LOW FIELD SIDE	HIGH FIELD SIDE
$\theta = 55^{\circ}$	$\langle 100 \rangle$	1.7 ± 0.2 Oe	Cannot be resolved	1.68 Oe	0.2 Oe
$\theta = 35^{\circ}$	$\langle 110 \rangle$	3.4 ± 0.2 Oe	2.0 ± 0.2 Oe	3.5 Oe	2.0 Oe
$\theta = 90^{\circ}$	$\langle 110 \rangle$	No lines found	No lines found	Zero intensity	Zero intensity
$\theta = 70^{\circ}$	$\langle 111 \rangle$	Cannot be resolved	1.4 ± 0.3 Oe	0.07 Oe	1.56 Oe
$\theta = 0^{\circ}$	$\langle 111 \rangle$	No lines found	No lines found	Zero intensity	Zero intensity

observed at higher modulation levels, where the components were not resolved.

The intensities of the lines of spectrum (D) are difficult to measure accurately; however, an estimate of their intensities relative to the lines of spectrum (A) indicated that they could be due to a quadrupole term in the Hamiltonian $P\left\{I^2-\frac{1}{3}I(I+1)\right\}$ with $|P|$ between 1.5 and 2.5 oersted.

The splittings of the spectrum (D) lines which were obtained from the measurements described here, were explained quantitatively by Loubser (1965) by using second order perturbation theory for the so-called "forbidden" $\Delta m = \pm 1$ lines, as developed by Bleaney (1951). The value of the coefficient P of the quadrupole term in the spin Hamiltonian had to be assigned a value of -2.0 ± 0.2 oersted $= -5.6 \pm 0.5$ Mc/s, in order to fit the experimental values. The correspondence obtained by Loubser is shown in Table 5.2. (The nuclear Zeeman term was taken to be -0.374 Oe for ^{14}N in the magnetic field used 3370 Oe). The $\Delta m = \pm 2$ lines will be displaced by only 0.75 Oe on either side of the isotropic centre line of spectrum (A), and thus, as expected were never resolved in this investigation.

From this value found by Loubser for the coefficient P, the quadrupole coupling constant eqQ for nitrogen can be calculated and compared with the values found for nitrogen in other compounds, and with values quoted in the literature for the valence electron of nitrogen. It follows from the theory (Bleaney 1951) that

$$P = \tfrac{3}{4}\, eqQ \qquad (5.2)$$

Where:

q = Electric field gradient at the nitrogen nucleus.

Q = Quadrupole moment of the nucleus.

The value of Q for ^{14}N is believed to be between 0.016 x $10^{-24}cm^2$ and 0.0071 x $10^{-24}cm^2$ (Lin 1960, Kato and Nakahara 1959 and Bassompierre 1955).

If it is assumed that the unpaired electron is responsible for the total field gradient, then it follows from the theory for a p electron that

$$q = -2e\left\langle \left\{ Z^2 - \tfrac{1}{2}\,(x^2+y^2) \right\} / r^5 \right\rangle$$
$$= -2e\, P_N \qquad (5.3)$$

Where $P_N = 1.9 \times 10^{24} cm^{-3}$ is the value calculated by

Smith et al from the nitrogen hyperfine constants.

From the experimentally measured value of P for spectrum (D) it is found that

$$eqQ = -7.5 \pm 0.6 \text{ Mc/s.}$$

Using the value of $q = 1.82 \times 10^{15}$ e.s.u. which is calculated from expression 5.3 above

$$Q = 0.057 \times 10^{-24} \text{cm}^2$$

This is about four times larger than the largest accepted value, and also larger than the upper limit of the quadrupole moment as predicted by the nuclear shell model.

If the value of q is taken as 3.6×10^{15} e.s.u. as estimated by Townes and Schawlow (1955) for a valency electron of nitrogen, a value of

$$Q = 0.011 \times 10^{-24} \text{cm}^2$$

is obtained, which is surprisingly close to the accepted value.

A possible explanation for this may be that the unpaired electron polarizes and distorts the other electrons around the nucleus so much that "antishielding" occurs and the field gradient is increased by a factor of four or five. This perturbation of the closed electron shells by an external unpaired electron will affect the magnetic hyperfine splittings only very slightly (Sternheimer 1952).

5.2.5. Spectrum (E).

This spectrum consists of two weak lines about 200 times less intense than the lines of spectrum (A) when Ho || <100>. They are illustrated for this orientation in Figure 5.1, and are thought to arise from hyperfine splitting by the ^{15}N isotope. This isotope, being 0.365% abundant and with nuclear spin $I = \frac{1}{2}$, would be expected to give rise to two weak lines of intensity 1/180 of that of the spectrum (A) lines.

The average separation between the two lines of spectrum (E) with Ho || <100> is 48.4 Oe. Using this value, the ratio of the magnetic moment of ^{15}N to that of ^{14}N is found to be

$$\frac{\mu_{^{15}N}}{\mu_{^{14}N}} = 0.72 \pm 0.02$$

The accepted ratio is 0.701, so that it can be confidently stated that spectrum (E) is really due to ^{15}N.

The presence of this spectrum due to ^{15}N serves to remove any doubt that the observed E.P.R. spectra are really due to the presence of substitutional nitrogen atoms in isolated positions in the diamond lattice. It is clear that although the electron is tightly bound, the degree to which it is confined to a particular nitrogen-carbon bond is less than is suggested by the work by Smith et al.

A more detailed theoretical investigation is needed to find an acceptable wave function explaining all the observed facts. This is currently being undertaken by Schonland and Every (1965).

5.3. O.A. in the U.V.-VIS Region.

The O.A. spectra for the five specially selected specimens, which were shown by the E.P.R. studies to contain only paramagnetic nitrogen in detectable quantities, were obtained. The O.A. spectra of two of these

specimens, D6 and D7, are illustrated in Figure 5.3. To obtain these spectra it proved necessary in all cases to work with very thin specimens (of the order of 0.1 to 0.2 mm) as the absorption coefficient between 4 eV and the fundamental absorption edge (5.4 eV) is in general large.

The form of the absorption spectrum characteristic of all diamonds containing only paramagnetic nitrogen in detectable amounts with E.P.R. absorption, has been found to be the same. By using an appropriate normalizing factor all the spectra obtained can, within the limits imposed by experimental technique, be brought into coincidence.

No fine structure was found in the spectra recorded at room temperature. At liquid nitrogen temperature some structure was observed between 4 eV and 5 eV. This is shown for specimen D6, in Figure 5.3. Imperfectly resolved lines were observed at 4.07 eV, 4.15 eV, 4.24 eV, 4.58 eV and 4.64 eV.

5.4. O.A. in the I.R. Region.

The five specimens, mentioned in the previous sections, all exhibited the intrinsic bands of diamond between 0.185 eV and 0.5 eV and, in addition, a completely

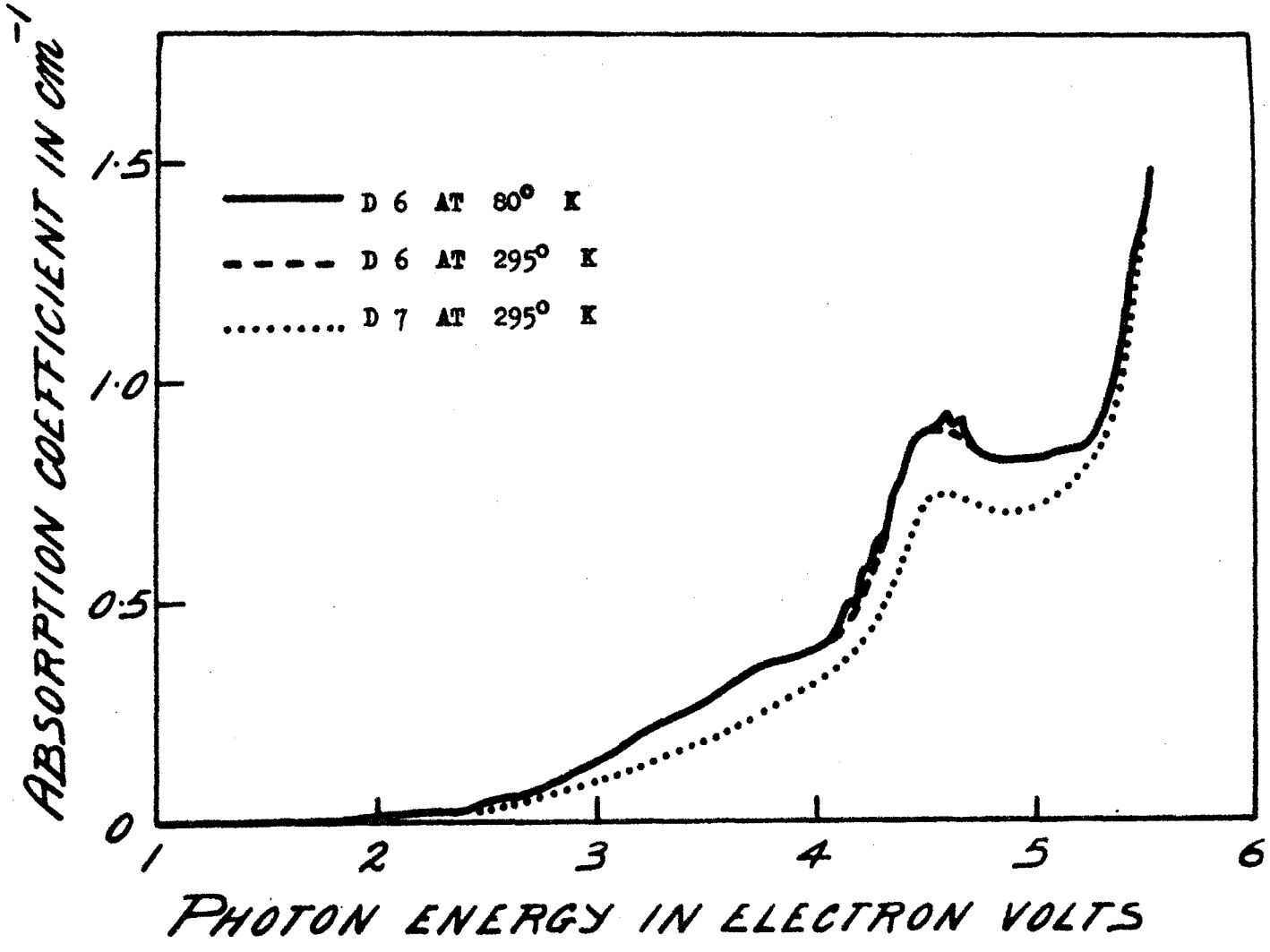

FIGURE 5.3 OPTICAL ABSORPTION SPECTRA OF SPECIMENS D6 AND D7 WHICH CONTAIN PARAMAGNETIC NITROGEN

new band system. This new system in specimen D6, which definitely contains no 4150A-centres, and probably no non-paramagnetic nitrogen, is shown in Figure 5.4.

The main features of the new system are:

a) The main band, with its peak at 0.140 eV.

b) A small sharp peak at 0.167 eV, and possibly

c) A broad saddle between 0.155 eV and 0.166 eV.

The uncertainty about the saddle arises because this occurs in the spectral region of the main band due to non-paramagnetic nitrogen platelets.(0.159 eV). The situation where a weak A-band due to platelet nitrogen is obviously present in a specimen D8, containing dispersed paramagnetic nitrogen as well, is illustrated in Figure 5.5.

The secondary absorption edge at 3.7 eV, associated with nitrogen platelets, does not help to resolve the uncertainty as to whether the broad saddle is due to dispersed or platelet nitrogen, because it cannot be resolved from the intense U.V. absorption arising from nitrogen platelets. However, the following facts suggest that the saddle is really part of the I.R. system specific to paramagnetic nitrogen:

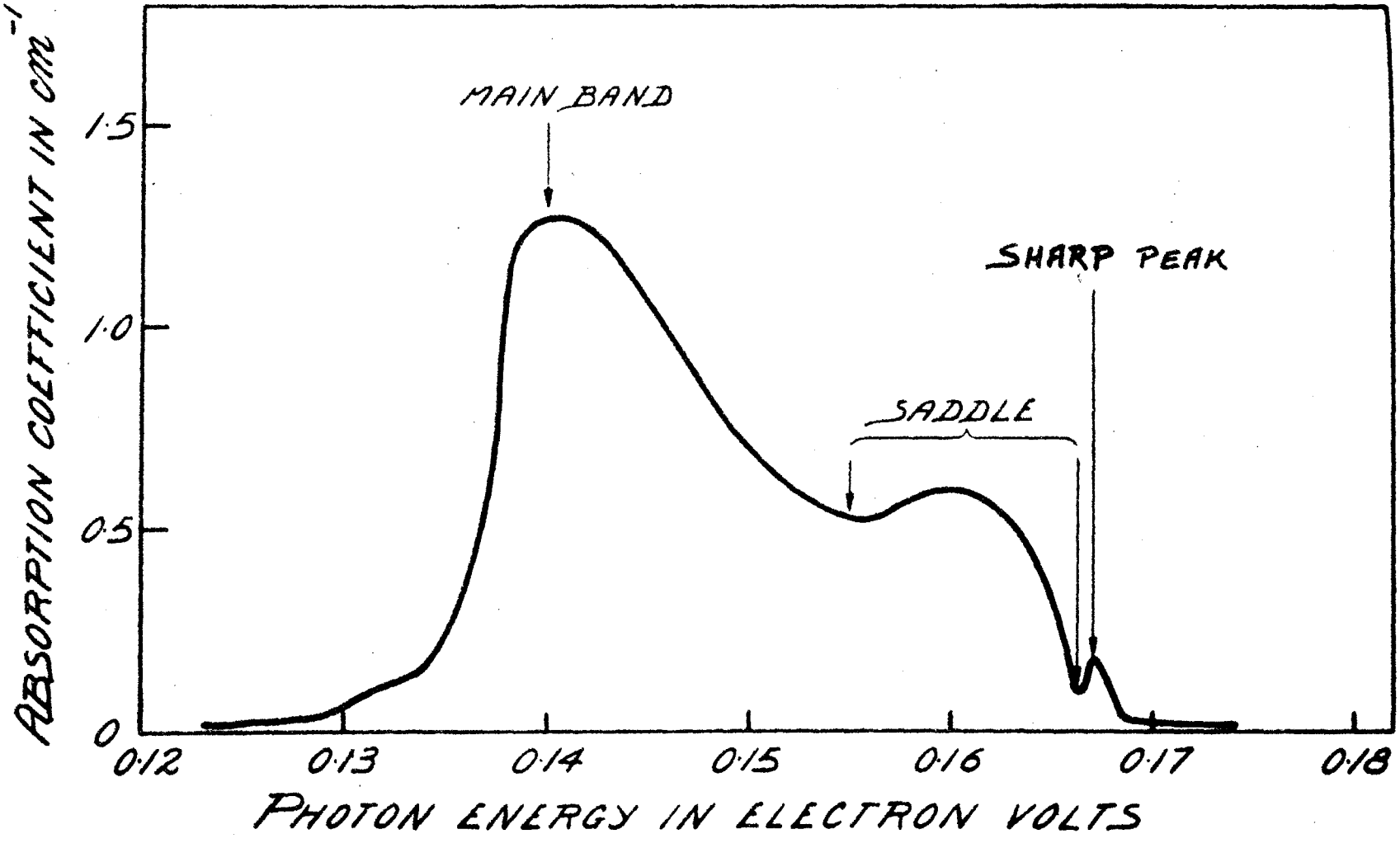

FIGURE 5.4 INFRA-RED ABSORPTION SPECTRUM OF NATURAL DIAMOND D6, WHICH CONTAINS PARAMAGNETIC NITROGEN.

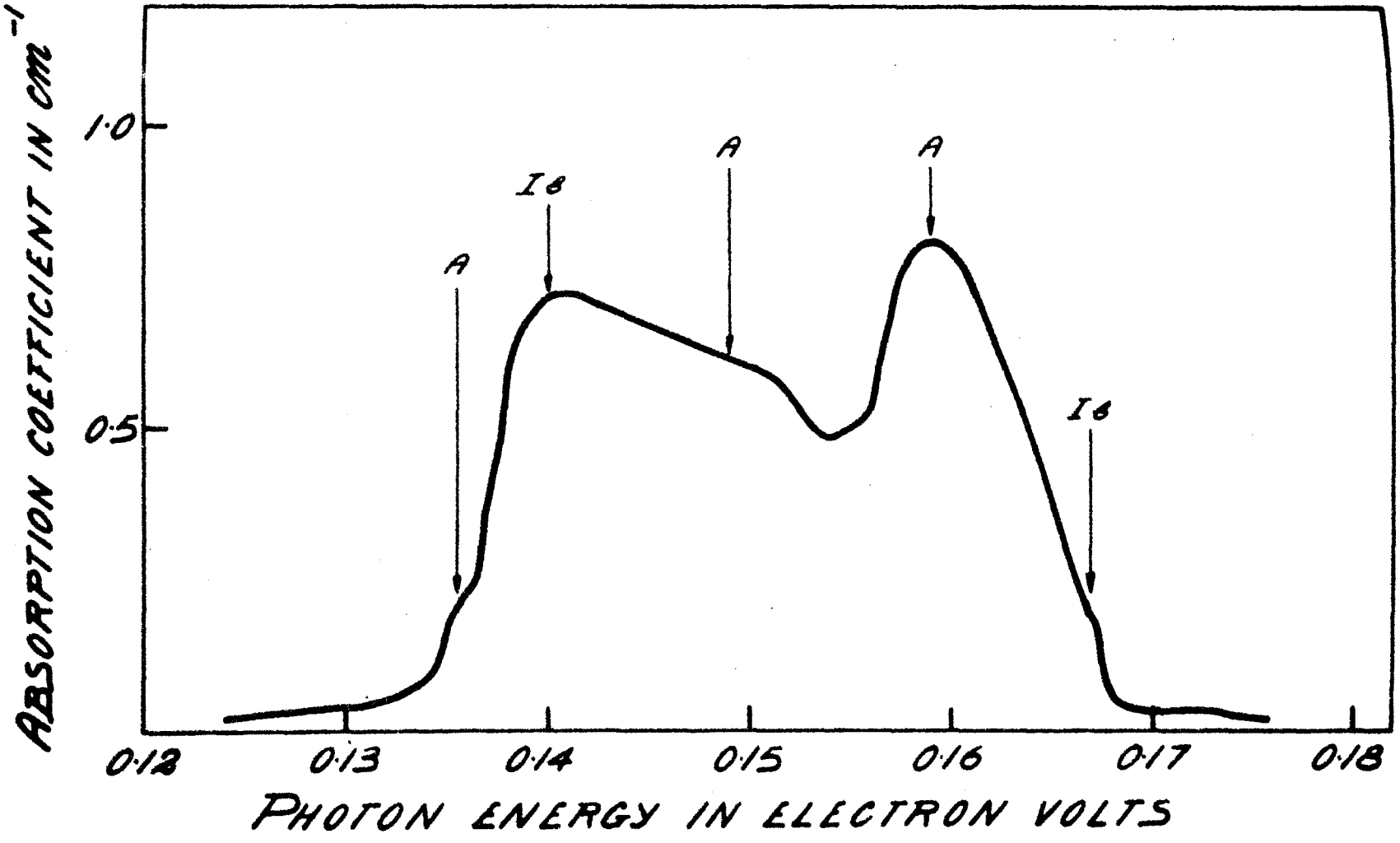

FIGURE 5.5 INFRA-RED ABSORPTION SPECTRUM OF SPECIMEN D8 CONTAINING BOTH NON-PARAMAGNETIC AND PARAMAGNETIC NITROGEN. THE PARAMAGNETIC NITROGEN FEATURES ARE LABELLED Ib.

a) The shape of the saddle is not precisely that of a weak 0.159 eV band.

b) Several specimens show spectra of exactly the form of Figure 5.4. This implies either that this is the true paramagnetic nitrogen spectrum, or that the non-paramagnetic to paramagnetic nitrogen ratio is precisely the same for each of these specimens, which appears improbable.

c) A similar saddle is observed in synthetic diamond; this will be discussed in Chapter VII.

It is of interest to note that the so-called A and B bands, due to non-paramagnetic nitrogen and 4150A-centres respectively, and the band system observed in paramagnetic nitrogen-containing specimens, can all co-exist in one specimen. This is illustrated in Figure 5.6 (Specimen D9).

5.5. Correlation between the Absorption Features.

It is difficult to measure accurately all the absorption features believed to be related to paramagnetic nitrogen in diamond in the same specimen, since the

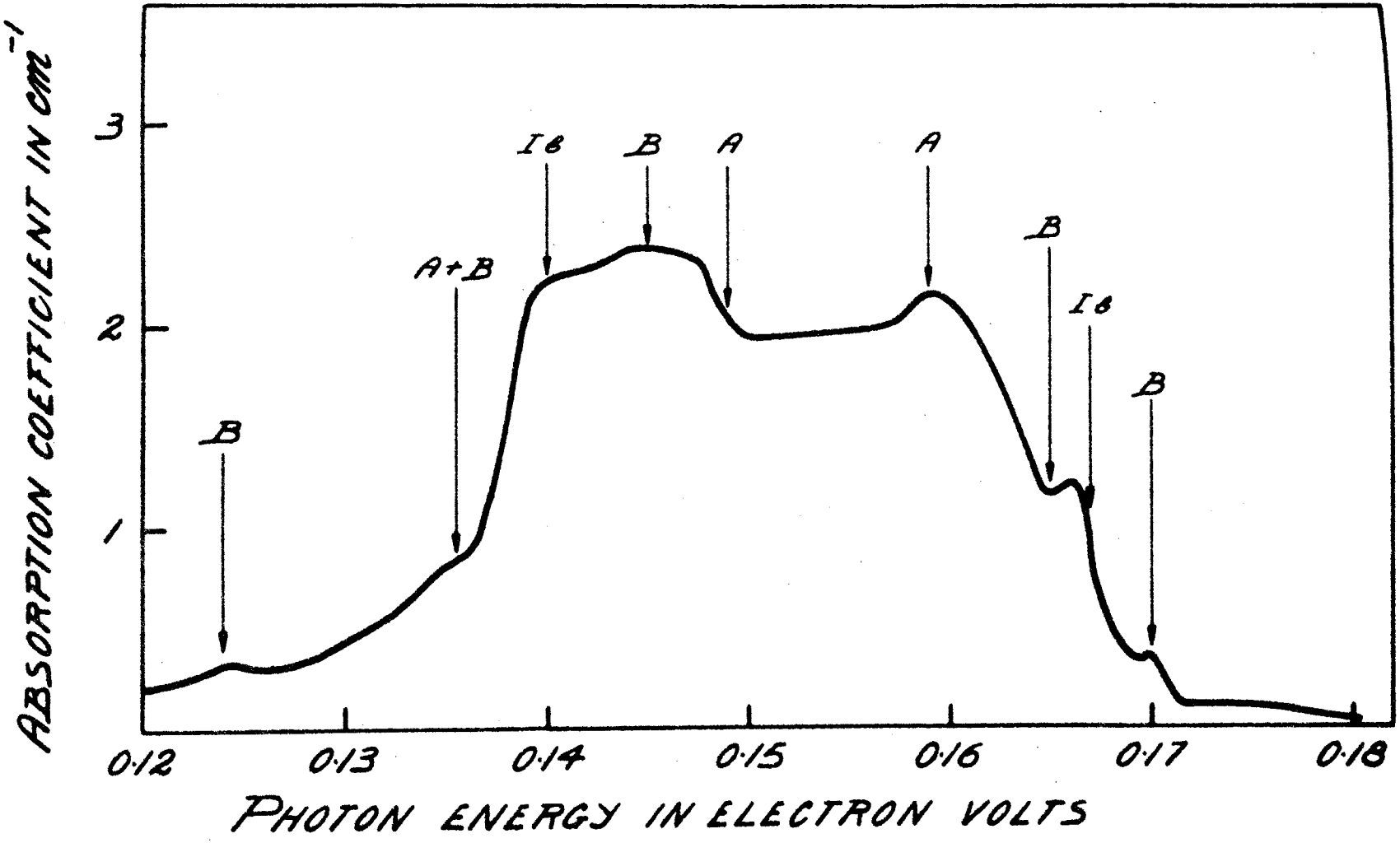

FIGURE 5.6 INFRA-RED ABSORPTION SPECTRUM OF SPECIMEN D9 ILLUSTRATING THE CO-EXISTENCE OF NON-PARAMAGNETIC NITROGEN (A), PARAMAGNETIC NITROGEN (Ib) AND 4150A-CENTRES (B).

U.V.-bands are intense and the I.R. bands are much weaker. For accuracy, thin specimens are needed in the former case, thick specimens are needed in the latter.

In the five specially selected specimens, the I.R. and E.P.R. spectra were measured when the specimens were relatively thick (2 to 3mm). I.R. measurements through various portions of the diamonds revealed that the absorbing centres were homogeneously distributed. The specimens were then thinned to about 0.2 mm, and the accurate U.V. measurements made.

The strengths of the E.P.R. and I.R. absorption were assessed by measuring the areas enclosed by the band systems. In the case of the U.V. features, this was not possible, as the major part of the absorption is a continuum; the slope of the absorption curve at 2.6 eV was therefore taken as a measure of the U.V. absorption intensity.

Linear correlation coefficients were calculated, and these are listed in Table 5.3. The significantly high values obtained indicate that there is a common cause for all three absorption systems, which, from E.P.R. evidence, is identified, as single substitutional nitrogen atoms in the paramagnetic configuration.

TABLE 5.3

LINEAR CORRELATIONS BETWEEN THE ABSORPTION FEATURES IN PARAMAGNETIC NITROGEN CONTAINING DIAMONDS

ABSORPTION FEATURES	CORRELATION COEFFICIENT
E.P.R./U.V.	0.94
E.P.R./I.R.	0.99
I.R./U.V.	0.94

5.6. Discussion.

It is now certain that the intense E.P.R. spectrum first observed by Smith et al (1959 a), who referred to it as the A-spectrum, arises from nitrogen in isolated substitutional positions in the diamond lattice. Many other E.P.R. lines, which are due to the interaction of the unpaired electron with the 1.1% abundant ^{13}C isotope, and the interaction of the small quadrupole moment of the nitrogen nucleus with the field gradient, occur in addition to this spectrum. These lines were catalogued so that they will not be confused with E.P.R. lines due to other defect centres in paramagnetic nitrogen containing diamonds.

The presence of nitrogen atoms in the paramagnetic configuration has the effect of introducing a strong absorption continuum beginning at 2.4 eV and stretching to the fundamental absorption edge at 5.4 eV. This continuum may be explained by postulating that the ground state of the extra unpaired electron of the isolated nitrogen atom is at about 3.0 eV above the valence band (2.4 eV below the conduction band). Transitions from this level to the conduction band would be expected to give rise to absorption beginning at 2.4 eV, and

increasing with an increase in photon energy. The general shape of the absorption continuum is similar to that of the U.V. band associated with irradiation damage and believed to be due to transitions from the ground state to the conduction band, as the result of experiments which will be described in Chapter VIII. Further evidence for this postulate of the position within the gap of the ground state of the unpaired electron was subsequently obtained by Vermeulen (1965) from a study of the photoconduction spectra of one of the specimens used in this study.

The I.R. bands originating from nitrogen in the paramagnetic configuration in diamond, occur in the region of the fundamental optical vibrational frequencies of the diamond lattice, despite the fact that absorption associated with single-phonon processes is explicitly forbidden in diamond. From the E.P.R. data it appears that the paramagnetic nitrogen centre is essentially a dipole whose axis is directed along one C-N bond. Such centres can locally destroy the symmetry of the lattice and thereby permit an electromagnetic coupling to the fundamental optical vibrational frequencies.

CHAPTER VI.

CLASSIFICATION OF DIAMONDS.

6.1. Introduction.

Robertson et al (1934, 1936) originally divided natural diamonds into two groups, Type I and Type II, on the basis of differences in a wide variety of physical properties. More recent investigations (e.g. Clark et al 1956 a), as well as this study, reveal that the basis of the classification of Robertson et al is the presence of the secondary absorption edge, (due to non-paramagnetic nitrogen) and 4150A-centres in Type I, and the absence of these defect centres in the Type II diamond.

Custers (1952, 1955) has sub-divided Type II diamonds into subgroups; Type IIa, which are insulators and Type IIb, which exhibit p-type semiconducting properties and are usually blue.

Although not describing all the defect centres known to occur in diamond this classification had definite merit as a convenient and brief definition of the properties of a particular diamond being described. However, diamonds containing paramagnetic nitrogen do not

fit into this system of classification.

6.2. Proposed New Classification.

From this study it became evident that the large majority of diamonds contain substitutional nitrogen in two different configurations. All the other defect centres, except those attributed to graphitic regions and acceptor centres, were also only detected in nitrogen-containing specimens and are therefore thought to be associated in some way with nitrogen.

It is therefore proposed that the sole criterion for diamonds being divided into two main types be taken as the presence or absence of nitrogen. Thus any diamond containing any nitrogen in detectable amounts will be classified as Type I, whereas any specimen in which no nitrogen can be identified will be classified as Type II.

As the nitrogen at this stage can be identified as being in two different substitutional configurations, it is further proposed that Type I diamonds be subdivided into Ia and Ib Types, depending upon whether the nitrogen occurs in platelet, non-paramagnetic form, or singly in dispersed, paramagnetic form.

As before Type II diamonds, in which no nitrogen

can be identified, will be subdivided according to their electrical properties, Type IIa specimens being insulators and Type IIb diamonds being semiconductors due to the presence of acceptor centres.

The characteristic physical properties of the various types of natural diamond are set out in Table 6.1. Also included in this table is the morphology, which the diamonds investigated in this study were found to exhibit. It can be seen that the presence and configuration of substitutional nitrogen in natural diamonds appear to effect the crystal morphology, however, it must be emphasised that this statement is based merely on the observations made during this study, and is essentially highly speculative.

6.3. Discussion.

In Table 6.1 no mention was made of the 4150A-centres. These occur in the great majority of Type Ia diamonds, but the nature of these centres is not sufficiently well understood to form the basis of a useful classification system.

TABLE 6.1

CHARACTERISTIC ABSORPTION PROPERTIES OF THE DIAMOND TYPES

TYPE	CHARACTERISTIC DEFECT CENTRES	CHARACTERISTIC U.V.-VIS, O.A. FEATURES	CHARACTERISTIC I.R., O.A. FEATURES	CHARACTERISTIC E.P.R. ABSORPTION FEATURES	ELECTRICAL RESISTANCE (Ohm. cm.)	CRYSTAL MORPHOLOGY
Ia	Nitrogen in Platelet form (Elliot 1960)	Secondary absorption edge (Clark et al 1956a)	A-bands (Sutherland et al 1954)	None (This study	10^{15} and above	Well-defined faces. Dodecahedra and Octahedra
Ib	Nitrogen in dispersed form (This study)	Paramagnetic nitrogen bands (This study)	Paramagnetic nitrogen bands (This study)	Paramagnetic nitrogen spectrum. (This study)	10^{15} and above	Poorly defined faces. Cubes.
IIa	No nitrogen; Structural defects (Clark et al 1956b)	Absorption tail between 2.0 eV and 5.4 eV (Clark et al 1956b)	None, only intrinsic bands of diamond (Lax and Burstein)	Single isotropic line (This study)	10^{3} to 10^{15}	No faces. Nondescript

TABLE 6.1 (Continued)

TYPE	CHARACTERISTIC DEFECT CENTRES	CHARACTERISTIC U.V.-VIS, O.A. FEATURES	CHARACTERISTIC I.R., O.A. FEATURES	CHARACTERISTIC E.P.R. ABSORPTION FEATURES	ELECTRICAL RESISTANCE (Ohm. cm.)	CRYSTAL MORPHOLOGY
IIb	No nitrogen; Acceptor centres (Wedepohl 1957b)	Absorption tail between 1.0 eV and 2.0 eV (Wedepohl 1957b)	Acceptor bands (Wedepohl 1957b)	None (This study)	50 to 1,000	No faces. Nondescript

The validity of this system of classification may be questioned in view of the possibility of a large measure of overlap between classes. However, from the survey of many natural diamonds it was evident that, while some overlap between classes was found, for the great majority of diamonds the characteristics of one particular class are dominant, and those of other classes, if present, are very much weaker.

CHAPTER VII.

SYNTHETIC DIAMONDS.

7.1. Introduction.

Although sought for very hard, a technique for producing diamond synthetically from graphite was not found until 1955 when the first successful synthesis was reported by Bundy et al (1955). Since then the problem has been investigated extensively by various laboratories, and today the technique for producing diamonds synthetically is well established.

In brief, synthetic diamond growth occurs only at high temperatures and pressures in the presence of certain molten metals which serve as solvents for carbonaceous material. The zones in the pressure/temperature phase diagram of carbon in which diamond can be grown from graphite have been determined for a number of metals. These zones are bounded by the melting line of the metal-carbon eutectic, and by the diamond-graphite equilibrium line. The experimentally determined equilibrium line agrees very closely with the linear extrapolation of the thermodynamically calculated line

proposed by Berman and Simon (1955), viz.

$$P \text{ (k bar)} = 7.1 + 0.027\ T\ (^{o}K).$$

Very little has been published about the occurence of defect centres in synthetic diamond. As these diamonds are generally dark yellow, substantial concentrations of defect centres of some form can be expected. In view of the classification system proposed in the previous chapter the question arose: can synthetic crystals be classified according to the proposed scheme, and if so, to which type do they belong? It was therefore decided to extend the survey of defect centres in diamond to include synthetic diamond. For this purpose batches of synthetic diamonds were grown using various metal solvents under several conditions of growth. The crystals obtained ranged in size from about 200 microns to about 500 microns, and exhibited a distinct dark-yellow to amber colour.

7.2. Ferro-Magnetic Impurities.

In distinction to natural diamonds, all the synthetic diamond crystals exhibited ferromagnetism.

X-ray fluoresence and diffraction analysis revealed the presence of inclusions of the solvent metal used to grow the crystals, which in most cases was ferromagnetic (e.g. iron, cobalt or nickel). In no instance could any of the included metal be found in solid solution in the diamond lattice. Careful investigations of the lattice parameters and density of the crystals revealed no metal atoms in solid solution in specimens containing up to 3% metal impurities by weight.

It appears evident therefore that most synthetic diamond samples contain included solvent metal giving rise to ferromagnetism; not being in solid solution in the diamond lattice, and will therefore not be classified as defect centres in diamond.

7.3. E.P.R. Measurements.

Huggins and Cannon (1962) briefly reported E.P.R. spectra which they, on rather indirect evidence, attributed to the presence of paramagnetic nitrogen in synthetic diamonds. Powder samples of average crystal size 400 microns, selected from batches grown under several conditions of growth, were investigated in more detail.

The majority of these samples exhibited the E.P.R. spectrum shown in Figure 7.1. The isotropic g-value of 2.0024 ± 0.0005 found for the system is the same, within experimental error, as that observed for natural Type Ib diamond.

The spectra differ from those observed in natural diamond in that the lines are considerably broader than that observed in natural diamond. The line widths ΔH (measured between maxima and minima of the first derivative spectra) are between 0.3 Oe and 1.0 Oe in natural Type Ib diamond. The central line of the synthetic diamond spectrum (Figure 7.1) has ΔH = 7.9 Oe ± 0.5 Oe. This broadening is believed to be due mainly to the presence of the ferromagnetic inclusions discussed in the previous section, which not being uniform in composition, and not randomly dispersed through the crystal, provides different magnetic field strengths, to which the paramagnetic centres are subject.

To check this latter point, crystals were grown using a non-ferromagnetic alloy, "Bright-Ray-S" (80% Ni, 20% Cr) as solvent. The E.P.R. spectrum exhibited by these crystals is shown in Figure 7.2. It can be seen that the central isotropic line is much narrower

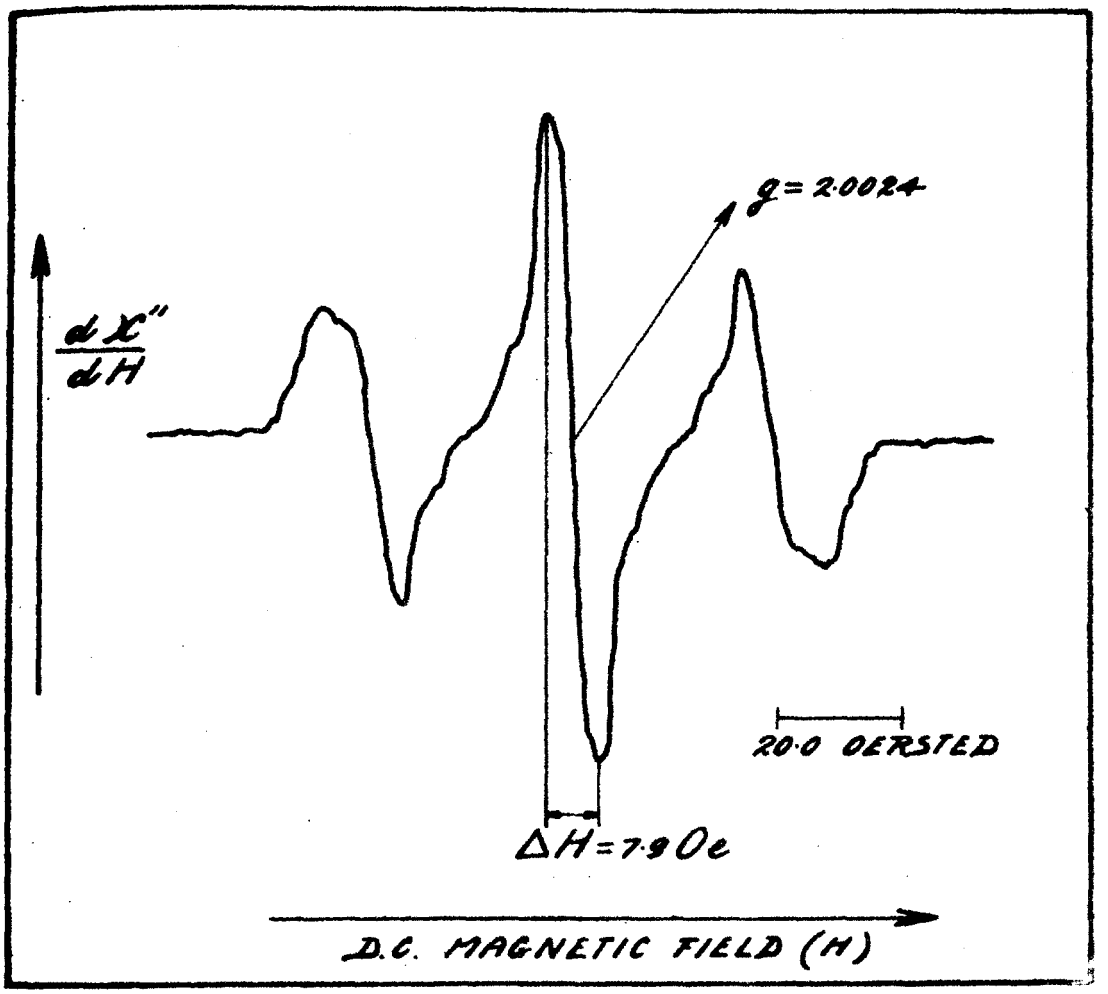

FIGURE 7.1 ROOM TEMPERATURE FIRST DERIVATIVE E.P.R. SPECTRUM OF SYNTHETIC DIAMOND, BATCH S.D.1, WHICH CONTAINS FERROMAGNETIC INCLUSIONS.

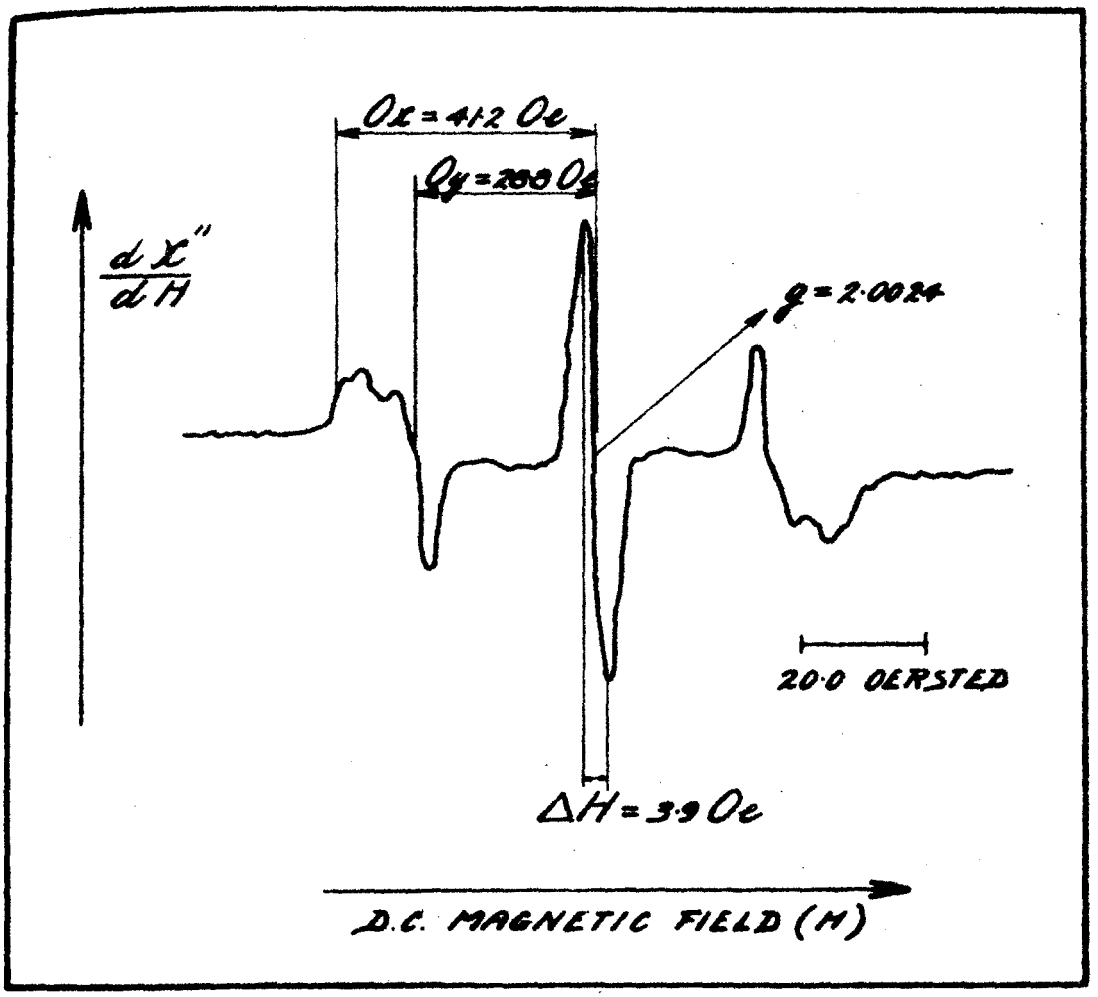

FIGURE 7.2 ROOM TEMPERATURE FIRST DERIVATIVE E.P.R. SPECTRUM OF SYNTHETIC DIAMOND, BATCH S.D.2, GROWN FROM NON-FERROMAGNETIC SOLVENT.

(ΔH = 3.9 Oe $\pm$ 0.5 Oe).

The three satellite lines arising from hyperfine splitting by the ^{14}N nucleus (referred to as spectrum (A) in Chapter V) have in this case the shape to be expected from an assembly of many crystals in random orientation. Using the same type of theory as that developed by Sands (1955), it can be shown that the maximum and minimum values of the spacing between hyperfine lines, A and B, can be readily obtained from the shape of the first derivative E.P.R. spectra for polycrystalline samples. Thus referring to Figure 7.2, the following values were obtained for the hyperfine constants:

$$A = Ox = 41.2 \text{ Oe} \pm 0.8 \text{ Oe}.$$
$$B = Oy = 28.8 \text{ Oe} \pm 0.6 \text{ Oe}.$$

This is in good agreement with the values of 40.8 Oe and 29.2 Oe obtained by Smith et al (1959 a) and there is therefore no doubt that the E.P.R. spectrum exhibited by synthetic diamond is due to the presence of paramagnetic nitrogen.

The amount of this paramagnetic nitrogen can vary between large limits (10^{14} atoms/cc to 10^{18} atoms/cc)

and depends on the environment in which the crystals are grown. By outgassing the synthesis capsule and then flushing it with nitrogen prior to subjection to synthesis conditions, the E.P.R. line intensity could be enhanced, whilst by taking precautions to exclude nitrogen from growing synthetic diamond; by flushing the outgassed capsule with purified argon, batches have been obtained in which the characteristic nitrogen spectra are absent.

7.4. Optical Measurements in the U.V. and VIS Region.

Several of the larger clear synthetic diamond crystals were selected for optical measurements. The specimens were too small for accurate quantitative measurement of absorption spectra, but the transmission spectra are sufficiently good for qualitative comparison with those obtained for natural Type Ib diamonds.

In Figure 7.3 transmission curves obtained from a natural Type Ib and a synthetic diamond are compared. It can be seen that the two curves are, as expected, very similar in nature.

7.5. Infra-red Measurements.

Charette (1961) measured several synthetic

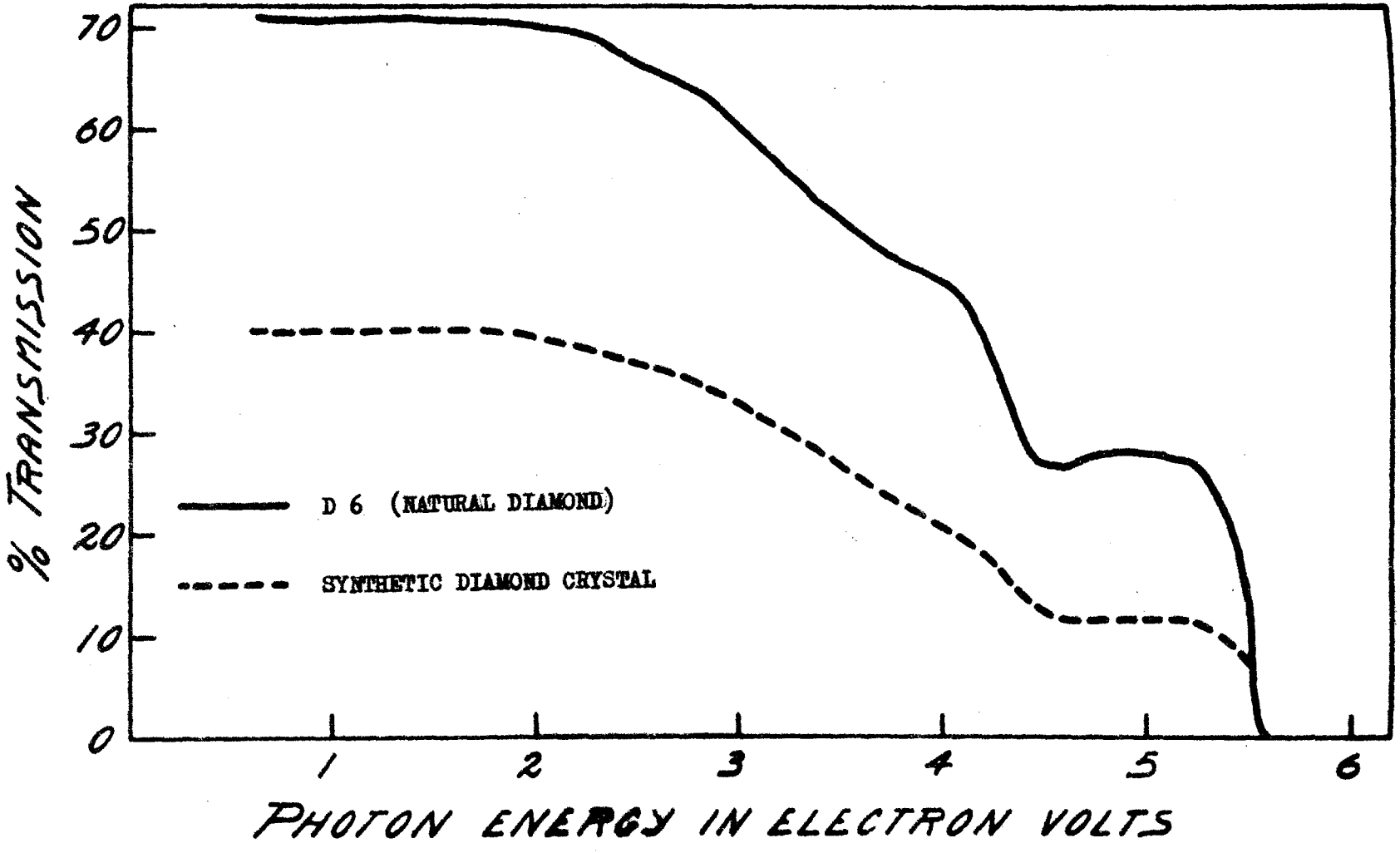

FIGURE 7.3 COMPARISON OF THE OPTICAL TRANSMISSION CURVES OBTAINED FOR NATURAL DIAMOND D6 AND A SYNTHETIC DIAMOND CRYSTAL SELECTED FROM BATCH S.D.2.

diamond specimens produced by the same technique as the batches used in this study. He reported the existence of the band system between 1000 and 1500 cm^{-1}, reproduced in Figure 7.4, but was not able to interpret or explain its origin.

Several synthetic diamond specimens were investigated in this survey. The spectra obtained confirm Charette's observations and are also closely analogous to those observed in natural Type Ib diamond (Figure 5.4). In view of this evidence, there seems no doubt that Charette's band system is due to paramagnetic nitrogen.

In both Charette's measurements and those of this study, a saddle appears between 0.155 eV and 0.166 eV. This is the saddle which could not positively be ascribed to paramagnetic nitrogen from measurements on natural diamond. Its size and shape in relation to the main band, at 0.140 eV, is the same as in natural Type Ib diamonds. It appears improbable that it can be due to the A-band system (which arises from non-paramagnetic nitrogen condensed into platelets) as it does not seem likely that migration and condensation of nitrogen into platelets could occur in the time necessary for the growth of the synthetic diamonds studied (of the order of minutes at

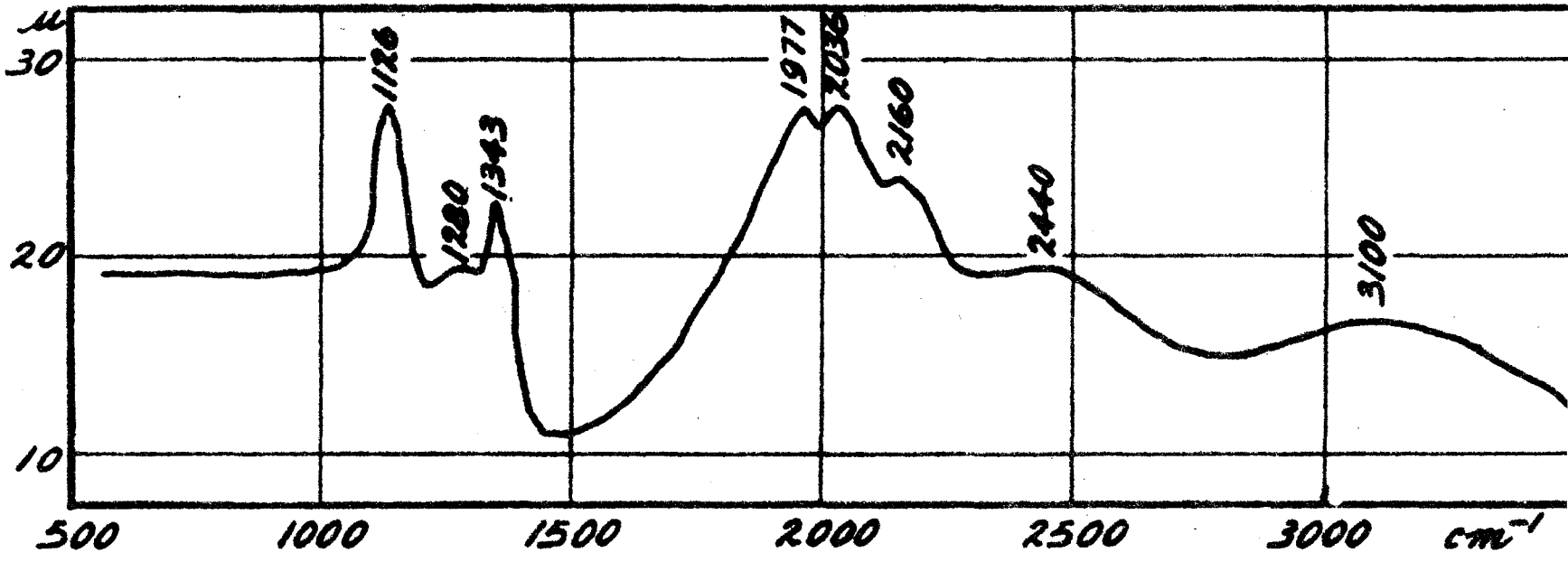

FIGURE 7.4 INFRA-RED SPECTRUM OF A SYNTHETIC DIAMOND CRYSTAL. REPRODUCED FROM CHARETTE (1961).

about 1600°C). In support, specimens grown at a higher temperature, and held at that temperature about five times longer, did not show a detectable increase in the saddle strength relative to the main line at 0.140 eV.

7.6. Doping Experiments.

7.6.1. General.

By introducing foreign atoms into the diamond lattice, defect centres can be produced, which can then be compared with the unidentified defects occuring in natural diamond specimens. In theory this can be effected in either of two ways. Firstly, by diffusion-doping, where a foreign atom is incorporated by solid state diffusion at high temperature in an existing crystal, or secondly, by growth-doping where foreign atoms are incorporated during crystal growth.

Diffusion doping experiments up to 2000°C, at high pressure, so as not to graphitize the diamond, were tried with a great variety of elements. No defects could be introduced in natural diamond crystals by this technique, presumably because this temperature is too low, or because the foreign atoms formed stable carbides at

the diamond surface.

Diamond synthesis offers an ideal opportunity for growth-doping. This was attempted by incorporating compounds, known to be unstable under diamond synthesis conditions, between the graphite and solvent metal interfaces; where diamond growth is believed to take place. Unfortunately the presence of these additional compounds made diamond synthesis very difficult, and diamond crystals could only be grown from ferromagnetic solvent metals. The crystals obtained were very small ($\pm$ 150 microns) and of such poor quality that no optical measurements could be made. They were therefore only studied by E.P.R. absorption, and this was further complicated by the presence of ferromagnetic inclusions in these crystals.

The synthetic diamond specimens obtained when Li, Be, Na, Mg, Si, P, S or As were present in the growth environment all exhibited only the E.P.R. spectrum illustrated in Figure 7.1 and were coloured dark yellow. There is therefore no positive evidence that any of these elements were incorporated in solid solution in the diamond lattice. It may be possible that atoms of these elements cannot exist in solid solution in the diamond

lattice, or that they formed a stable alloy with the solvent metal and were therefore not available for incorporation. Judging from the E.P.R. spectrum (Figure 7.1) it appears that nitrogen from the air, present in the growth environment, was apparently incorporated in isolated substitutional positions. This is not unexpected since nitrogen incorporation frequently occurs during synthetic diamond growth.

The specimens obtained when either boron or aluminium was present exhibited no E.P.R. absorption although air was present in the growth environment. The aluminium doped crystals were colourless and the boron doped crystals dark blue to indigo. It therefore appears that boron and aluminium were incorporated in substitutional positions, thus creating acceptor centres which compensated the substitutional nitrogen donor centres, but not giving rise to any E.P.R. absorption as discussed in § 4.6.3.

7.6.2. Nitrogen Doping.

Although nitrogen is incorporated readily in all synthetic diamond crystals in isolated substitutional positions, an attempt was made to increase the nitrogen

content by growth doping, to determine whether a different nitrogen configuration could be obtained. This was accomplished by incorporating sodium azide (NaN_3), a good nitrogen generator, in the growth environment. The same difficulties, described in the previous section, were encountered and again only E.P.R. spectra broadened by ferromagnetic inclusions, could be obtained. No detailed analysis of the results could therefore be carried out. These experiments were limited to a minimum, because of the potential danger of explosions due to the presence of NaN_3 at high temperatures in the pressure vessel.

The E.P.R. spectra exhibited by the crystals grown with various ratios by weight, of NaN_3 to graphite, are described in Table 7.1 and illustrated in Figure 7.5. It is clear that when the doping was low, the usual paramagnetic nitrogen spectrum was obtained. With increased doping the spectrum became much broader and the satellite hyperfine lines apparently less intense. The colour of the specimens changed to yellow-green. After heavy doping a broad single line, which narrowed on still heavier doping, was obtained (Table 7.1). These specimens exhibited a dark green colour and the total amount of paramagnetic centres became less.

TABLE 7.1

SYNTHETIC DIAMOND-GROWTH DOPING WITH NITROGEN

(All the E.P.R. spectra were obtained from 0.5g samples)

BATCH NO.	RATIO NaN_3/GRAPHITE BY WEIGHT	E.P.R. SPECTRUM	COLOUR	ESTIMATED NUMBER OF PARAMAGNETIC CENTRES PER cc.
S.D.1	0	Paramagnetic nitrogen Figure 7.1	Yellow	2×10^{17}
S.D.3	1/1000	Paramagnetic nitrogen Figure 7.5 (a)	Dark Yellow	1×10^{18}
S.D.4	1/250	3 Broad overlapping lines Figure 7.5(b)	Yellow Green	3×10^{17}
S.D.5	1/80	Single broad line $\Delta H \approx 20$ Oe Figure 7.5 (c)	Green	2×10^{16}
S.D.6	1/20	Single narrower line $\Delta H \approx 13$ Oe	Dark Green	5×10^{15}

FIGURE 7.5 FIRST DERIVATIVE E.P.R. SPECTRA OBTAINED FROM THE NITROGEN-DOPED SYNTHETIC DIAMOND CRYSTALS.

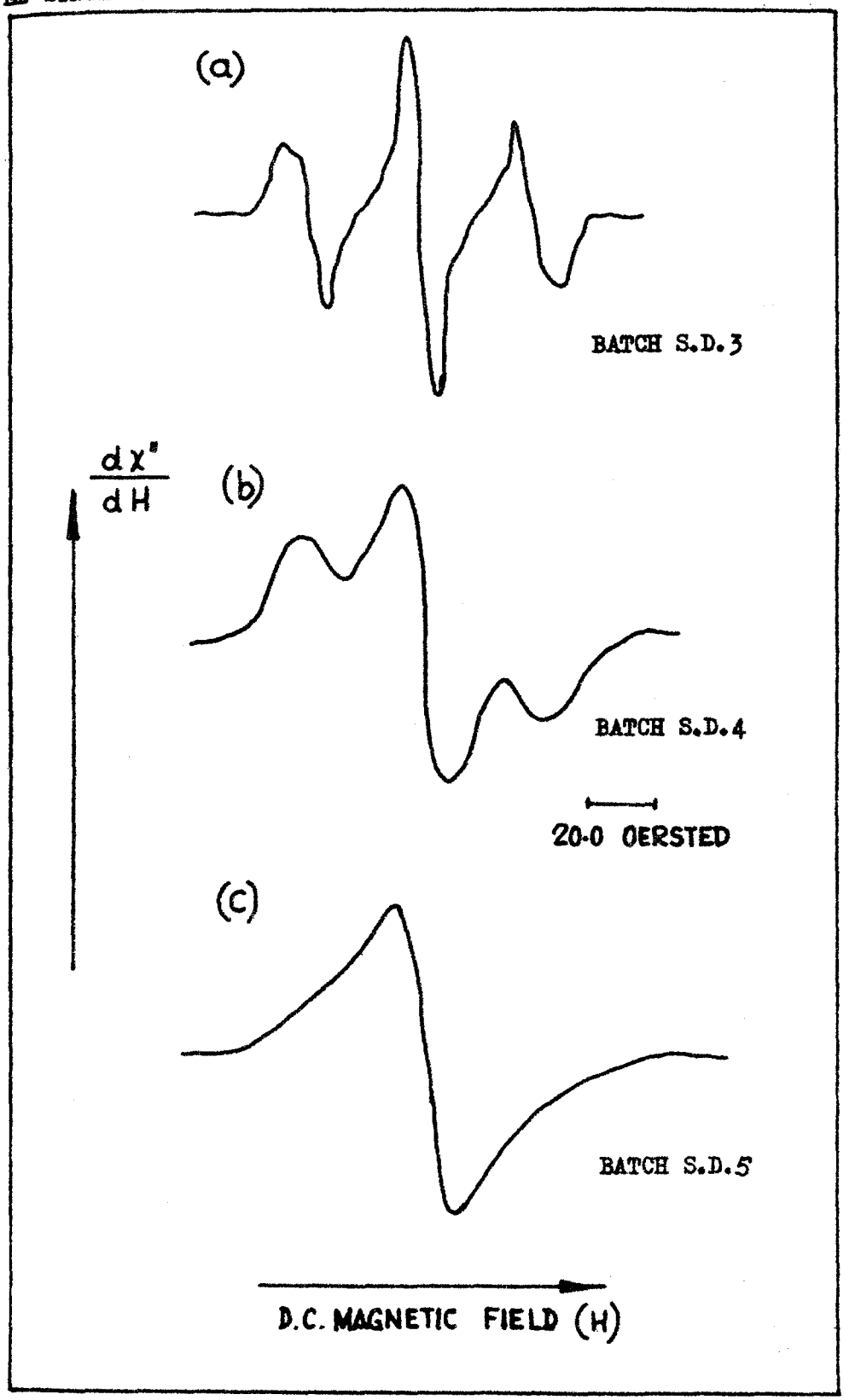

The crystals of batches S.D.3 (little doping) and S.D.6 (heavy doping), were mixed in equal amounts. The spectrum obtained from this mixture was very similar to that obtained from batch S.D.4 (medium doping). It is therefore concluded that the crystals of batch S.D.4 exhibit two superimposed spectra; arising from paramagnetic nitrogen in isolated positions and from the defects responsible for the single E.P.R. line.

Additional growth doping experiments with various sodium containing compounds indicated that the single E.P.R. line does not originate from Na, but from the nitrogen. From the evidence available it appears that substitutional nitrogen does not remain in isolated positions on heavy doping, but forms aggregates. Some of these aggregates are presumably non-paramagnetic, which would account for the fact that the number of paramagnetic centres becomes less when the nitrogen doping is increased. Others, giving rise to the single line may consist of substitutional nitrogen atoms in positions so close to one another that exchange interaction, as described in § 4.11.3, is effected.

The heavily doped crystals all had a green colour. The GR1 band, found in irradiated natural diamond,

which is known to arise from the presence of either vacancies or interstitials (ϕ 4.7.1), is known to impart a green colour to many diamond specimens. However, there is no reason to expect that heavy nitrogen doping would cause vacancies or interstitials; it is therefore suggested that the nitrogen aggregates responsible for the single E.P.R. line also give rise to an O.A. band in the red portion of the visible spectrum, which would cause a green colouration.

7.7. Discussion.

When no deliberate attempt is made to change the growth environment, synthetic diamond contain defect centres due to substitutional nitrogen in the paramagnetic configuration. This accounts for the dark yellow colour exhibited by these specimens. Synthetic diamonds can therefore be classified as Type Ib diamond.

On the contrary, the vast majority of all natural diamonds are Type Ia, Type Ib diamonds being rare exceptions. This is an expected result as the growth history of the specimens differs widely. Natural diamonds during growth and for subsequent millenia prior to kimberlite pipe formation, had probably been maintained at

a temperature sufficiently high for the processes of migration and condensation of nitrogen atoms into platelets to have been completed. This is certainly not true of the synthetic diamonds studied, whose total time at elevated temperature is measured in minutes.

Due to the nature of the crystals, no positive evidence could be obtained from growth doping experiments. However, the evidence indicates that boron or aluminium in substitutional positions can be responsible for the acceptor centres in natural diamonds, and that non-paramagnetic nitrogen aggregates can be present in synthetic diamond if the nitrogen concentration is very high. Evidence has been obtained to the effect that substitutional nitrogen aggregates, where exchange interaction takes place, can exist. These aggregates do not appear to give rise to an amber colour in the diamonds, as suggested in § 4.11.3, but are responsible for a green colouration.

CHAPTER VIII.

IRRADIATION DAMAGE IN TYPE Ia DIAMOND.

8.1. Introduction.

As most of the defect centres in natural diamond, described in Chapter IV, could not be identified, but appeared to be associated with nitrogen, it was decided to try to synthesize them by creating defects in specimens containing only the two known nitrogen configurations. Such specimens were therefore irradiated with fast electrons, whereby vacancies and interstitials were created. During subsequent heat treatment, these point defects might be expected to combine with the nitrogen, thus forming new defect centres; and ultimately, at very high temperatures, substitutional nitrogen migration to other configurations might be effected with a vacancy mechanism. The first stage in this programme was to irradiate Type Ia diamonds.

The results of irradiation damage and limited heating in Type Ia diamonds are described in this chapter. Many phenomena which were not understood, or were unknown in the past were encountered. An effort was

therefore made to pursue this first stage in the programme as extensively as possible.

8.2. Existing Knowledge.

As described in § 2.3.1., the Reading workers found that irradiation with electrons of energy between 0.3 and 0.8 MeV produces two O.A. systems in all diamonds. These are a band with its maximum at approximately 2.0 eV, known as G.R.1, and the U.V. band which extends from 2.8 eV to the fundamental absorption edge 5.4 eV. They are illustrated in Figure 8.1, and are thought to result from the creation of single vacancies and/or interstitial carbon atoms. Electrons of energy greater than 0.8 MeV produce additional absorption most easily observed at 2.696 eV, (which was termed the "absorption tail" in § 4.5) and thought to be associated with so-called "graphitic regions" arising from multiple defect generation.

The component lines of the G.R.1 band, measured at 80°K, are very much sharper in the case of electron irradiation than that for gamma-ray or neutron irradiation, although in each case irradiation is carried out nominally at room temperature. After heating gamma-ray or neutron irradiated diamond at 350°C, the G.R.1 is

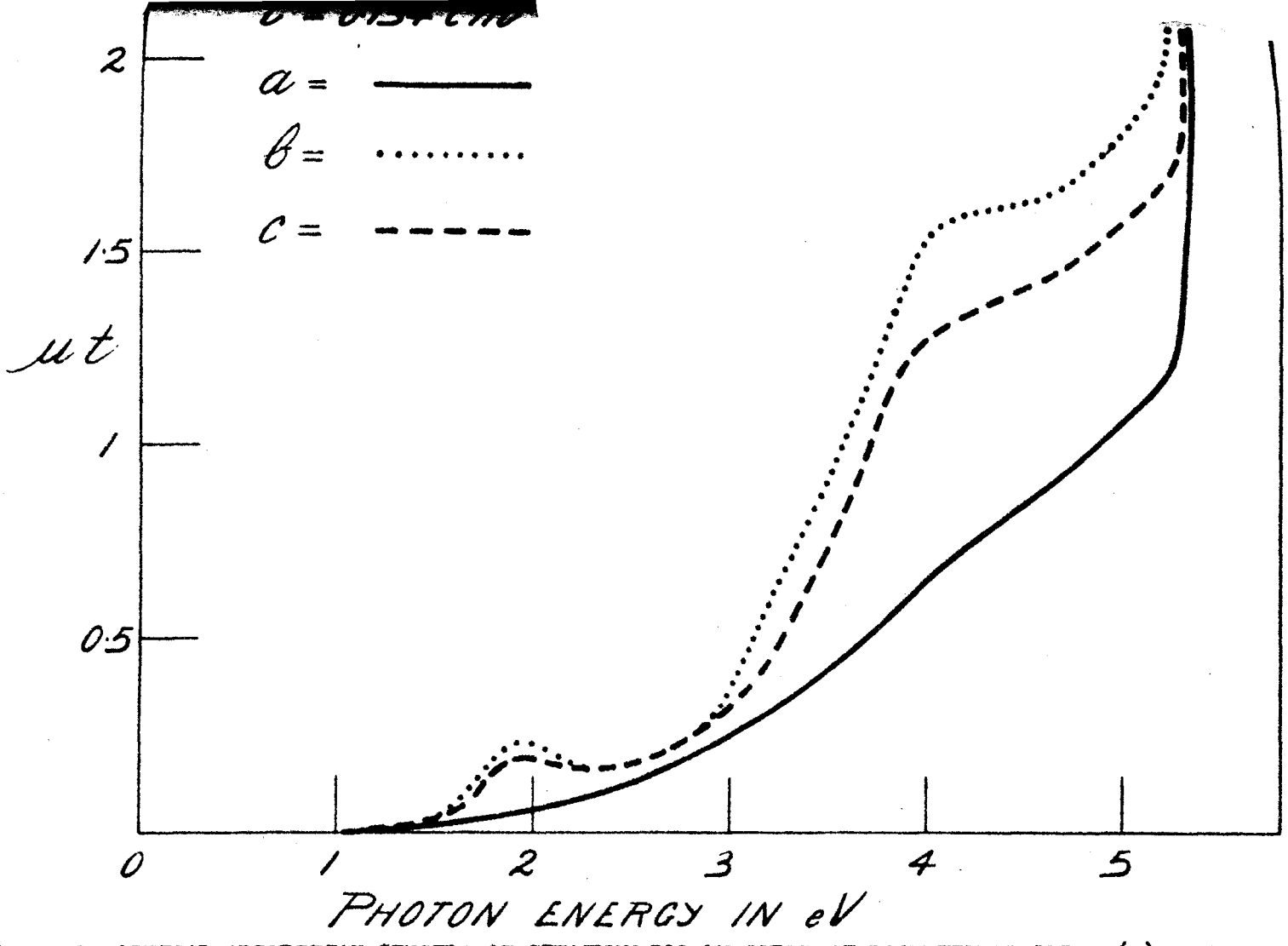

FIGURE 8.1 OPTICAL ABSORPTION SPECTRA OF SPECIMEN D11 MEASURED AT ROOM TEMPERATURE. (a) IN THE ORIGINAL CONDITION. (b) AFTER ELECTRON IRRADIATION. (c) AFTER HEATING AT 500°C.

reduced in size, and the form of the remaining G.R.1 absorption is the same as that observed for electron irradiation.

Clark et al (1956 a) explained the breadth of the lines in the case of neutron and gamma-ray irradiation as being due to perturbation effects arising from close interstitial/vacancy pairs. These close pairs recombine at 350°C, leaving only that absorption due to isolated and unperturbed defects (either vacancies or interstitials). In the case of electron irradiation at 20°C, it was suggested that this recombination of close pairs occurs during the irradiation, due to the high local temperatures which accompany bombardment with a high intensity electron beam.

Coulson and Kearsley (1957) found by a molecular-orbital calculation that an isolated neutral vacancy would have an electronic transition of about 2.0 eV, which is approximately the energy, 1.67 eV, of the principal G.R.1 line. More recently Yamaguchi (1962, 1963) performed a similar calculation. He evaluated the values of the intra-atomic orbitals in a modified way and concluded that the G.R.1 band can originate from some transition in a neutral interstitial, while the

U.V. band maximum value would correspond to transitions in a negatively charged vacancy. ~~(These contradictory theoretical results were discussed in Harwell lately; however, with the present state of knowledge the dispute could not be resolved.)~~

Faulkner and Lomer (1962) observed complex E.P.R. spectra in 2 MeV electron irradiated diamond which may be due to multiple defects. Baldwin (1963) demonstrated that the E.P.R. absorption induced in diamond by 0.75 MeV electron irradiation has the appearance of a single line, but is in fact composed of three superimposed lines arising from so-called A, B and C centres. The A-centre was shown to be due to isolated carbon vacancies. Recent workers, however, have not been able to reproduce Baldwin's results.

Pringsheim (1953) found that the last four lines of the 4150A system were enhanced when a neutron irradiated Type I diamond was heated in the dark at about 300°C. This enhancement could be optically bleached with light of energy greater then 2.3 eV. This was interpreted by Pringsheim as resulting from perturbations, induced by irradiation damage, in the neighbourhood of the 4150A-centres. He argued that the form of the perturbation is

reversibly altered by heating to about 300°C, making transitions to certain vibrational levels of the excited state more probable, and thus enhancing certain lines; bleaching reverses this process.

8.3. Specimen Selection.

A total of six diamonds was selected for detailed study. The amount of nitrogen present in platelet form was determined for each specimen by optical absorption techniques as described by Kaiser and Bond (1959). Details of the specimens are listed in Table 8.1.

8.4. Results.

8.4.1. Irradiation.

Irradiation was carried out as described in Chapter III, electron energy was maintained at 0.78 MeV throughout to avoid the possibility of multiple defect generations occurring.

After irradiation, specimens D_{11}, D_{12} and D_{13} each exhibited a G.R.1 and a U.V. band. The nitrogen-containing diamonds (D_{12} and D_{13}) showed, in addition, an absorption system between 3.1 eV and 3.8 eV, which

TABLE 8.1

DESCRIPTION OF THE SPECIMENS

SPECIMEN NUMBER	"TYPE"	APPROXIMATE NITROGEN CONCENTRATION (ATOMS/cc.)	4150A SYSTEM	APPROXIMATE IRRADIATION DOSE ELECTRONS/cm^2
D11	IIa	None detectable	None	2×10^{18}
D12	Ia	2.0×10^{20}	None	2×10^{18}
D13	Ia	7.0×10^{18}	None	2×10^{18}
D14	Ia	3.0×10^{20}	None	1×10^{18}
D15	Ia	8.8×10^{19}	None	6×10^{18}
D16	Ia	2.8×10^{20}	Very strong	4×10^{18}

will be referred to as the N.D.1 band. This is illustrated in Figures 8.1 and 8.2 for D_{11} and D_{12} respectively. Because of the decrease in density of the absorption centres with depth below the surface of a diamond after electron irradiation, the total absorption μt has been quoted, rather than the absorption coefficient μ; t is the specimen thickness.

The N.D.1 band in D_{12}, measured at room temperature and at 80°K, is shown in more detail in Figure 8.3. The structure of N.D.1 was found to be the same in all the specimens studied. The energies of the lines are listed in Table 8.2, where those of the 4150A system are included for comparison.

As suggested by Clark et al (1956 a) and Dyer and Matthews (1957) for other characteristic diamond systems (including G.R.1), it appears that the N.D.1 band consists of a principal line of lowest energy; additional less sharp lines arise from the interaction between the main electronic transition and vibrational states of the crystal. In this respect the system is quite typical of diamond.

From Table 8.2. it is clear that by chance the principal line of the N.D.1 band coincides in wavelength

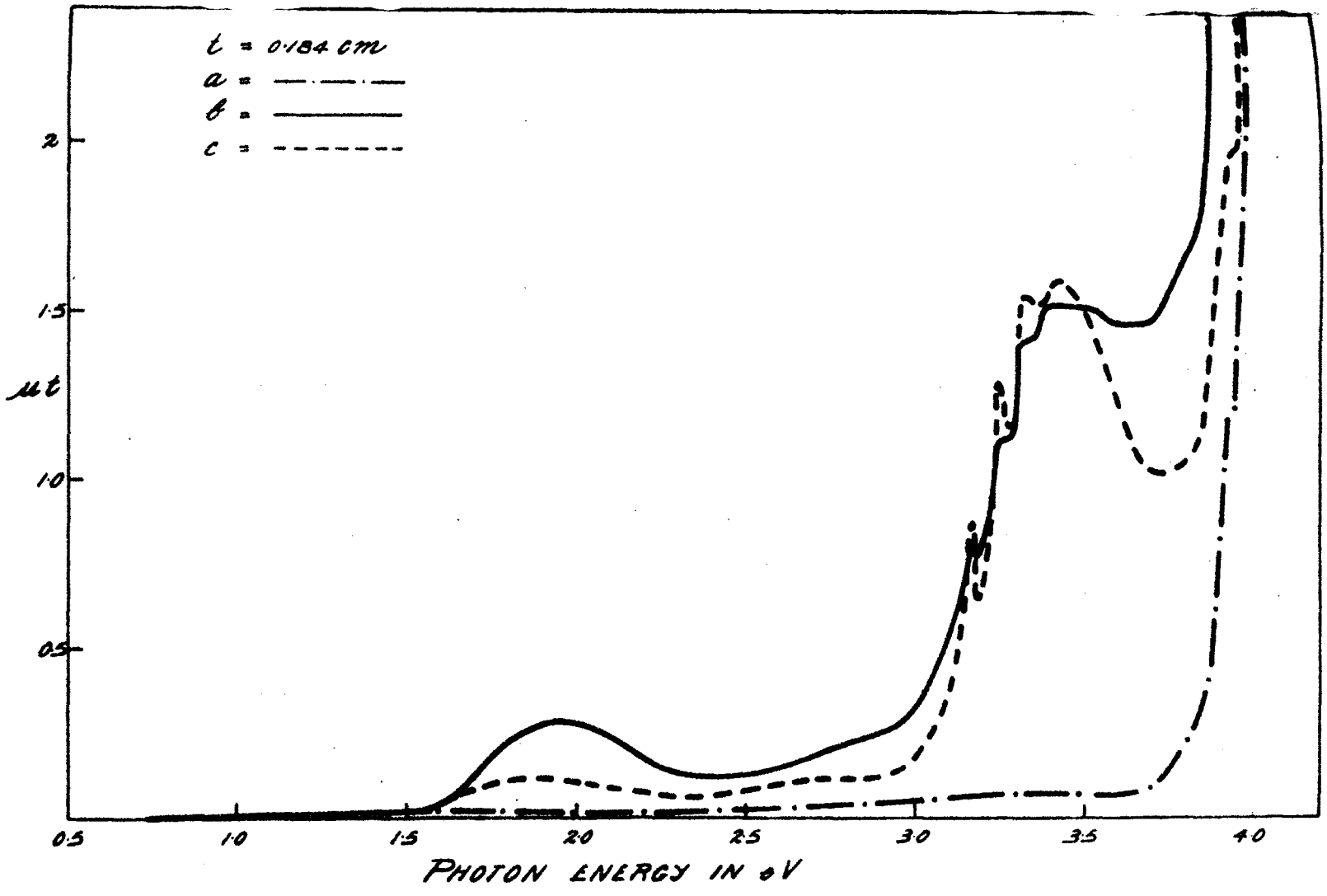

FIGURE 8.2 OPTICAL ABSORPTION SPECTRA OF SPECIMEN D12 MEASURED AT ROOM TEMPERATURE. (a) IN THE ORIGINA CONDITION. (b) AFTER ELECTRON IRRADIATION. (c) AFTER SUBSEQUENT HEATING AT 500°C IN THE DARK.

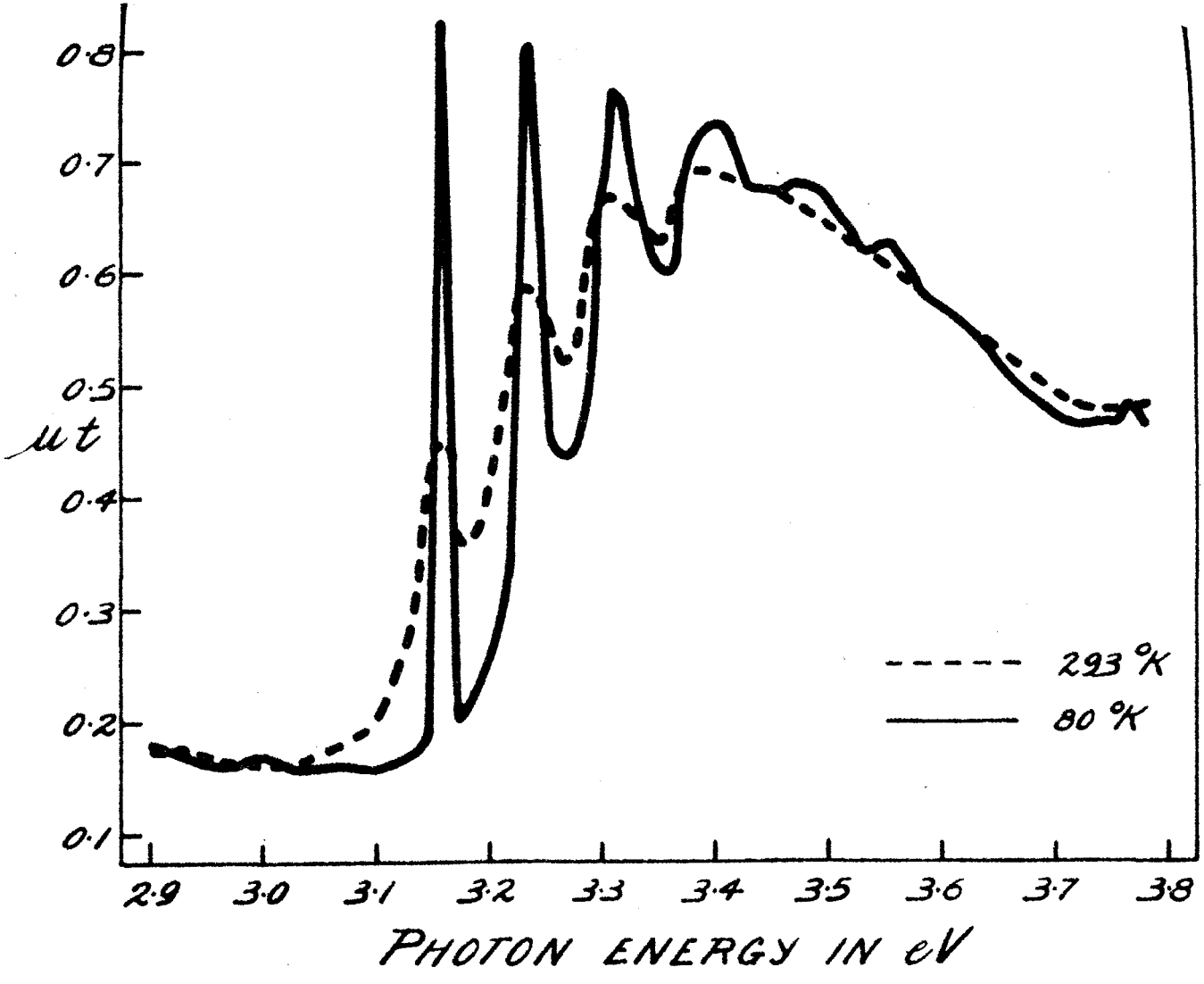

FIGURE 8.3 THE N.D.1 OPTICAL ABSORPTION BAND MEASURED AT ROOM TEMPERATURE AND AT LIQUID NITROGEN TEMPERATURE.

TABLE 8.2

ENERGIES OF THE MAIN OPTICAL ABSORPTION FEATURES OF THE N.D.I. AND 4150A BANDS

OPTICAL ABSORPTION FEATURE	POSITION IN eV	
	N.D.I. BAND	4150A BAND
Lower energy limit	3.10	2.95
Principal line	3.16	3.00
Second line	3.24	3.09
Third line	3.31	3.16
Fourth line	3.40	3.24
Fifth line	3.48	3.31
Sixth line	3.55	3.37
Higher energy limit	3.80	3.60

with the third line of the 4150A band. Furthermore, because the lines of the N.D.1 band have about the same spacing, (about 0.08 eV) as those of the 4150A band, the first four lines of the N.D.1 band coincide in wavelength with the last four lines of the 4150A band. This fact was verified by irradiation of specimen D_{16} which contained a large 4150A band. After irradiation the N.D.1 band is observed to be superimposed on the 4150A band, and it appears as if the last four lines of the 4150A band are enhanced by irradiation.

It is thus clear that Pringsheim's suggestion that the observed absorption in the region 3.1 eV to 3.8 eV after irradiation was due to a modification of the 4150A system, is incorrect. The N.D.1 band is completely independent of the presence or absence of the 4150A band, and is a system in its own right.

8.4.2. E.P.R. and I.R. Spectra after Irradiation.

The E.P.R. and infra-red spectra of all specimens were recorded before and after irradiation. No changes were observed at this or subsequent stages in the infra-red, so no further mention will be made of these measurements.

Before irradiation no E.P.R. absorption was detected in D_{12} and D_{13}. A single isotropic line, which was associated with the C.A. "absorption tail" and attributed to the presence of graphitic regions in § 4.5.3. was observed in D_{11} (Type IIa).

After irradiation, the line found in D_{11} was enhanced; this is presumably due to the superimposition of the A, B and C lines reported by Baldwin (1963) upon the existing Type IIa line. In both D_{12} and D_{13} a strong isotropic line was observed, that in D_{12} being seven times, and in D_{13} twice as large as the total line intensity in D_{11} after irradiation.

In neither specimen was it possible to resolve the induced line into component lines, and the line width (measured between maxima of the first derivative spectrum) of 1.9 Oe $\pm$ 0.3 Oe was the same in each case. The spectrum measured for specimen D_{12} is shown in Figure 8.4; the total line intensity corresponds to a defect centre concentration of approximately 10^{17}/cc.

8.4.3. Heat Treatment at 500°C of the Irradiated Specimens.

Specimens D_{11}, D_{12} and D_{13} were now heated in

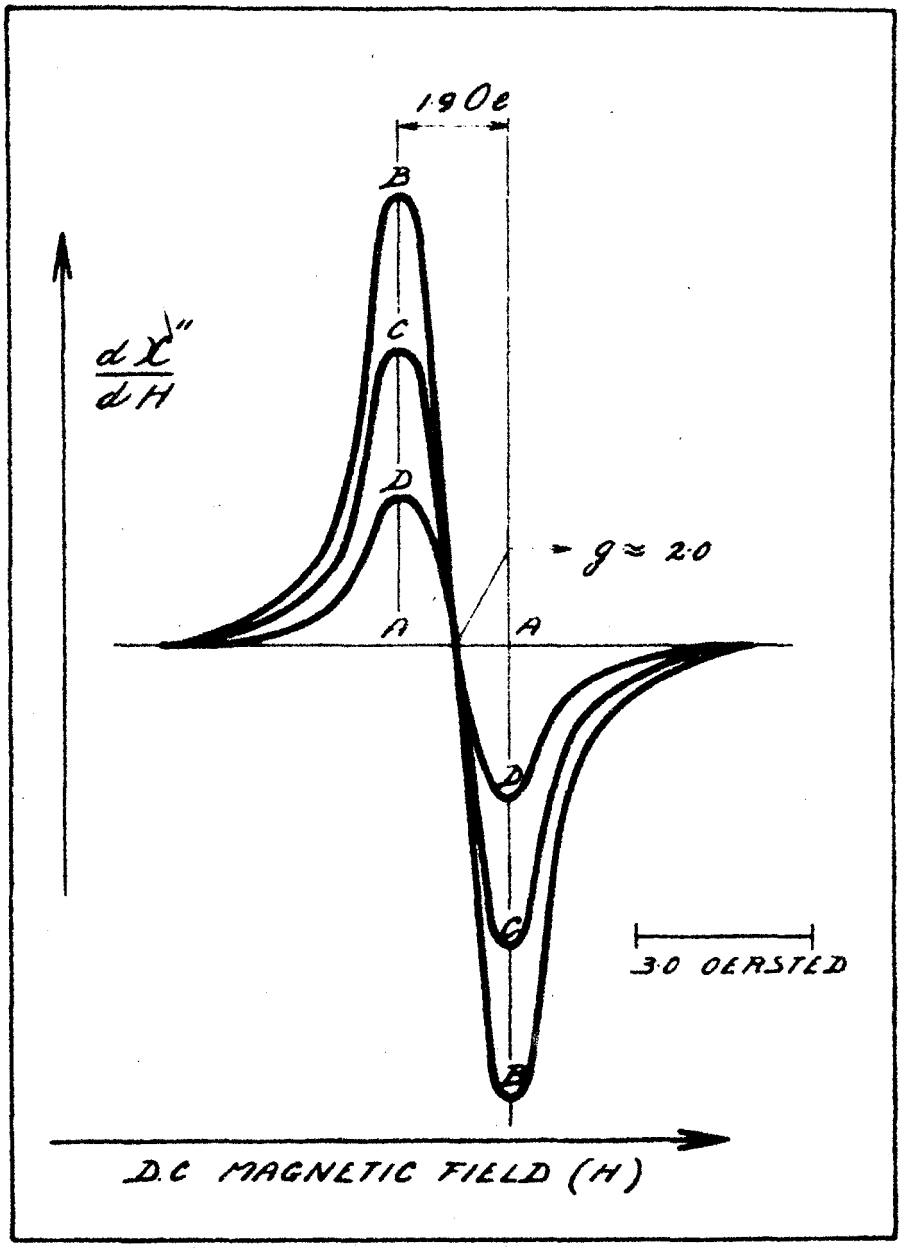

FIGURE 8.4 FIRST DERIVATIVE E.P.R. SPECTRA OF SPECIMEN D12.

(a) IN THE ORIGINAL CONDITION.

(b) AFTER ELECTRON IRRADIATION.

(c) AFTER SUBSEQUENT HEATING AT 500°C.

(d) AFTER ILLUMINATION WITH MERCURY LIGHT.

the dark for four hours at 500°C in vacuo. In D_{11} (Type IIa) the effect was to reduce the strengths of G.R.1 and the U.V. band. This is an expected result as Clark et al (1956 a) have shown that at about 350°C limited vacancy interstitial recombination occurs leading to just such a reduction in absorption. In both nitrogen-containing specimens these bands were observed to decrease by an amount greater than that observed in D_{11}. Furthermore, the reduction appeared specimen dependent, D_{12} showing a greater decrease than D_{13}. At the same time an increase in the N.D.1 band was observed which showed a similar specimen dependence - i.e. an increase proportional to the nitrogen concentration. This is illustrated for D_{12} in Figure 8.2.

The change in intensity of the E.P.R. line as a result of this treatment was not consistent - in specimen D_{12} the line decreased substantially (Figure 8.4); in D_{13} it was found to increase in intensity.

8.4.4. Reversible Optical Bleaching of the Irradiation Induced Bands.

The specimens were now exposed to alternate bleaching and heating cycles. Bleaching was done at room

temperature for periods of 10 minutes, using light from a quartz envelope high pressure mercury lamp. Heating was carried out in the dark for four hour periods at 500°C.

In both D_{12} and D_{13} exposure to mercury light resulted in an increase in the size of G.R.1 and the U.V. band while the N.D.1 band and the E.P.R. line were reduced in size; prolonging the time of exposure beyond 10 minutes resulted in no further change. The Type IIa specimen D_{11} was unaffected.

Heating of D_{12} and D_{13} at 500°C for four hours restored the N.D.1 band and the E.P.R. line to their former strengths, while G.R.1 and the U.V. band were correspondingly reduced. Again D_{11} was unaffected. These changes are illustrated in Figures 8.4 and 8.5.

The strengths of the N.D.1 and G.R.1 bands were measured by obtaining the integrated total absorption between 3.1 and 3.8 eV for N.D.1, and between 1.65 eV and 2.4 eV for G.R.1. A qualitative measure of the behaviour of the U.V. band was obtained by recording the total optical absorption at 2.85 eV for each specimen after each stage in the treatment.

These band strengths, together with that of the

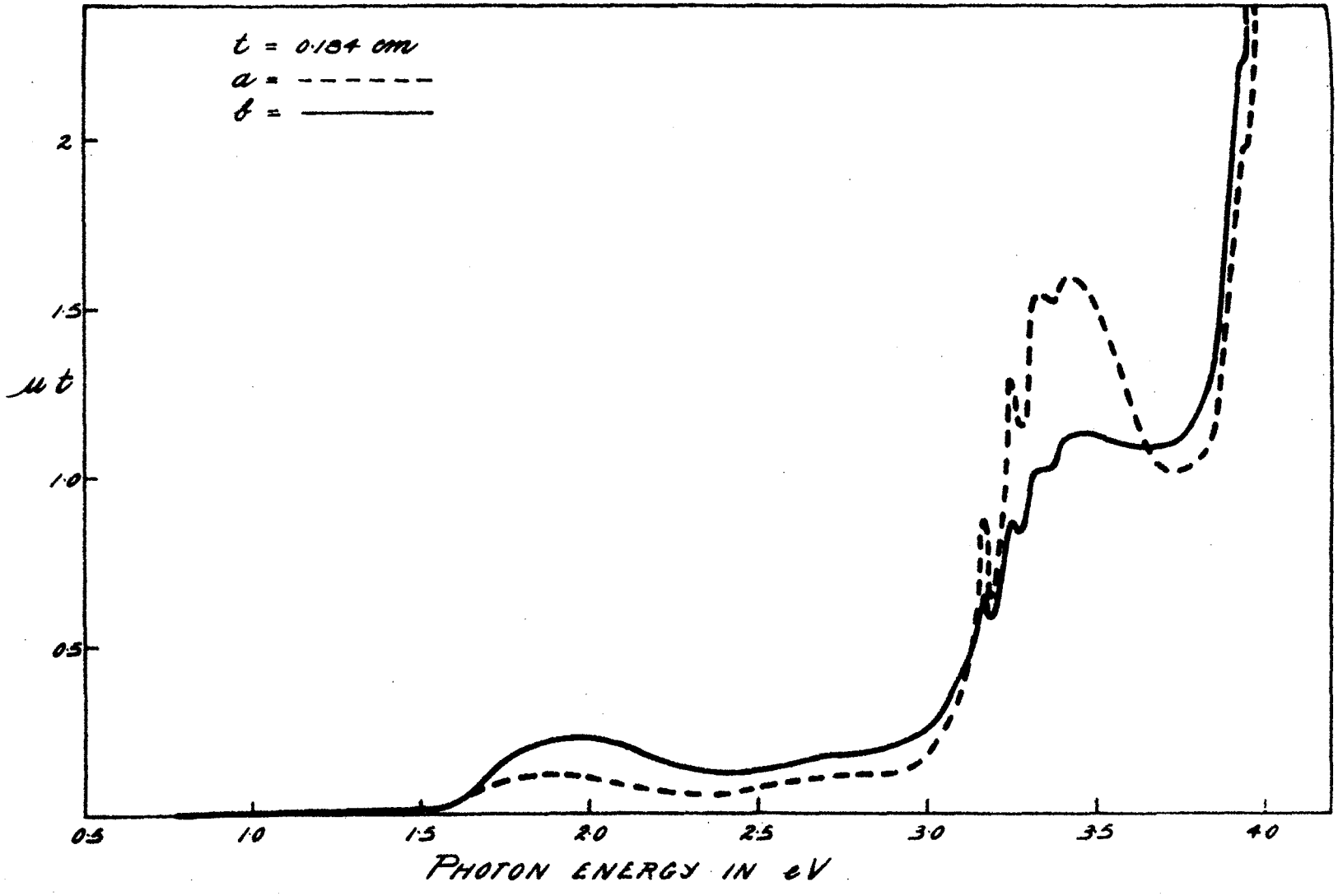

FIGURE 8.5 OPTICAL ABSORPTION SPECTRA OF THE ELECTRON IRRADIATED SPECIMEN D12 AT ROOM TEMPERATURE.

(a) AFTER HEATING AT 500°C. (b) AFTER SUBSEQUENT ILLUMINATION WITH MERCURY LIGHT.

E.P.R. line, are plotted as a function of treatment for each specimen in Figures 8.6a, b, c and d. It can be seen that each of the bands has undergone cyclic reduction and enhancement in D_{12} and D_{13}, while in D_{11} those bands (G.R.1 and the U.V. band) which are observed are not affected. In addition, there is a slow reduction in the maximum strength of each band with time of heating. This is due to annealing processes which, over periods of hundreds of hours at this temperature, cause other changes which will be discussed in the next chapter, but which are not marked for the first thirty hours of heating.

The rate of bleaching was not investigated in detail, but it was found that it was not greatly affected by cooling the specimen to 80°K during bleaching. It was also established that no detectable bleaching of thermally enhanced bands occurred during spectrophotometric measurement, due to the low level of light intensity in the instrument.

8.5. Discussion of the Cycling Effects in Irradiated Type Ia Diamonds.

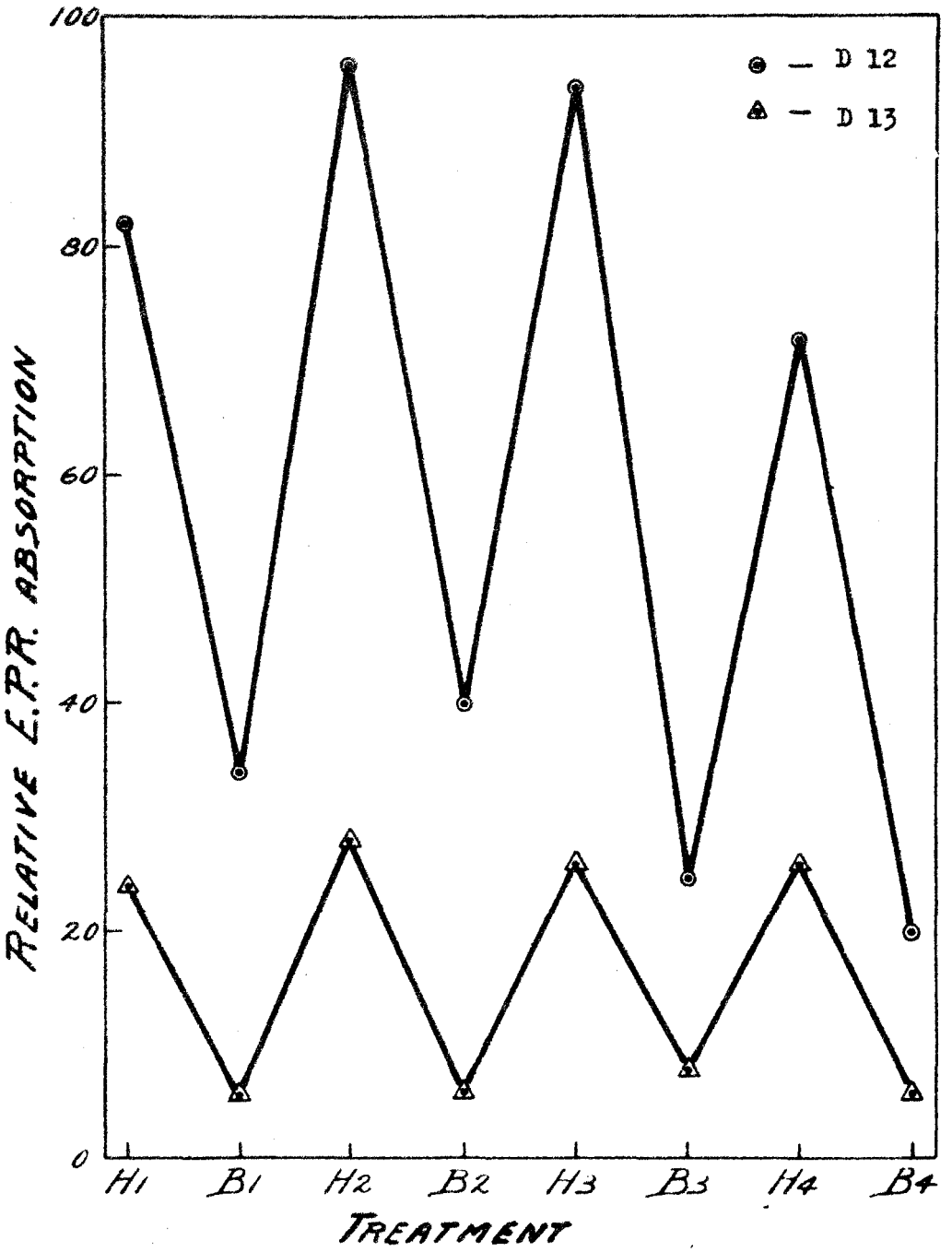

FIGURE 8.6a CYCLING IN THE STRENGTH OF THE E.P.R. LINE. TREATMENTS H_1, H_2, ETC. REFER TO HEATING FOR 4 HOUR PERIODS AT 500°C IN THE DARK; B_1, B_2, ETC. TO SUBSEQUENT ILLUMINATION WITH MERCURY LIGHT.

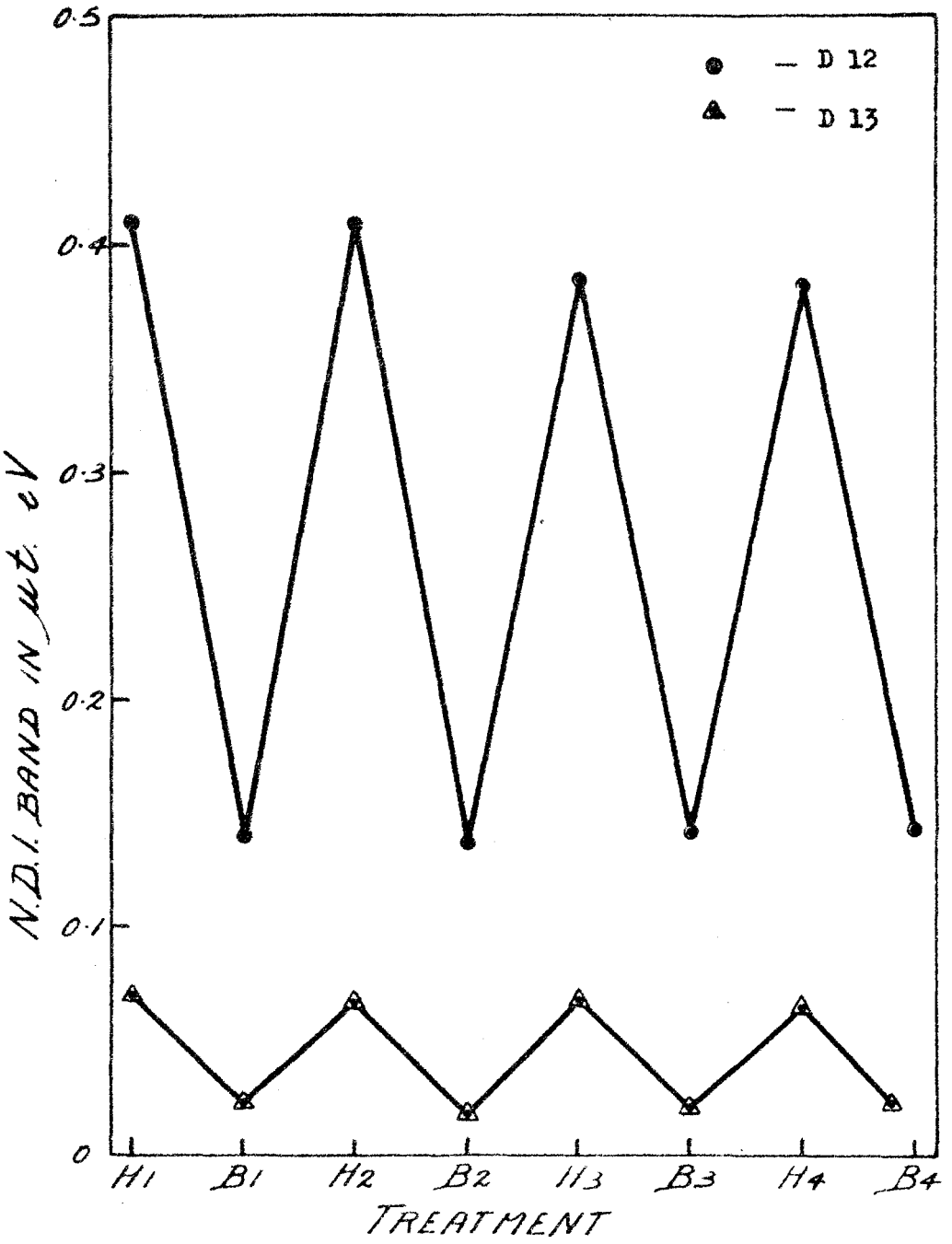

FIGURE 8.6b CYCLING IN THE STRENGTH OF THE N.D.1 BAND. TREATMENTS H_1, H_2, ETC. REFER TO HEATING FOR 4 HOUR PERIODS AT 500°C IN THE DARK; B_1, B_2, ETC. TO SUBSEQUENT ILLUMINATION WITH MERCURY LIGHT.

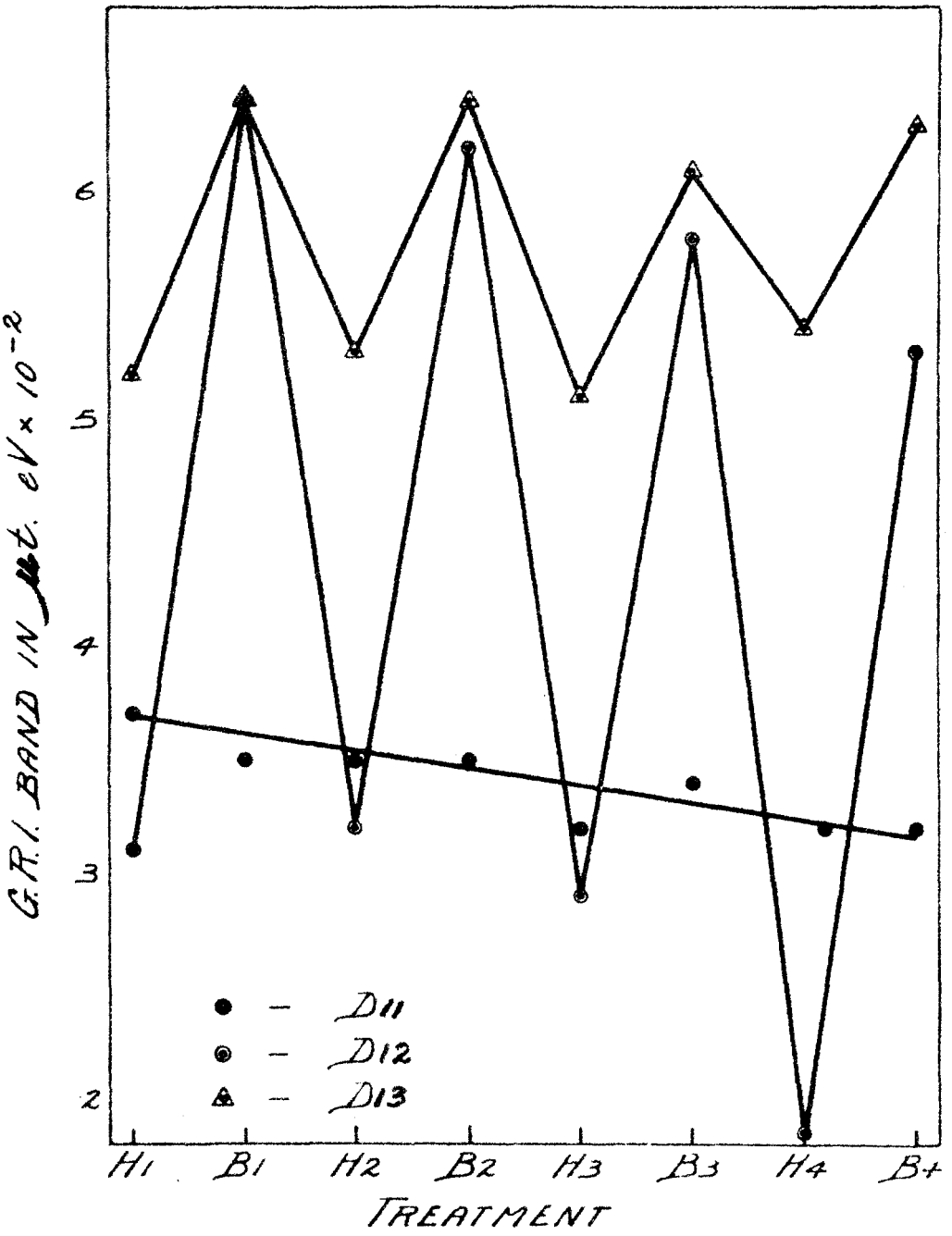

FIGURE 8.6c CYCLING IN THE STRENGTH OF THE G.R.1 BAND. TREATMENTS H_1, H_2, ETC. REFER TO HEATING FOR 4 HOUR PERIODS AT 500°C IN THE DARK; B_1, B_2, ETC. TO SUBSEQUENT ILLUMINATION WITH MERCURY LIGHT.

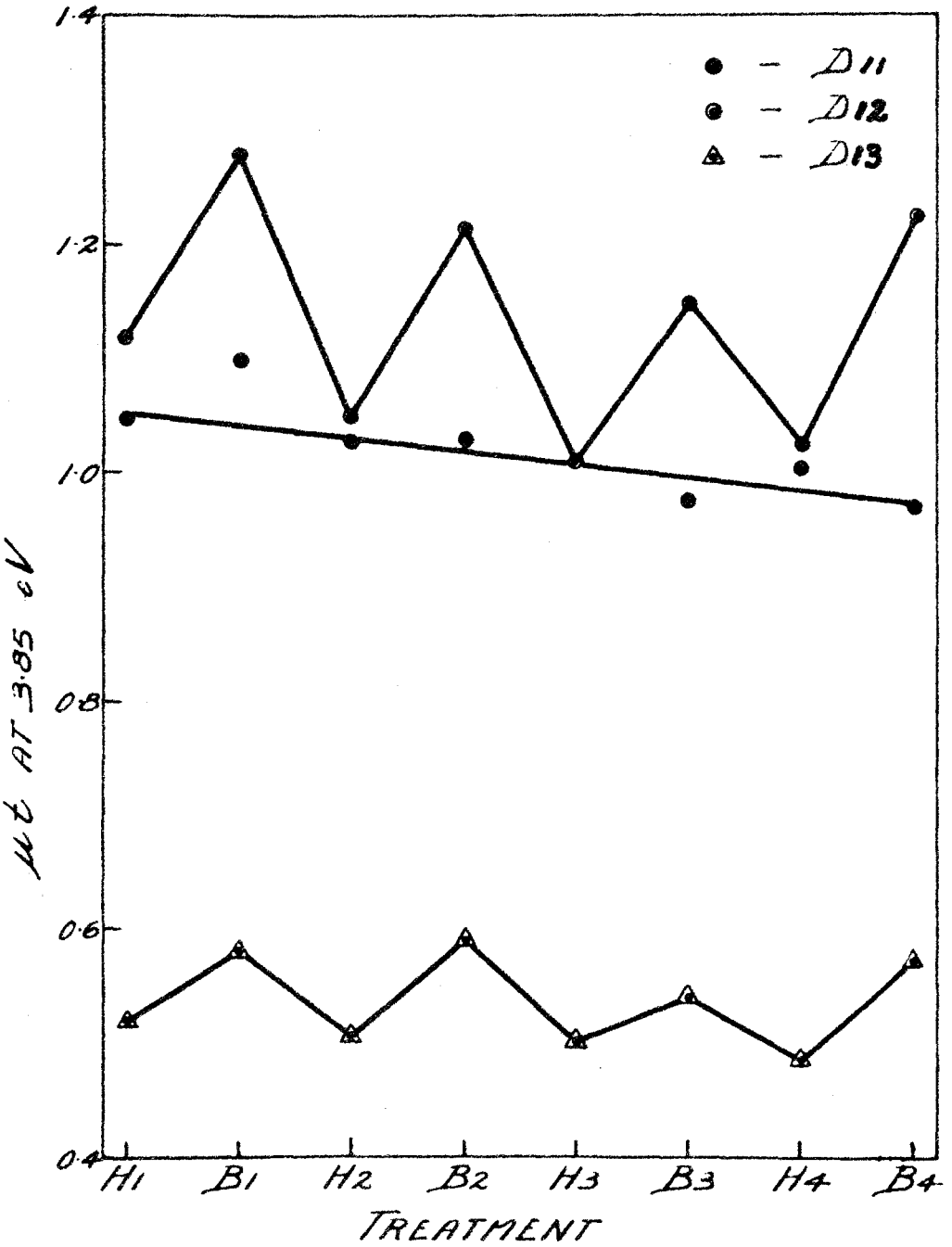

FIGURE 8.6d CYCLING IN THE STRENGTH OF THE U.V. BAND. TREATMENTS H_1, H_2, ETC. REFER TO HEATING FOR 4 HOUR PERIODS AT 500°C IN THE DARK; B_1, B_2, ETC. TO SUBSEQUENT ILLUMINATION WITH MERCURY LIGHT.

8.5.1. Proposed Model.

The cyclic behaviour of N.D.1, G.R.1 and the U.V. band can be explained by the model illustrated in Figure 8.7a, b and c.

The N.D.1 centre consists of a ground state and a main excited state. This gives rise to the principal absorption line at 3.16 eV. Additional excited levels arise from the interaction between the main electronic transition and vibrational states of the crystal. As transfer of electrons from these excited levels to the conduction band occurs even at low temperatures, the levels must lie just below the conduction band. If one assumes a gap of about 0.1 eV between the top of the N.D.1 system and the conduction band, the ground state of the system must lie at about 1.5 eV above the valence band.

The parallel behaviour of G.R.1 and the U.V. band suggests that these are two transitions within the same centre. The G.R.1 band arises in a manner completely analogous to that described for N.D.1. The principal line is at 1.68 eV, and the band extends to about 2.4 eV. The U.V. band is explained by transitions from the ground state of the G.R.1-centre to the conduction band. The

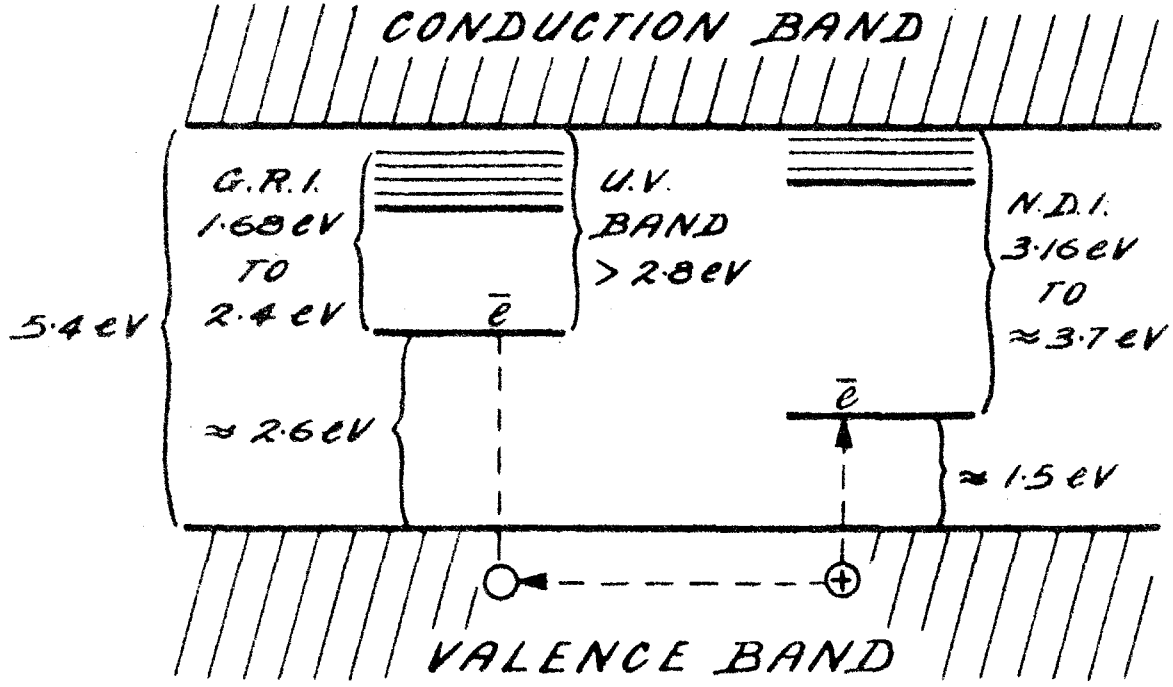

FIGURE 8.7a SCHEMATIC ILLUSTRATION OF THE ELECTRON TRANSFER INVOLVED IN THE CYCLING OF THE N.D.1, G.R.1 AND U.V. BANDS BY THERMAL ACTIVATION.

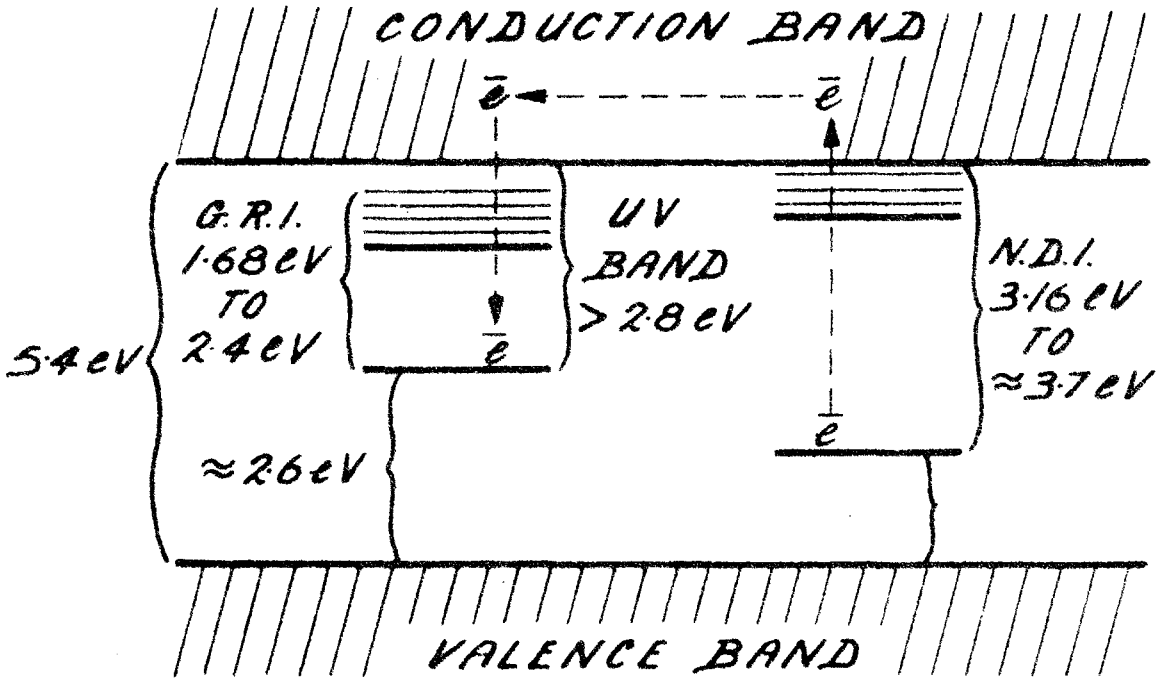

FIGURE 8.7b SCHEMATIC ILLUSTRATION OF THE ELECTRON TRANSFER INVOLVED IN THE CYCLING OF THE N.D.1, G.R.1 AND U.V. BANDS BY ILLUMINATION WITH THE 3.40 eV MERCURY LINE.

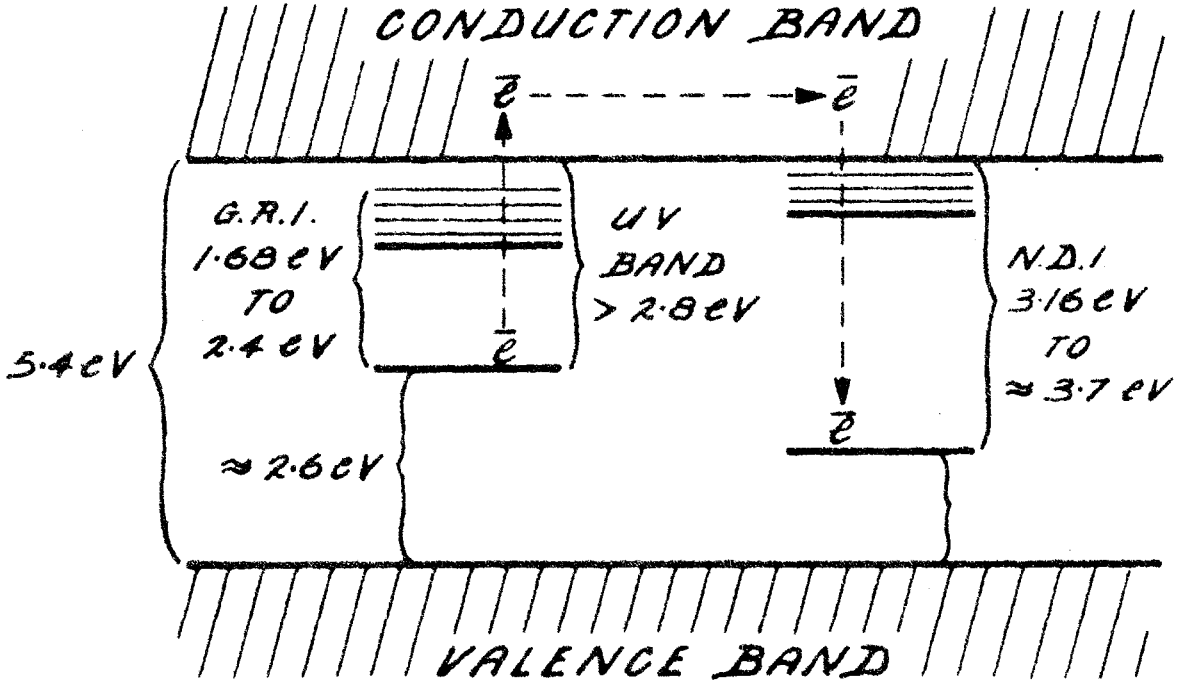

FIGURE 8.7c SCHEMATIC ILLUSTRATION OF THE ELECTRON TRANSFER INVOLVED IN THE CYCLING OF THE N.D.1, G.R.1 AND U.V. BANDS BY ILLUMINATION WITH THE 2.84 eV MERCURY LINE.

width of the U.V. band (> 1.6 eV) is consistent with this proposition. As the U.V. band begins absorbing at about 2.8 eV, the ground state of the G.R.1-centre is fixed at about 2.6 eV above the valence band.

It is also proposed that the N.D.1-centre is optically inactive when neutral, and acts as an acceptor. Thermal activation of an electron from the valence band to the N.D.1 ground state renders this band optically active. The positive hole so generated is captured by a G.R.1-centre (which thus acts as a donor) and the G.R.1-centre is thereby rendered optically inactive.

Illumination with light in the N.D.1 band raises electrons to the excited states of this band; these electrons are thermally excited to the conduction band (a small step energetically) and are captured by ionized G.R.1-centres. This restores the original condition, where the G.R.1-centre is unionized and optically active; the N.D.1 band is bleached.

The N.D.1 band extends from 3.1 eV to 3.8 eV and the U.V. band associated with G.R.1 extends from about 2.8 eV to 5.4 eV. There is thus a considerable measure of overlap of the two bands, and light of 3.4 eV will serve both to transfer electrons from N.D.1 to G.R.1

(Figure 8.7b) and in the reverse direction (Figure 8.7c), as both G.R.1 and N.D.1-centres, when optically active, are ionized by this energy of light. Thus final electron population of these two levels will be some equilibrium state depending upon the relative absorption coefficient of the two systems at the energy of excitation. This is believed to be the reason why it was never possible to bleach the N.D.1 band completely.

8.5.2. Experiments Designed to Test the Model.

a) Illumination with Monochromatic Light:

The U.V. and N.D.1 bands do not overlap completely. There is the spectral region from about 3.8 eV to 5.4 eV where only the U.V. band is presumed to be absorbing. However, this is not available for experiment, as the very strong secondary absorption edge arising from nitrogen platelets is dominant over this range of photon energies.

In addition there is a narrow spectral region from 2.8 eV to 3.1 eV in which only the U.V. band is absorbing, albeit very weakly. If the proposed model is correct, it should be possible to bleach G.R.1-centres and enhance the N.D.1 band by illumination in this

spectral region. Specimen D_{14} was exposed to the 2.84 eV mercury emission line, selected using a quartz monochromator, and the expected affect was observed, but was small. Accordingly an interference filter was introduced into the optical path to increase the spectral purity of the light by reducing the intensity of the stray light of energy greater than 3.0 eV. With this modification, the enhancement of N.D.1 was doubled, while still not being quite complete as gauged by the size of N.D.1 after thermal enhancement. The strengths of the N.D.1 band at various stages are listed in Table 8.3. Corresponding changes in G.R.1 and the U.V. band were also observed (i.e. reduction in these bands wherever N.D.1 increased and vice versa).

As expected, exposure of the specimen to the 2.27 eV mercury line caused no observable change in any band, irrespective of its condition of enhancement.

b) Irradiation of Type IIb Diamond.

If, as is believed, G.R.1 is a donor centre, it should interact with the acceptor centres (ϕ 4.6.1) known to exist in semi-conducting Type IIb diamond. These acceptors are quite different to the N.D.1-centres, and lie at 0.34 eV above the valence band. Thermal activation

TABLE 8.3

EFFECTS OF ILLUMINATION ON THE N.D.I. BAND IN D_{14}

NOMINAL TREATMENT	LIGHT SOURCE	STRENGTH OF N.D.I. BAND μt.eV
Heating for 4 hours at 500°C	-	0.038
Illumination for 16 hours	3.40 eV Mercury line from monochromator	0.006
Illumination for 50 hours	2.84 eV Mercury line from monochromator	0.014
Illumination for 16 hours	3.40 eV Mercury line from monochromator	0.004
Illumination for 50 hours	2.84 eV Mercury line from monochromator plus filter	0.026

of electrons to this level occurs at room temperature, and the G.R.1 band would therefore be expected to be in the bleached condition after room temperature irradiation. As a result of this proposal the effects of irradiating Type IIb diamonds were subsequently studied in detail by Ferdinando (1965). Briefly it was found that neither the G.R.1 band, nor the U.V. band, could be observed in irradiated Type IIb diamonds, although the irradiation dose was shown to be quite sufficient to produce these bands in Type IIa diamonds which do not contain acceptor centres.

No E.P.R. absorption could be detected in the specimens studied, either before or after irradiation.

8.6. Investigation of the N.D.1-Centre.

8.6.1. Experimental Results.

It was at this stage not clear whether N.D.1-centres are formed as a result of irradiation damage, or whether they are always present in Type Ia diamond, but are optically inactive until G.R.1 donor centres are created. D_{14} was therefore selected as having the highest platelet nitrogen concentration observed in this study,

and was irradiated at a very low dose rate, the specimen being held at about 200°K during irradiation. At five stages during the total irradiation the specimen was allowed to warm up to room temperature and the optical absorption measured. At no stage was the N.D.1 band detected. The optical absorption spectra before irradiation and after the final dose are shown in Figure 8.8. This shows that the N.D.1 band normally observed arises from the localised heating associated with normal room temperature irradiation, estimated by Clark et al (1956 b) to be equivalent to about 350°C.

D_{14} was now heated together with D_{15}, a specimen in which a large N.D.1 band had been developed by irradiation and heat treatment, and then bleached to is minimum by mercury light. Stages in the sequence of heating and optical bleaching of these two specimens are listed in Table 8.4. Only changes in the strength of N.D.1 are shown; however, corresponding changes in G.R.1 and the U.V. band were also observed (i.e. a reduction in these bands wherever N.D.1 was observed to increase, and vice versa).

It is clear that temperatures in the range 180-250°C are adequate to develop an N.D.1 band by electron

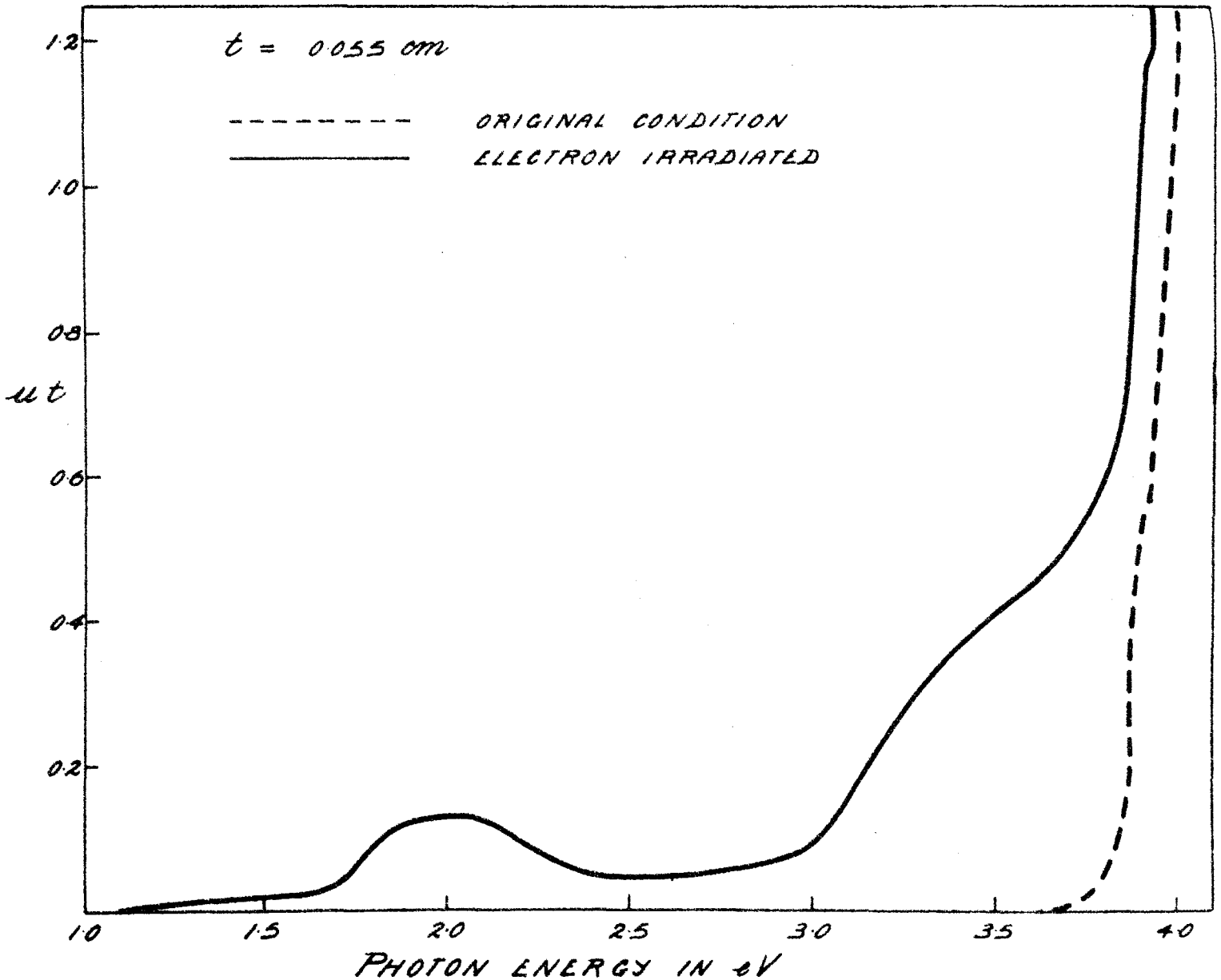

FIGURE 8.8 OPTICAL ABSORPTION SPECTRA OF SPECIMEN D14 BEFORE AND AFTER ELECTRON IRRADIATION AT 200°K.

TABLE 8.4

EFFECTS OF TREATMENT ON THE N.D.I. BAND IN D_{14} AND D_{15}

TYPE OF TREATMENT	TIME IN HOURS	TEMPERATURE IN ^{o}C	STRENGTH OF THE N.D.I. IN $\mu t.eV$	
			D_{14}	D_{15}
Heating	15	140	0	0.350
Bleaching	0.1	25	0	0.351
Heating	18	180	0	0.483
Bleaching	0.1	25	0	0.349
Heating	4	215	0	0.465
Bleaching	0.1	25	0	0.350
Heating	15	250	0.027	0.538
Bleaching	0.1	25	0	0.351
Heating	46	250	0.032	0.540
Bleaching	0.1	25	0.004	0.349
Heating	64	410	0.036	0.980
Bleaching	0.1	25	0.006	0.350
Heating	4	500	0.038	1.143
Bleaching	0.1	25	0.005	0.351
Heating	16	200	0.018	0.493
Bleaching	0.1	25	0.005	0.350

transfer in D_{15} where N.D.1-centres already exist; however, this temperature is not sufficient to create the centres in D_{14} which had been irradiated at low temperatures. Higher temperatures serve to develop N.D.1 fully in D_{14}, after which reheating at 200°C results in a marked enhancement of the N.D.1 band, although this temperature was earlier ineffective.

8.6.2. Proposed Model for N.D.1-Centres.

The N.D.1-centre appears to be the result of the combination of an irradiation damage product and nitrogen in platelet form. Such evidence as is available suggests that the irradiation damage product concerned is an interstitial; this will be discussed fully in a later section. For convenience of description this assignment of interstitial atoms in combination with platelets will be made to N.D.1-centres. The G.R.1-centres are identified as the other irradiation damage product - namely vacancies.

When electron irradiation is done carefully at low temperatures, the interstitials are not mobile; or, if mobile, have insufficient energy to overcome an activation energy barrier preventing interstitial/nitrogen

platelet combination. Thus no N.D.1-centres are formed. Heating to a temperature of about 200°C can therefore not result in the appearance of the N.D.1 band, although this temperature is shown to be sufficient to excite electrons on to the N.D.1-centres, and render them detectable in absorption if they already exist.

At about 250°C the interstitials attach themselves to substitutional nitrogen in platelet form and N.D.1-centres are created.

The cyclic behaviour of the E.P.R. line is consistent with its being due either to ionized N.D.1-centres or to ionized G.R.1-centres; the absence of E.P.R. absorption in irradiated Type IIb diamonds, which contain ionized G.R.1-centres, suggests strongly that these centres cannot be responsible for the E.P.R. line. It is thus concluded that at least part of the observed E.P.R. line is associated with ionized N.D.1-centres. The apparent inconsistent behaviour of the E.P.R. line when an irradiated Type Ia diamond is first heated at 500°C ($\oint$ 8.4.3), may be due to additional E.P.R. absorption, superimposed on the line under discussion, and arising from centres which are annealed during the first heat treatment after irradiation.

8.7. Investigation of the Thermal Activation Process.

8.7.1. Experimental Results.

The rates of thermal enhancement of the N.D.1 band were now investigated, initially in the two irradiated specimens D_{13} and D_{15}.

The specimens were first bleached using mercury light until no further change in absorption was observed. They were then heated for increasing periods of time in the dark at 400°C for a total of 47 hours and then at 500°C for a further five hours. After each heat treatment the specimens were cooled rapidly and optical absorption measurements made.

The behaviour of G.R.1 and N.D.1 for specimen D_{15} is shown in Figure 8.9. Similar results were obtained for D_{13}. If the two processes - growth of N.D.1 and decrease of G.R.1 - are directly related, then it may simply be shown that the size of the N.D.1 band at any stage is given by:

$$S_{N_j} = S_{N_o} + k(S_{G_o} - S_{G_j}) \qquad (8.1)$$

Where S_{N_o} and S_{G_o} are the size of N.D.1 and G.R.1

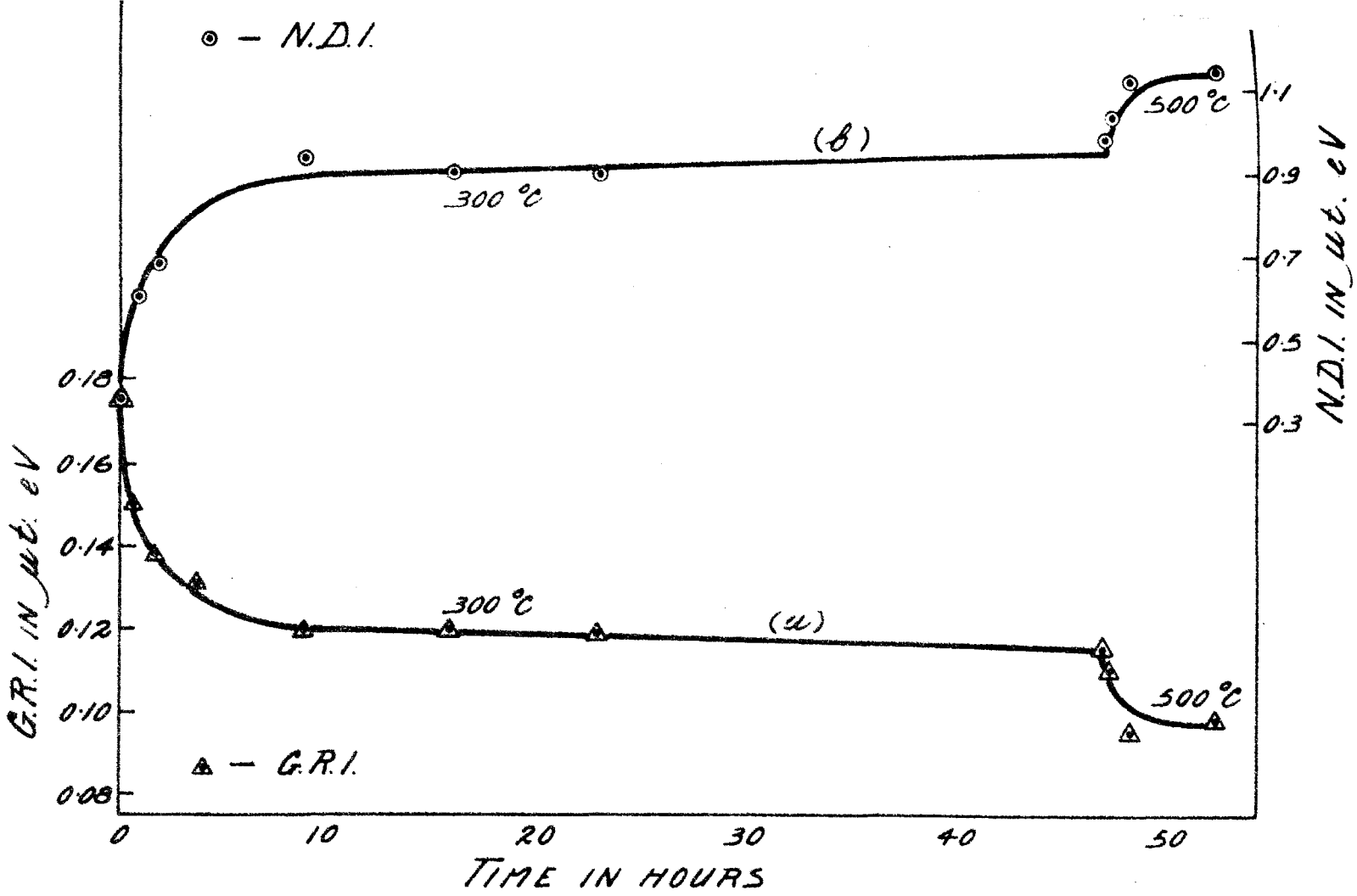

FIGURE 8.9 RATE CURVES OBTAINED BY HEATING D15, ILLUSTRATING THE SIMILAR BEHAVIOUR OF THE G.R.1 AND N.D.1 BAN (a) WAS FITTED TO THE VALUES FOR THE DECREASE OF G.R.1. (b) WAS CALCULATED FROM (a) BY EQN. 8.1 TO REPRESENT A CORRESPONDING INCREASE IN N.D.1. THE CIRCLES REPRESENT THE EXPERIMENTAL VALUES FOR THE INCREASE IN N.D.1.

respectively before heating; and S_{N_j} and S_{G_j} are their sizes after the jth heating stage.

In Figure 8.9, curve (a) was fitted to the experimental values for decay of G.R.1. Curve (b) was derived by transforming curve (a) according to eqn. (8.1). It can be seen that the transformed curve is an excellent fit to the experimental points for growth of N.D.1. This establishes that the two processes are directly related.

Figure 8.10 demonstrates the behaviour of N.D.1 in D_{15} after a series of isothermal heatings in the dark at different temperatures. The specimen was restored to the optically bleached condition after every heat cycle at a given temperature. It can be seen that the band strength rises rapidly to a nearly constant "final value" which changes very little with prolonged heating at a specific temperature. The "final value" of the band strength is different for each of the temperatures employed.

8.7.2. Proposed Model.

Several possible models have been considered to explain this temperature dependence of the "final value." Possibly the simplest is to postulate that the N.D.1-

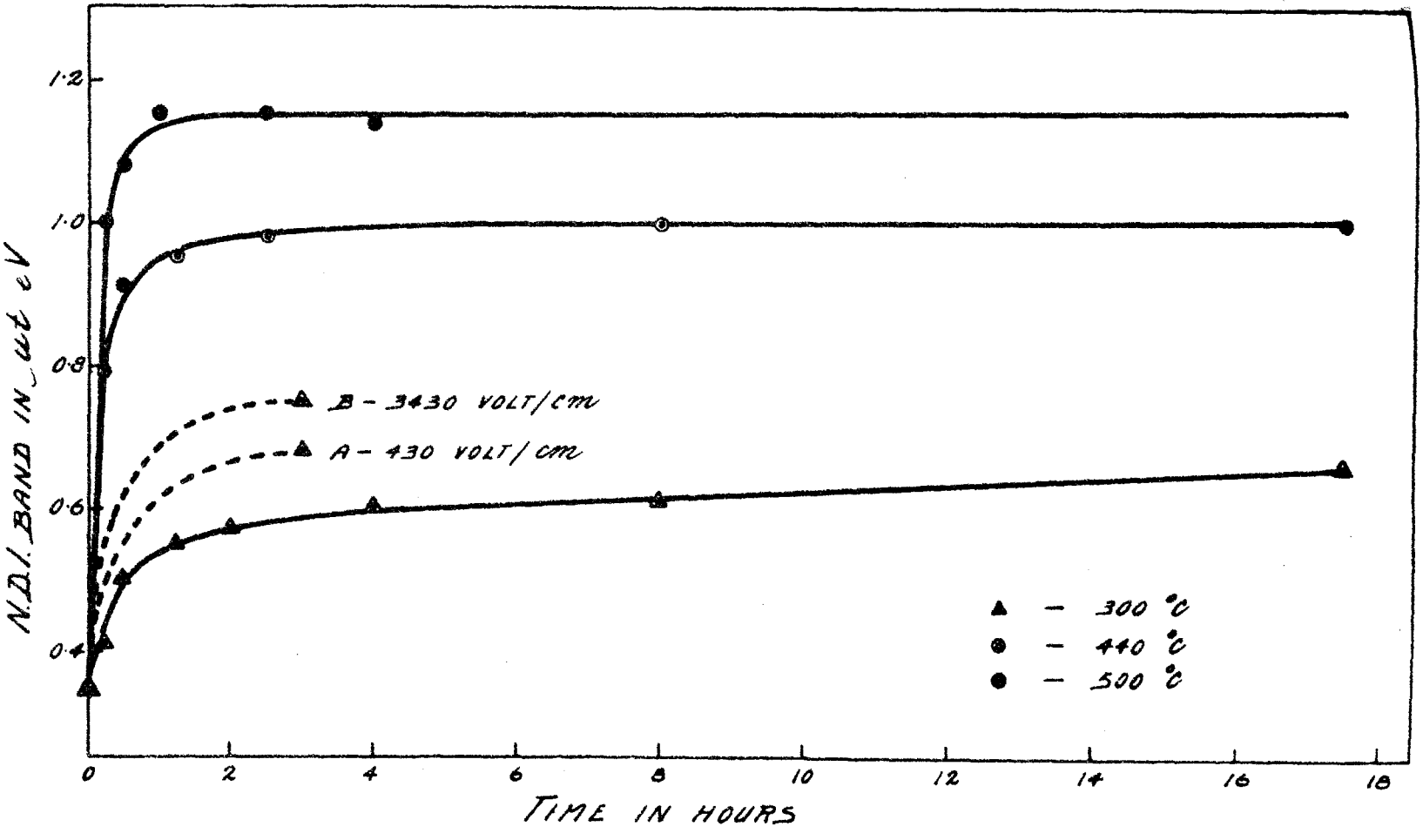

FIGURE 8.10 THE EFFECT OF ISOTHERMAL HEATING IN THE DARK ON THE STRENGTH OF THE N.D.1 BAND IN SPECIMEN WHERE CONSIDERABLE CLUSTERING OF N.D.1 CENTRES IS EXPECTED. BY HEATING FOR 3 HOURS AT 300°C WITH APPLIED ELECTRIC FIELDS, POINTS A AND B WERE OBTAINED.

centres are of more than one kind, each having a ground state at a different energy above the valence band. Against this is the fact that no evidence of multiple levels is observed optically. On the contrary, the N.D.1 band has an extremely sharp main line, indicating well defined ground and excited states for the centre.

Postulation of a third trapping centre for the positive holes arising from thermal excitation of electrons on to the N.D.1 acceptor states would explain the temperature dependence of the "final value" of the G.R.1, but would, however, not account for the parallel effect observed for the N.D.1 band.

Another possibility is that the observed "final value" of the bands represents the equilibrium distribution of electrons between the two systems at a particular temperature. The "final value" should then be the same irrespective of the path taken to achieve it. Thus it should be possible to decrease the size of the N.D.1 band in a specimen that was heated to 500°C by reheating it in the dark at a lower temperature of say, 300°C, - to the value as would be obtained if the specimen in the bleached condition were heated to 300°C. No such effect was observed.

It is now proposed that the N.D.1-centres are in general not randomly distributed through the specimen, but occur in clusters. The process of activating the N.D.1-centre consists of the excitation of an electron to the N.D.1 acceptor level and the capture of the positive hole by a G.R.1-centre. Initially the process proceeds rapidly. When, however, an appreciable number of N.D.1-centres are activated, positive holes find it increasingly difficult to escape from the clusters, as they are subject to retrapping by activated N.D.1-centres.

In addition, at the stage when many of the N.D.1-centres of a cluster are activated, the positive hole arising from ionization of a neutral N.D.1-centre is subjected to the attractive Coulomb field of the activated centres. This constitutes an energy barrier to escape of the positive hole from the cluster, which would thus be a thermally activated process, and strongly temperature dependent.

Qualitatively it can be shown that this mechanism can give rise to the observed effects. A quantitative calculation has not been attempted as the number of unknown parameters is too large for the result to be meaningful.

8.7.3. Experiments Designed to Test the Model.

It is believed that clustering of N.D.1-centres arises from the presence of a number of interstitial carbon atoms on each nitrogen platelet. If this is the case, the degree of clustering can to some extent be controlled by adjusting the ratio of interstitials arising from irradiation, to the number of platelets.

In specimen D_{15} the concentration of platelets is only moderately high, while the irradiation dose is large, and a considerable degree of clustering may be expected. In specimen D_{14} the platelet concentration is much higher and the irradiation dose much lower (Table 8.1); one therefore expects clustering to be low.

In Figure 8.11 the N.D.1 growth rate curves are plotted for various temperatures of heating of D_{14}. Comparing these with those shown in Figure 8.10 for D_{15}, it can be seen that, where clustering is a minimum, the temperature dependence of the "final value" of the band strengths is very much smaller.

Another expected consequence of the clustering of the N.D.1-centres is a broadening of the associated E.P.R. line. Unfortunately the observed E.P.R. lines in irradiated Type Ia diamonds probably do not originate

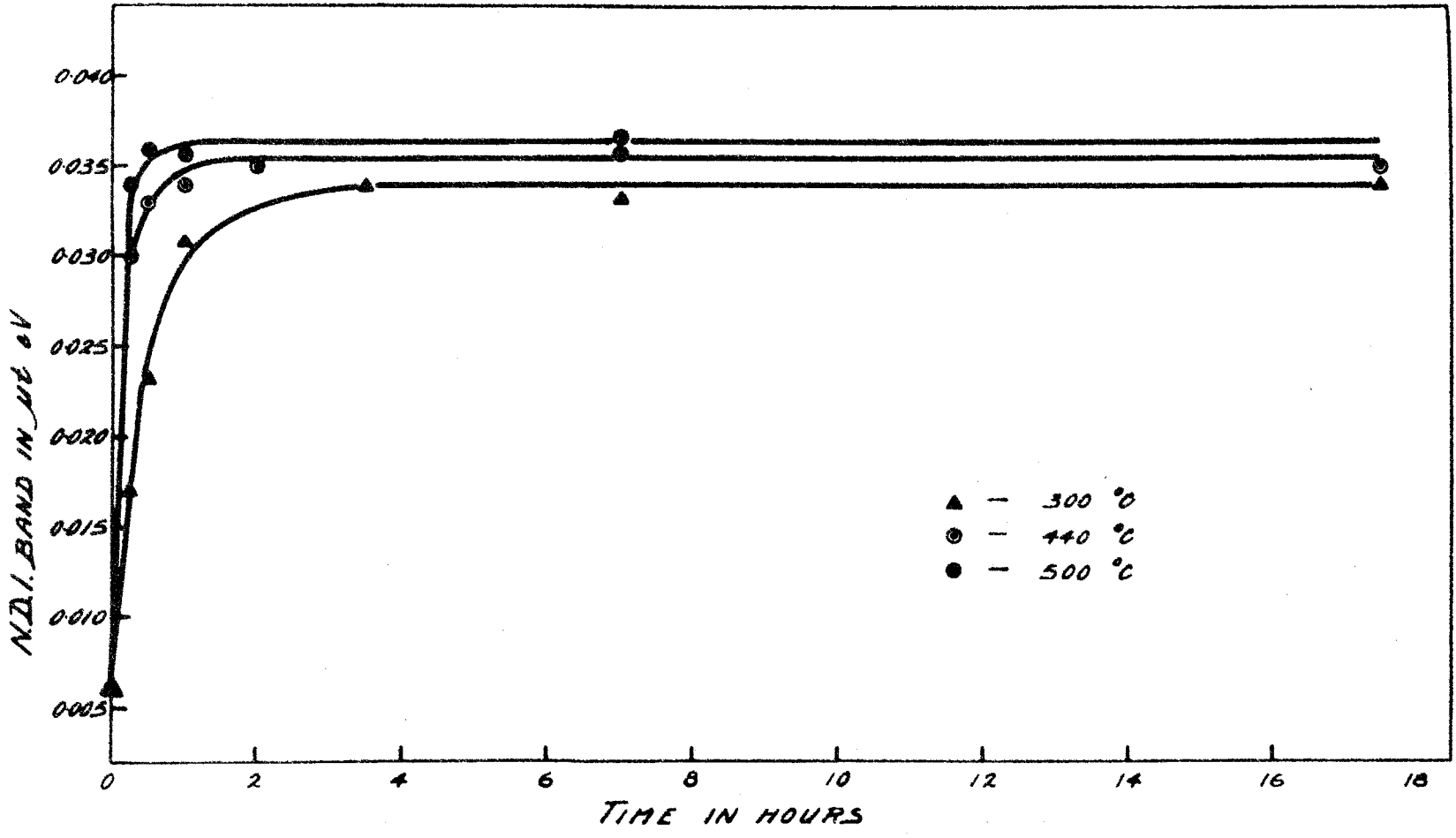

FIGURE 8.11 THE EFFECT OF ISOTHERMAL HEATING IN THE DARK ON THE STRENGTH OF THE N.D.1 BAND IN SPECIMEN D14, WHERE CLUSTERING OF N.D.1 CENTRES IS EXPECTED TO BE A MINIMUM.

from N.D.1-centres alone. This makes an assessment of line broadening due to clustering of N.D.1-centres difficult. The lines found in D_{14} and D_{15} appeared similar in shape, the line widths being 1.6 Oe $\pm$ 0.3 Oe for D_{14} where clustering is expected to be low and 2.0 Oe $\pm$ 0.3 Oe for D_{15} where considerable clustering is expected.

The effect of an applied electric field on the rate of growth of the N.D.1 band during heating was now studied. Electric fields of 430 volt/cm. and 3430 volt/cm. were applied to specimen D_{15} during the whole period of heating at 300°C. An initial rapid fall in resistance was observed as the specimen attained furnace temperature. This was followed by a steady increase in specimen resistance to a constant maximum value. This is consistent with electron or hole mobility being involved in the activation of the N.D.1 band and the simultaneous reduction of G.R.1.

The values obtained for the strengths of G.R.1 and the N.D.1 band after heating were not the same as when no field was applied. G.R.1 was smaller and the N.D.1 band larger than expected for heat treatment at this temperature. This effect was the more marked with the higher field applied during heating (Figure 8.10).

It thus appears that the applied field has the effect of aiding the escape of positive holes from substantially ionized clusters of N.D.1-centres, by imposing a directional mobility to the random motion of the positive hole, and by helping to counteract the effect on the hole of the space charge arising from clustered ionized defects.

8.8. Discussion.

The effect of irradiation with electrons of energy below 0.8 MeV is to create single vacant atomic sites and interstitial carbon atoms in the diamond lattice. If the irradiation is performed at room temperature, localized heating occurs as a result of the irradiation process, leading to limited defect mobility. However, if the irradiation is performed at low temperature, the defects are effectively immobile and do not react with each other, or with impurity centres.

When a Type Ia diamond, irradiated at low temperature, is heated to about 250°C, limited vacancy interstitial recombination occurs. Apart from this effect, no annealing of G.R.1 is observed (even at temperatures up to 450°C), but a new band - N.D.1 - is formed. This is consistent with G.R.1 being associated with one type

of damage product which is not mobile below 500°C and N.D.1 with the other. For this reason it is suggested that the G.R.1-centre is a vacancy, and that N.D.1-centres are associated with interstitials. ^ The discussion will, in this thesis the foregoing assumption is taken to be the case. however, not materially be affected if the role of vacancies and interstitials is interchanged.

The production of the N.D.1-centre demonstrates interstitial mobility. This centre, to become observable, requires thermal activation of electrons from the valence band to its ground state; this, however, does not explain its absence before heating to 250°C, as temperatures well below this are sufficient for the thermal activation process to occur. Therefore the fact that N.D.1 only appears after heating to about 250°C can only be explained by assuming that at this temperature the interstitial is mobile.

The N.D.1 band is always observed in irradiated Type Ia diamonds which have been heated in the temperature range 250°C - 500°C. It is never observed in nitrogen-free diamond, and its strength for a given irradiation dose depends upon the nitrogen content of the specimen. As expected, irradiation treatments (x-rays and electrons of energy below 0.3 MeV) which do not produce displacement

of carbon atoms in the diamond lattice, do not produce any N.D.1 band even when followed by appropriate heat treatment. It is therefore concluded that the N.D.1-centre is an interstitial carbon atom anchored at substitutional nitrogen atoms in platelet form.

To be more specific about the mechanism of N.D.1-centre formation is difficult, because, although the concept of nitrogen segregated into a platelet configuration is well established, the precise arrangement of the atoms in the platelet is speculative. The presence of these defects, however, is known to cause an expansion of the diamond lattice normal to the platelet. One would therefore expect regions where the diamond lattice is in compression as well as regions where the lattice is dilated. The regions where the lattice is in compression will be unfavourable locations for an interstitial; and may present an energy barrier to a mobile interstitial; thus preventing it from combining with a nitrogen platelet. At about 250°C the interstitial presumably has enough kinetic energy to overcome this energy barrier and is probably anchored in the platelet region where the lattice is dilated.

The rate of thermal enhancement of N.D.1 can be explained by assuming that the N.D.1-centres are not randomly distributed through the crystal but occur in clusters. These clusters probably arise from the presence of a number of interstitial carbon atoms anchored to each nitrogen platelet.

This proposed atomic model for an N.D.1-centre is in agreement with subsequent very recent results of Runciman (1965), who, not being aware of this study, investigated the splitting of the so-called "enhanced line of the 4150A system" as described by Pringsheim, under an applied uniaxial stress. Polarization spectra were obtained for stress applied along the three principal directions $\langle 100 \rangle$, $\langle 110 \rangle$ and $\langle 111 \rangle$. From these Runciman ascribed this line, the principal or zero phonon line of N.D.1 to: "a monoclinic [hko] centre, of which an example might be a vacancy at 000 plus an interstitial at $1\frac{1}{2}0$". It is therefore now suggested that the N.D.1-centre comprises a substitutional nitrogen atom at 000 plus an interstitial at $1\frac{1}{2}0$.

The G.R.1 band arises from transitions from the ground state of a vacancy to excited states, the ground state being about 2.6 eV above the valence band, with the

principal excited state at 1.68 eV above this. The U.V. band arises from transitions from the ground state of the same centre, a vacancy, to the conduction band. The width of this band (>1.6 eV) is consistent with this proposition. In Type IIa diamonds which contain no nitrogen in detectable amounts, only G.R.1 and the U.V. band can be detected after irradiation, although vacancies and interstitials are created. It appears therefore that the interstitials are optically inactive.

The G.R.1-centre acts as an electron donor - the N.D.1-centre as an electron acceptor. Therefore the magnitude of G.R.1 after irradiation is not a measure of the irradiation damage produced in any diamond containing acceptor centres, as the vacancy is optically inactive after having donated an electron.

CHAPTER IX.

ANNEALING OF IRRADIATION DAMAGE IN TYPE Ia DIAMOND.

9.1. Introduction.

The effects of isothermal heat treatment at temperatures between 500° and 1200°C on the defect centres induced by 0.78 MeV electron irradiation in Type Ia diamonds, were now studied.

As shown in the previous chapter, the carbon interstitials created by irradiation damage are mobile and combine with the nitrogen platelets in Type Ia diamonds at 250°C. Thus the N.D.1 band is produced. The other product of irradiation damage, vacancies, is not mobile below 500°C, and is responsible for the G.R.1 and U.V. bands.

Heat treatment at 500°C or higher temperatures is expected to render the vacancies mobile as well, thus creating the possibility of interaction between mobile vacancies and nitrogen platelets or N.D.1-centres. These effects are described in this chapter.

9.2. Existing Knowledge.

The effect of heat treatment between 300 and 900°C on the O.A. bands produced by 1.0 MeV electron irradiation in diamond, was first studied by Clark et al (1956 b). They found that:

a) Heat treatment between 300 and 400°C causes a general reduction in all the irradiation induced absorption. From additional evidence obtained by a study of gamma and neutron irradiation, Clark et al concluded that this effect is due to the recombination of those interstitials and vacancies which are near neighbours.

b) Heat treatment of irradiated Type IIa diamonds causes a great reduction in G.R.1 and the U.V. band, and the formation of a band between 2.1 and 2.8 eV, called TH5. From a study of the kinetics of the decay of G.R.1 and the associated growth of TH5, Clark et al concluded that the TH5 centres arise from pairs of G.R.1-centres, and therefore ascribed the TH5 band to divacancies.

c) Subsequent heat treatment of a Type IIa diamond up to 900°C results in the decay of TH5 and the growth of the absorption tail (ϕ 4.5.1). The absorption tail was ascribed to the presence of amorphous or graphitic regions, produced by the agglomeration of

G.R.1-centres. After this treatment no G.R.1 band could be detected in the specimens.

d) When an irradiated Type I diamond was heat-treated between 500 and 900°C the G.R.1 and U.V. bands annealed out more rapidly than in Type IIa diamonds. Associated with this annealing was the growth of a large band, the 5032A band, between 2.4 and 3.0 eV. This was attributed by Clark et al to the anchoring of G.R.1-centres at crystal defects present only in Type I diamonds. In addition to the 5032A band, a small band called H2, around 1.6 eV, was found. No explanation was offered for the formation of this small additional absorption feature.

More recently Palmer (1961) studied the kinetics of annealing of irradiation damage in Type IIa diamonds, and concluded that the partial annealing of both G.R.1 and the U.V. band at temperatures up to 600°C is identical. At higher temperatures the U.V. band cannot be measured because of the formation of the absorption tail. Contrary to the findings of Clark et al, however, Palmer found that the G.R.1 band never annealed out completely at these temperatures, and in fact exhibited a slight increase in strength after heat treatment at 900°C.

In order to explain these effects, Palmer suggested that the annealing of the G.R.1 band occurs by the migration of some unspecified impurities or imperfections to G.R.1-centres. The specimen dependence of the rate of annealing of the G.R.1 band, was then attributed to the presence of different concentrations of these unspecified defects in various specimens.

9.3. Isothermal Annealing.

The six irradiated specimens, D_{11} to D_{16}, which were described in the previous chapter, were subjected to isothermal heat treatment at 500, 600 and 700°C for prolonged periods of time, and for further shorter intervals at 900 and 1200°C.

As described before, the N.D.1-centres in the nitrogen containing specimens are electron acceptors, the G.R.1-centres donors, and electron transfer from G.R.1 to N.D.1 is effected by thermal activation. Heat treatment will therefore produce thermal ionization of these defects as well as annealing. The heat treatment was therefore carried out in the dark and O.A. measurements made prior to, and after, subsequent illumination with unfiltered mercury light. Thus an indication could be obtained from

the strength of the O.A. bands, as to the extent of annealing of defect centres.

The presence or absence, of 4150A-centres in these specimens, had no apparent effect on the changes brought about by isothermal heat treatment. The concentration of nitrogen in platelet form, however, was found to have a profound effect. In order to facilitate presentation of the results, only three specimens, in which only nitrogen platelets in widely varying amounts could be detected, will be discussed in detail. The effects observed in these specimens are representative of the effects of heat treatment in all the specimens studied.

The amount of substitutional nitrogen present in non-paramagnetic platelet form (Table 8.1) in these specimens, was as follows:

Specimen D_{11}	Specimen D_{12}	Specimen D_{13}
None detectable	2×10^{20} atoms/cc	7×10^{18} atoms/cc

Only changes in the N.D.1, 5032A, G.R.1 and H2 bands, produced by heat treatment and subsequent exposure to unfiltered mercury light at room temperature after every heating stage, could be measured quantitatively.

This was accomplished by obtaining the integrated total absorption $\mu t.eV$ (t = specimen thickness) between 3.1 and 3.7 eV for N.D.1, 2.4 and 2.95 eV for 5032A, 1.65 and 2.4 eV for G.R.1 and 1.2 eV and 2.0 eV for the H2 band. These values are listed in Tables 9.1, 9.2 and 9.3 for specimens D_{11}, D_{13} and D_{12} respectively, and are illustrated graphically in Figure 9.1.

9.4. Effects of Isothermal Heat Treatment.

9.4.1. Presentation of the Results.

In general the effects of isothermal heat treatment of the irradiated Type Ia and Type IIa specimen appear to be fourfold. These effects are:

a) Annealing of defect centres. This is manifested by the disappearance of the G.R.1 and N.D.1 bands.

b) Production of new defect centres. This is manifested by the growth of two new O.A. bands, namely the 5032A and H2 bands.

c) Thermal bleaching of the G.R.1 and 5032A bands. Apparently this process modifies the electronic configuration of the defect centres only, and not the atomic arrangement, because this bleaching effect can be

TABLE 9.1

THE EFFECT OF ISOTHERMAL HEAT TREATMENT ON THE OPTICAL ABSORPTION BANDS IN SPECIMEN D11

(Values in brackets were obtained after exposure to mercury light subsequent to heating in the dark)

TEMPERATURE IN ^{o}C	TOTAL HEATING TIME IN HOURS	STRENGTH OF G.R.I. $\mu t.eV$
-	-	0.064
500	4	0.037 (0.035)
500	16	0.032 (0.032)
500	24	0.035 (0.035)
500	32	0.030 (0.030)
500	58	0.030 (0.031)
500	157	0.027 (0.029)
500	320	0.027 (0.025)
500	632	0.023 (0.024)
500	791	0.025 (0.025)
600	66	0.021 (0.022)
600	207	0.017 (0.018)
600	368	0.013 (0.012)
600	700	0.007 (0.006)
600	1125	0.003 (0.003)
700	25	0.002 (0.002)
700	150	0.002 (0.001)
700	400	zero (zero)

TABLE 9.2

THE EFFECT OF ISOTHERMAL HEAT TREATMENT ON THE OPTICAL ABSORPTION BANDS IN SPECIMEN D13

(Values in brackets were obtained after exposure to mercury light subsequent to heating in the dark)

TEMPERATURE IN °C	TOTAL HEATING TIME IN HOURS	STRENGTH OF G.R.I. (μt.eV)	STRENGTH OF N.D.I. (μt.eV)	STRENGTH OF 5032A (μt.eV)
-	-	0.083	0.028	zero
500	4	0.052 (0.064)	0.071 (0.023)	zero (zero)
500	16	0.054 (0.063)	0.066 (0.023)	zero (zero)
500	24	0.055 (0.042)	0.067 (0.020)	zero (zero)
500	32	0.042 (0.064)	0.064 (0.017)	zero (zero)
500	58	0.042 (0.054)	0.068 (0.018)	zero (zero)
500	157	0.036 (0.049)	0.066 (0.012)	zero (zero)
500	320	0.036 (0.040)	0.061 (0.016)	0.003 (0.003)
500	632	0.027 (0.033)	0.061 (0.014)	0.002 (0.004)
500	791	0.026 (0.035)	0.055 (0.013)	0.007 (0.006)
600	66	0.021 (0.023)	0.051 (0.012)	0.010 (0.008)
600	207	0.011 (0.014)	0.040 (0.009)	0.014 (0.015)
600	368	0.008 (0.006)	0.032 (0.006)	0.019 (0.017)
600	700	0.001 (0.002)	0.017 (0.005)	0.028 (0.028)
600	1125	zero (zero)	0.008 (0.002)	0.035 (0.034)
700	25	zero (zero)	0.003 (zero)	0.035 (0.036)
700	150	zero (zero)	zero (zero)	0.038 (0.037)
700	400	zero (zero)	zero (zero)	0.038 (0.036)

THE EFFECT OF ISOTHERMAL HEAT TREATMENT ON THE OPTICAL ABSORPTION BANDS IN SPECIMEN D12.

(Values in brackets were obtained after exposure to mercury light subsequent to heating in the dark)

TEMPERATURE IN °C	TOTAL HEATING TIME IN HOURS	BAND STRENGTH (μt.eV)			
		G.R.I.	N.D.I.	5032A	H2
-	-	0.096	0.196	zero zero	zero (zero)
500	4	0.031(0.068)	0.410(0.140)	zero zero	zero (zero)
500	16	0.015(0.053)	0.385(0.144)	0.006(0.003)	zero (zero)
500	24	0.013(0.050)	0.382(0.128)	0.017(0.011)	zero (zero)
500	32	0.005(0.049)	0.354(0.113)	0.018(0.018)	zero (zero)
500	58	zero (0.035)	0.340(0.102)	0.031(0.026)	0.001 (zero)
500	157	zero (0.017)	0.203(0.057)	0.046(0.049)	0.001(0.001)
500	320	zero (0.010)	0.171(0.048)	0.047(0.057)	0.019(0.002)
500	632	zero (0.004)	0.135(0.032)	0.059(0.066)	0.0[illegible](0.004)
500	652	zero (0.002)	0.144(0.020)	0.057(0.073)	0.030(0.004)
500	791	zero (0.002)	0.137(0.025)	0.055(0.068)	0.033(0.006)
600	66	zero (zero)	0.016(0.003)	0.064(0.093)	0.057(0.014)
600	207	zero (zero)	zero (zero)	0.064(0.107)	0.064(0.019)
600	368	zero (zero)	zero (zero)	0.065(0.105)	0.061(0.017)
600	700	zero (zero)	zero (zero)	0.065(0.106)	0.063(0.020)
600	1125	zero (zero)	zero (zero)	0.064(0.107)	0.065(0.018)
700	25	zero (zero)	zero (zero)	0.066(0.106)	0.066(0.019)
700	150	zero (zero)	zero (zero)	0.063(0.108)	0.064(0.019)
700	400	zero (zero)	zero (zero)	0.064(0.107)	0.064(0.020)

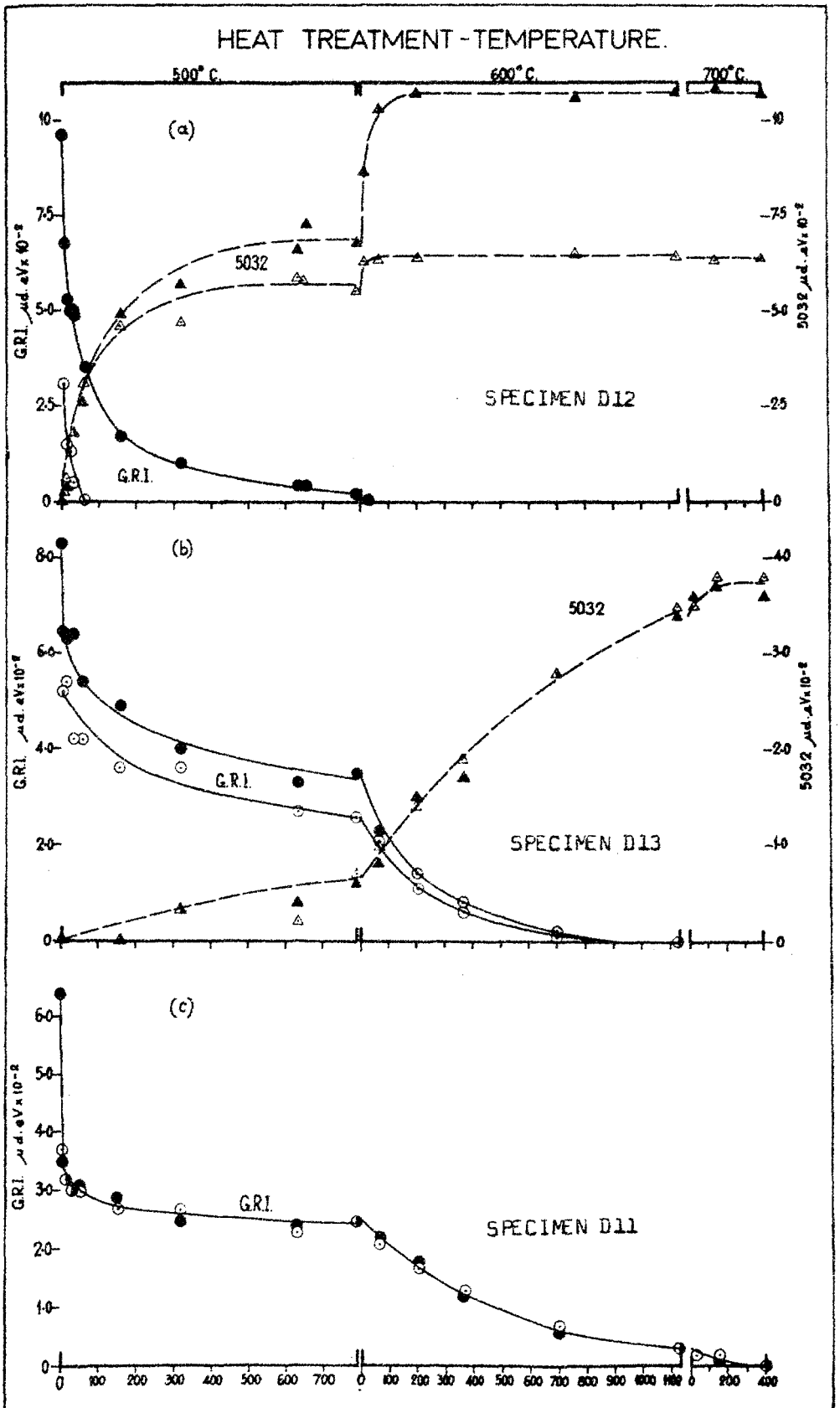
HEAT TREATMENT - TEMPERATURE.
500° C.
600° C.
700° C.
(a)
5032
G.R.I.
SPECIMEN D12
(b)
5032
G.R.I.
SPECIMEN D13
(c)
G.R.I.
SPECIMEN D11
HEAT TREATMENT - TIME IN HOURS

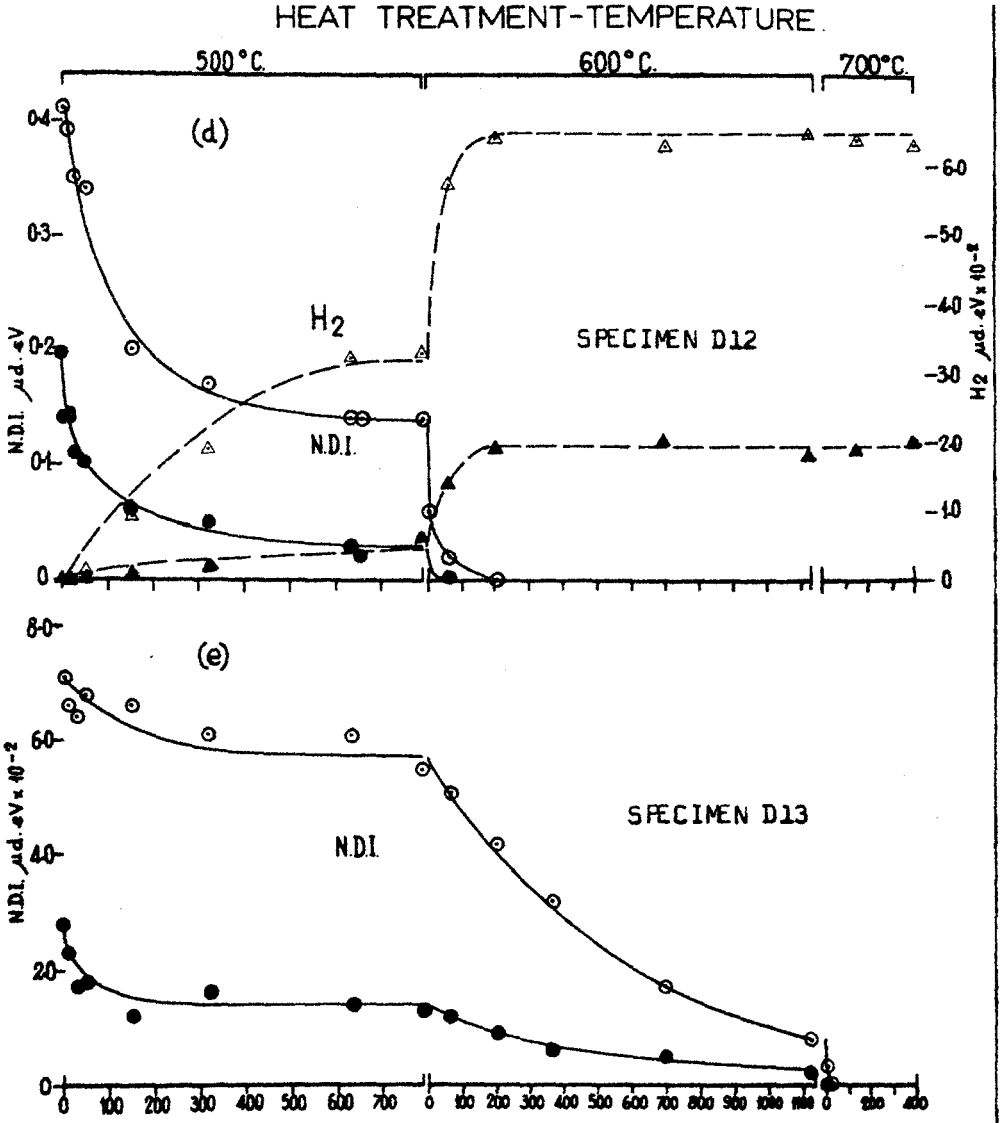

FIGURE 9.1

THE EFFECT OF ISOTHERMAL HEAT TREATMENT AT 500°C, 600°C AND 700°C ON THE STRENGTH OF :

(a) GRI (CIRCLES) AND 5032A (TRIANGLES) IN SPECIMEN D12

(b) GRI (CIRCLES) AND 5032A (TRIANGLES) IN SPECIMEN D13

(c) GRI (CIRCLES) IN SPECIMEN D11

(d) N.D.I. (CIRCLES) AND H_2 (TRIANGLES) IN SPECIMEN D12

(e) N.D.I. (CIRCLES) IN SPECIMEN D13

OPEN SYMBOLS REPRESENT THE VALUES OBTAINED AFTER HEAT TREATMENT IN THE DARK, FILLED IN SYMBOLS AFTER SUBSEQUENT EXPOSURE TO MERCURY LIGHT

reversed by exposure to mercury light.

d) Thermal enhancement of the N.D.1 and H2 bands. Again this process can be reversed by exposure to mercury light, and is therefore ascribed to a modification of the electronic configuration of the defect centres.

It is therefore necessary to take into account the state of charge of the defect centres if the changes in their atomic structure, brought about by isothermal heat treatment, are to be followed by optical absorption. Thus the magnitude of the N.D.1 and the H2 bands after heat treatment in dark was taken as a measure of the number of these centres present. Similarly the magnitude of the G.R.1 and 5032A bands after subsequent exposure to mercury light, was taken as a measure of the number of these centres.

Using this approach the effects of isothermal heat treatment will now be discussed with reference to Figure 9.1 and Tables 9.1, 9.2 and 9.3.

9.4.2. General Effects.

The first four hour heating stage at 500°C caused a rapid annealing of G.R.1-centres in all the specimens. The actual amount by which G.R.1 decreased

was specimen dependent, being 42% in D_{11} (Type IIa) and only 29% and 23% respectively in the Type Ia specimens D_{12} and D_{13}.

Following Clark et al (1956 b) this effect is attributed to vacancy/interstitial recombination. As no such marked decrease in N.D.1 is observed, the required interstitials presumably do not, in the case of Type Ia diamond, derive from this source.

That the reduction in G.R.1 is much larger for Type IIa diamond is to be expected, as, in the absence of platelets interstitial traps of the N.D.1-centre type are not present, and presumably a larger proportion of interstitials are available for recombination. Further, as the interstitials have been deduced to be mobile below 250°C (ϕ 8.6.2 and ϕ 10.4.1), the fact that this decrease is only observed at a higher temperature must be ascribed to a recombination activation energy barrier.

There remains the problem that the reduction in Type Ia diamond is as large as observed. This can be explained by postulating that interstitials close to vacancies are not as mobile as those at greater distances - i.e. there is a degree of stability associated with close vacancy/interstitial pairs.

That this stability postulate is reasonable, derives from Clark et al (1956 b). They show that close pairs gives rise to line broadening in for example neutron irradiated diamond, and that this broadening persists above the temperature at which it is now shown (ϕ 8.6.2 and ϕ10.4.1) that interstitials are mobile. If the interstitials which form close pairs with vacancies are free to move - thus recombining with or moving away from the vacancies - sharpening of the G.R.1 lines should be observed. This is not the case. Only when the temperature is raised to 300°C or above, does line sharpening occur, and this is associated with a decrease in G.R.1 strength, indicating that the close vacancy/interstitial pairs are removed by mutual recombination.

9.4.3. Specimen Dependent Effects.

Further isothermal heat treatment produced permanent changes in the absorption spectra which differed for each specimen and will therefore be discussed separately.

1) Specimen D_{11} (No Nitrogen Platelets Detectable).

The significant points observed during heat

treatment of this specimen are as follows: (Figure 9.1c)

a) At 500°C - Apart from the initial decrease in G.R.1 discussed above, G.R.1 anneals very slowly during the 791 hours of heating at this temperature.

b) At 600°C - G.R.1 anneals more rapidly to about 5% of its original value after 1125 hours. During this stage a TH5 band develops.

c) At 700°C - The remainder of G.R.1 anneals out after 400 hours. During this stage TH5 anneals out and an absorption tail forms.

d) Up to 1200°C - No further changes.

e) No thermal ionization or optical bleaching effects can be detected.

f) As G.R.1 was annealed out completely by the heat treatment, and no increase of this band at 900°C (as reported by Palmer 1961) was found, a further two irradiated Type IIa specimens were subjected to similar isothermal heat treatment. Again in both cases the G.R.1 band was annealed out permanently by prolonged heat treatment at 600 and 700°C. The time of heat treatment was about ten times longer than that reported by Palmer.

2) Specimen D_{13} (Nitrogen Platelet Concentration 7×10^{18} atoms/cc)

The significant points observed during heat treatment of this specimen are as follows: (Figures 9.1b & 9.1e).

a) At 500°C - G.R.1 anneals more rapidly than in D_{11}. N.D.1 anneals more slowly than G.R.1. A small 5032A band develops.

b) At 600°C - G.R.1 anneals out after 800 hours. N.D.1 anneals to about 10% of its original value after 1125 hours. The 5032A band grows.

c) At 700°C - The N.D.1 band anneals out after 25 hours. 5032A reaches a steady maximum value.

d) Up to 1200°C - No further changes.

e) Electron exchange effects - i.e. the reversible thermal enhancement of N.D.1 and thermal bleaching of G.R.1 are observed. No such effects are observed in the strength of the 5032A band.

3) Specimen D_{12} (Platelet Nitrogen Concentration 2×10^{20} atoms/cc).

The significant points observed during heat treatment of this specimen are as follows: (Figures 9.1a

& 9.1d).

a) At 500°C - G.R.1 anneals more rapidly than in D_{13} to about 2% of its original value. N.D.1 anneals more slowly than G.R.1. A 5032A band and an H2 band develop.

b) At 600°C - G.R.1 anneals out after 25 hours. N.D.1 anneals out after 200 hours. The 5032A and H2 bands reach steady maximum values after 150 hours.

c) 700°C to 1200°C - No further changes.

d) More complex electron exchange effects occur. These are thermal enhancement of N.D.1 and H2, and thermal bleaching of G.R.1 and 5032A.

9.4.4. Electron Exchange Effects.

The isothermal heat treatment did not produce any electron exchange effects in the Type IIa diamond (D_{11}). Electron exchange effects between N.D.1 and G.R.1, but not involving 5032A-centres are observed in D_{13}. These effects are explained by the discussion presented in Chapter VIII. In D_{12}, however, some additional electron exchange interactions are observed, which will now be described in more detail.

1) G.R.1 and N.D.1.

As mentioned in Chapter VIII, the G.R.1 band is bleached when an irradiated Type Ia specimen is heated in the dark but the thermal bleaching is not complete. However, after 58 hours isothermal annealing at 500°C the G.R.1 band in specimen D_{12} (high platelet nitrogen concentration) can be completely bleached thermally. This can be explained as follows:

Although vacancies and interstitials are produced in equal amounts, not all the interstitials combine with nitrogen platelets to form N.D.1-centres. Thus there are initially more vacancies (G.R.1-centres) than N.D.1-centres, and the excess vacancies cannot be ionized thermally, so that the G.R.1 band is not bleached completely. The G.R.1-centres, however, anneal more rapidly than N.D.1-centres, and after about 58 hours heat treatment at 500°C, equal amounts remain, so that the heat treatment also results in complete bleaching of the G.R.1 band. The N.D.1 band is never bleached completely by subsequent illumination with light in this band, as this energy of light also causes electron transfer from G.R.1-centres to N.D.1-centres as was discussed in the previous chapter.

2) 5032A Band and the H2 Band.

Also during the first 58 hours at 500°C, a 5032A band was formed, which exhibited no effects due to thermal ionization. As soon as G.R.1 was reduced beyond the point at which it could be completely bleached, however, the 5032A band (which was growing in size) became subject to thermal bleaching and optical enhancement.

Furthermore, after this first 58 hours an H2 band also developed, and was found to be subject to thermal enhancement and optical bleaching effects.

This situation is illustrated in Figure 9.2 which is the O.A. spectrum, measured at 80°K, of D_{12} after 550 hours at 500°C, before and after exposure to mercury light. Figure 9.3 is the O.A. spectrum of the same specimen after all heat treatment (up to 1200°C) had been completed. Measurement in this case was made at room temperature.

It was found that heat treatment in the dark at any temperature above 150°C serves to enhance H2 and to bleach the 5032A band. Exposure to mercury light serves to bleach H2 and enhance the 5032A band; this cycling of the band strengths can be repeated indefinitely.

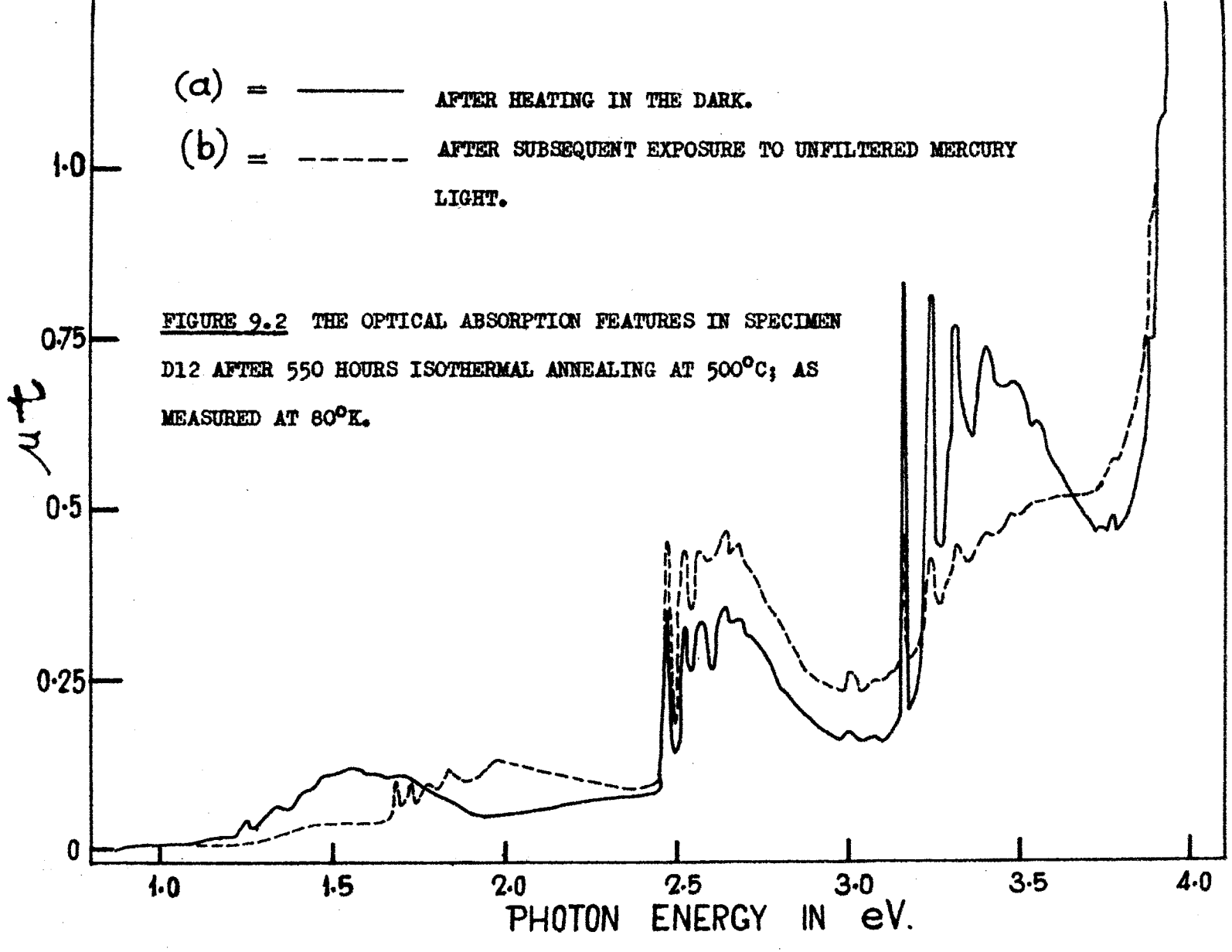

FIGURE 9.2 THE OPTICAL ABSORPTION FEATURES IN SPECIMEN D12 AFTER 550 HOURS ISOTHERMAL ANNEALING AT 500°C; AS MEASURED AT 80°K.

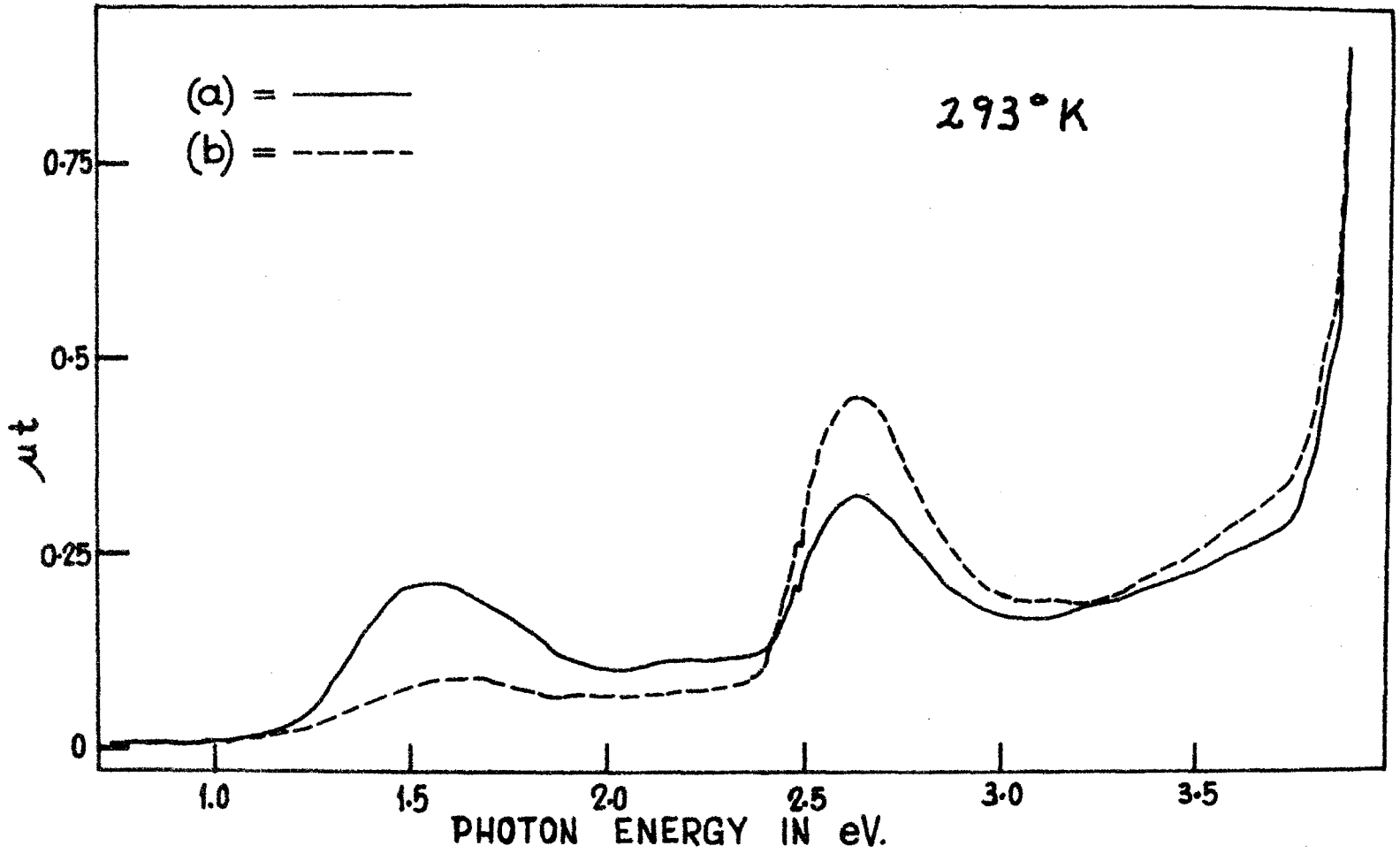

FIGURE 9.3 CYCLING OF THE H_2 AND 5032A BANDS IN SPECIMEN D12 AFTER ANNEALING UP TO 1200°C.

(a) AFTER HEAT TREATMENT IN THE DARK.

(b) AFTER SUBSEQUENT ILLUMINATION WITH MERCURY LIGHT.

The effect of both time and temperature upon the growth of H2, and the simultaneous reduction of the 5032A band, are illustrated in Figure 9.4 for another Type Ia diamond, D_{14}, which had previously been heated for 700 hours at 600°C after irradiation.

The effect of illumination with monochromatic light of various wavelengths was investigated by heating D_{14} in the dark at 500°C for four hours and then exposing it to a particular mercury emission line until no further change in band strength could be detected. The results are listed in Table 9.4. It is evident from this study that only light of energy greater than 2.27 eV is effective in reversing the changes brought about by heat treatment in the dark.

The reversible changes brought about by heat treatment and illumination are probably due to charge transfer between the 5032A and H2 centres. No simple mechanism can be suggested, however, as it is clear from Figure 9.4 that at least two other broad optical absorption features, between 3.0 and 3.7 eV, and between 2.0 and 2.4 eV, are involved as well.

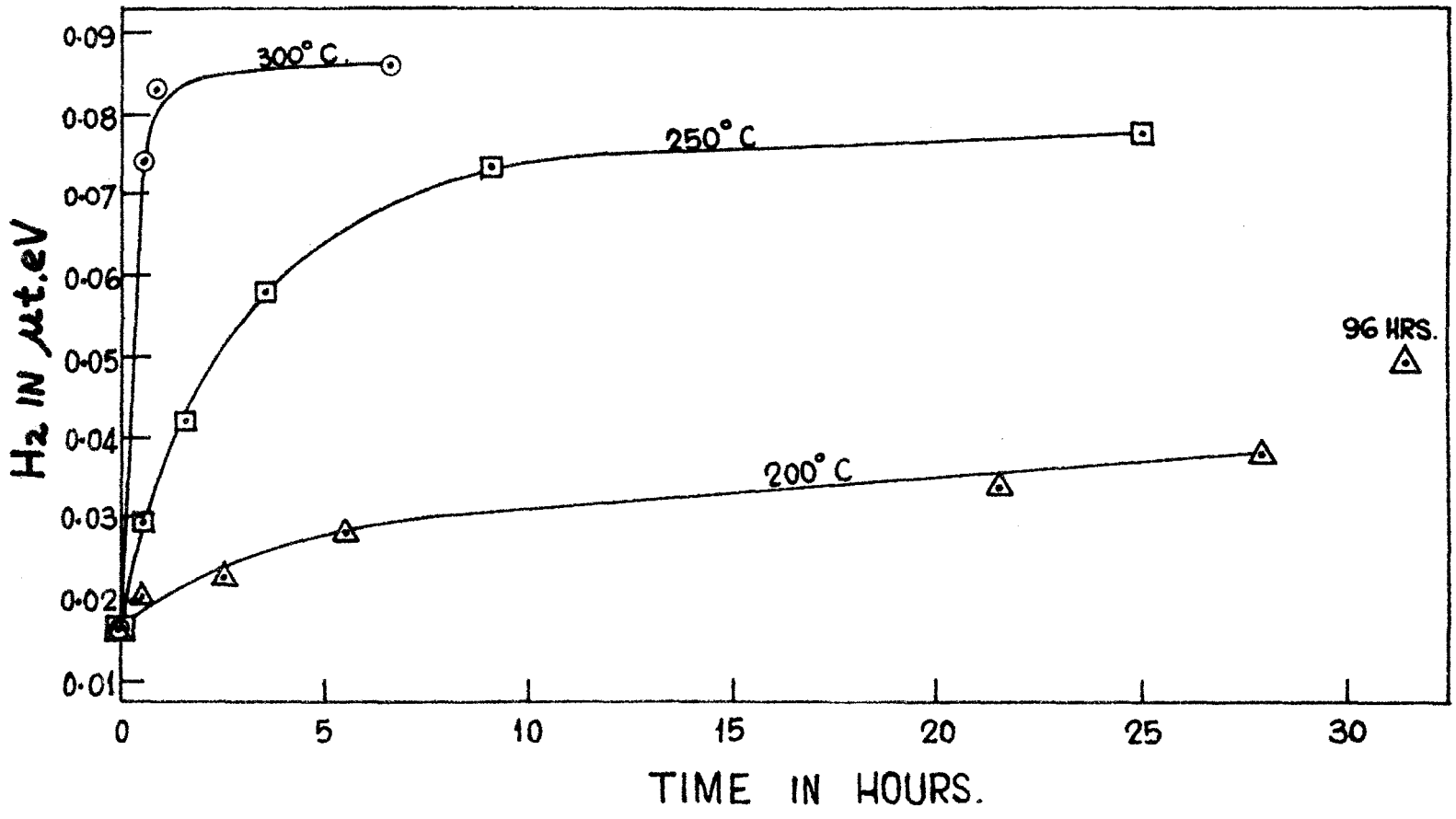

FIGURE 9.4a THE EFFECT OF ISOTHERMAL HEAT TREATMENT IN THE DARK ON THE STRENGTH OF THE H_2 BAND.

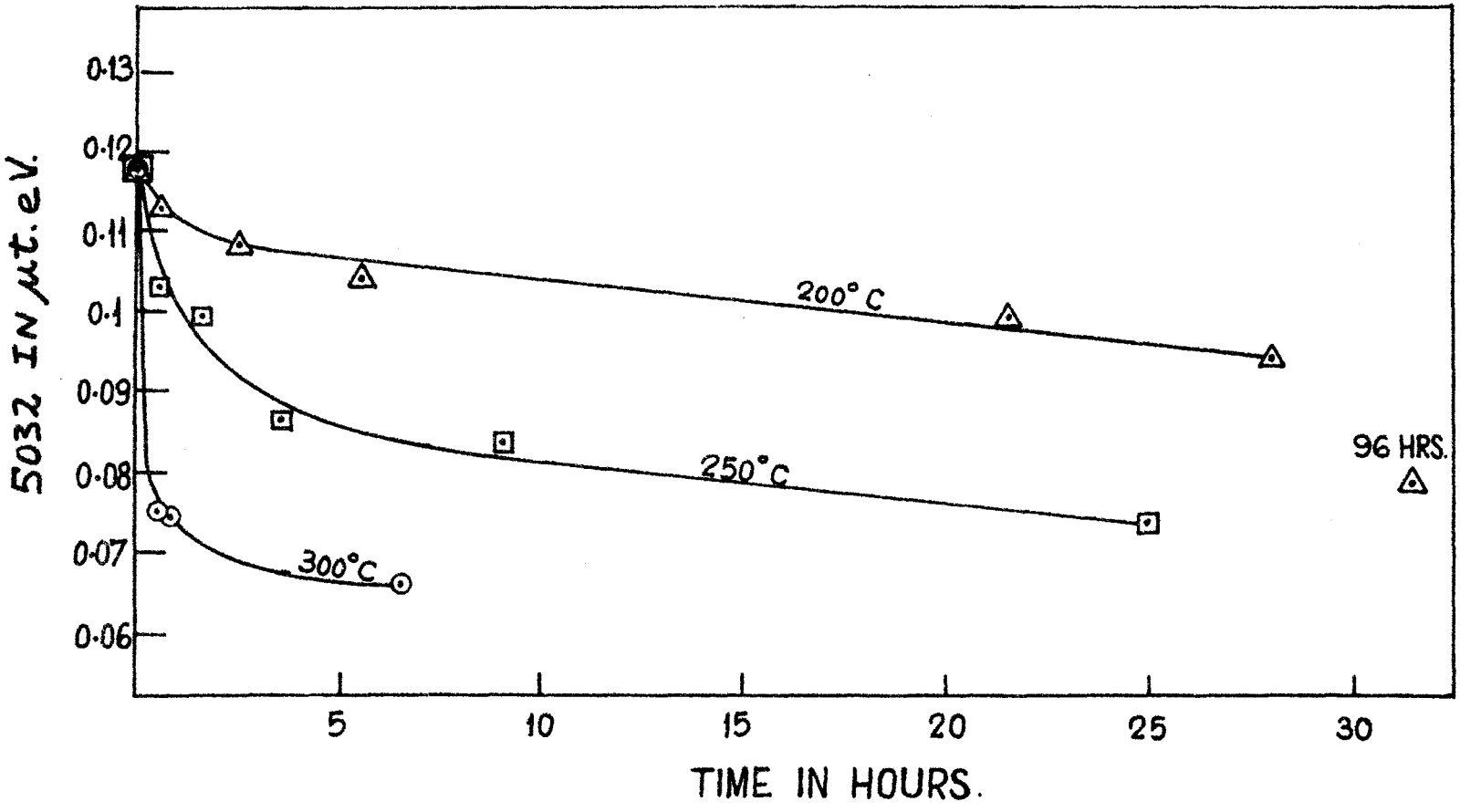

FIGURE 9.4b THE EFFECT OF ISOTHERMAL HEAT TREATMENT IN THE DARK ON THE STRENGTH OF THE 5032A BAND.

TABLE 9.4

THE EFFECT OF ILLUMINATION WITH MONOCHROMATIC LIGHT ON THE 5032A AND H2 BANDS IN D14

NOMINAL TREATMENT	ENERGY OF LIGHT IN eV	BAND STRENGTH (μt.eV)	
		5032A	H2
Heat 500°C	-	0.063	0.084
Illumination	1.98	0.062	0.085
Illumination	2.14	0.063	0.082
Illumination	2.27	0.089	0.049
Heat 500°C	-	0.064	0.073
Illumination	2.84	0.118	0.017
Heat 500°C	-	0.062	0.074
Illumination	3.40	0.117	0.018

9.5. 5032A-Centres.

A 5032A band is formed only in diamonds containing nitrogen platelets by heat treatment at temperatures in excess of about 500°C after irradiation. The strength of the band depends both on the irradiation dose and the nitrogen platelet concentration.

As the band is only formed at temperatures of 500°C and above, by which time all interstitials have been trapped to form N.D.1-centres, it appears that the 5032A-centre must be formed by the combination of a vacancy and a nitrogen platelet. 500°C is presumed, therefore, to be the temperature at which vacancy mobility first occurs.

This deduction is supported by independent observations of Clark (1962), who subjected twelve diamond samples to an equal dose of neutron irradiation and subsequently heated these specimens simultaneously at 750°C, after which 5032A bands were formed. In Figure 9.5 Clark's results are represented schematically by plotting the log of the strength* of the secondary absorption edge, which is a

---

*i.e. slope of line joining points on the absorption curve at 3.8 and 3.9 eV.

measure of the amount of nitrogen platelets (Kaiser and Bond 1959), as a function of the strength of the 5032A band produced in each specimen. Although not reported by Clark, a linear correlation coefficient r = 0.89 is found between the strength of the 5032A band and the logarithm of the strength of the secondary absorption edge.

As the formation of a 5032A-centre involves migration of one of the primary products of irradiation damage (a vacancy) to a nitrogen platelet, it is reasonable to assume that other traps for such a defect can exist in diamond. A direct correlation between the amount of nitrogen platelets and the 5032A band produced will therefore not be expected.

If the concentration of traps other than platelets be S, and the concentration of sites on platelets available for 5032A-centre formation be P, then, very simply, the fraction of vacancies forming 5032A-centres is given by

$$F = \frac{P}{S + P}$$

i.e. the 5032A band strength is proportional to $F/S+P$. As S is unknown, and may be expected to vary from

FIGURE 9.5 SCHEMATIC ILLUSTRATION OF THE RESULTS OF CLARK (1962), DEMONSTRATING THE RELATION BETWEEN THE STRENGTH OF THE SECONDARY ABSORPTION EDGE IN A SPECIMEN AND THE STRENGTH OF THE 5032A BAND PRODUCED BY NEUTRON IRRADIATION AND SUBSEQUENT HEAT TREATMENT.

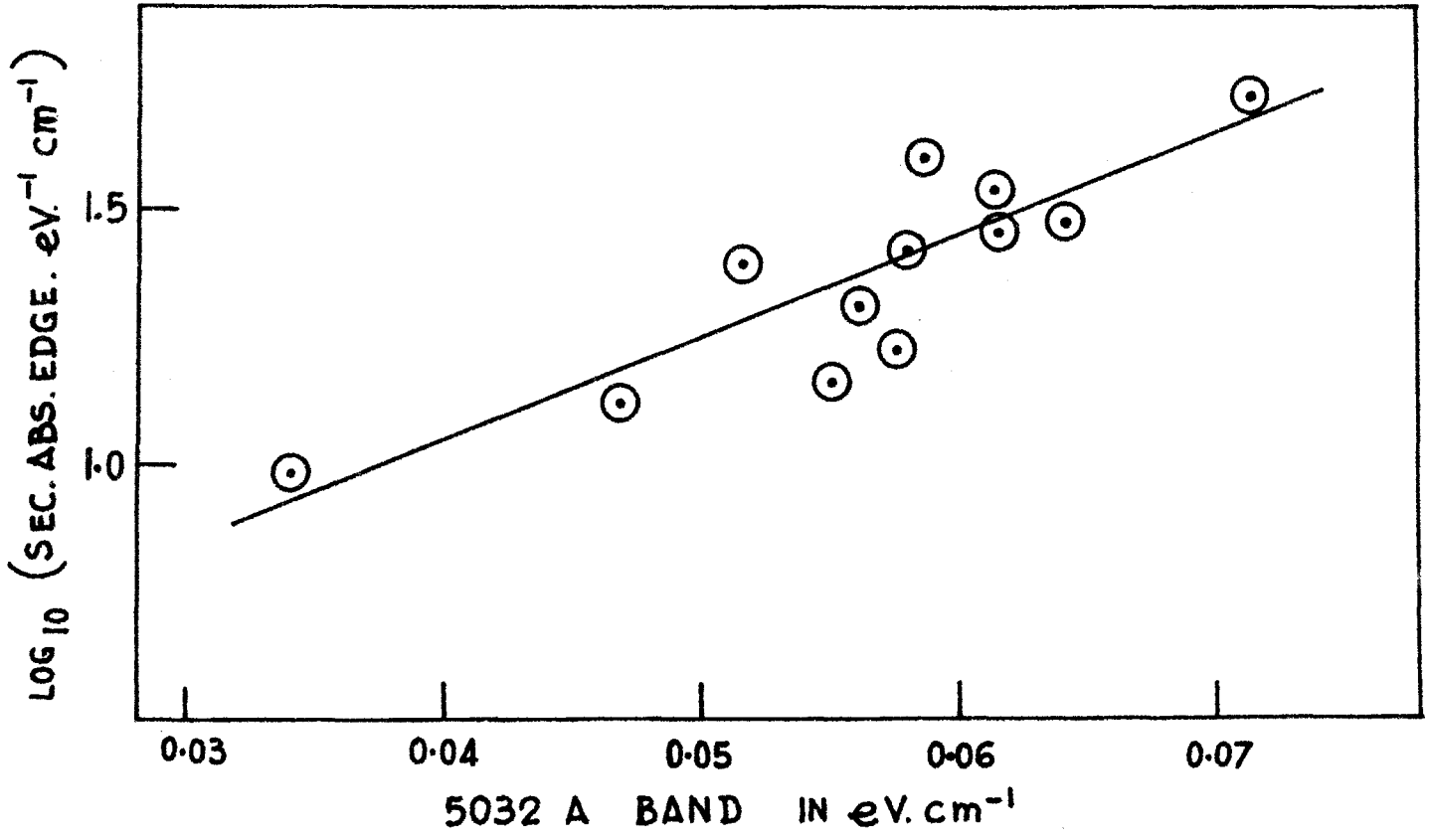

specimen to specimen, as formal analysis of this data is not justified; however, it may readily be shown that, when the ratio $^{P}/_{S+P}$ has values between about 0.2 and 0.9, it is closely proportional to the characteristic of the logarithm of P.

Measurements by Elliot et al (1958) and Clark et al (1962) on the polarisation of the green luminesence associated with a 5032A-centre indicate that the centre has <110> symmetry. The simplest model will therefore be a vacancy anchored in a next nearest neighbour position to a substitutional nitrogen atom of a nitrogen platelet.

No E.P.R. or I.R. spectra, which could be associated with 5032A-centres, could be detected.

9.6. Annealing of G.R.1-Centres.

9.6.1. Investigation of the Nitrogen Dependence.

From the detailed results reported for three specimens, it is clear that the rate of annealing of the G.R.1 band depends on the amount of nitrogen in platelet form present in the specimens. This observation was confirmed by a study of an additional five specimens.

It therefore appears certain that the rate of annealing of G.R.1 is indeed controlled to a large extent by the impurity content of the specimens. The specific impurity involved, appears to be nitrogen in platelet form, which is known to be immobile at temperatures up to 1200°C. The proposal of Palmer (1961) that G.R.1-centres are immobile below 1000°C and anneal by the migration of impurities to them, is therefore probably not correct. A more feasible explanation would be that the annealing of the G.R.1 band is due to the migration of vacancies.

The vacancies in irradiated Type Ia diamonds are ionized by heat treatment above 180°C, because of the presence of N.D.1-centres which are acceptors. When the nitrogen platelet concentration is high, so is the N.D.1-centre concentration, and consequently a large fraction of the G.R.1-centres is ionized. In Type IIa diamonds the vacancies are not ionized. This difference in the state of charge of vacancies may account for the nitrogen dependence of the rate of annealing of G.R.1 if an ionized vacancy is more mobile than one in the neutral state.

In order to investigate this possibility, two specimens cut from the same diamond block and having a homogeneous nitrogen content of 2×10^{20} atoms/cc in

platelet form, were irradiated together to a dose of approximately 10^{18} electrons/cm^2. The specimens were heated together in a large furnace at 500°C, one being kept in total darkness. A quartz lens was used to focus light from a mercury lamp on to the other, in order to effect electron transfer from N.D.1-centres to G.R.1-centres. Thus the G.R.1-centres in the specimen kept in darkness would be ionized during heat treatment, whereas the same centres in the other specimen would be largely neutral.

After annealing these specimens for 400 hours the residual G.R.1 band in the specimen kept in the dark (G.R.1-centres ionized), contrary to expectation, was found to be 5% larger than the residual G.R.1 band in the specimen exposed to mercury light. The experimental error in measuring these bands is estimated to be about 3%, so that the observed difference may or may not be real.

In carrying out this experiment it was realized that a negative result would be completely inconclusive, as the relaxation time of the electronic processes may well be much shorter than the time taken for a single vacancy jump. In such an event, optical de-ionization would be completely ineffective in affecting the vacancy

mobility, as thermal re-ionization of the vacancy would occur before the vacancy could move. Only if the time taken for an electron to be transferred from a neutral vacancy to an N.D.1-centre, by the process of ϕ 8.5.1, is comparable to, or longer than, the time for a single vacancy jump, can any positive result be expected from the experiment.

9.6.2. Proposed Model.

The following mechanism is now proposed to explain the effect of nitrogen platelets on the rate of annealing of G.R.1-centres.

The vacancies created by irradiation damage are immobile. At about 500°C they become mobile, but at this stage do not have enough energy to overcome an activation energy barrier to mutual combination with each other; thus if no nitrogen platelets are present, very little annealing of the G.R.1 band occurs. At higher temperatures the vacancies have sufficient energy to overcome the energy barrier preventing them from combining; double and multiple vacancies are formed. The G.R.1 band in Type IIa specimens therefore decays, and other absorption features such as the TH5 band and the absorption tail are

formed.

In discussing such a mechanism one has to consider why the mobile vacancies, in view of the difficulty of combining with each other, do not escape at the surfaces of the crystal. This query cannot be answered adequately; however, it appears that the crystal surfaces of diamonds present a barrier to the escape of considerable numbers of vacancies, because the decay of the G.R.1 band is always associated with the growth of other optical absorption features in all specimens.

In Type Ia diamonds the activation energy barrier preventing nitrogen platelet/vacancy combination is probably lower. This is an expected result as James and Evans (1965) showed that the diamond lattice on either side of a nitrogen platelet is in compression. Such defects will therefore be ideal sinks for vacancies, which, being mobile at 500°C, are expected to migrate to, and combine with the platelets. G.R.1 would therefore anneal rapidly and correspondingly a 5032A band will be formed.

From Figure 9.1 it is evident that the 5032A band in D_{12} and D_{13} can continue to grow after the G.R.1 band has annealed completely. In fact, the growth of the 5032A band appears to correlate more closely with the

decay of the N.D.1 band, rather than with that of the G.R.1 band. It has been shown however, that N.D.1-centres arise from the combination of an interstitial and a nitrogen platelet. Annealing of N.D.1-centres will therefore not be expected to produce any new centres which could account for the formation of the 5032A band.

The continued growth of the 5032A band after the disappearance of G.R.1 can be accounted for by considering ionized vacancies, which are optically inactive (§ 9.4.4.). As is manifested by the unbleachable component of the N.D.1 band during this stage, some vacancies in the system are permanently ionized and do not contribute to the strength of the G.R.1 band. Therefore after G.R.1 has disappeared, there are still some vacancies left, which can participate in further 5032A-centre formation.

Subsequently a similar phenomenon was observed by Dyer and Ferdinando (1965) in semiconducting Type IIb diamonds. In these specimens no G.R.1 band is observed after irradiation, as all the vacancies are ionized by the naturally occuring acceptor centres at room temperature. After heat treatment at 900°C, however, the usual absorption tail is formed, although no decay in the G.R.1

band could of course be detected.

9.7. H2 Centres.

Unlike the 5032A band, the H2 band is not well known as a product of the annealing of irradiation damage in diamond, presumably because it is not as readily formed as the 5032A band. The H2 band formed in D_{12}, after heat treatment at 500°C, and measured at room temperature and at 80°K, is shown in Figure 9.6. The energies of the main optical absorption features are listed in Table 9.5. As this absorption system is situated in the near infra-red region the lead-sulphide detector available on the Unicam S.P. 700 spectrophotometer was used. This arrangement did not offer good resolution; however, lines further into the infra-red region, not observed by Clark et al (1956 b) with a Hilger Uvispek spectrophotometer, could be detected. As suggested by Clark et al for other characteristic diamond systems such as the 4150A band, it appears that the H2 band consists of a principal line of lowest energy; additional less sharp lines arise from the interaction between the main electronic transition and vibrational states of the crystal. In this respect the system is quite typical of diamond.

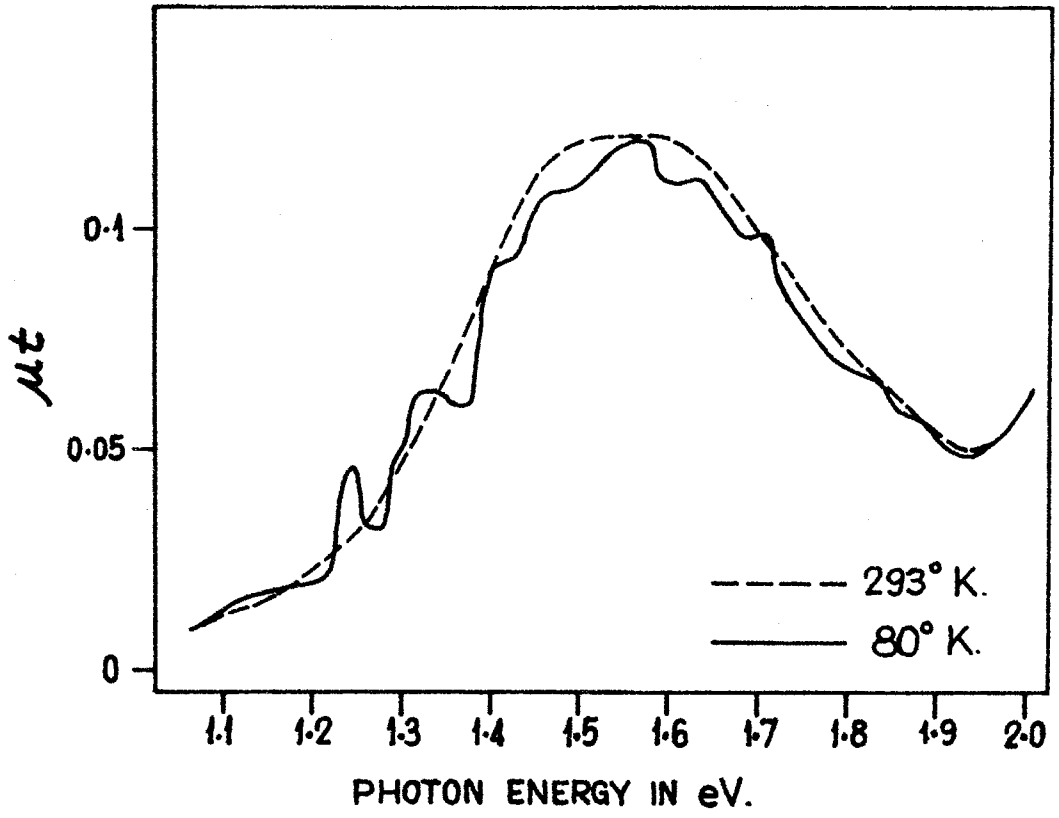

FIGURE 9.6 THE H_2 OPTICAL ABSORPTION BAND AS MEASURED AT ROOM TEMPERATURE AND AT LIQUID NITROGEN TEMPERATURE.

TABLE 9.5

ENERGIES OF THE MAIN OPTICAL ABSORPTION FEATURES OF THE H2 BAND

OPTICAL ABSORPTION FEATURE	POSITION IN eV
Lower energy limit	1.20
Principal line	1.25
Second line	1.32
Third line	1.40
Fourth line	1.47
Fifth line	1.56
Sixth line	1.63
Higher energy limit	2.00

No E.P.R. or I.R. spectra which could be associated with H2 centres could be detected.

An H2 band could only be produced by the annealing of irradiation damage in specimens containing more than 10^{19} atoms/cc nitrogen in platelet form. In these specimens the H2 band could be produced readily when the heat treatment was carried out over long periods at 500°C or 600°C. When similar specimens were heated at 900°C directly after irradiation, however, no H2 band was produced, although once an H2 band is developed in a crystal, it is stable to temperatures well above 900°C.

Some further indirect information on the nature of H2 centres was obtained from a study of irradiation damage in Type Ib diamonds. (Which contain nitrogen, not as platelets, but in dispersed form.) This will be discussed fully in the next chapter. Briefly, however, it was found that an N.D.1 band is also produced in these specimens by irradiation damage. The formation of this N.D.1 band, however, occurs at a lower temperature than in specimens containing nitrogen platelets. Subsequent heat treatment at temperatures above 500°C resulted in the decay of G.R.1 and the growth of a band similar to the 5032A band in platelet containing specimens.

However, no additional band analogous to the H2 band has been formed by any treatment in these specimens.

The evidence therefore indicates that the formation of an H2 centre is associated with the annealing of a product or products, of irradiation damage and substitutional nitrogen, specifically in platelet form. Any model for the H2 centre will at this stage be speculative; however, the following tentative proposal may explain H2 centres in terms of nitrogen platelets, interstitials and vacancies.

Vacancies and interstitials are produced by irradiation damage; the interstitials are mobile at temperatures below 250°C, the vacancies not. The interstitials migrate to nitrogen platelets, which as described in § 8.8 produce both regions where the diamond lattice is in compression, and regions where the lattice is dilated. (An activation energy barrier is presented to interstitial/platelet combination, so that an interstitial would not combine with the platelet as readily as in Type Ib specimens.)

At 250°C the interstitial has enough energy to overcome the energy barrier preventing combination with a platelet, and is presumably anchored in the platelet

region where the diamond lattice is dilated, thus relieving strain.

At temperatures of 500°C or above, the vacancies become mobile and the nitrogen platelets will act as ideal sinks for them. A vacancy will therefore be trapped, in the region where the lattice is in compression, presumably in a second nearest neighbour position to provide <110> symmetry, to produce a 5032A-centre. At this stage some vacancies may also, however, be trapped by N.D.1-centres, which compromise a platelet with an anchored interstitial; thus forming an H2 centre. Vacancy-interstitial recombination is prevented as the irradiation induced defects are pinned to different locations in the platelet region. In the case of dispersed substitutional nitrogen, vacancy-interstitial recombination is expected, and no additional band such as the H2 band will be formed.

Such a model does not explain why no H2 centres were formed in specimen D_{13} which contained only few nitrogen platelets. However, in this instance the very few N.D.1-centres may have been formed in positions far away from the vacancies, where they are not readily accessible for H2 formation.

CHAPTER X.

IRRADIATION DAMAGE IN TYPE Ib DIAMOND.

10.1. Introduction.

In order to produce defect centres in diamond which are associated with substitutional nitrogen in the paramagnetic configuration, the effects of irradiation damage and subsequent annealing in Type Ib diamonds were now investigated. After heat treatment the vacancies and interstitials created by irradiation are expected to combine with this isolated substitutional nitrogen, thus forming defect centres different from those in Type Ia diamonds where the nitrogen is in platelets.

Four Type Ib specimens, in which only the defect centres identified as substitutional paramagnetic nitrogen could be detected, were therefore irradiated with 0.78 MeV electrons. Two of these specimens were specially thinned to about 0.8 mm, so that any absorption due to induced defect centres could be measured up to 5.4 eV, this being necessary as the absorption due to paramagnetic nitrogen is large between 3.0 and 5.4 eV.

10.2. Defects induced Below Room Temperature.

In Type Ia diamonds, an N.D.1 band is produced by room temperature irradiation. If the irradiation is carried out below room temperature at minus 80°C, no N.D.1 band results, but after subsequent heat treatment at 250°C, the N.D.1 band is formed. It was concluded that the N.D.1 band produced by room temperature irradiation is due to the combination of an interstitial with a nitrogen platelet, as a result of the localised heating associated with electron irradiation. In order to minimize this, two Type Ib specimens were now irradiated at a very low dose rate while being cooled by a mixture of solid carbon dioxide and acetone, to a total dose of 1×10^{18} electrons/cm^2. A Type Ia and a Type IIa specimen were included with the Type Ib specimens as a reference.

The O.A. bands induced by this treatment in the specimens are listed in Table 10.1. As expected, no N.D.1 band was induced in Type IIa specimen at this or at later annealing stages. Neither was any N.D.1 band induced in the Type Ia specimen; the temperature in the localised regions where atomic displacements took place was therefore below 250°C. Each Type Ib specimen, however, exhibited a large N.D.1 band, and a G.R.1 band

TABLE 10.1

OPTICAL ABSORPTION BANDS PRODUCED BY IRRADIATION AT LOW TEMPERATURES

SPECIMEN	TYPE	NITROGEN CONCENTRATION (ATOMS/cc)	IRRADIATION DOSE (ELECTRONS/cm^2)	BAND STRENGTH	
				N.D.I. ($\mu t.eV$)	G.R.I. ($\mu t.eV$)
D16	IIa	None detectable	1×10^{18}	None detectable	0.053
D17	Ia	2×10^{20}	1×10^{18}	None detectable*	0.058
D18	Ib	1×10^{18}	1×10^{18}	0.384	0.017
D19	Ib	3×10^{17}	1×10^{18}	0.295	0.021

* After 20 hours heat treatment at $400^{\circ}C$, a value of 0.108 was obtained.

about one third the size of those induced in the other specimens, although all the specimens were subjected to identical irradiation treatment. This is shown in Figure 10.1.b for specimen D_{18}.

The E.P.R. spectrum of D_{18} before and after this irradiation treatment is shown in Figures 10.2a and b. Apparently a single isotropic E.P.R. line superimposed on the isotropic central line of the paramagnetic nitrogen E.P.R. spectrum was induced by this treatment.

10.3. Comparison of the N.D.1-Centres in Type Ia and Ib Diamond.

The first question to be resolved is whether the apparent N.D.1 band formed in Type Ib diamond, is the same as that in Type Ia specimens, and whether in fact it is reasonable to expect identity.

In the sense that both are thought to represent substitutional nitrogen in combination with an irradiation induced defect (interstitial), one expects similarity; however, as the nitrogen configuration is different in each case, some modification is probable.

FIGURE IV.1 OPTICAL ABSORPTION SPECTRA OF SPECIMEN D18 MEASURED AT ROOM TEMPERATURE.

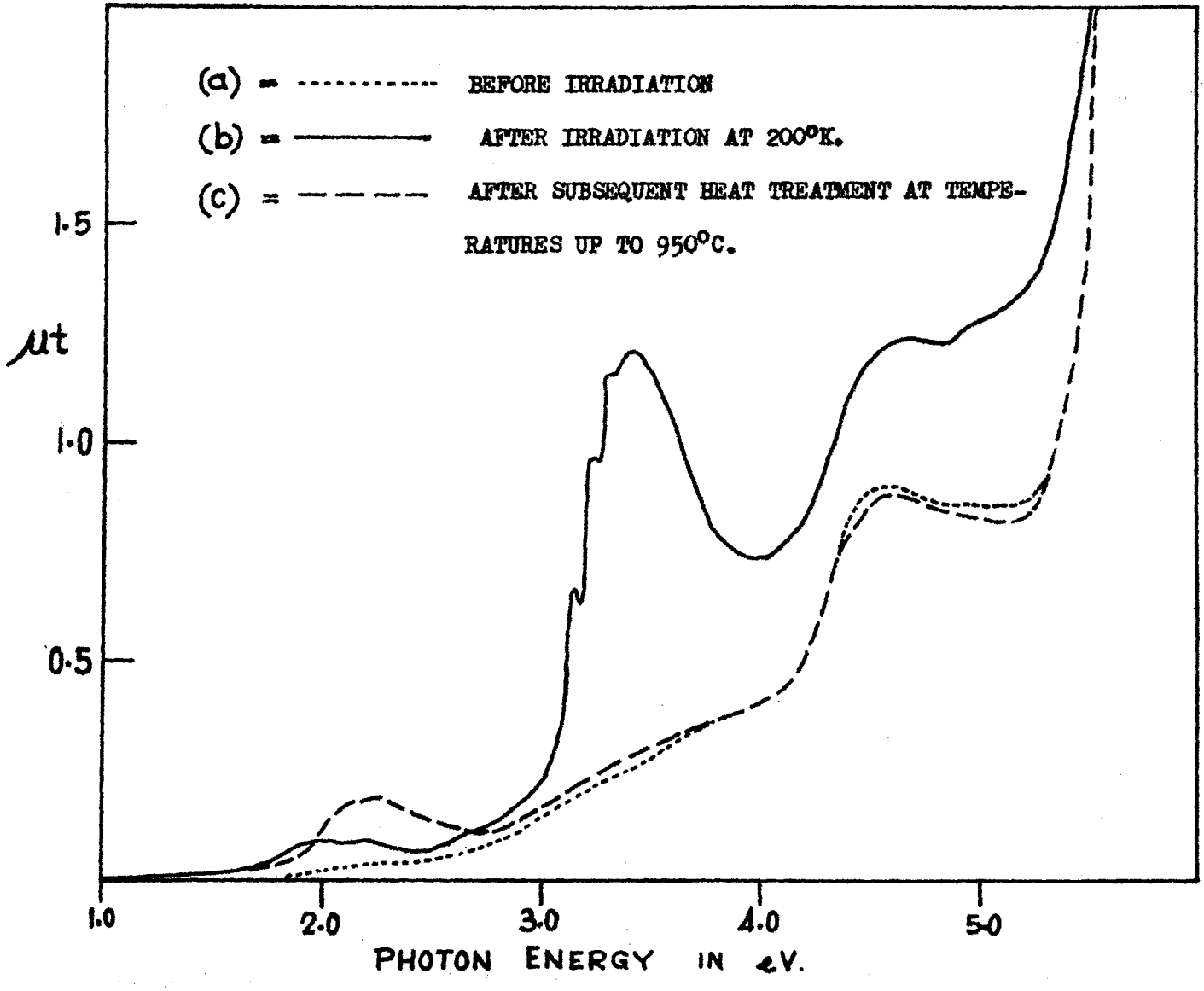

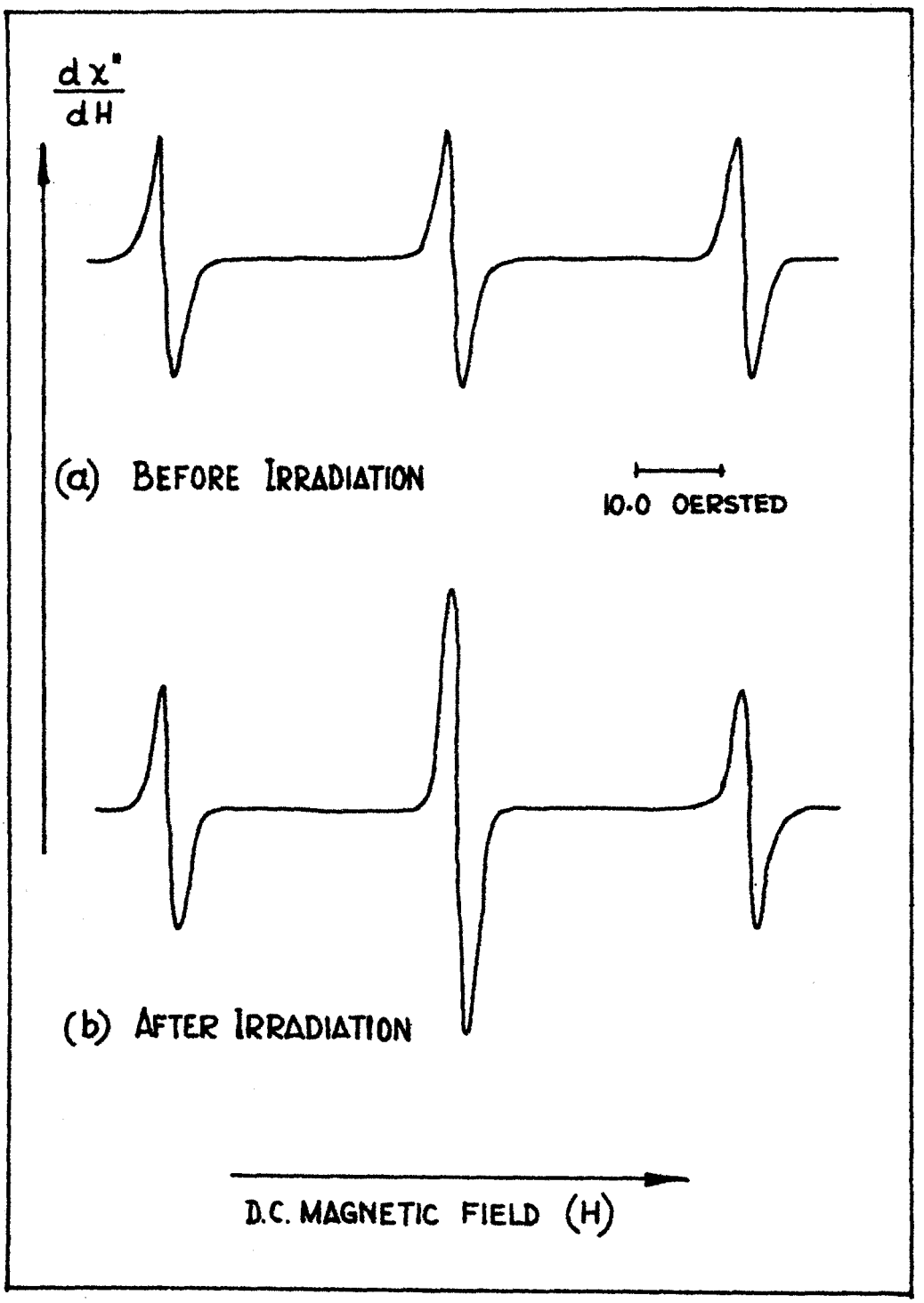

FIGURE 10.2 FIRST DERIVATIVE E.P.R. SPECTRA OF SPECIMEN D18 WITH THE D.C. MAGNETIC FIELD APPLIED IN A (100) DIRECTION, BEFORE AND AFTER IRRADIATION AT 200°K.

10.3.1. Points of Similarity.

a) As just mentioned both are associated with irradiation damage and substitutional nitrogen, and formed at relatively low temperatures.

b) The energies at which the main and excited state lines of the N.D.1 in Type Ia and Type Ib diamonds occur, as measured at 80°K, cannot be distinguished with the Unicam spectrophotometer. This is illustrated in Figure 10.3.

c) Both N.D.1-centres appear to interact electronically with G.R.1-centres. After irradiation of the Type Ib specimens G.R.1 is small and N.D.1 large - this being equivalent to the thermally activated state in Type Ia diamonds (Chapter VIII.).

10.3.2. Points of Difference.

a) Temperature of formation: In Type Ia diamond N.D.1 formation can be inhibited by irradiating at minus 80°C, subsequent heating at 250°C then promotes N.D.1 formation. In Type Ib diamond N.D.1 is formed during irradiation at minus 80°C; lower temperatures may, however, be

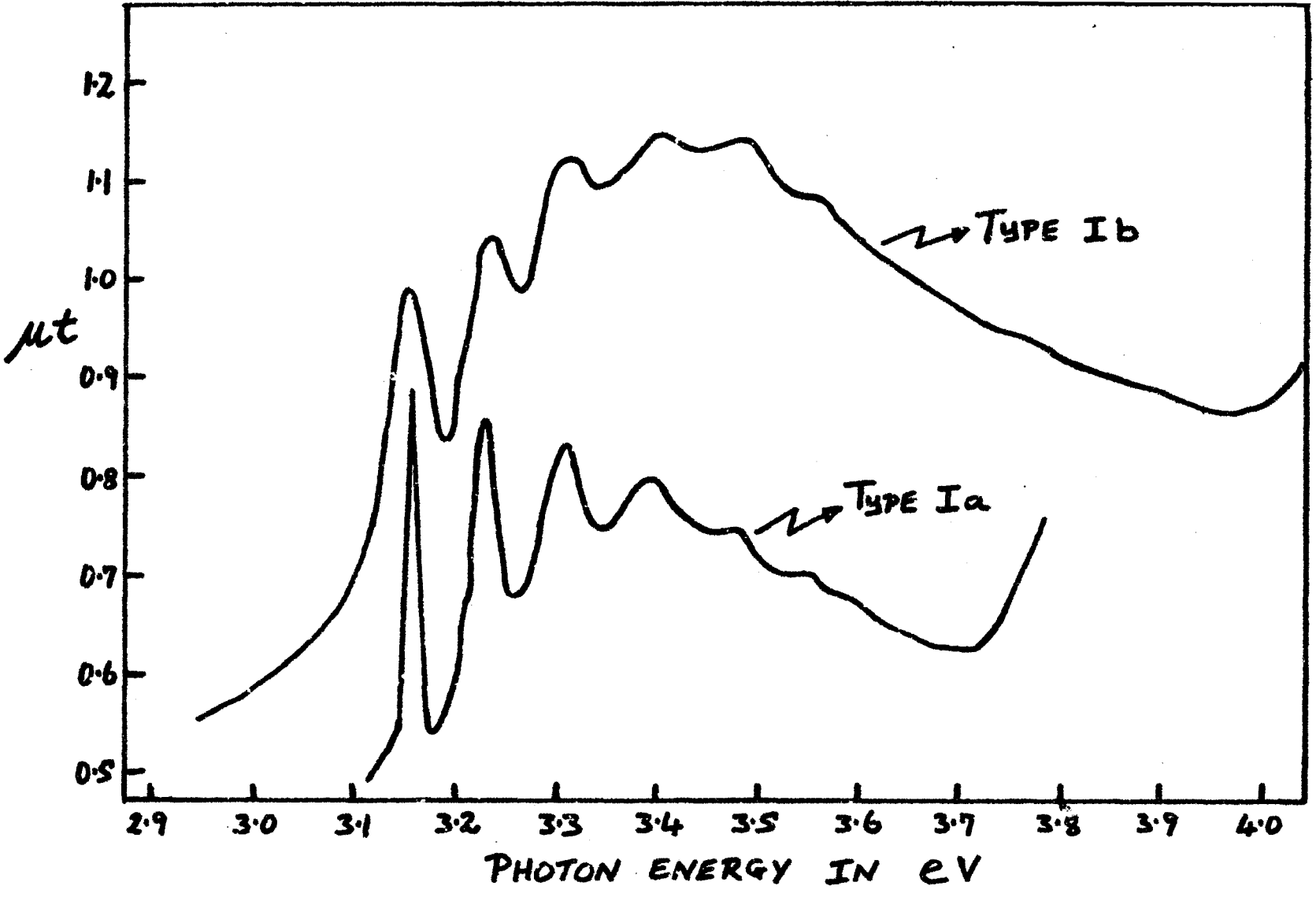

FIGURE 10.3 COMPARISON OF THE N.D.1 BANDS IN IRRADIATED TYPE Ia AND TYPE Ib DIAMOND.

effective in inhibiting N.D.1 formation.

b) Overall width of the band: In Type Ia diamonds the N.D.1 band is found between 3.1 and 3.7 eV. The lower energy limit of the N.D.1 band in Type Ib diamond is also at 3.1 eV. It is difficult to determine the higher energy limit, because of the overlapping absorption due to paramagnetic nitrogen in this region; however, this band appeared to extend to 4.0 eV (Figure 10.3).

c) Broader component lines: As is evident from Figure 10.3 the N.D.1 band in Type Ia diamond consists of sharper component lines than the N.D.1 band in Type Ib diamond, both being recorded at liquid nitrogen temperature.

d) Interaction with G.R.1: After irradiation the N.D.1 in Type Ib diamonds is large - G.R.1 is small. It therefore appears that thermal activation of N.D.1-centres and consequent bleaching of G.R.1 occurs at room temperature. In Type Ia diamond this process only becomes evident at about 180°C.

10.4. N.D.1-Centres in Type Ib Diamond.

10.4.1. Formation of N.D.1-Centres.

As mentioned above N.D.1-centres form at a lower temperature in Type Ib diamond, than in Type Ia's. This difference can be accounted for by assuming that the interstitial is mobile, but that the activation energy barrier for interstitial/nitrogen platelet combination (§ 8.8) is the limiting condition for N.D.1 formation in Type Ia diamond.

The lattice strain around an isolated substitutional nitrogen atom is presumably very different from that around a nitrogen platelet in that no large regions where the lattice is in compression is expected. In Type Ib diamond one therefore expects a lower activation energy barrier for interstitial/nitrogen combination, and interstitial mobility is probably the limiting condition for N.D.1-centre formation.

10.4.2. Electronic Configuration.

To account for the observations described in Chapter VIII the N.D.1 ground state was placed at approximately 1.5 eV above the valence band. Thermal activation

of an electron from the valence band to this ground state could be observed at about 180°C.

If the N.D.1-centres in Type Ib diamond are analogous to those in Type Ia specimens, the ground state must be sufficiently near to the valence band to be available to electrons at room temperature.

The position of the ground state of the N.D.1-centre in a Type Ib diamond is of course not certain. The acceptor level in semi-conducting Type IIb diamonds (ϕ 4.6) is 0.34 eV above the valence band. Thermal activation of electrons to this level occurs at room temperature. It thus appears reasonable to assume that the ground state of N.D.1 should lie at about 0.5 eV above the valence band. The N.D.1 then arises from transitions from this ground state to a series of excited states of increasing energy, with the principal excited state at 3.16 eV above the ground state. The excited state of highest energy is about 4.0 eV above the ground state, i.e. 4.5 eV above the valence band, this being derived from the high energy limit of the N.D.1 band.

The excited state of greatest energy of the N.D.1-centre in Type Ia specimens was estimated to be 5.2 eV above the valence band. The process of electron transfer

from N.D.1 to G.R.1-centres in a Type Ib diamond by illumination in the N.D.1 band, will therefore not be as effective as in the Type Ia case, as the electrons must be thermally excited across a larger gap between the excited states and the conduction band.

10.4.3. General.

From the foregoing it appears that the N.D.1-centre in both Type Ia and Ib diamond comprises an interstitial in combination with substitutional nitrogen. The difference in nitrogen configuration, however, leads to differences in the temperature of formation and in the positions of the levels within the forbidden gap; however, the energy difference between the ground and excited states are the same in both cases.

10.5. Investigation of the Electron Exchange Effects.

If the foregoing deductions are correct, the effects of thermal enhancement and optical bleaching noted for N.D.1 in Type Ia diamond should be the same for Type Ib diamond, with the difference, however, that the temperature scale is lowered. The effect of illumination with monochromatic light on the N.D.1 and G.R.1 bands

in the irradiated Type Ib specimen, D_{18}, was therefore investigated.

These observations are listed in Table 10.2 and can be summarised as follows:

a) Illumination in the N.D.1 band with the 3.40 eV mercury line at room temperature, (to effect electron transfer from N.D.1 to G.R.1) causes no observable change. This is an expected result as thermal activation of electrons from the valence band to the N.D.1 ground state occurs at room temperature. The positive holes so generated are captured by G.R.1-centres, thus reversing the effect of illumination.

b) When the specimen is kept at liquid nitrogen temperature during illumination in the N.D.1 band and subsequent measurement of the absorption spectra, some bleaching of N.D.1 and corresponding enhancement of G.R.1 is effected.

c) This effect can be partially reversed by subsequent exposure to the 2.84 eV mercury line. This line is in the narrow spectral region where the U.V. band is absorbing but N.D.1 is not (ϕ 8.5.2). Some electron transfer from G.R.1

TABLE 10.2

THE EFFECT OF ILLUMINATION WITH MONOCHROMATIC LIGHT ON THE OPTICAL ABSORPTION BANDS IN SPECIMEN D18

NOMINAL TREATMENT	TEMPERATURE IN ^{o}K	N.D.I. ($\mu t.eV$)	G.R.I. ($\mu t.eV$)
Irradiation at solid CO_2 temperature	-	0.384	0.016
Illumination : 3.40 eV mercury line	293	0.385	0.017
Illumination : 3.40 eV mercury line	80	0.266	0.023
Illumination : 2.84 eV mercury line	80	0.318	0.019
Warm up	293	0.386	0.015

back to N.D.1 via the conduction band is therefor expected.

d) When the specimen is allowed to warm up to room temperature, the original band strengths are completely restored.

This evidence is fairly satisfactory, but it is not very clear why the optical bleaching of N.D.1 is more limited than in the Type Ia case. This may be accounted for, however, by considering that the excited state of highest energy of N.D.1 is only 4.5 eV above the valence band, whereas this value was estimated to be 5.2 eV in Type Ia diamond (§ 10.4.2).

10.6. The Effects of Heat Treatment.

The Type Ib specimens were now subjected to heat treatment. The effects on the strengths of the irradiation induced bands are listed in Table 10.3. As heat treatment can produce ionization by thermal excitation of the induced defects as well as annealing, the heating was carried out in the dark and O.A. measurements were made prior to and after subsequent illumination with unfiltered mercury light. Thus an indication could be obtained as to what changes resulted from

TABLE 10.3

THE EFFECT OF HEAT TREATMENT ON THE OPTICAL ABSORPTION BANDS IN SPECIMEN D18

(Values in brackets were obtained after exposure to mercury light subsequent to heating in the dark)

TEMPERATURE IN °C	HEATING TIME IN HOURS	BAND STRENGTH IN μt.eV		
		N.D.I.	G.R.I.	6400A
20	-	0.384	0.017	zero
140	21	0.396 (0.380)	0.012 (0.015)	zero (zero)
200	22	0.378 (0.321)	0.009 (0.014)	zero (zero)
250	15	0.325 (0.259)	0.006 (0.014)	zero (zero)
300	17	0.273 (0.177)	0.004 (0.010)	zero (zero)
360	64	0.235 (0.151)	0.002 (0.007)	zero (zero)
400	40	0.198 (0.132)	zero (0.008)	zero (zero)
500	45	0.087 (0.056)	zero (zero)	zero (zero)
600	67	zero (zero)	zero (zero)	0.078 (0.076)
700	180	zero (zero)	zero (zero)	0.077 (0.076)
950	25	zero (zero)	zero (zero)	0.078 (0.077)

annealing of the centres, or from thermal ionization only.

10.6.1. Effect on N.D.1.

After heat treatment at 140 and 200°C the lines of the N.D.1 band became much sharper and in appearance resembled the N.D.1 band in Type Ia diamond more closely. Furthermore as is evident from Table 10.3, the N.D.1 band could now be partially bleached with mercury light at room temperature! It appears therefore that the N.D.1-centres were modified by this heat treatment. Apparently there is a multiplicity of interstitial/substitutional nitrogen arrangements which comprise N.D.1-centres, and they are subject to modification by heat treatment. The previous discussion of possible levels in the forbidden gap produced by N.D.1-centres is therefore not general. It appears to explain the behaviour of N.D.1-centres after irradiation at a specific temperature, but does not account for the behaviour of N.D.1-centres after modification by mild heat treatment.

Apart from the electron exchange effects which could be reversed by exposure to mercury light, the values obtained for the strength of the N.D.1 band after heating in the dark became progressively lower, until after

67 hours at 600°C it could no longer be detected. It is evident therefore that considerable annealing of N.D.1-centres occurs at temperatures below 500°C. This is not the case in Type Ia diamond, and it must be concluded therefore that N.D.1-centres in Type Ib diamond are less stable than those in Type Ia diamond.

This is not inconsistent with the earlier suggestion of an energy barrier to N.D.1 formation in Type Ia diamond, where the interstitial is envisaged as trapped in a potential well. It will therefore not be liberated as readily as when in combination with an isolated substitutional nitrogen atom, a combination which is more easily formed.

10.6.2. Effect on G.R.1.

Apart from thermal bleaching, which could be restored by illumination with mercury light, heat treatment at temperatures up to 250°C did not alter the G.R.1 band permanently. Subsequent heat treatment up to 360°C, however, caused a rapid decrease of about 40% in the strength of G.R.1, which was not further effected by another 40 hours heating at 400°C.

It is tempting to compare this effect with the analogous drop observed in Type Ia and Type IIa diamond. However, the G.R.1-centre in the case of Type Ib diamond is known to be very largely ionized, and the band observed represents only a small fraction of the true centre concentration. Thus marked changes in the apparent strength may be expected if only limited changes in other centres affecting electron distribution occur.

At 500°C, the remainder of the observable G.R.1 band disappears. Again it is difficult to infer whether this is due to annealing of the centres or to more complete ionization. However, at this temperature unionized vacancies are known to be mobile, although ionized vacancies probably require a rather higher temperature. (5032A band continues to grow after G.R.1 has apparently disappeared in Type Ia diamonds - Figure 9.1.) Thus, possibly at 500°C, and certainly at 600°C, a new band due to vacancy/nitrogen combination might be expected.

Such a new band, between 1.92 and 2.45 eV, was developed during heat treatment at 600°C. This will be referred to as the 6400A band. The O.A. spectrum of D_{18} after this treatment is shown in Figure 10.1c. Illumination with mercury light after heat treatment in the

dark did not affect the strength of this band. Heat treatment at higher temperatures was also ineffective in producing further changes in the O.A. spectrum.

10.6.3. Effect on the E.P.R. Spectrum.

The apparent single E.P.R. line superimposed on the central line of the paramagnetic nitrogen spectrum, annealed during all the heat treatment stages. After treatment at 600°C this line could not be detected; the E.P.R. spectrum now being the same as before irradiation.

10.7. 6400A-Centres.

The 6400A band developed in a Type Ib specimen, D_{20}, measured at room temperature and at 80°K, is shown in Figure 10.4. The energies of the main O.A. features are listed in Table 10.4. Like all the other band systems found in diamond (N.D.1, 4150A, 5032A, G.R.1, H2 and 14,500A), the 6400A system also consists of a principal line of lowest energy and additional less sharp lines arising from the interaction between the main electronic transition and vibrational states of the crystal.

All the specimens in which a 6400A band was developed, fluoresced with a red colour when exposed to

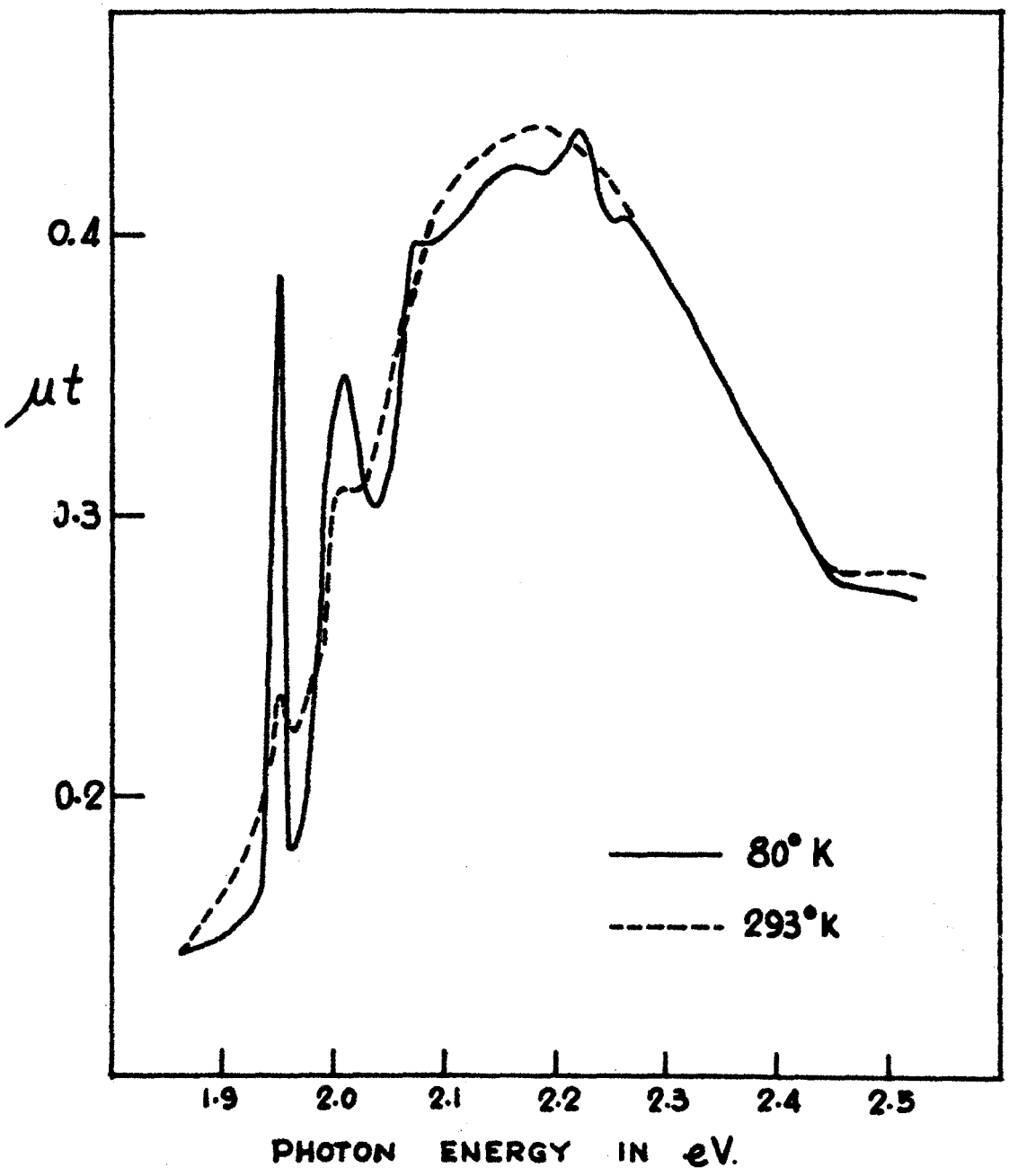

FIGURE 10.4 THE 6400A BAND IN TYPE Ib SPECIMEN D20, AS MEASURED AT ROOM TEMPERATURE AND AT 80°K.

TABLE 10.4

ENERGIES OF THE MAIN OPTICAL ABSORPTION FEATURES OF THE 6400A BAND

OPTICAL ABSORPTION FEATURE	POSITION IN eV
Lower energy limit	1.92
Principal line	1.95
Second line	2.01
Third line	2.08
Fourth line	2.16
Fifth line	2.22
Sixth line	2.27
Higher energy limit	2.45

mercury light. It therefore appears that, like the 4150A and 5032A systems, the 6400A system also has an associated fluorescence spectrum which, judging from the colour of the luminesence, may be the mirror image of the absorption system.

The 6400A band is produced only in Type Ib specimens, and by the same treatment that produces the 5032A band in Type Ia diamonds. It is therefore proposed that the 6400A-centre also consists of a vacancy in combination with substitutional nitrogen, the nitrogen in this case being in the isolated paramagnetic configuration.

The 6400A-centres appear to be non-paramagnetic and do not produce any I.R. absorption features.

10.8. Defects Induced at Room Temperature.

In addition to the experiments described above, the remaining two Type Ib specimens, which were not specially thinned, were now irradiated at room temperature with 0.78 MeV electrons to a considerable higher dose of approximately 5×10^{18} electrons/cm^2. The O.A. spectrum, as measured at liquid nitrogen temperature, of one of these, D_{21}, before and after this irradiation, is illustrated in Figures 10.5a and b.

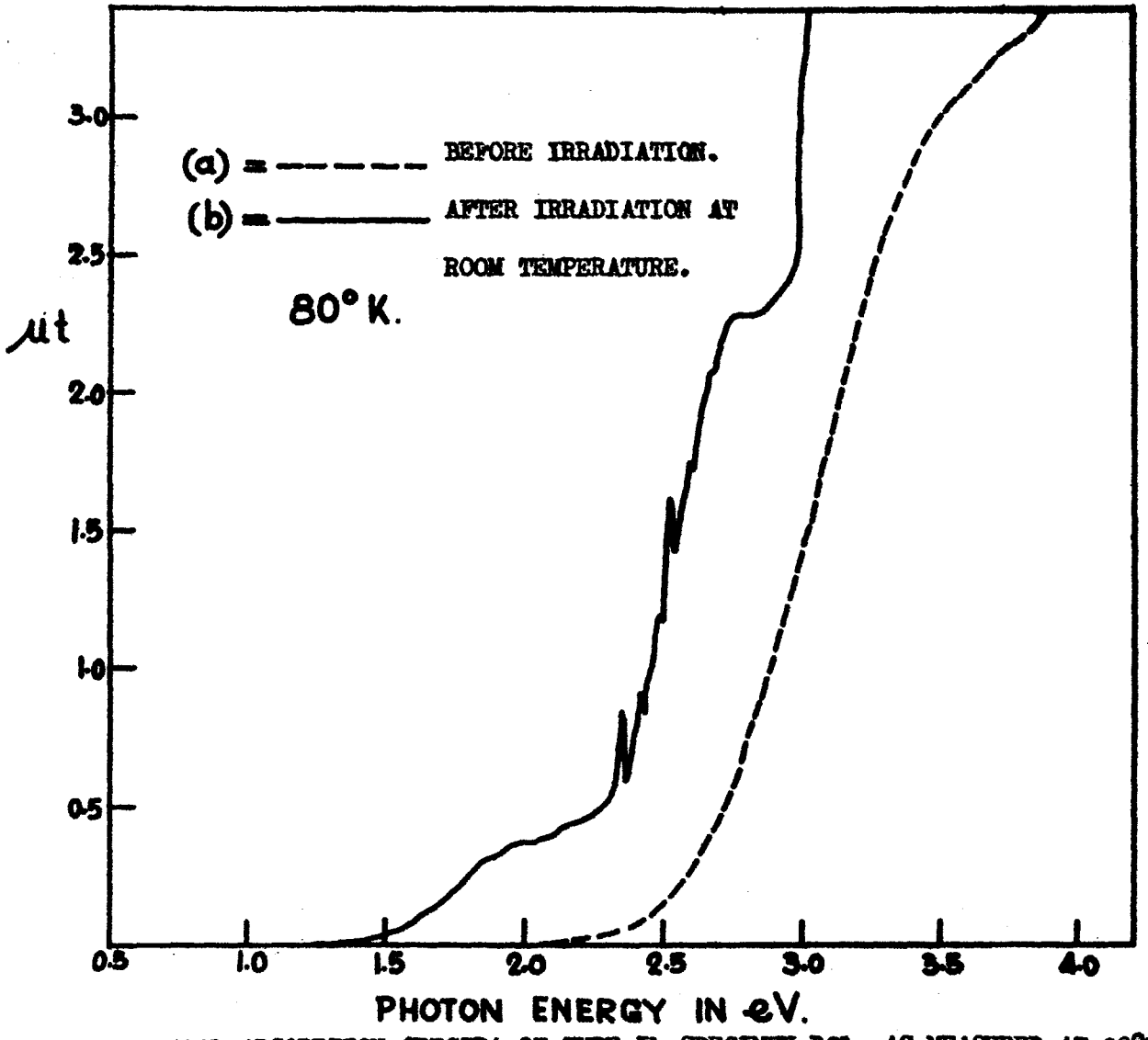

FIGURE 10.5 OPTICAL ABSORPTION SPECTRA OF TYPE Ib SPECIMEN D21, AS MEASURED AT 80°K.

The following O.A. features were introduced by this irradiation treatment:

a) A broad structureless band between 1.5 and 2.3 eV. This is in the region where the G.R.1 band is normally found (1.65 to 2.4 eV), and it is therefore not possible to determine whether a G.R.1 band is present as well.

b) A band system between 2.3 and 2.5 eV with an apparent sharp principal line at 2.35 eV, and less sharp associated lines at 2.42 and 2.49 eV.

c) Another band system between 2.5 and 2.9 eV with an apparent sharp principal line at 2.52 eV, and less sharp lines at 2.6 and 2.68 eV.

d) At photon energies greater than 3.0 eV the absorption was so large that no measurements could be made. It is not certain whether this is due to a very large N.D.1 band.

The E.P.R. spectrum of the same specimen before and after irradiation with Ho // <100> , is illustrated in Figures 10.6a and b. A complicated anistropic E.P.R. spectrum was induced by this irradiation treatment. This spectrum did not lend itself to any simple analysis, and still has to be analysed in more detail. No I.R.

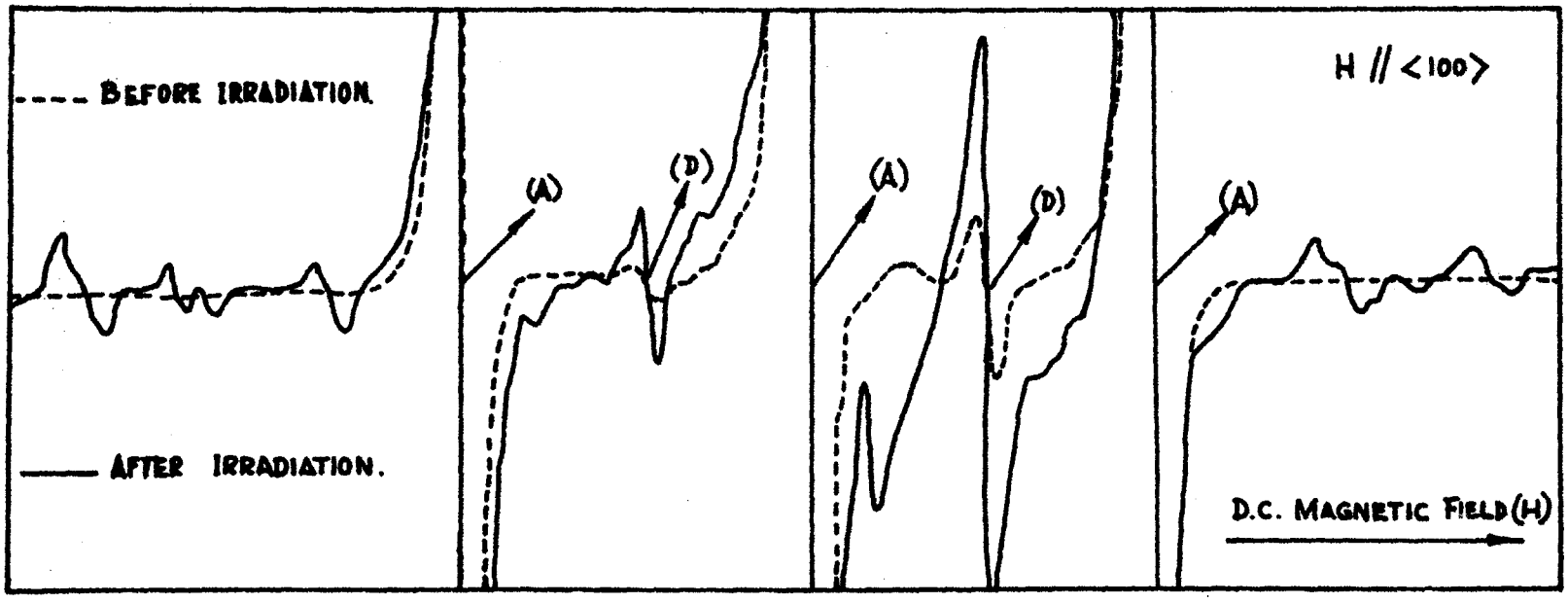

FIGURE 10.6 FIRST DERIVATIVE E.P.R. SPECTRA OF TYPE Ib SPECIMEN D21, BEFORE AND AFTER IRRADIATION AT ROOM TEMPERATURE.

absorption features other than those ascribed to the paramagnetic nitrogen were found.

The specimens were now heated at 500°C for 30 hours. The E.P.R. spectrum exhibited by D_{21} after this treatment is similar to that observed after irradiation of the Type Ib specimens at low temperature (Figure 10.2b). The set of anisotropic lines annealed out, and only the spectrum due to paramagnetic nitrogen with an isotropic line superimposed on the central line could be detected.

The O.A. spectrum after this treatment is illustrated in Figure 10.7a. This spectrum is similar to that obtained after irradiating a Type Ib specimen at low temperature (Figure 10.1b), and exhibits only a large N.D.1 and a small G.R.1 band. As is evident from Figure 10.7a the N.D.1 band is still very large, so that no reliable deductions as to the sharpness of the component lines can be made.

Further heat treatment at 600°C for 75 hours had the same effect as when the specimens subjected to low temperature irradiation were heated at this temperature, namely: complete annealing of G.R.1, N.D.1 and the superimposed E.P.R. line, and the production of a

6400A band. The O.A. spectrum of D_{21} after this heat treatment is illustrated in Figure 10.7b.

10.9. Discussion.

In general the effects of irradiation damage in Type Ib diamond are similar to those observed in Type Ia specimens only if the irradiation is carried out at 200°K. In every aspect, however, significant differences, which are attributed to the difference in the nitrogen configuration, are observed.

Most striking of these differences is the fact that N.D.1-centres form at a lower temperature in Type Ib than in Type Ia diamonds. This is attributed to different states of strain in the host lattice which are expected to exist around an isolated substitutional nitrogen atom and a nitrogen platelet. Thus a lower activation energy barrier to interstitial/nitrogen combination exists in Type Ib diamond.

Because of the specific nitrogen configuration, the N.D.1-centres in Type Ib diamonds apparently produce acceptor levels much closer to the valence band than the N.D.1-centres in Type Ia specimens. Thus electron transfer from N.D.1 to G.R.1 occurs at room temperature.

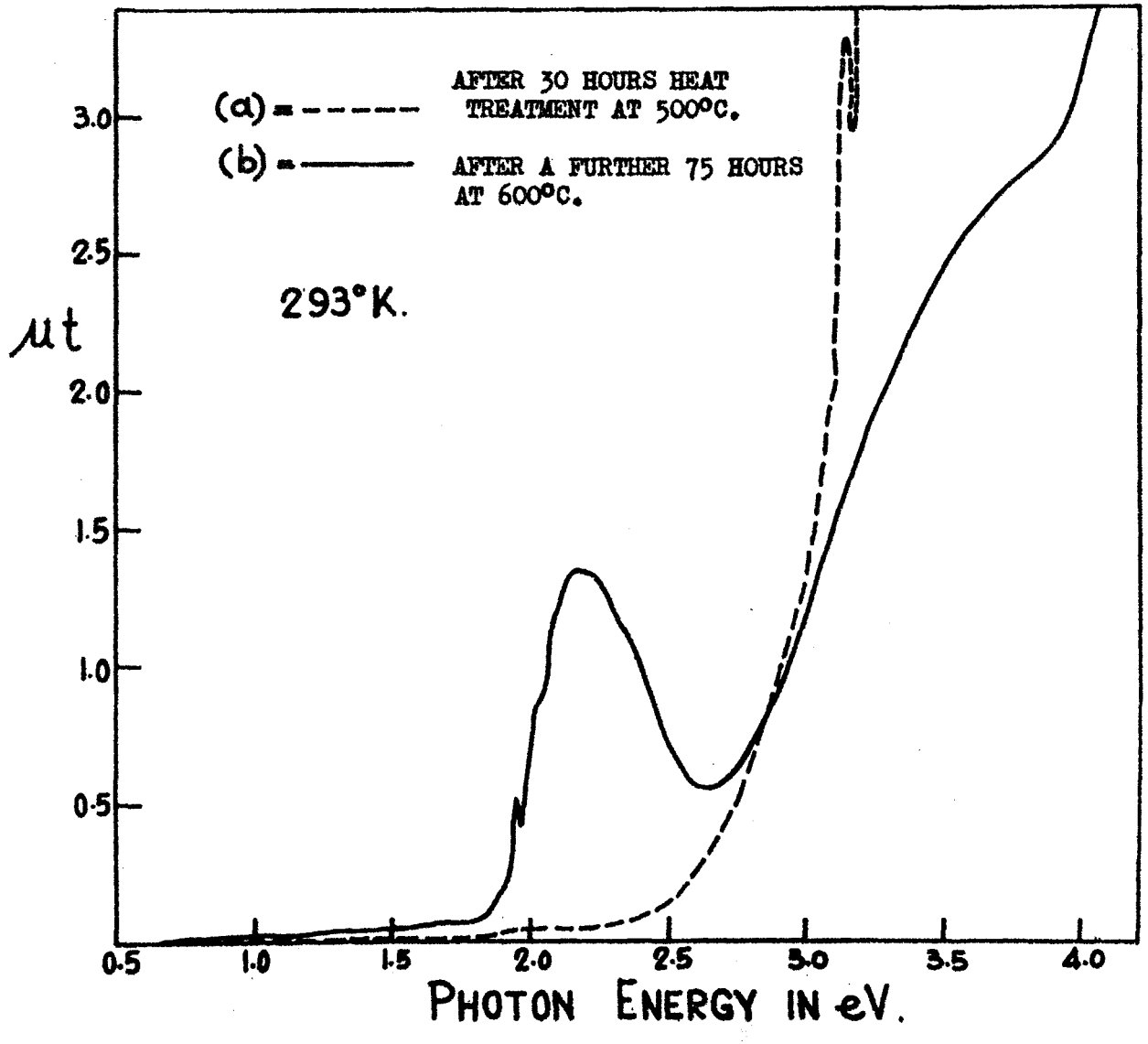

FIGURE 10.7 OPTICAL ABSORPTIC SPECTRA OF SPECIMEN D21, WHICH WAS IRRADIATED AT ROOM TEMPEI TURE.

A large proportion of the vacancies is therefore ionized and optically inactive. The magnitude of G.R.1 after irradiation is therefore not a measure of the irradiation damage produced in a Type Ib diamond.

The nature of the nitrogen configuration in Type Ib diamond is simpler than that of nitrogen platelets. Contrary to expectation, however, this investigation has revealed that the effects of irradiation damage in Type Ib diamond are much more complicated than in Type Ia specimens.

When subjected to heat treatment at about 200°C the N.D.1 band in Type Ib diamond becomes sharper, and the band now interacts differently with G.R.1. This phenomenon is not well understood at all, but tends to indicate multiplicity of interstitial/nitrogen arrangements which comprise N.D.1-centres.

If the irradiation is carried out at room temperature the process is even more complicated. Additional O.A. and E.P.R. spectra, which anneals out at 500°C, are produced. This is never observed in the other diamond types. The nature of the defect centres responsible for these additional spectra, cannot be deduced at this stage. These defect centres are formed below 500°C

and are not stable at this temperature. After being annealed out, no new O.A. or E.P.R. spectra are found. It therefore appears that they are associated only with substitutional nitrogen atoms in isolated positions and interstitials, situated in various different orientations, relative to the nitrogen.

The N.D.1-centres in Type Ib anneal more readily than those in Type Ia diamond. This is not unexpected as an interstitial is expected to be more loosely bound to an isolated substitutional nitrogen atom than to a nitrogen platelet.

The annealing of G.R.1 in Type Ib diamond is analogous to that of G.R.1 in Type Ia's and can also be best explained by considering vacancies which become mobile around 500°C and are trapped by substitutional nitrogen atoms. An analogue of the 5032A-centre (vacancy plus nitrogen platelet), the 6400A-centre (vacancy plus isolated substitutional nitrogen), is therefore obtained. No analogue of the H2 band is found in Type Ib diamond. Again this is not unexpected as it is not considered likely that an interstitial and a vacancy can co-exist at or near a single isolated substitutional nitrogen atom.

CHAPTER XI.

CONCLUSION.

11.1. Results of this Study.

From the survey of natural diamond it became evident that all the diamond specimens encountered in practice contain defect centres. The most abundant defects are those attributed to substitutional nitrogen segregated into platelets, which are found in 98% of all natural diamond. Only a small group of transparent natural diamonds contain substitutional nitrogen in isolated lattice positions. A new classification system for diamond, based on the presence or absence of these defect centres, is proposed, and accordingly specimens containing substitutional nitrogen in platelets and in isolated positions were classified as Type Ia and Type Ib diamonds respectively.

In about 2% of all natural diamonds no nitrogen can be detected. These specimens are classified as being Type II, and were subdivided as Type IIa diamonds, which contain graphitic regions, and Type IIb diamonds, which are semiconductors due to the presence of acceptor centres.

Apart from these four defect centres, an additional seven defect centres were found to occur only, in Type I diamonds. Although they could not be identified from their characteristic O.A. and E.P.R. spectra, these defects are thought to be associated with nitrogen in some way.

From the evidence it appears that the substitutional nitrogen in diamond was originally incorporated in isolated substitutional positions, and migrated with a vacancy mechanism to the more stable platelet configuration. It is quite possible that nitrogen in intermediate stages remained in the diamond lattice and is responsible for some of the unidentified defect centres.

In order to investigate the feasibility of this proposal, it was decided to try to convert substitutional nitrogen in isolated positions to the platelet configuration and vice versa, with a vacancy mechanism. Specimens containing these two nitrogen configurations were therefor irradiated with 0.78 MeV electrons to introduce vacancies.

After irradiation, hitherto unknown effects were observed and a general investigation of irradiation damage in diamond was therefore conducted. This yielded

information on the nature of vacancies and interstitial carbon atoms in diamond, and models were proposed to explain the effects of irradiation damage in terms of immobile vacancies, mobile interstitials which combine with substitutional nitrogen, and charge transfer between these centres.

Heat treatment of the irradiated specimens also produced unknown effects, and the annealing of irradiation damage in diamond was therefore studied in some detail. Models were proposed to explain these effects in terms of the combination of mobile vacancies with each other, with nitrogen platelets, with substitutional nitrogen in isolated positions, and with a nitrogen platelet with an anchored interstitial and charge transfer between the resulting defect centres.

It was shown that vacancies act as electron donors and interstitials in combination with substitutional nitrogen as acceptors. When ionized, the vacancies are optically inactive and the G.R.1 band observed in diamonds after irradiation is therefore not always a measure of the vacancies produced. An estimate of vacancy and interstitial mobility in diamond could be obtained. It is suggested that interstitials are mobile

below 250°C and that vacancies become mobile at temperatures of about 500°C.

Two of the unidentified defect centres found in natural diamond, G.R.1 and 5032A-centres, were encountered in the study of irradiation damage. From the information obtained it is now suggested that the G.R.1-centre is a vacancy, and the 5032A-centre a vacancy in combination with a nitrogen platelet.

The other defect centres, which are formed by irradiation damage and subsequent heat treatment, are:

a) Interstitials which are optically inactive.

b) N.D.1-centres, which are ascribed to the combination of an interstitial and substitutional nitrogen in any of the two known configurations.

c) 6400A-centres, ascribed to the combination of a vacancy and substitutional nitrogen in isolated positions.

d) H2 centres which are thought to arise from a vacancy and an interstitial pinned to different locations in a nitrogen platelet.

No evidence of any substitutional nitrogen migration was observed after heat treatment at temperatures

up to 1200°C.

11.2. Suggestions for Further Research.

It is obvious that this study on the nature of defect centres in diamond is by no means complete. In fact, it can rather be regarded as opening the field for further studies based on the same approach, as it demonstrates the importance of employing more than one experimental method to investigate a variety of defect centres in all the diamond types simultaneously, rather than concentrating on the application of one specific technique to a defect centre in a particular type of diamond.

Suggestions for further research can be grouped in two categories:

a) Further investigations on the effects described in this study.

More work on a number of the effects described in this study should lead to valuable information. Some suggestions are:

1. Growth doping of synthetic diamond with emphasis on growing good quality crystals suitable for optical absorption measurements.
2. Irradiation damage at liquid nitrogen and

possibly lower temperatures, without warm up prior to absorption measurements. In particular, if such a study is conducted on Type Ib specimens, formation of the N.D.1 band should only occur after subsequent heating and an idea of interstitial mobility can be obtained.

3. Investigation of the I.R.R. absorption induced by irradiation damage in different types of diamond employing a more sensitive spectrometer and a higher irradiation dose.

4. Investigation of the symmetry of the irradiation induced defect centres using polarisation of luminescence and optical bleaching with polarised light, where appropriate. If successful such evidence would remove the uncertainty that exists about the proposed models.

5. A study of the photoconduction expected to be associated with the cycling in bandstrength of the optical absorption bands induced by irradiation, which would lead to a better understanding of the charge transfer involved

between defect centres.

b) Attempts to change the substitutional nitrogen configuration.

The programme to change the substitutional nitrogen configuration in diamond was only just started. It was suggested that vacancies were attached to nitrogen in the two known substitutional configurations by heat treatment after irradiation. No evidence of nitrogen migration with a vacancy mechanism was obtained after heat treatment up to 1200°C. Following this with further heat treatment at higher temperatures up to about 2500°C is bound to promote nitrogen migration. As diamond reverts to graphite above 1700°C at atmospheric pressure, this will have to be conducted under suitable high pressures. The trouble involved in conducting such experiments in the diamond stable region of the carbon equilibrium diagram, should be more than rewarded by the wealth of information that can be obtained.

REFERENCES.

Abragam, A., and Pryce, M.H.L., 1951, Proc. Roy. Soc. A 205, 135.

Ashby, M.F. and Brown, L.M., 1963a, Phil. Mag. 8, 1083.

Ashby, M.F. and Brown, L.M., 1963b, Phil. Mag. 8, 1649.

Baldwin, J.A., 1963, Phys. Rev. Letters 10, 220.

Bassompierre, A., 1955, Disc. Faraday Soc. 19, 260.

Bastin, J.A., Mitchell, E.W.J. and Whitehouse, J., 1959, Brit. J. Appl. Phys. 10, 412.

Bell, M.D. and Leivo, W.J., 1961, Bull. Amer. Phys. Soc. 6, 142.

Berman, R. and Simon, F., 1955, Z.F. Elektrochem. 59, 333.

Bleaney, B., 1951, Phil. Mag. 42, 441.

Bube, R.H., 1960, Photoconductivity of Solids, John Wiley and Sons, New York, p.64.

Bundy, F.P., Hall, H.T., Strong, H.M. and Wentorf, R.H., 1955, Nature 176, 51.

Charette, J.J., 1961, J. Chem. Phys. 35, 1906.

Clark, C.D., 1955, PhD. Thesis, Reading University.

Clark, C.D., 1962, Proc. 1st Int. Congress on Diamonds in Industry, Paris, p.253.

Clark, C.D., Ditchburn, R.W. and Dyer, H.B., 1956a, Proc. Roy. Soc. A234, 363.

Clark, C.D., Ditchburn, R.W. and Dyer H.B., 1956b, Proc. Roy. Soc. A237, 75.

Clark, C.D., Kemmey, P.J. and Mitchell, E.W.J., 1961, Disc. Faraday Soc. 31, 96.

Clark, C.D., Maycraft, G.W. and Mitchell, E.W.J., 1962, J. Appl. Phys. 33, 378.

Cork, J.N., 1942, Phys. Rev. 62, 80 and 494.

Coulson, C.A. and Kearsley, M.J., 1957, Proc. Roy. Soc. A241, 433.

Crookes, W., 1909, Diamonds, 108-110 (Harper Mag. London)

Custers, J.F.H., 1952, Physica 18, 489.

Custers, J.F.H., 1955, Nature 176, 173.

Dean, P.J., 1965, Private Communication.

Dexter, D.L., 1958, Solid State Phys., 6, 353.

Dugdale, R.A., 1953, Brit. J. Appl. Phys. 4, 334.

Duncan, I., 1963, PhD. Thesis, Reading University.

Dyer, H.B. and Ferdinando, P., 1965, Private Communication.

Dyer, H.B. and Matthews, I.G., 1957, Proc. Roy. Soc. A243, 320.

Elliot, R.J., 1960, Proc. Phys. Soc., 76, 787.

Elliot, R.J., Matthews, R.G. and Mitchell, E.W.J., 1958, Phil. Mag. 3, 36C.

Evans, T. and Phaal, C., 1962, Proc. Roy. Soc., A270, 538.

Every, A.G., 1965, Private Communication.

Faulkner, E.A. and Lomer, J.N., 1962, Phil. Mag. 7, 1995.

Feher, G., Hensel, J.C. and Gere, E.A., 1960, Phys. Rev. Letters 5, 309.

Ferdinando, P., 1965, Private Communication.

Frank, F.C., 1956, Proc. Roy. Soc. A237, 168.

Frank, F.C., 1964, Proc. Phys. Soc. 84, 745.

Glendennin, L.E., 1948, Nucleonics 2, 12.

Henneberke, G., 1960, Nuclear Instrum. 7, 89.

Holland, M.B., 1964, Private Communication.

Holland, M.B. and Raal, F.A., 1964, Private Communication.

Horszowski, S.M., 1963, J. Sci. Instrum. 40, 532.

Huggins, C.M., and Cannon, P., 1962, Nature 194, 329.

James, P.F. and Evans, T., 1965, Phil. Mag. 11, 113.

Kaiser, W. and Bond, W.L., 1959, Phys. Rev. 115, 857.

Kato, Y. and Nakahara, C., 1959, J. Phys. Soc. Japan 14, 690.

Kemmey, P.J. and Mitchell, E.W.J., 1960, Proc. Int. Conf. on Semi-conductor Phys. (Prague), p. 919.

Kinchin, G.H. and Pease, R.S., 1955, Rep. Prog. Phys. 18, 1.

Lang, A.R., 1964, Proc. Phys. Soc. 84, 871.

Lark-Horovitz, K. and Johnson, V.A. (Ed.), 1959, Solid State Physics 6, Academic Press.

Lax, M. and Burstein, E., 1955, Phys. Rev. 97, 39.

Levy, P.W., and Krammerer, O.F., 1955, Phys. Rev. 100, 1787.

Lin, C.C., 1960, Phys. Rev. 119, 1027.

Lomer, W.M., and Cottrell, A.H., 1955, Phil. Mag. 46, 711.

Loubser, J.H.N., 1965, Private Communication.

Ludwig, G.W., and Woodbury, H.H., 1962, Solid State Physics 13, 223.

McKinley, W.A. and Feshbach, H., 1948, Phys. Rev. 74, 1759.

Matthews, I.G., 1956, PhD. Thesis, Reading University.

Maycraft, G.W., 1960, PhD. Thesis, Reading University.

Mykolatewycz, R., Kalnajs, J. and Smakula, A., 1964, J. Appl. Phys. 35, 1773.

Palmer, D.W., 1961, PhD. Thesis, Reading University.

Peter, F., 1923, Z. Physik 15, 358.

Pough, F.H., and Rogers, T.H., 1947, Amer. Min. 32, 31.

Pringsheim, P., 1953, Phys. Rev. 91, 551.

Pryce, M.H.L., 1950, Proc. Phys. Soc. A63, 25.

Raal, F.A., 1957, Amer. Min. 42, 354.

Raal, F.A., 1958, Proc. Phys. Soc. 71, 846.

Raal, F.A., 1959, Proc. Phys. Soc. 74, 647.

Robertson, R., Fox, J.J. and Martin, A.E., 1934, Trans. Roy. Soc. A232, 463.

Robertson, R., Fox, J.J. and Martin, A.E., 1936, Proc. Roy Soc. A157, 579.

Runciman, A., 1965, Private Communication.

Sands, R.H., 1955, Phys. Rev. 99, 1222.

Seitz, F., 1940, The Modern Theory of Solids, McGraw-Hill, New York.

Seitz, F., 1949, Disc. Faraday Soc. 5, 271.

Seitz, F. and Koehler, J.S., 1956, Solid State Phys. 2, 305.

Schonland, D. and Every, A.G., 1965, Private Communication.

Silsbee, R.H., 1957, J. Appl. Phys. 28, 1246.

Slichter, C.P., 1955, Phys. Rev. 99, 479.

Smakula, A., 1930, Z. Physik 59, 603.

Smith, W.V., Sorokin, P.P., Gelles, I.L. and Lasher, G.J., 1959a, Phys. Rev. 115, 1546.

Smith, W.V., Gelles, I.L., and Sorokin, P.P., 1959b, Phys. Rev. Letters 2, 39.

Smith, S.D. and Hardy, J.R., 1961, Phil. Mag. 6, 1163.

Smith, S.D., Hardy, J.R. and Mitchell, E.W.J., 1962, Proc. Exeter Conf. on Phys. of Semiconductors, p. 592.

Sternheimer, R., 1952, Phys. Rev. 86, 316, 595A.

Sutherland, G.B.B.M., Blackwell, D.E. and Simeral, W.G., 1954, Nature 174, 901.

Tagaki, M. and Lang, A.R., 1964, Proc. Roy. Soc. A281, 310.

Thompson, D.O., Blewitt, T.H. and Holmes, D.K., 1956, J. Appl. Phys. 28, 742.

Townes, C.H. and Shawlow, A.L., 1955, Microwave Spectroscopy, McGraw-Hill, New York, p. 243.

Vermeulen, L., 1965, Private Communication.

Wagoner, G., 1961, Bull, Amer. Phys. Soc. 6, 129.

Wedepohl, P.T., 1957a, PhD. Thesis, Reading University.

Wedepohl, P.T., 1957b, Proc. Phys. Soc. B70, 177.

Wedepohl, P.T., 1963, Private Communication.

Wright, A., 1961, Private Communication.

Yamaguchi, T., 1962, J. Phys. Soc. Japan 17, 1359.

Yamaguchi, T., 1963, J. Phys. Soc. Japan 18, 368.